Vol. 62 March, 1958 No. 3

THE JOURNAL OF PHYSICAL CHEMISTRY

(Registered in U. S. Patent Office)

CONTENTS

Notes

THE JOURNAL OF PHYSICAL CHEMISTRY

(Registered in U. S. Patent Office)

Published monthly by the American Chemical Society at 20th and Northampton Sts., Easton, Pa.

Second-class mail privileges authorized at Easton, Pa.

The *Journal of Physical Chemistry* is devoted to the publication of selected symposia in the broad field of physical chemistry and to other contributed papers.

Manuscripts originating in the British Isles, Europe and Africa should be sent to F. C. Tompkins, The Faraday Society, 6 Gray's Inn Square, London W. C. 1, England.

Manuscripts originating elsewhere should be sent to W. Albert Noyes, Jr., Department of Chemistry, University of Rochester, Rochester 20, N. Y.

Correspondence regarding accepted copy, proofs and reprints should be directed to Assistant Editor, Allen D. Bliss, Department of Chemistry, Simmons College, 300 The Fenway, Boston 15, Mass.

Business Office: Alden H. Emery, Executive Secretary, American Chemical Society, 1155 Sixteenth St., N. W., Washington 6, D. C.

Advertising Office: Reinhold Publishing Corporation, 430 Park Avenue, New York 22, N. Y.

Articles must be submitted in duplicate, typed and double spaced. They should have at the beginning a brief Abstract, in no case exceeding 300 words. Original drawings should accompany the manuscript. Lettering at the sides of graphs (black on white or blue) may be pencilled in and will be typeset. Figures and tables should be held to a minimum consistent with adequate presentation of information. Photographs will not be printed on glossy paper except by special arrangement. All footnotes and references to the literature should be numbered consecutively and placed in the manuscript at the proper places. Initials of authors referred to in citations should be given. Nomenclature should conform to that used in *Chemical Abstracts*, mathematical characters marked for italic, Greek letters carefully made or annotated, and subscripts and superscripts clearly shown. Articles should be written as briefly as possible consistent with clarity and should avoid historical background unnecessary for specialists.

Notes describe fragmentary or incomplete studies but do not otherwise differ fundamentally from articles and are subjected to the same editorial appraisals as are articles. In their preparation particular attention should be paid to brevity and conciseness. Material included in Notes must be definitive and may not be republished subsequently.

Communications to the Editor are designed to afford prompt preliminary publication of observations or discoveries whose value to science is so great that immediate publication is imperative. The appearance of related work from other laboratories is in itself not considered sufficient justification for the publication of a Communication, which must in addition meet special requirements of timeliness and significance. Their total length may in no case exceed 500 words or their equivalent. They differ from Articles and Notes in that their subject matter may be republished.

Symposium papers should be sent in all cases to Secretaries of Divisions sponsoring the symposium, who will be responsible for their transmittal to the Editor. The Secretary of the Division by agreement with the Editor will specify a time after which symposium papers cannot be accepted. The Editor reserves the right to refuse to publish symposium articles, for valid scientific reasons. Each symposium paper may not exceed four printed pages (about sixteen double spaced typewritten pages) in length except by prior arrangement with the Editor.

Remittances and orders for subscriptions and for single copies, notices of changes of address and new professional connections, and claims for missing numbers should be sent to the American Chemical Society, 1155 Sixteenth St., N. W., Washington 6, D. C. Changes of address for the *Journal of Physical Chemistry* must be received on or before the 30th of the preceding month.

Claims for missing numbers will not be allowed (1) if received more than sixty days from date of issue (because of delivery hazards, no claims can be honored from subscribers in Central Europe, Asia, or Pacific Islands other than Hawaii), (2) if loss was due to failure of notice of change of address to be received before the date specified in the preceding paragraph, or (3) if the reason for the claim is "missing from files."

Subscription Rates (1958): members of American Chemical Society, $8.00 for 1 year; to non-members, $16.00 for 1 year. Postage free to countries in the Pan American Union; Canada, $0.40; all other countries, $1.20. Single copies, current volume, $1.35; foreign postage, $0.15; Canadian postage $0.05. Back volumes (Vol. 56-59), $15.00 per volume; (starting with Vol. 60) $18.00 per volume; foreign postage $1.20, Canadian, $0.40; $1.75 per issue, foreign postage $0.15, Canadian postage $0.05.

The American Chemical Society and the Editors of the *Journal of Physical Chemistry* assume no responsibility for the statements and opinions advanced by contributors to This Journal.

The American Chemical Society also publishes *Journal of the American Chemical Society, Chemical Abstracts, Industrial and Engineering Chemistry, Chemical and Engineering News, Analytical Chemistry, Journal of Agricultural and Food Chemistry* and *Journal of Organic Chemistry*. Rates on request.

THE JOURNAL OF PHYSICAL CHEMISTRY

(Registered in U. S. Patent Office)

VOLUME 62 APRIL 1, 1958 NUMBER 3

THE SOLUTION POLYMERIZATION OF STYRENE AND METHYL METHACRYLATE

BY J. P. VAN HOOK[1] AND A. V. TOBOLSKY

Contribution from the Frick Chemical Laboratory, Princeton University, Princeton, N. J.

Received April 30, 1957

The investigation of the polymerization of styrene in benzene and CCl_4 at 30.5° has shown that the value of A'' increases substantially upon dilution of the monomer. The results indicate that CCl_4 has a much greater effect than benzene in increasing the value of A'' for styrene. The value of A'' for various monomer concentrations was calculated from the equation $A'' = k_d f[I][M_{av}]^2/R_p^2$ considering $k_d f$ to be constant ($k_d f$ is constant for rates of initiation greater than 5×10^{-9} mole/l./sec. (previous paper)). The results obtained for the styrene–benzene system were checked by subjecting the polymer to viscometric analysis for the evaluation of A'. A' has been set equal to A'' for the bulk polymerization of styrene. The results for several monomer concentrations are in very good agreement thus confirming that the rate of initiation is constant with varying [M]. Brief data for the methyl methacrylate–solvent systems show that A'' does not change with dilution of the monomer.

Introduction

As a continuation of the previous paper in this series in which the initiator efficiency of Azo I (2,2′-azo-bis-isobutyronitrile) in the bulk polymerization of styrene and methyl methacrylate was investigated, this paper studies the solution polymerization of these monomers at 30.5° to determine the possible variation of f' and/or A' on dilution with benzene and carbon tetrachloride.

Bradbury and Melville[2] have reported an increase in A'' on dilution with benzene for the polymerization of styrene and butyl acrylate at 60° using labeled Azo I as the initiator. The basic equation used was

$$A'' = \frac{k_d f\ [I][M_{av}]^2}{R_p^2}$$

(in our connotation; for a summary of the basic kinetic expressions see Paper II). The rate of polymerization was determined by the usual gravimetric method and the rate of initiation ($2k_d f.[I]$) by radioactive assay on the initiator and polymer. The reason for this behavior in A'' was not clear but Burnett and Loan[3] recently have published a report on the polymerization of methyl methacrylate, methyl acrylate and vinyl acetate in benzene solution and have given a kinetic analysis of these systems proposing that the transfer radical from benzene (phenyl radical) has a decided chemical effect on the kinetics, the effect being quite different for each monomer system. Burnett's equation to explain the kinetics in such solution polymerizations is

$$\frac{R_p^2}{[M_{av}]^2} = \frac{k_d f[I]}{A'' + K_1 \dfrac{[S]^2}{[M_{av}]^2} + K_2 \dfrac{[S]}{[M_{av}]}} \qquad (1)$$

where K_1 is a group constant consisting of the rate constants for polymerization, transfer to solvent, termination of two solvent radicals, and radical attack (phenyl radical) on the monomer to initiate a chain. K_2 is likewise a combination of the polymerization rate constant, transfer to solvent constant, termination of radicals by interaction of a phenyl radical with a polymeric radical and phenyl radical attack on a monomer to initiate a chain. In this equation the value of the group expression in the denominator on the right-hand side should increase with increasing S/M ratio, the increase being very proncunced at low monomer concentration.

Considering the same solvent participation as Burnett and Loan an expression relating P_n and R_p is obtained

(1) This paper is based upon a dissertation submitted by James P. Van Hook in partial fulfillment of the requirements for the degree of Doctor of Philosophy at Princeton University.

(2) J. H. Bradbury and H. W. Melville, *Proc. Roy. Soc. (London)*, **A222**, 456 (1954).

(3) G. M. Burnett and L. D. Loan, *Trans. Faraday Soc.*, **51**, 214 (1955).

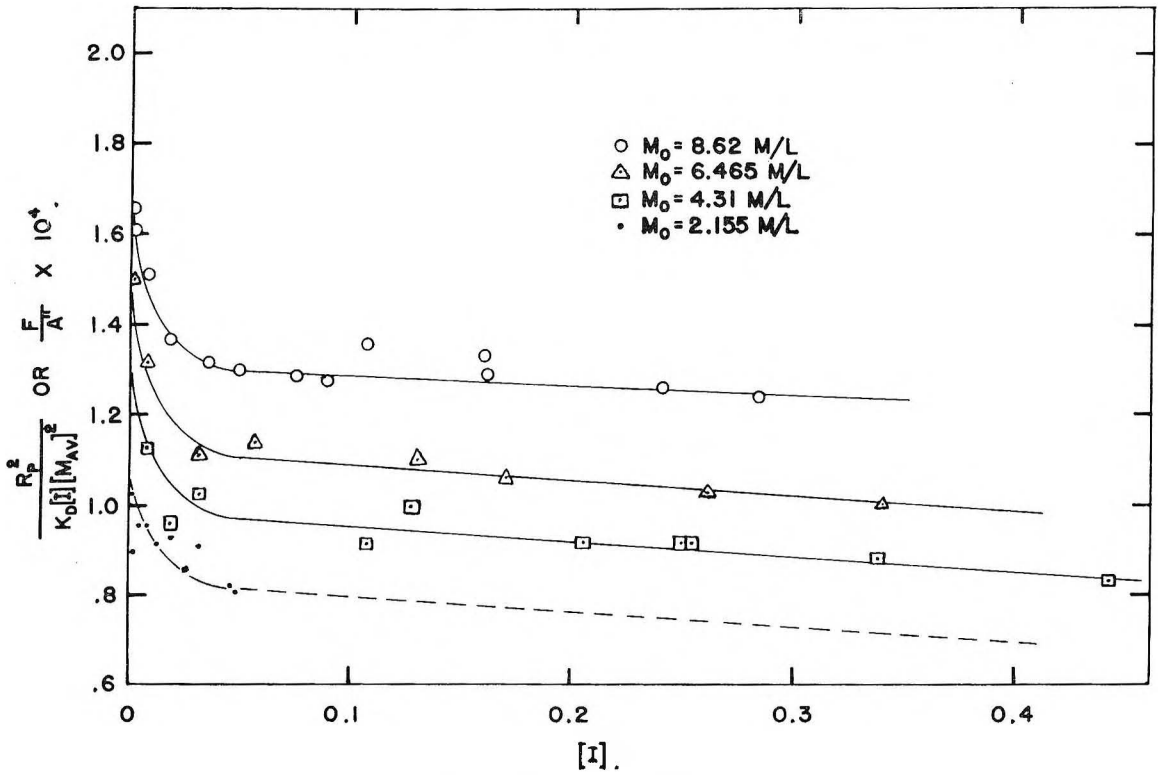

Fig. 1.—Styrene–benzene–azo I at 30.5°.

$$\frac{1}{P_n} = C_{tr,m} + C_{tr,s}\frac{[S]}{[M_{av}]} + \frac{R_p}{[M_{av}]^2}\left[A' + K_1\frac{[S]^2}{[M_{av}]^2} + K_2\frac{[S]}{[M_{av}]}\right] \quad (2)$$

where the group value in the brackets can be determined by a plot of $1/P_n$ *versus* $R_p/[M_{av}]^2$ for polymer prepared at various S/M ratios. The value of A' obtained in this manner is valid regardless of any assumptions concerning the efficiency of initiation.

The value of the denominator in equation 1 is obtained by measuring the rate at various Azo I concentrations and assuming f to be constant with [I]. This assumption is valid but subject to the provision in Paper II, that is, that the rate of initiation be greater than 5×10^{-9} mole/l./sec.

Since styrene chains terminate by direct combination,[4] hence $A' = A''$ for this particular monomer, a comparison of these values (terms in brackets in equation 1 and 2) will yield insight into the validity of these expressions for the solution polymerization of styrene in benzene. These terms were not compared in the case of styrene in CCl_4 as the molecular weight of the polymer was too low to use the viscosity technique for the determination of P_n; likewise, because with CCl_4 the $C_{tr,s}$ ($[S]/[M_{av}]$) term in equation 2 was much too large to permit a plot of $1/P_n$ *versus* $R_p/[M_{av}]^2$ for the evaluation of A'.

No such extensive work was performed on the methyl methacrylate solvent systems as there were brief indications that A'' or A' was constant with dilution.

(4) J. C. Bevington, H. W. Melville and R. P. Taylor, *J. Poly. Sci.*, **12**, 449 (1954).

Experimental

Materials.—Styrene, methyl methacrylate and Azo I were purified in the same manner as in the previous paper. Benzene, Mallinckrodt, Analytical Grade and carbon tetrachloride, Mallinckrodt, Low Sulfur Content, were used without further purification.

Procedure.—The gravimetric method for the determination of the rate of polymerization and the viscosity technique for the evaluation of P_n have been presented previously. The equation used to convert intrinsic viscosity into P_n was that given by Mayo, *et al.*,[5] $\log P_n = 3.2004 + 1.3699 \log [\eta]$.

Results and Discussion

The values of $R_p/[M_{av}]^2$ $[I]k_d$ or f/A'' at various initiator concentrations were obtained for the polymerization of styrene in benzene at monomer concentrations of 8.62, 6.465, 4.310 and 2.155 moles/liter. The value of k_d used was 10^{-7} sec.$^{-1}$ in accordance with Paper I. The plot of these data in Fig. 1 shows reasonable linearity of the major portion of the curve at all monomer concentrations. The entire data is given in Table I. From a consideration of Paper II the substantial increase of f/A'', for any particular monomer concentration, at low initiator concentration is to be expected due to the decrease in magnitude of the secondary combination wastage reaction. This decided increase in efficiency is realized even at monomer concentrations down to 25%. It is unreasonable to propose that at constant monomer concentration A'' is decreasing rapidly at low [I] as the solution in this region should be approaching ideality.

The values of $A'' + K_1/[S]^2/[M_{av}]^2) + K_2$ ($[S]/[M_{av}]$) from equation 1 were obtained for constant $k_d f$ ($k_d f = 6.44 \times 10^{-8}$), that is, at rates of

(5) F. R. Mayo, R. A. Gregg and M. S. Matheson, *J. Am. Chem. Soc.*, **73**, 1691 (1951).

TABLE I

POLYMERIZATION OF STYRENE IN BENZENE

Expt. no.	Azo I concn., mole/l.	$[M_{av}]$, mole/l.	$R_p \times 10^7$, mole/l./sec.	Intrinsic viscosity
	M_0 = 8.62 moles/l.			
2-177-1	0.283	8.10	152.0	0.642
2-177-2	.2405	8.16	142.0	.660
2-177-3	.1612	8.32	120.0	.811
2-171-1	.160	8.32	121.5	...
2-101-4	.107	8.40	101.5	.825
2-171-3	.0893	8.40	90.0	...
1-111-6	.0750	8.46	83.3	1.048
2-95-2	.0488	8.41	67.0	1.205
2-98-1	.0352	8.43	57.5	1.305
2-171-6	.01805	8.52	42.4	...
1-81-1	.00780	8.50	29.2	2.170
1-67-3	.00195	8.56	15.3	3.630
	M_0 = 6.465 moles/l.			
3-43-1	0.340	6.09	112.1	0.445
3-43-2	.261	6.18	101.3	.488
2-165-6	.1835	6.20	95.5	.565
3-43-3	.170	6.23	83.6	.550
3-43-4	.1305	6.28	74.7	.595
2-165-4	.113	6.28	78.9	.618
2-165-1	.0654	6.33	63.3	.685
3-43-5	.0565	6.36	51.1	.860
1-104-1	.0312	6.33	37.2	1.140
1-73-1	.00780	6.38	20.45	1.840
1-51-1	.00195	6.39	10.89	3.040
	M_0 = 4.310 moles/l.			
2-179-3	0.443	3.90	76.3	...
2-179-4	.338	3.99	69.0	...
3-45-1	.255	3.97	60.7	0.315
2-179-5	.250	4.06	61.5	.380
3-45-2	.205	4.02	55.3	.395
3-45-3	.1275	4.06	45.9	.415
3-45-4	.1089	4.14	41.2	.490
3-45-5	.0633	4.18	35.0	.585
1-104-2	.0312	4.19	23.7	.775
2-163-1	.01940	4.18	18.0	0.971
1-73-2	.00780	4.20	12.47	1.340
1-51-2	.00195	4.21	5.70	2.155
	M_0 = 2.155 moles/l.			
3-47-1	0.0483	2.01	12.6	0.382
1-111-4	.0465	2.05	12.7	.360
1-104-3	.0312	2.04	10.88	.468
1-111-3	.0264	2.06	9.80	.496
1-111-2	.01858	2.07	8.61	.536
1-111-1	.01340	2.08	7.30	.610
1-73-3	.00780	2.08	5.68	.710
3-47-2	.00555	2.06	4.73	.860
1-51-3	.00195	2.11	2.87	1.305
3-47-4	.000924	2.05	2.04	1.642

initiation greater than 5×10^{-9} mole/l./sec. and are given in Fig. 2 labeled as A'' on the ordinate. Likewise, the value of $A'' + K_1([S]^2/[M_{av}]^2) + K_2([S]/[M_{av}])$ at various monomer concentrations determined from equation 2 is also given in Fig. 2. The ordinate in this case is designated as A'. A typical linear plot of $1/P_n$ *versus* $R_p/[M_{av}]^2$ (M_0 = 6.465) for the determination of A' is given in Fig. 3. The agreement between A' and A'' for all monomer concentrations is very good (as a consequence of termination by combination A' has been set equal to A'' for the bulk polymerization of styrene) thus the expected equality of A' and A'' with varying $[M_0]$ is realized, showing the constancy in the rate of initiation.

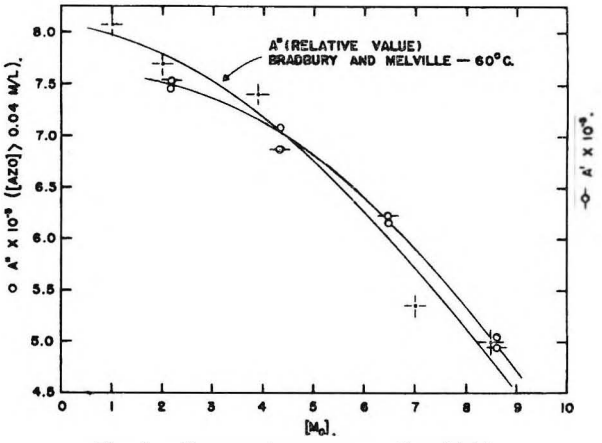

Fig. 2.—Styrene–benzene–azo I at 30.5°.

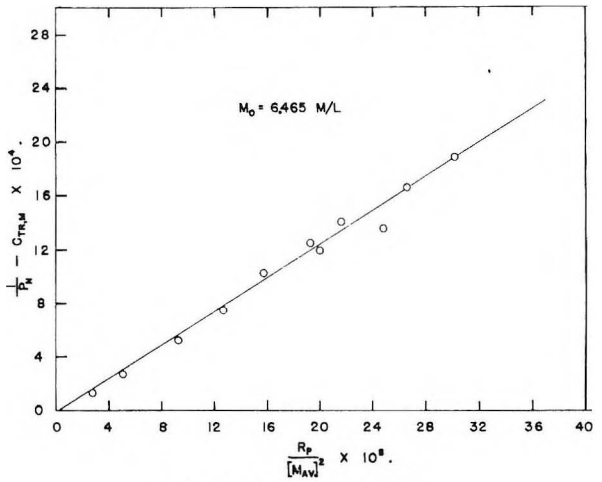

Fig. 3.—Styrene–benzene.

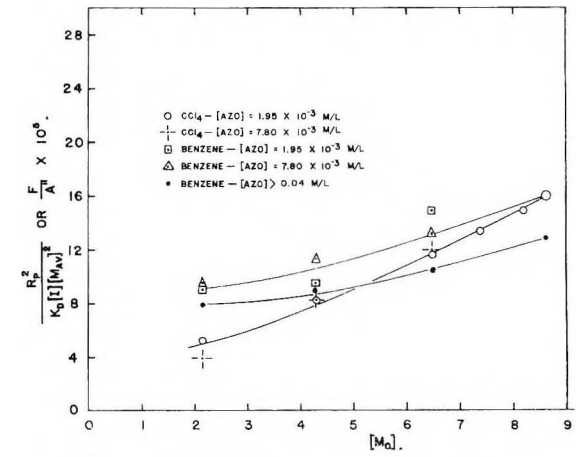

Fig. 4.—Solution polymerization of styrene.

The data of Bradbury and Melville[2] for the polymerization of styrene in benzene at 60° have also been plotted in Fig. 2. A comparison of their data at 60° with our results at 30.5° shows that the change in A'' (and hence A') at both temperatures is essentially the same.

In an attempt to fit the A' (P_n measurements) results to the equation of Burnett and Loan (equation 1) the equation $Y = A' + K_1([S]^2/[M_{av}]^2) + K_2([S]/[M_{av}])$ was set up and Y (our varying A') was plotted against [S]/[M]. Instead of the slope of this curve increasing with increasing S/M, the slope decreased. This effect is not understood. Possibly the relatively large value of the chain transfer to styrene term has particular significance in that even at low benzene concentrations the concentration of styrene transfer radicals becomes very important and initiation and the various termination steps due to these radicals should be included in the kinetic scheme.

To compare the effect of CCl_4 with that of benzene in the polymerization of styrene, f/A'' is plotted in Fig. 4 against $[M_0]$. The curves show that CCl_4 has a much greater effect than benzene in increasing the value of A'' on dilution. Unfortunately the A' values could not be checked by molecular weight measurements using the intrinsic viscosity equation.

The work on the methyl methacrylate solvent systems at low initiator concentration (1.95 and 7.80×10^{-3} mole/l.) showed that A'' or f/A'' is constant with monomer concentration for both benzene and CCl_4 dilution. No $\bar{P}_n$ data were obtained on polymethyl methacrylate samples.

BIMOLECULAR, UNIMOLECULAR AND SOLVENT CONTRIBUTIONS TO THE RATE OF HYDROLYSIS OF BENZOYL CHLORIDE, IN ACETONE–WATER MIXTURES[1]

BY M. J. KELLY[2] AND G. M. WATSON[2]

The Agricultural and Mechanical College of Texas, College Station, Texas

Received May 8, 1957

The rates of hydrolysis of benzoyl chloride were determined at high water concentrations in acetone–water mixtures. These results and those of previous investigators are correlated using reasonable assumptions. A change from a bimolecular to a unimolecular mechanism is indicated as water concentration increases. The reaction rate constants have been calculated for each process. The solvent contribution to the over-all process has been separated from these rate constants and the specific reaction rate constants, exclusive of solvent contributions, have been calculated. An equation is presented, expressing explicitly the magnitudes of the bimolecular, unimolecular and solvent contributions to the observed reaction rate constant.

Introduction

A study of the results and conclusions of previous investigators,[3-8] who have studied rates of hydrolysis of benzoyl chloride in mixed solvents, indicates a large body of evidence supporting the existence of two possible mechanisms. In the region of low water concentration rather conclusive evidence is available[3a,6] for the existence of a bimolecular mechanism. As the water concentration is increased, there is evidence of a concurrent unimolecular mechanism.[3a,6] At water concentrations of 50% w./w. and 0°, Gold[6] has satisfactorily shown that the contribution of the unimolecular mechanism to the over-all rate is of considerable magnitude.

A drastic increase in the rate of hydrolysis occurs at higher water concentrations; however, no satisfactory measurements were available corresponding to rate constants in excess of 3×10^{-3} sec.$^{-1}$. Apparently, the determinations of rate constants with sufficient precision under conditions where fast rates prevail has been a deterring factor to the logical extension of the investigations. The present investigation extends the results to higher water concentrations and temperatures, with corresponding rates measured increasing some fifty-fold over the higher rates previously measured. With the present measurements it has been possible to develop a more detailed basis showing changes in mechanism as well as solvent effects.

Experimental

Reagents.—The acetone used was Eimer and Amend C.P. grade. It was tested for moisture by a modified Karl Fisher method and was found to contain less than 0.3% water. Several comparative experiments were also performed using Eastman Spectro grade acetone (which had been distilled through a Snyder column from calcium chloride). Within the precision of the rate measurements no difference was noted. The benzoyl chloride used was J. T. Baker Analyzed Reagent grade. The experimentally determined freezing point was −0.7° as compared to a recorded value of −0.5°.

Apparatus. Thermometers.—The temperatures were measured with mercury-in-glass thermometers, graduated in tenths of a degree. The thermometers were calibrated over the temperature range used against a thermometer recently certified by the National Bureau of Standards. The temperature of the reacting mixture was regulated within ±0.02°.

The conductance of the reaction mixture was measured by a wheatstone bridge, preamplifier, phase-shifting network and oscilloscope. Using the technique described by Lamson[9] resistance balance, exclusive of reactance balance, could be obtained. The assembly was designed for rapid balancing. Removable platinum bead electrodes sealed in glass capillaries at a fixed distance were used. The electrodes were streamlined and positioned to allow rapid stirring of

(1) Presented before the Division of Physical and Inorganic Chemistry at 131st Meeting of the American Chemical Society, Miami, Florida, April 7–12, 1957.

(2) Oak Ridge National Laboratory, Oak Ridge Tenn.

(3) (a) B. L. Archer and R. F. Hudson, *J. Chem. Soc.*, 3259 (1950); (b) B. L. Archer, R. F. Hudson and J. E. Wardill, *ibid.*, 888 (1953).

(4) (a) G. Berger and S. C. G. Olivier, *Rec. trav. chim.*, **46**, 516 (1927); (b) G. E. K. Branch and A. C. Nixon, *J. Am. Chem. Soc.*, **58**, 2499 (1936).

(5) D. A. Brown and R. F. Hudson, *J. Chem. Soc.*, 3352 (1953).

(6) V. Gold, J. Hilton and E. G. Jefferson, *ibid.*, 2756 (1954).

(7) R. F. Hudson and J. E. Wardill, *ibid.*, 1729 (1950).

(8) J. F. Norris and H. H. Young, *J. Am. Chem. Soc.*, **57**, 1420 (1935).

(9) W. L. Lamson, *Rev. Sci. Inst.*, **9**, 272 (1938).

the solution without cavitation effects. The limiting precision of the conductance methods was ±0.1%.

A recorder with a chart speed of one inch per second was used as a linear time base when the rate of reaction was extremely rapid. Tapping a telegraph key caused a pip on the chart related to zero time by the distance traveled. Successive points could be taken easily within one second providing the proper bridge settings were previously chosen.

Procedure.—Large quantities of the desired acetone–water mixtures were prepared by weight. For a given experiment, a portion of one of the prepared acetone–water solutions was allowed to attain thermal equilibrium in the reaction vessel. A known weight of benzoyl chloride was injected by a syringe with excellent dispersion of the reactant into the rapidly stirred mixture. The conductance bridge had been pre-set to balance at a resistance value expected shortly after the reaction was started. The initial resistance and those following where balance would occur at convenient intervals had been previously recorded. The balancing times were recorded by tapping the telegraph key as balance occurred at the successive resistance settings.

Since the initial concentration of benzoyl chloride varied from 0.005 to 0.015 M, the reaction was pseudo first order. The experimentally determined specific reaction rate constants were obtained from the slopes of the plots of log $(l_\infty - l_t)$ *versus* time, where l_∞ and l_t were the observed conductances at "infinite" and at time, t, respectively. "Infinite time" was taken in excess of ten reaction half lives.

Results

The experimental results are summarized in Table I and are also presented graphically in Fig. 1. The results of previous investigators are also presented in Fig. 1. Measurements were not performed at water concentrations above 70% by weight because the rate of solution of the benzoyl chloride approached the rate of hydrolysis. The temperature dependence of the observed reaction rate constants determined in this and other investigations are shown in Fig. 2.

TABLE I

OBSERVED SPECIFIC REACTION RATE CONSTANTS FOR THE HYDROLYSIS OF BENZOYL CHLORIDE IN VARIOUS ACETONE–WATER MIXTURES

Temp., °C.	No. of determinations	Water concn. Wt. %	Water concn. Moles/l.	Obsd. $10^3\,k$, sec.$^{-1}$
0	3	70.0	37.7	2.97 ± 0.03
15	4	60.0	31.5	4.59 ± .06
	3	70.0	37.4	15.9 ± .1
25	4	40.0	19.9	1.65 ± .01
	3	50.0	25.4	4.31 ± .06
	4	60.0	31.2	12.4 ± .1
	4	70.0	37.0	42.8 ± .5
35	3	12.3	5.5	0.352 ± .008
	3	23.6	11.0	1.04 ± .01
	2	30.0	14.3	1.79 ± .00
	3	40.0	19.6	3.89 ± .06
	9	50.0	25.2	9.9 ± .1
	4	60.0	30.9	31.8 ± .8
	4	70.0	36.8	99.0 ± 2.2
40	3	70.0	36.7	160.0 ± 3
45	1	12.2	5.5	0.719
	4	18.2	8.3	1.34 ± 0.02
	5	30.0	14.2	3.93 ± .07
	4	40.0	19.4	9.31 ± .05
	4	50.0	24.9	25.8 ± .1
	4	60.0	30.6	77.8 ± .2
55	4	24.4	11.0	4.81 ± .05
	3	30.0	14.0	8.34 ± .07
	4	40.0	19.2	21.0 ± .2
	3	50.0	24.7	57.1 ± .2
	3	60.0	30.3	169 ± 6

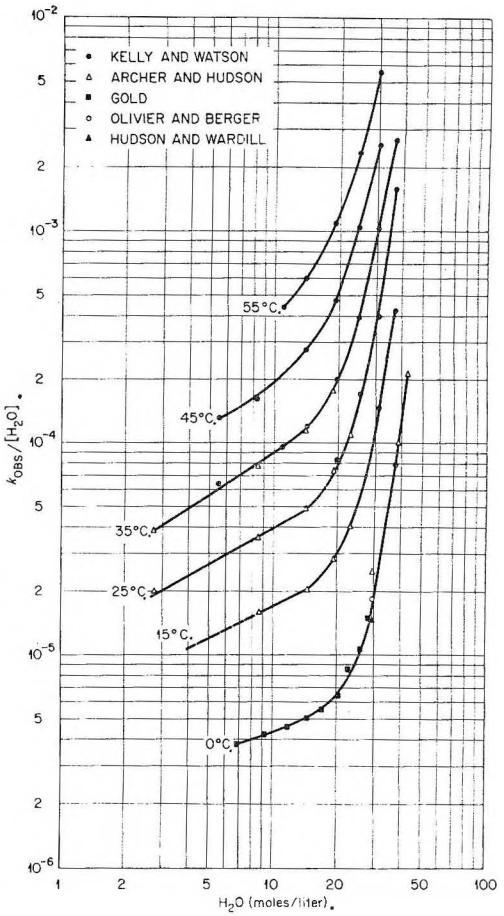

Fig. 1.—Observed reaction rate constants *vs.* water concentration.

Discussion of Results

It has been postulated[10] that the hydrolysis of benzoyl chloride can occur by either or both of two mechanisms. The first is a bimolecular reaction. The second is comprised by a rate-controlling ionization of the benzoyl chloride followed by rapid reaction with water. The type of mechanism prevailing depends on the properties of the solvent system.

Archer and Hudson,[3a] as well as Gold,[6] have suggested that curvature of the relation between log $k_{obs}/[H_2O]$ and $(D - 1)/(2D + 1)$ might indicate the change of mechanism in the hydrolysis reaction. This treatment follows from Kirkwood's theory of dipole solvation.[11] Gold[6] extrapolated the linear portion of the curve obtained at 0°. He found the difference between the experimental points and the extrapolation at 50% acetone–water to be in good agreement with the value of the unimolecular rate constant derived from competition experiments.

As an alternate approach which may also be used to demonstrate the change in mechanism let us look at Fig. 1. It is noted that abrupt changes in slope occur. Assuming that the linear portion of the

(10) E. D. Hughes, *Trans. Faraday Soc.*, **37**, 603 (1941).
(11) J. G. Kirkwood, *J. Chem. Phys.*, **2**, 351 (1934).

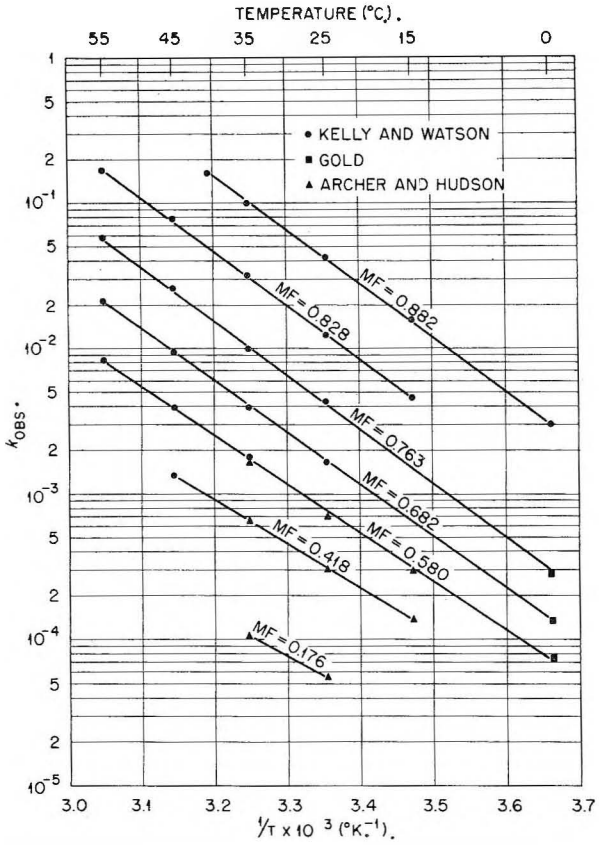

Fig. 2.—Temperature dependence of k_{obs} at various mole fractions of water.

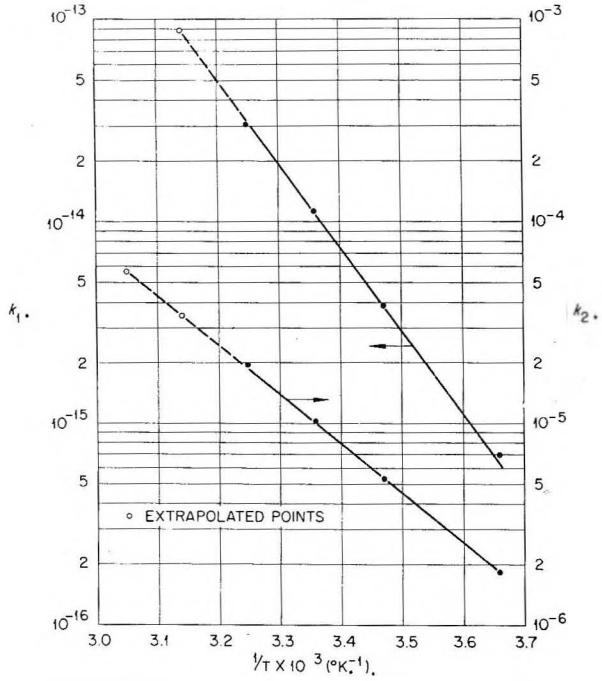

Fig. 3.—Temperature dependence of k_1 and k_2.

curve is representative of a single mechanism, presumably a bimolecular reaction, any departure from linearity might indicate that a unimolecular mechanism is responsible for part of the observed rate constant.

Since the data available in the present investigation are more extensive at higher water concentrations than those available to other workers, the particular shapes of the curves were better defined. Accordingly, it was possible to separate these curves into two concurrent components. One component was assumed to be the bimolecular mechanism and the other the unimolecular mechanism.

The assumed mechanisms which can occur simultaneously are

$$C_6H_5COCl + H_2O \rightleftharpoons [C_6H_5C(OH)_2Cl]^{\ddagger} \xrightarrow{k_2} \text{products, and} \quad (1)$$

$$C_6H_5COCl \xrightarrow[\text{slow}]{k_1} C_6H_5CO^+ + Cl^- \quad (2)$$

$$C_6H_5CO^+ + H_2O \xrightarrow{\text{fast}} C_6H_5COOH + H^+$$

The constants, k_2 and k_1, are defined as independent of solvent effects. Under the experimental conditions the corresponding constants, $\bar{k}_2$ and $\bar{k}_1$, include solvent effects. In order to obtain k_1 and k_2 from the solvent-dependent constants, the reasoning outlined below is used.

In pure acetone at infinite dilution

$$r_1 = k_2[C_6H_5COCl][H_2O]$$

and

$$r_2 = k_1[C_6H_5COCl]$$

With excess water present r_1 becomes

$$r_3 = \bar{k}_2[C_6H_5COCl][H_2O] = k_2[H_2O]^n[C_6H_5COCl][H_2O]$$

and r_2 becomes

$$r_4 = \bar{k}_1[C_6H_5COCl] = k_1[H_2O]^q[C_6H_5COCl]$$

By the above postulations

$$\bar{k}_2 = k_2[H_2O]^n \text{ and } \bar{k}_1 = k_1[H_2O]^q$$

In the experimental work a large excess of water is always present; so

$$r_{obs} = k_{obs}[C_6H_5COCl] = r_3 + r_4$$

or

$$k_{obs}[C_6H_5COCl] = k_2[H_2O]^n[C_6H_5COCl][H_2O] + k_1[H_2O]^q[C_6H_5COCl]$$

and

$$k_{obs} = k_2[H_2O]^n[H_2O] + k_1[H_2O]^q$$

where r_{obs} and k_{obs} are the observed rate and specific reaction rate constants, respectively. To be consistent with Fig. 1, the rate function is altered to

$$\frac{k_{obs}}{[H_2O]} = k_2[H_2O]^n + k_1[H_2O]^{q-1}$$

At low water concentrations, $k_1[H_2O]^{q-1}$ is assumed to be negligible since solvation is necessary to lower the activation energy of the ionization to accessible values.[12] Extending the linear portion of the curve, and assuming that the straight line represents the contribution of $k_2[H_2O]^n$, then $k_1[H_2O]^{q-1}$ may be determined by subtracting this curve from the experimental curve. Two components were thus obtained which were found to be linear within experimental error at 0, 15, 25 and 35°. Data at 45 and 55° were not available at sufficiently low water concentrations so that the unimolecular contribution could be neglected.

(12) C. K. Ingold, "Structure and Mechanism in Organic Chemistry," Cornell University Press, Ithaca, N. Y., 1953, Chap. 7.

This separation leaves the expressions $\bar{k}_2 = k_2 \cdot [H_2O]^n$ and $\bar{k}_1/[H_2O] = k_1[H_2O]^{q-1}$ which may be expressed as

$$\log \bar{k}_2 = \log k_2 + n \log [H_2O]$$

and

$$\log \frac{\bar{k}_1}{[H_2O]} = \log k_1 + (q - 1) \log [H_2O]$$

When $\log \bar{k}_2$ is plotted *versus* $\log [H_2O]$, n appears as the slope of the plotted function. Plots made at 0, 15, 25 and 35° indicate n to be linearly dependent on temperature and can be represented by the empirical function

$$n = 0.0092T - 2.14$$

where T is the absolute temperature.

Similar plots of $\log \bar{k}_1/[H_2O]$ *versus* $\log [H_2O]$ yield a value of $(q - 1)$ of 7 ± 0.5, which appears to be independent of temperature at 0, 15, 25 and 35°.

The reaction rate constants exclusive of solvent effects for both the bimolecular and unimolecular reactions can now be determined from

$$k_2 = \frac{\bar{k}_2}{[H_2O]^n}$$

and

$$k_1 = \frac{\bar{k}_1}{[H_2O]^q}$$

The values of k_2 and k_1 are found to be constant independent of water concentration within experimental error at constant temperature. The calculated values are listed in Table II.

The observed reaction rate constant may now be expressed by the equation

$$k_{obs} = k_2[H_2O]^{(0.0092T-1.14)} + k_1[H_2O]^8$$

The calculated values of k_{obs} from this equation agree with observed experimental data to within $\pm 10\%$ throughout the entire range of temperatures and concentrations studied in this investigation as well as with the published results of previous investigators. The values of k_1 and k_2 listed at 45 and 55° were obtained by extrapolation of the temperature dependence plots as shown in Fig. 3. The energy of activation of the bimolecular process corresponds to 11.0 kcal. This would represent the energy of activation in acetone at infinite dilution. This value is in excellent agreement with the value determined at zero mole fraction of water in acetone by calculation from the data shown in Fig. 2. The energy of activation of the unimolecular process is 20.0 kcal./mole. The minimum energy of activation for this process would correspond to the ionization energy of benzoyl chloride in pure acetone at infinite dilution. From electrostatic considerations of the solvent only, this value is calculated to be 10.5 kcal./mole at 50° which shows the above value is reasonable.

TABLE II

COEFFICIENTS DERIVED ASSUMING SEPARATE CONCURRENT PROCESSES

Temp., °C.	q	n	$10^6 k_2$	$10^{16} k_1$
0	8	0.370	1.81	6.90
15	8	.496	5.32	38.9
25	8	.613	10.3	112
35	8	.692	19.0	300
45	8	.786[a]	33.4[a]	880[a]
55	8	.877[a]	56.6[a]	2100[a]

E_1 = 20.0 kcal./mole E_2 = 11.0 kcal./mole

[a] Extrapolated from data at lower temperatures.

Acknowledgment.—The authors are grateful to Dr. B. A. Soldano for helpful discussions and suggestions made during preparation of this manuscript.

A KINETIC THEORY FOR THE OXIDATION OF CARBONIZED FILAMENTS

BY G. BLYHOLDER, J. S. BINFORD, JR., AND H. EYRING

Department of Chemistry, University of Utah

Received May 20, 1957

A considerable amount of data on the carbon-oxygen reaction has been collected from the literature, evaluated and expressed in such a manner that comparisons can be made. A theory is proposed which applies to the temperature range from 750 to 2000°. In particular, the unusual maximum in the Arrhenius plot is explained on a theoretical basis.

Introduction

The kinetics of the reactions of graphite with such oxidizing gases as oxygen, water and carbon dioxide have been studied intensively for a number of years.[1] In this paper we formulate a kinetic theory for the carbon–oxygen reaction which incorporates data found in the literature dealing with the oxidation of carbonized filaments. The various workers in this field often have emphasized the differences in the data which they gathered. We believe that these differences arise from differences in the extent of graphitization, crystallite size and impurities in the carbon filaments. Several unusual general features of the reaction rate have been found and require explanation. There is a low temperature region (750–1000°) in which the rate increases exponentially with an activation energy of from 25 to 30 kcal. mole^{-1} followed by an intermediate region (1000–1700°) in which the rate reaches a maximum value at from 1000 to 1400° and then decreases more or less exponentially. Beyond this region at least two investigators, Meyer[2] for O_2, H_2O and CO_2 and Sihvonen[3] for H_2O, observe another exponential increase in rate with an activation energy value of from 70 to 90 kcal. mole^{-1}.

(1) I. Langmuir, *J. Am. Chem. Soc.*, **37**, 1154 (1915).
(2) L. Meyer, *Trans. Faraday Soc.*, **34**, 1056 (1938).
(3) V. Sihvonen, *Ann. Acad. Sci. Fenn.*, **A41**, No. 3 (1934).

Description of Experiments

Following Langmuir's[1] example, a number of workers have used the hot filament technique. The method is to heat a carbon fiber, such as a lamp filament, by its own electrical resistance and expose it to the oxidizing gas. The temperature is observed by means of an optical pyrometer. In general no attempt was made to preheat the gases. The effect of a cold gas impinging on a hot filament might change a first-order reaction. This has been shown to be true in the case of the steam–carbon reaction below 1100° by Binford and Eyring.[4] The advantages of the hot filament technique are obvious. There is no necessity of constructing an elaborate furnace with the high temperature and high vacuum requirements needed for an adequate study of the kinetics.

The experiments fall into two categories. A flow system was employed by Meyer,[2,5,6] Duval[7] and Sihvonen[8–10] in which a gas stream was allowed to pass over the filament thus sweeping the reaction products out of the reaction chamber. Strickland-Constable[11,12] and Eucken[13] on the other hand used a static system in which the reaction chamber was evacuated and then a known amount of gas admitted. Rates were determined by following the pressure or by a gas analysis at the end of the run.

Properties of Graphite and Carbonized Filaments.—The workers whose data are reported here all had different sources for their filaments. Strickland-Constable states that his filaments were carbonized at 2000°. The history of the filaments used by other workers is unknown. Meyer cracked methane at 2000° on his filaments. Strickland-Constable did this a few times but said it made no appreciable difference in his data. Since the temperature reported by Strickland-Constable is much less than the 3000° used to make artificial graphite, his filaments would be expected to have had considerable amounts of hydrogen left in them. Other workers may reasonably be presumed to have filaments which were prepared in a similar fashion but with somewhat different starting materials, temperature of carbonization and times of carbonization. With these differences, the filaments used by different workers can be expected to have somewhat different surface areas, porosities, extent of graphitization, crystallite size and impurities. None of the workers reported Brunauer, Emmett, Teller surface area measurements. The differences in activation energy and order between the data for carbon filaments and those given for spectrographic graphite by Blyholder and Eyring[14] also lead to the conclusion that the carbonized filaments are not completely graphitized and contain enough impurities to affect the oxidation kinetics.

Ruff[15] recognized the wide variation in crystallinity of graphite resulting from differences in source or heat treatment. He proposed that the so-called "beta-graphite" is nothing but graphite with an imperfect crystallinity and that the crystal is perfected continuously as the temperature is increased. Recent data have been obtained which indicate a rapid increase in crystallization rate in the temperature region of 1000 to 1200°. Schaeffer, Smith and Polley[16] studying the effects of heat treatment on various commercial carbon blacks have made some interesting discoveries. The bulk resistivity of a sample passes through a minimum at 1000–1200° and increases at higher temperatures as the crystal is perfected. X-Ray diffraction data have shown that above 1000° the diffuse lines become sharper and new reflection angles appear, a clear indication of crystal growth. In addition to this, adsorption isotherms indicate a decrease in surface heterogeneity above 1000°.

Some mass spectrographic data on graphite sublimation have been published recently by Honig.[17] Activation energies for evaporation of negative fragments varying from C_1 to C_6 have been determined by heating a graphite filament with an electric current. The $\Delta E^{\ddagger}$ value found for C_1 is 177 ± 10 kcal. and values for the other species are of the same order of magnitude.

Kinetics of the Carbonized Filament-Oxygen Reaction.—The majority of the literature on the oxidation of carbon filaments deals with oxygen. The experimental data obtained by using the hot filament technique are found in Fig. 1. To provide a basis for comparison all rate constants have been converted to actual rates of disappearance of carbon at a chosen pressure. For the data chosen this pressure is 10 μ Hg. This value was chosen because it required the least amount of extrapolation for the data as a whole.

In order to describe the maximum in the Arrhenius plot followed by an exponential increase in the rate of oxidation, two different types of reaction sites are required. We shall refer to the sites as type 1 and type 2. The rate of reaction expressed in moles carbon cm.$^{-2}$ min.$^{-1}$ is the sum of the processes on the two types of sites as

$$v = k_{-1}\theta_1 fN + k_{-2}\theta_2(1 - f)N \qquad (1)$$

where

N = total no. of edge carbon atoms per cm.^{2}
f = fraction of edge carbon atoms which are type 1
$1 - f$ = fraction of edge carbon atoms which are type 2
θ_1 = fraction of type 1 sites which are covered by oxygen
θ_2 = fraction of type 2 sites which are covered by oxygen
k_{-1} = rate constant for type 1 surface oxide leaving surface
k_{-2} = rate constant for type 2 surface oxide leaving surface

Using the steady-state assumptions that $d\theta_1/dt = 0$ and $d\theta_2/dt = 0$ we obtain the familiar Langmuir isotherms

$$\theta_1 = \frac{k_1 p}{k_{-1} + k_1 p} \qquad (2)$$

$$\theta_2 = \frac{k_2 p}{k_{-2} + k_2 p} \qquad (3)$$

where

k_1 = rate constant for the formation of type 1 surface oxide
k_2 = rate constant for the formation of type 2 surface oxide
p = oxygen pressure

(4) J. S. Binford, Jr., and H. Eyring, THIS JOURNAL, 60, 486 (1956).
(5) L. Meyer, *Z. physk. Chem.*, 17B, 385 (1932).
(6) H. Martin and L. Meyer, *Z. Elektrochem.*, 41, 136 (1936).
(7) X. Duval, *J. Chem. Phys.*, 47, 339 (1950).
(8) V. Sihvonen, *Z. Elektrochem.*, 36, 806 (1930).
(9) V. Sihvonen, *ibid.*, 40, 456 (1934).
(10) V. Sihvonen, *Trans. Faraday Soc.*, 34, 1052 (1938).
(11) R. F. Strickland-Constable, *ibid.*, 43, 769 (1947).
(12) R. F. Strickland-Constable, *ibid.*, 40, 333 (1944).
(13) A. Eucken, *Z. ang.-Chem.*, 43, 986 (1930).
(14) G. Blyholder and H. Eyring, THIS JOURNAL, 61, 682 (1957).
(15) O. Ruff, *Trans. Faraday Soc.*, 34, 1022 (1938).
(16) W. D. Schaeffer, W. R. Smith and M. H. Polley, *Ind. Eng. Chem.*, 45, 1721 (1953).
(17) R. E. Honig, *J. Chem. Phys.*, 22, 126 (1954).

The first-order reaction observed from about 700 to 1600° is assigned to type 1 site. From Fig. 1 it is observed that the rate on this site passes through a maximum somewhere between 1000 and 1400°. At higher temperatures the rate, still first order, decreases rapidly until a temperature is reached where a zero-order reaction takes over and the rate again increases with a higher activation energy. Since this zero-order reaction cannot be occurring on type 1 sites, it is assigned to type 2 sites. The value of f controls the reaction in a manner shown by equation 1. To obtain an expression for f we make the steady state assumption that $df/dt = 0$ at any given temperature. Consider the following species to be present on the graphite surface

Species	No. of species per cm.
Total number type 1 sites	fN
Bare type 1 sites	$fN(1 - \theta_1)$
Covered type 1 sites	$fN\theta_1$
Bare type 2 sites	$(1 - f)N(1 - \theta_2)$
Covered type 2 sites	$(1 - f)N\theta_2$

and consider the following processes to occur on the surface: (1) type 1 surface oxide is formed; (2) type 2 surface oxide is formed; (3) type 1 surface oxide leaves the surface; (4) type 2 surface oxide leaves the surface; (5) bare type 1 sites are converted to type 2 sites with a first-order constant k_3; (6) type 1 surface oxide becomes a type 2 site. The first-order rate constant for this process is k_4; (7) type 2 sites are converted to type 1 sites at a rate which is proportional to the number of type 2 sites and to the rate of type 1 surface oxide leaving the surface. The rate of this process is given by $(1/\alpha)k_{-1}\theta_1(1 - f)N$ where $1/\alpha$ is the proportionality constant. The reasonableness of process 7 will be shown when the physical interpretation of the kinetics is discussed. These processes have an effect on $N(df/dt)$ as shown below

Process	Effect on $N\frac{df}{dt}$
1	None
2	None
3	$(n - 1)k_{-1}fN\theta_1$
4	$n'k_{-2}(1 - f)N\theta_2$
5	$-k_3fN(1 - \theta_1)$
6	$-k_4fN\theta_1$
7	$\frac{1}{\alpha}k_{-1}\theta_1(1 - f)N$

where

n = no. of type 1 sites produced when type 1 oxide leaves the surface
n' = no. of type 1 sites produced when type 2 oxide leaves the surface

Thus the steady-state condition which determines f is

$$N\frac{df}{dt} = (n - 1)k_{-1}fN\theta_1 + n'k_{-2}(1 - f)N\theta_2 - k_3fN(1 - \theta_1) - k_4fN\theta_1 + \frac{1}{\alpha}k_{-1}\theta_1(1 - f)N \quad (4)$$

$$\frac{df}{dt} = 0$$

The expression for f then, including all seven processes, is

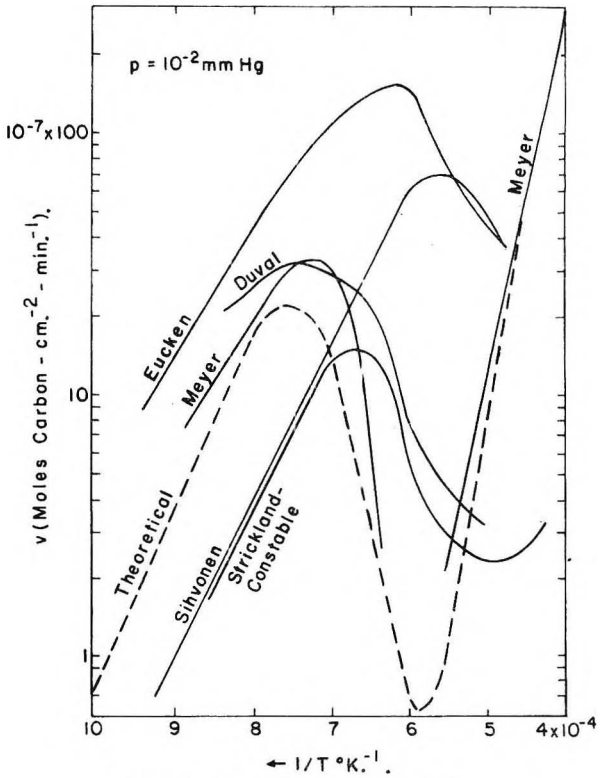

Fig. 1.—Carbon–oxygen reaction.

$$f = \frac{n'k_{-2}\theta_2 + \frac{1}{\alpha}k_{-1}\theta_1}{(1 - n)k_{-1}\theta_1 + n'k_{-2}\theta_2 + k_3(1 - \theta_1) + k_4\theta_1 + \frac{1}{\alpha}k_{-1}\theta_1} \quad (5)$$

The value 2 is arbitrarily chosen for n', the number of type 1 sites formed when a type 2 oxide leaves the surface. The calculations are actually quite insensitive to the value assigned to n'. It was found, however, that in order to give a satisfactory representation of the observed data, the quantity n had to be given a value of 1. The significance of this is that when a type 1 site burns it exposes a new type 1 site. Since this type 1 reaction is always observed to be first order we may see from equation 2 that we must have $k_{-1} >> k_1p$, and therefore $\theta_1 = k_1p/k_{-1}$, a quantity which is very much less than 1. Similarly since the type 2 reaction is observed to be zero order, this means that $k_{-2} \ll k_2p$ and equation 3 gives $\theta_2 = 1$. This leads to the expression for the rate of reaction

$$v = k_1fNp + k_{-2}(1 - f)N \quad (1)'$$

and f becomes

$$\frac{n'k_{-2} + \frac{1}{\alpha}k_1p}{n'k_{-2} + k_3 + \frac{k_4k_1p}{k_{-1}} + \frac{1}{\alpha}k_1p} \quad (5)'$$

In the above development, the maximum in the Arrhenius plot is achieved by decreasing the value of f. The value of f decreases because type 1 sites are converted to type 2 sites by processes 5 and 6. Processes 5 and 6 are then competitive ways of doing the same thing and so either one or the other will dominate its competitor. In order for f to have a steady-state value it is necessary to have the re-

verse process of a type 2 site yielding a type 1 site. Processes 4 and 7 are competitive ways of doing this. Again one will be expected to dominate the other. The fact that f must be independent of the pressure limits the ways in which processes 4 through 7 may be combined. A consideration of equation 5 reveals that if f is to be pressure independent two cases are possible.

Case I

$$n'k_{-2} \gg \frac{1}{\alpha} k_1 p \quad \text{and} \quad k_3 \gg \frac{k_4 k_1 p}{k_{-1}}$$

Here process 5 dominates process 6 and 4 dominates 7. The expression for f in equation 5′ then simplifies to

$$f = \frac{n'k_{-2}}{n'k_{-2} + k_3} = \frac{1}{1 + \dfrac{k_3}{n'k_{-2}}}$$

Case II

$$\frac{1}{\alpha} k_1 p \gg n'k_{-2} \quad \text{and} \quad \frac{k_4 k_1 p}{k_{-1}} \gg k_3$$

Here we merely reverse the conditions of case I with a corresponding reversal in the dominant processes. Examination of equation 5′ now shows

$$f = \frac{\dfrac{1}{\alpha} k_1 p}{\dfrac{k_4 k_1 p}{k_{-1}} + \dfrac{1}{\alpha} k_1 p}$$

$$f = \frac{1}{\alpha \dfrac{k_4}{k_{-1}} + 1}$$

Since there is no way of calculating these constants independently we combine them into one constant

$$k = \alpha \frac{k_4}{k_{-1}}$$

and write

$$f = \frac{1}{1 + k}$$

We note that both case I and case II lead to the same type of expression for f.

One may get an idea of the relative sizes of f at various temperatures by extrapolating the low temperature first-order rate curve in Fig. 1 linearly beyond the temperature where the rate goes through a maximum. The ratio of the actual rate to the extrapolated rate is a measure of the value of f at the temperature in question. One can immediately see that f decreases very rapidly with temperature and at temperatures 100° or more above the temperature of the maximum rate the quantity $f = 1/(1 + k)$ may be replaced by $f = 1/k$ in case II. The temperature coefficient of k may be determined by examining the rate expression for the type 1 reaction given by the first term in equation 1′.

$$v = k_1 f N p = \frac{C_1 N p e^{-\Delta H_1^{\ddagger}/RT}}{C e^{-\Delta H^{\ddagger}/RT}}$$

or

$$v = \frac{C_1 N p}{C} e^{-(\Delta H_1^{\ddagger} - \Delta H^{\ddagger})/R}$$

where

$\Delta H^{\ddagger}$ = over-all activation energy for k
$\Delta H_1^{\ddagger} - \Delta H^{\ddagger}$ = effective heat of activation in the range of decreasing rate
C_1, C = constants that have negligible temperature dependence

We choose -65 kca. as a typical value of $\Delta H_1^{\ddagger} - \Delta H^{\ddagger}$. A reasonable value for $\Delta H_1^{\ddagger}$ is 30 kcal. leaving a value of 95 kca.. for $\Delta H^{\ddagger}$.

Similarly for case I we have

$$f = \frac{1}{1 + \dfrac{k_3}{n'k_{-2}}}$$

reducing to

$$f = n'k_{-2}/k_3$$

Thus

$$v = k_1 f N p = C_1 N p e^{-\Delta H_1^{\ddagger}/RT} \frac{n' C_{-2} e^{-\Delta H_{-2}^{\ddagger}/RT}}{C_3 e^{-\Delta H_3^{\ddagger}/RT}}$$

$$v = \frac{C_1 C_{-2}}{C_3} N p n' e^{-(\Delta H_1^{\ddagger} + \Delta H_{-2}^{\ddagger} - \Delta H_3^{\ddagger})/RT}$$

where

$\Delta H_{-2}^{\ddagger}$ = activation energy for type 2 oxide leaving the surface
$\Delta H_3^{\ddagger}$ = activation energy for surface rearrangement of carbon atoms
C_{-2}, C_3 = constants with negligible temperature dependence

A reasonable value for $\Delta H_{-2}^{\ddagger}$ is 80 kcal. and since $\Delta H_1^{\ddagger} + \Delta H_{-2}^{\ddagger} - \Delta H_3^{\ddagger} = -65$ kcal. we have $\Delta H_3^{\ddagger} = 175$ kcal. The choice between case I and II is arbitrary. In light of the kinetic data of Honig[17] for sublimation of graphite, however, it appears that 175 kcal. is at least of the correct order of magnitude for the migration of carbon fragments over the graphite surface. We will give below the calculations for case I.

At 1200°K. the velocity of the reaction is given by

$$v = k_1 f N p$$

We take f to be unity and choose an energy value of 30 kcal. for $\Delta H_1^{\ddagger}$. Expressing p in mm. and applying a surface roughness factor of 100 to the experimental data in Fig. 1 we obtain

$$k_1 N = 0.27 e^{-30,000/2T}$$

At 2300°K. the rate of reaction, being primarily on type 2 site, is given by

$$v = k_{-2}(1 - f)N$$

At these high temperatures $(1 - f)$ may be replaced by 1 which gives

$$v = k_{-2} N$$

Choosing $\Delta H_{-2}^{\ddagger} = 80$ kcal. and applying a roughness factor of 100 to the experimental data we obtain

$$k_{-2} N = 3.7 e^{-80,000/2T}$$

The roughness factor of 100 is arbitrarily chosen.

The value taken for N in the rate equation can vary slightly as a result of variation in the extent of graphitization, but a value of 10^{15} atoms cm.$^{-2}$ should be of the right order of magnitude or

$$N = 1.7 \times 10^{-9} \text{ moles/cm.}^2$$

We have then the rate constant values

$$k_1 = 1.6 \times 10^8 e^{-30,000/2T} \text{ min.}^{-1} \text{ mm. Hg}^{-1}$$
$$k_{-2} = 2.2 \times 10^9 e^{-80,000/2T} \text{ min.}^{-1}$$

We now have for k_3 the expression

$$k_3 = C_3 e^{-176,000/2T}$$

To establish the value of C_3 we choose a rate for experimental data at 1400°K. Here the value of f is seen to be about 0.3 and this leads to the expression for k_3

$$k_3 = 4.2 \times 10^{24} e^{-176,000/2T} \text{ min.}^{-1}$$

The theoretical curve is given by substituting these values into equation 1′ at $p = 10^{-2}$ mm.

Discussion

Up to this point we have developed a mathematical theory with little regard for the physical nature of the sites involved. We shall now present a physical model for these sites. Due to the speculative nature of the reaction details, this model will be pursued only to its broad outline. From the information presented in the section entitled "Properties of Graphite and Carbonized Filament," we conclude that the carbonized filaments whose oxidation is discussed here are not graphite but are a partially graphitized hydrocarbon material. In this state the filaments may be roughly regarded as graphite with hydrogen as an impurity disrupting the graphitic structure throughout the entire filament. Type I sites are on this hydrocarbon material. Type 2 sites are the graphite lattice undisturbed by hydrogen or other impurities. This view is supported by the similarity in activation energy and order of reaction between the oxidation of type 2 sites and the oxidation of pure graphite reported by Blyholder and Eyring.[14] Process 1 has a disrupted lattice which directly or indirectly involves hydrogen in the activated complex for the formation of type I surface oxide. Process 2, which is the formation of type 2 surface oxide, involves only graphitic carbon and oxygen in its activated complex. Processes 3 and 4 are similar except that, whereas in process 3 the surface oxide breaks loose from a hydrocarbon material, in process 4 the oxygen must remove a carbon atom from a graphite lattice undisturbed except for the surface oxide. Apparently process 4 is much more difficult than process 3. Process 5 is the graphitization process in which hydrogen leaves the material and the carbon atoms organize themselves into a graphite structure. Process 6 results from the oxygen in type 1 surface oxide breaking loose from the surface with hydrogen rather than carbon, thus leaving unhydrogenated carbon which can form a graphitic structure characteristic of type 2 sites. In a partially hydrogenated graphite lattice there will be some type 1 and some type 2 sites. Due to the decomposition of the type 1 oxide the lattice will be disrupted to the extent that the type 2 sites, which are dependent upon a stable graphite lattice, will become type 1 sites. This is process 7. The α in the proportionality constant of process 7 is by this model simply the average number of type 1 sites which must be removed to convert a type 2 site to a type 1 site. All impurities including lattice imperfections will play the role that we have outlined for hydrogen. Hydrogen has been specifically cited here because of its predominance over other impurities in carbonized filament.

Acknowledgment.—The authors gratefully acknowledge support from the U. S. Air Force under contract No. AF 22(038)20839.

BURNING-RATE STUDIES. PART 6. EFFECT OF CHEMICAL COMPOSITION ON THE CONSUMPTION RATE OF VARIOUS NITRIC ACID SYSTEMS

BY A. GREENVILLE WHITTAKER

Contribution from the Chemistry Division, Research Department, U. S. Naval Ordnance Test Station, China Lake, California

Received June 17, 1957

Each of the compounds nitromethane, nitroethane, and 2-nitropropane in stoichiometric mixture with 99% nitric acid was previously shown to give a low pressure step in its consumption rate curve. This study showed that the addition of small amounts of potassium nitrate or nitrogen tetroxide completely removed the low pressure step or greatly diminished it. Addition of nitrogen pentoxide increased the low pressure step and moved it to lower pressure. The effect of addition of small amounts of *gem*-dinitropropane was also studied and found to produce results similar to those given by nitrogen tetroxide addition. All results are discussed in terms of a previously proposed hypothesis which describes the observed effects in terms of chemical reactions taking place in the liquid phase preheat zone.

Introduction

Previous studies on the combustion of nitroparaffin–99% nitric acid systems showed that they gave a low pressure step in their consumption rate curves.[1] This phenomenon was discussed in terms of a hypothesis which described the phenomenon in terms of a set of reactions occurring in the liquid phase preheat zone. According to the hypothesis, addition of NO_3^- or N_2O_4 to these systems should vitiate or greatly diminish the low pressure step, and the addition of NO_2^+ should increase the low pressure step and move it to lower pressure. These predicted qualitative effects were investigated by the addition of KNO_3, N_2O_4 and N_2O_5 to these systems and observing the results. *gem*-Dinitropropane was shown to be a probable liquid phase reaction intermediate in the system 2-nitropropane–nitric acid.[1] It was found that this compound had a marked effect on the consumption rate curve of this system. Its effect on the consumption rate

(1) A. G. Whittaker and H. Williams, THIS JOURNAL, **61**, 388 (1957).

curves of the other nitroparaffin systems were studied also. All the results appear to be interpretable in terms of the proposed hypothetical mechanism of the low pressure step.

Materials.—The preparation and purity of the HNO_3, nitromethane, nitroethane, 2-nitropropane and N_2O_4 are described in previous publications.[2,3] All the systems discussed below were prepared with 99% nitric acid. The KNO_3 was reagent grade material which was dried *in vacuo* in the presence of P_2O_5. *gem*-Dinitropropane was obtained as a technical grade material from commercial solvents. It was purified by slow vacuum sublimation in the presence of P_2O_5. Its melting point was found to be 53.7 to 54.3°. The literature value is given as 53.0°. The N_2O_5 was prepared by oxidizing N_2O_4 with an excess of ozone. The product was a dry white powder which decomposed slowly at room temperature. Because of this, these mixes were made up and burned as quickly as possible in order to minimize the effects of decomposition.

Apparatus and Procedure.—The apparatus and procedure used to make the consumption rate measurements was the same as that described previously.[1] All systems were made in such proportions as to be exactly stoichiometric to CO_2, H_2O and N_2. No additional fuel was added to the systems containing KNO_3 because it was not considered to take part in the combustion reactions. This assumption was supported by the fact that X-ray diffraction studies showed that the KNO_3 remaining in the bottom of the combustion tube was unchanged by the combustion of the mixture. No surface corrections were applied to any of the burning rate measurements. This was somewhat unfortunate, because it was found near the end of the study that some of the systems burned with an unusually deep meniscus. Consequently, their consumption rates are not directly comparable with systems that burned with a normal meniscus shape. Fortuitously the effects under investigation did not depend on the absolute value of the consumption rate; hence, the absence of surface corrections is not critical. In general the consumption rate at any particular pressure is not particularly important; however, the consumption rate curve is of primary importance. Although no consumption rate curves are shown they will be discussed frequently and should be interpreted as the graph that results when the log of the consumption-rate is plotted against the log of the pressure. Thus, if the consumption rate curve is said to be linear it means that the data will give a straight line on this log–log plot.

Results and Discussion

The pressure range covered for the various systems given in the following tables was determined by two features. The lowest pressure reported was at or near the lowest pressure at which ignition and sustained combustion could be obtained. The highest pressure for a given system was the pressure at which the system went into turbulent combustion. This means that only the smooth burning portion of the consumption rate curves was considered. Consumption rate data obtained on the various systems studied are given in Tables I–IV.

An hypothetical mechanism was proposed previously which can be used to describe the low pressure step in terms of reactions assumed to be occurring within the liquid phase preheat zone.[1] The essential features of the mechanism are recapitulated briefly as

$$2HNO_3 \rightleftharpoons N_2O_5 + H_2O \quad (1)$$

$$N_2O_5 \rightleftharpoons NO_2^+ + NO_3^- \quad (2)$$

$$N_2O_5 \longrightarrow N_2O_4 + {}^1/_2O_2 \quad (3)$$

$$N_2O_4 \rightleftharpoons NO^+ + NO_3^- \quad (4)$$

$$NO_2^+ + RNO_2 \longrightarrow \text{Products} + Q \quad (5)$$

(2) A. G. Whittaker, H. Williams and P. M. Rust, *ibid.*, **60**, 904 (1956).

(3) A. G. Whittaker, R. W. Sprague, S. Skolnik and G. B. L. Smith, *J. Am. Chem. Soc.*, **74**, 4794 (1952).

TABLE I

CONSUMPTION RATE OF SYSTEMS CONTAINING NITROGEN PENTOXIDE

Pressure, atm.	Consumption rate (cm./sec.) Nitromethane HNO_3	Nitromethane $N_2O_4 + HNO_3$[a]	2-Nitropropane HNO_3	2-Nitropropane $N_2O_4 + HNO_3$[a]	3rd column
10.5	...	...	...	...	0.119
11.2	...	0.080	...	...	.129
11.8	...	...	...	...	.147
12.5	...	.089	...	...	...
13.2	...	...	...	...	.156
14.6	0.086	.097	...	0.142	.603
18.0	.105	.119	0.181	.201	.724
21.4	.141	.385	.236	.772	.852
24.8	.188	.454	.823	...	1.16
28.2	.215	.472	.890	.966	1.55[b]
31.6	.236	.505	...	...	
35.0	.277	.519	1.02	1.11	
38.4	.355				
41.8	.464	.600	1.08	1.40[b]	
48.6	.524	1.44[b]	1.09		
55.4	.567				
62.2	.598[b]		1.46[b]		

	3rd column		5th column	6th column
CH_3NO_2	65.06	$CH_3CHNO_2CH_3$	24.98	25.75
HNO_3	28.78	HNO_3	70.11	66.84
N_2O_5	5.15	N_2O_5	2.41	5.04
H_2O	1.02	H_2O	2.48	2.37

[a] Composition of mixtures, mole %.
[b] Turbulent combustion.

TABLE II

CONSUMPTION RATE OF NITROPARAFFINS WITH N_2O_4 OR N_2O_4 + (99%) HNO_3 AS OXIDIZERS

Pressure, atm.	Consumption rate (cm./sec.) Nitromethane $N_2O_4 + HNO_3$[a]	Nitroethane N_2O_4	Nitroethane $N_2O_4 + HNO_3$[a]		2-Nitropropane N_2O_4	2-Nitropropane $N_2O_4 + HNO_3$[a]
4.4	...	...	...	...	0.077	...
7.8	...	0.108	...	...	.125	...
9.5	0.062	...	...	...	...	...
11.2	.069	.151	0 068	0.068	.187	0.100
14.6	.092	.202	084	.086	.248	.135
18.0	...	.256	.109	.112	.311	...
21.4	.149	.299	.138	.167	1.94[b]	.212
24.8	...	.336	.207	.217	...	...
28.2	.205	1.96[b]	.295	.278	...	.323
31.6	...	...	.429	...	...	...
35.0	.258	...	.446	.405	...	.397
41.8	.321	...	.503	.484	...	.558
48.6	.377	...	.571	.524	...	.645
52.0	...	...	...	.584	...	.664
55.4	.471	...	.613	1.76[b]	...	1.75[b]
62.2	.578	...	1.88[b]	...	...	...
69.0	1.81[b]					

	2nd column		4th column	5th column		7th column
CH_3NO_2	62.37	$C_2H_5NO_2$	35.39	35.49	$CH_3CHNO_2CH_3$	24.70
HNO_3	33.84	HNO_3	59.84	58.91	HNO_3	70.07
N_2O_4	2.59	N_2O_4	2.65	3.55	N_2O_4	2.76
H_2O	1.20	H_2O	2.12	2.05	H_2O	2.47

[a] Composition mixtures, mole %.
[b] Turbulent combustion.

In the liquid phase the over-all reactions are assumed to take place. At the foot of the low pressure step the combustion is assumed to be controlled entirely by heat feedback from the fast vapor phase

TABLE III

EFFECT OF POTASSIUM NITRATE ON THE CONSUMPTION RATE OF NITROPARAFFIN-NITRIC ACID SYSTEMS

Pressure, atm.	Consumption rate (cm./sec.) Nitromethane[a]	Nitroethane[a]	2-Nitropropane[a]
7.8	0.085	...	0.069[c]
11.2	.139	0.130	.138
14.6	.200	.162	.195
18.0	.206	...	...
21.4	.259	.270	.299
28.2	.300	.381	.436
35.0	.341	.547	.571
41.8	.382	.627	.677
48.6	.438	.704	1.27[b]
55.4	.511	1.59[b]	
62.2	1.64[b]		

[a] Composition of mixtures, mole %.

	2nd column		3rd column		4th column
CH_3NO_2	60.11	$C_2H_5NO_2$	33.02	$CH_3CHNO_2CH_3$	23.71
HNO_3	36 11	HNO_3	62.24	HNO_3	71.18
KNO_3	2.50	KNO_3	2.53	KNO_3	2.61
H_2O	1.28	H_2O	2.20	H_2O	2.61

[b] Turbulent combustion. [c] Flameless combustion.

TABLE IV

CONSUMPTION RATES OF NITRIC ACID (99%) SYSTEMS CONTAINING *gem*-DINITROPROPANE

Pressure, atm.	Consumption rate (cm./sec.) Nitroethane, *gem*-dinitropropane, HNO_3[a]	2-Nitropropane, *gem*-dinitropropane, HNO_3[a]	*gem*-Dinitropropane HNO_3	*gem*-Dinitropropane $N_2O_4 + HNO_3$[a]
7.8	...	...	...	0.080
11.2	...	...	...	.096
12.9	...	...	0.115	...
14.6	0.067	0.100	.128[c]	.125
16.3	...	...	.175	...
18.0	...	...	.194	.142[c]
19.7	...	...	...	.221
21.4	.115	.154	.234	.237
28.2	.199	.225	.314	.319
35.0	.255	.323	.394	.399
38.4	...	...	...	.448
41.8	.337	.458	.480	1.44[b]
45.2	...	.524	1.88[b]	
48.6	.412	.847		
55.4	.494	.907		
62.2	.591	1.41[b]		
69.0	.691			
75.8	.722			
82.6	1.68[b]			

[a] Composition of mixtures, mole %.

CH_3NO_2	31.99	$CH_3CHNO_2CH_3$	22.26	$(CH_3)_2C(NO_2)_2$	33.47
HNO_3	62.93	HNO_3	72.48	HNO_3	61.12
$(CH_3)_2C(NO_2)_2$	2.87	$(CH_3)_2C(NO_2)_2$	2.69	N_2O_4	3.24
H_2O	2.21	H_2O	2.57	H_2O	2.17

[b] Turbulent combustion. [c] System burned flameless at and below this pressure.

reactions. This heat is used largely to evaporate liquid. Some of the heat decomposes nitric acid and produces N_2O_4 in the preheat zone according to reactions 1 and 3. The N_2O_4 dissociates according to reaction 4 to give NO_3^- which represses reaction 2 and causes the NO_2^+ concentration to be very small. This in turn limits reaction 5. As the rate increased due to increase in pressure the HNO_3 decomposition decreases because the dwell time in the preheat zone decreases and the surface temperature remains essentially constant.[4] This causes the N_2O_4 concentration to decrease and allows reaction 5 to become more prominent. Thus, a heat source appears within the liquid phase preheat zone. It is this extra production of heat within the preheat zone that caused the low pressure step to appear. As the rate increased further, all reactions in the preheat zone continue to be repressed; consequently, reaction 5 does not cause the rate to increase without limit. A leveling off of the consumption rate results which produces the top part of the step. This mechanism allows some qualitative predictions to be made concerning the effect on the low pressure step of compounds that change the concentration of NO_2^+, NO_3^- and N_2O_4. The addition of N_2O_5 would be expected to increase the NO_2^+ concentration according to reaction 2, and allow reaction 5 to become more prominent. It would be expected to show its effects as a lower rate and probably cause the rate to be somewhat enhanced everywhere. Qualitatively this is found to be the case and it may be regarded as a continuation of the study of the effect of decreasing the water content of the system.[1] In the nitromethane system the data in Table I show that the step occurs at a much lower pressure when N_2O_5 is added, and that the intensity of the step is greatly enhanced. In the 2-nitropropane system the step occurs at lower pressure with the addition of N_2O_5 but the intensity of the step is not changed much. It may be that these effects reflect the fact that the NO_2^+ attack would be on a primary hydrogen in the case of nitromethane and on a more reactive tertiary hydrogen in the case of 2-nitropropane. This may indicate that almost the maximum amount of reaction 5 takes place between 2-nitropropane and 99% nitric acid. Hence, the addition of N_2O_5 does not increase the extent of reaction 5 as much in this system. It is also interesting to note that the rate in the foot of the step is enhanced by the addition of N_2O_5 where reaction 5 is normally assumed to be negligible. This coupled with the fact that the low pressure step starts at a lower rate as the N_2O_5 content increases, supports the expectation that the addition of NO_2^+ ion increases the amount of reaction 5 taking place at all rates.

According to reaction 4, the addition of N_2O_4 to these systems will increase the nitrate ion concentration which in turn should decrease the NO_2^+ concentration by reversing reaction 2. This would have the effect of repressing reaction 5 which causes the low pressure step. The data in Table II show that qualitatively the results are compatible with this prediction in that the addition of N_2O_4 diminishes or vitiates the step. There was some possibility that NO^+ (produced in reaction 4) could be a reactive species associated with the production of the low pressure step. If this were true then the addition of N_2O_4 should enhance the step just as N_2O_5 did. Since this did not happen, the possibility that NO^+ is an important species is ruled out. The nitroethane system was somewhat "anomalous" in that the step did not disappear completely by addi-

(4) D. L. Hildenbrand and A. G. Whittaker, THIS JOURNAL, 69, 1024 (1965).

tion of N_2O_4 and the rates at the foot of the step were enhanced. This effect could result from the fact that reaction 5 may be significantly different in the case of attack on secondary hydrogens as compared to attack on primary or tertiary hydrogens as in nitromethane or 2-nitropropane, respectively. It is also possible that this system burns with a meniscus somewhat deeper than normal. This "anomalous" result of enhanced rates in the low pressure region was also noted in the case of water addition.[1] Again it could be due to a somewhat different reaction mechanism of the secondary hydrogens, or an abnormally deep meniscus. Since no high speed photographs were taken there is no direct evidence that the meniscus was abnormal. Moreover, the addition of water or N_2O_4 to the other systems caused no detectable abnormalities in meniscus shape. Since the step was not removed completely by the addition of fairly large amounts of N_2O_4, it is probable that the difference in reaction mechanism of the secondary hydrogens is the cause of the "anomalous" behavior. The data on the N_2O_4–nitroethane and 2-nitropropane systems shown in Table II indicate that with this oxidizer, the systems burned considerably faster than they do with nitric acid. Consequently, the effect of adding N_2O_4 to the nitric acid systems cannot be just a simple additive effect as if the two systems were burning independently. Indeed the N_2O_4 has an over-all depressing effect on the burning-rate of the nitric acid systems. Therefore, it must be involved in some reactions which are associated with nitric acid.

According to the above mechanism KNO_3 should have the same effect as the addition of N_2O_4 and for essentially the same reason. The data in Table III show that qualitatively the predicted results are obtained. Potassium nitrate has an advantage, in that it has a very low vapor pressure at the surface temperature of about 200°. Consequently, it is highly probable that it suppresses the low pressure step by affecting reactions in the liquid phase only. This then definitely locates the origin of the low pressure step as being due to liquid phase reactions. Unfortunately, the results are not as clean cut as desired because the consumption-rate curves are distorted somewhat by the unusual behavior of the systems containing KNO_3. Although it is evident that KNO_3 vitiates the low pressure step it is not clear what concentration is actually effective, because the concentration in the surface does not remain at the initial value. The low vapor pressure of the KNO_3 causes it to accumulate in the surface. However, some steady-state concentration is reached in each case because the excess either crystallizes out (as in the nitromethane system) or hangs up on the tube walls.

For the systems containing KNO_3 the consumption rate curves are not an extension of the low pressure foot of the step as might be expected. The consumption rate curves have about the same slope as the low pressure foot of the corresponding steps, but the rates are uniformly higher. Much of the unusual behavior of these systems was probably related to the fact that the KNO_3 caused the meniscus to be much deeper because the liquid tended to "hang up" on the tube walls. This extra burning surface caused the consumption rates to be significantly higher than the true burning rates. The depth of the meniscus appeared to be a compromise between the true burning rate, the viscous flow of the liquid, and the thermal gradients in the glass tube near the liquid surface. Since no high speed photographs were taken of these systems no quantitative surface corrections can be made. In the nitromethane system direct observation showed that the meniscus depth was a function of pressure. It appeared to go through a maximum at a consumption rate of about 0.2 cm./sec. Because of this the consumption rate curve has a slight downward curvature over the range 7.8 to 35 atmospheres. Above this pressure the depth was about constant, but larger than normal. A similar situation held for the nitroethane system except that the meniscus was generally much deeper than that of the nitromethane system and the maximum meniscus depth occurred at a rate of about 0.6 cm./sec. The 2-nitropropane system showed a smaller enhanced meniscus depth and it did not appear to go through a maximum; hence, its consumption rate curve is linear and displaced slightly to higher rates than the low pressure foot of its corresponding step.

The liquid "hang up" on the tube walls made it possible for significant amounts of KNO_3 to crystallize on the glass. This material became molten as the flame moved down the tube and resulted in a ring of molten KNO_3 following the burning surface as it progressed down the tube. This ring stayed approximately $^1/_8$" above the surface. After all the material had burned the molten KNO_3 solidified as a single mass just above the bottom of the tube. In the nitromethane system the KNO_3 crystallized at the interface between the preheat zone and the cool liquid. The crystals settled to the bottom of the tube, well ahead of the burning surface. In this case the amount of molten KNO_3 following the burning surface down the tube was very small. In the nitroethane and 2-nitropropane systems, the KNO_3 was sufficiently soluble due to the higher weight fraction of nitric acid in the systems, that it did not crystallize at the preheat zone-cool liquid interface. In these systems, the amount of molten KNO_3 just above the burning surface became rather large near the end of the combustion.

gem-Dinitropropane was shown to be a possible product[4] in reaction 5. In preliminary experiments it was added to the 2-nitropropane–97% nitric acid system. In this case it was found to be a slight inhibitor to the combustion process. It was shown that *gem*-dinitropropane starts to decompose rather rapidly at about 183°.[5] Unlike 2-nitropropane, one of the products of decomposition of *gem*-dinitropropane is N_2O_4; consequently, *gem*-dinitropropane can act as a source of N_2O_4. Hence, it would be expected to vitiate the low pressure step. The data in Table IV indicate that this result was obtained. Since the surface temperature of these systems is probably in the neighborhood of 200°, it is clear that this decomposition takes place in the last few microns of the preheat zone. This prob-

(5) A. G. Whittaker, *Rev. Sci. Inst.*, **28**, 360 (1957).

ably results in a rather high concentration of N_2O_4 right near the burning surface. In this way *gem*-dinitropropane can concentrate N_2O_4 in the region in which it is most effective in suppressing reaction 5. Previous studies showed that *gem*-dinitropropane is formed in the reaction between 2-nitropropane and nitric acid at about 160°.[1] Consequently, in the 2-nitropropane–nitric acid system *gem*-dinitropropane can be formed deep in the preheat zone and then decompose again right near the top of the preheat zone where the temperature is above 180°. This means that the system 2-nitropropane–nitric acid is somewhat unique in that one of the products of reaction 5 is a material which tends to inhibit reaction 5. Thus the inhibiting effect of *gem*-dinitropropane would be acting in the same direction as the shortening dwell-time for reactants in the preheat zone as consumption rate increases. This may be the reason why the change in slope in the upper part of the step is very sharp in the 2-nitropropane–nitric acid system as compared to the other nitroparaffin systems.

Table IV gives burning rate data for the system *gem*-dinitropropane–nitric acid and it can be seen that the consumption rate curve is linear and there is nothing unusual about the absolute value of the rates. If the above interpretation of the effect of N_2O_4 on the combustion of other nitroparaffin systems is correct, then addition of N_2O_4 to the *gem*-dinitropropane–nitric acid system should have no appreciable effect on the shape or absolute value of its consumption rate curve. The data in Table IV show this to be true. Both of these systems have a property of burning with and without flame. A comparison of rates in corresponding regions shows that the N_2O_4 does not alter the rate in either region. There is a discontinuity in the consumption rate curve at the point of transition from flameless to flame combustion. However, this is a true discontinuity and has no relation to the low pressure step which has been shown to be a continuous phenomenon.[2,3]

In view of the above and previous results, it appears that the proposed mechanism has been able to predict correctly several observable effects of chemical composition on the low pressure step, and has served as a good basis for correlating many phenomena observed in the combustion of nitric acid systems. Consequently, it continues to be an acceptable working hypothesis.

Acknowledgment. The author wishes to express his thanks to Mr. C. Stanifer and Mr. E. Dimitroff for their assistance in obtaining some of the consumption rate data.

MOLECULAR STRUCTURE AND PROPERTIES OF HYDROCARBONS AND RELATED COMPOUNDS*

BY JOHN B. GREENSHIELDS† AND FREDERICK D. ROSSINI

Chemical and Petroleum Research Laboratory, Carnegie Institute of Technology, Pittsburgh, Pennsylvania

Received June 21, 1957

Empirical equations, involving only structural parameters, are presented for calculating the isomeric variation in the values of certain physical and thermodynamic properties of the paraffin hydrocarbons. Those properties are the molal volume, the molal refraction, the standard heat of formation, the standard heat of vaporization (all at 25°), the normal boiling point and the boiling point at 10 mm. As an example of the extension of this type of correlation to other series of compounds, equations are presented for the isomeric variation in the values of the molal volume, the molal refraction and the normal boiling point of the saturated aliphatic alcohols. Each set of equations is preceded by a review of the literature describing closely allied investigations and is followed by a qualitative theoretical interpretation. The report concludes with a discussion of the possible extension of the isomeric variation type of correlation to other groups of compounds.

I. The Paraffin Hydrocarbons

1. Introduction and Review of Previous Investigations. The paraffin hydrocarbons seem to furnish a suitable foundation for the investigation of the structural dependence of isomeric variations in physical and thermodynamic properties. The interest in this class of compounds has led to a more nearly complete program of synthesis, purification and property determination than exists for any similar group of compounds. The absence of an observable dipole moment in the paraffins indicates that the isomeric variation in properties is entirely geometric in origin and subject to correlation involving only geometric factors. In all aliphatic compounds, and in alicyclic and aromatic compounds containing aliphatic side chains, the isomeric variation in properties depends to some degree upon the structural variations in the paraffin portion of the molecule.

Qualitative comparisons between the isomeric variation in properties and the differences in structure have been made by several investigators in conjunction with their determination of the physical and thermodynamic properties of the paraffin hydrocarbons.[1-8] These investigators recognized

(*) This investigation was performed as part of the work of the American Petroleum Institute Research Project 44. The material is taken from a dissertation submitted by John B. Greenshields to the Carnegie Institute of Technology in partial fulfillment of the requirements for the degree of Doctor of Philosophy.

(†) Holder of a Fellowship of the American Petroleum Institute Research Project 44.

(1) L. Clarke, *J. Am. Chem. Soc.*, **33**, 520 (1911).

(2) G. T. Morgan, S. R. Carter and A. E. Duck, *J. Chem. Soc.*, **127**, 1252 (1925).

(3) G. Edgar and G. Calingaert, *J. Am. Chem. Soc.*, **51**, 1540 (1929).

(4) A. L. Ward and S. S. Kurtz, Jr., *Anal. Chem.*, **10**, 559 (1938).

(5) C. E. Boord, *Petroleum Refiner*, **21**, 372 (1942).

(6) C. E. Boord, "The Science of Petroleum," Volume II, Oxford University Press, New York, N. Y., 1938, p. 1349.

(7) C. E. Boord, Advances in Chemistry Series No. 5, Progress in Petroleum Technology, American Chemical Society, Washington, 1951.

that both the number and relative position of side chains played key roles in determining the isomeric variations in such properties as the boiling point, density, refractive index and energy content.

These observations have generally led to attempts at a quantitative description as an increasing abundance of data has permitted a more precise evaluation of structural effects upon the values of properties. Those quantitative relationships in which the property variation among a group of isomers is expressed as a function of structural parameters alone may be conveniently separated into three categories: (1) total property group contribution methods; (2) homologous series methods and (3) isomeric variation methods in which the isomeric increment in the value of a property is correlated rather than the total value of the property for each isomer.

a. Total Property Group Contribution Methods.—An important type of correlation which has been excluded from this discussion is the generalized correlation in which isomeric variations in properties are neglected. These correlations usually express the value of a property as a function of the number and kinds of atoms and functional groups present in the molecule. Several investigators, however, have extended this method to include isomeric variations by the introduction of various structural contributions. Inasmuch as these correlations must express the value of a property as a function of both structure and molecular weight, they are most easily adapted to those properties which show a linear variation with change in molecular weight. This behavior is exhibited by the extensive intramolecular properties, such as the molal refraction and the standard heat of formation of the gas. Extensive intermolecular properties such as molal volume approach linear behavior, but intensive properties such as density, refractive index and boiling point do not. Nevertheless, a number of investigators have correlated such intensive properties with total value equations by expressing the property as a non-linear function of both the molecular weight and a term which is a linear combination of group and structural contributions. The group contribution method has thus been applied to the boiling point[9-14] by the use of non-linear functions although the correlation achieved is not as close as that obtained by the use of other analytical techniques.

A great number of group contribution equations have been proposed for the various thermodynamic properties such as heat of combustion, heat of formation, free energy of formation and entropy. Most of these correlations are quite general in nature and do not distinguish isomers. Some of the more recent formulations, however, are more detailed in their analysis of the isomeric differences in the values of these properties.[15-23]

b. Homologous Series Methods.—A large number of equations have been proposed for correlating the various physical and thermodynamic properties of the series of normal paraffin hydrocarbons and other "normal" series. These equations exhibit a wide variety of functional forms but are usually functions of a single variable, namely, the number of carbon atoms in the molecule or a closely related quantity. Several investigators have extended this homologous series method to the correlation of properties of several series of branched chain paraffins. Although homologous series correlations are, for practical purposes, capable of predicting values of properties for only a small fraction of the total number of paraffin isomers, they are generally more accurate than other methods in predicting values for those isomers for which they are applicable. Moreover, since only a single variable is involved, the variation in the values of properties among the members of a homologous series is subject to a simple graphical representation, which may be employed for the prediction of additional values by interpolation or extrapolation. This technique, in either graphical or analytical form, has been applied to the freezing point,[24] density,[24,25] molal volume,[26-28] refractive index,[24,25] boiling point,[29] and standard heat of formation.[30-32]

c. Isomeric Variation Methods.—In contrast to those methods previously discussed, this technique involves relationships in which an incremental difference in the values of properties is correlated rather than the total value of the property for each isomer. This incremental method has generally been employed by those investigators interested in constitutive influences upon the values of the properties of a set of isomers, and it was the method adopted in the present investigation. A. W. Francis[33,34] has applied a modification of this method to the correlation of the normal boiling points, densities and refractive indices for paraffin hydrocarbons containing 9 or more carbon

(8) F. D. Rossini, a chapter in Volume 1 of "Physical Chemistry of Hydrocarbons," Academic Press, New York, N. Y., 1950.
(9) C. R. Kinney, *J. Am. Chem. Soc.*, **60**, 3032 (1938).
(10) C. R. Kinney, *Ind. Eng. Chem.*, **32**, 559 (1940).
(11) C. R. Kinney and W. L. Spliethoff, *J. Org. Chem.*, **14**, 71 (1949).
(12) B. Nekrassow, *Z. physik. Chem.*, **A141**, 378 (1929).
(13) V. C. E. Burnop, *J. Chem. Soc.*, 826 (1938).
(14) F. Klages, *Ber.*, **76**, 788 (1943).
(15) M. Rebek, *Monatsh.*, **73**, 259 (1941).
(16) F. Klages, *Ber.*, **82**, 358 (1949).
(17) J. L. Franklin, *Ind. Eng. Chem.*, **41**, 1070 (1949).
(18) V. M. Tatevskii, *Doklady Akad. Nauk S. S. S. R.*, **75**, 819 (1950).
(19) V. M. Tatevskii, V. V. Korobov and E. A. Mendzheritskii, *ibid.*, **78**, 67 (1951).
(20) V. M. Tatevskii, *Zhur. Fiz. Khim.*, **25**, 241 (1951).
(21) V. M. Tatevskii, E. A. Mendzheritskii and V. V. Korobov, *Ser. Fiz. Mat. i Estest. Nauk.*, **3**, 83 (1951).
(22) J. W. Anderson, G. H. Beyer and K. M. Watson, *Natl. Petroleum News*, Tech. Sec., **36**, R476 (July 5, 1944).
(23) H. J. Bernstein, *J. Chem. Phys.*, **20**, 263 (1952).
(24) A. W. Schmidt, *Ber.*, **75**, 1399 (1942).
(25) A. W. Francis, *Ind. Eng. Chem.*, **33**, 554 (1941).
(26) G. Calingaert and J. W. Hladky, *J. Am. Chem. Soc.*, **58**, 153 (1936).
(27) G. Calingaert, H. A. Beatty, R. C. Kuder and G. W. Thomson, *Ind. Eng. Chem.*, **33**, 103 (1941).
(28) G. Egloff and R. C. Kuder, THIS JOURNAL, **45**, 836 (1941).
(29) G. Egloff, J. Sherman and R. B. Dull, *ibid.*, **44**, 730 (1940).
(30) E. J. Prosen, W. H. Johnson and F. D. Rossini, *J. Research Natl. Bur. Standards*, **37**, 51 (1946).
(31) Sr. M. Constance Loeffler, Thesis, Carnegie Institute of Technology, Pittsburgh, Pennsylvania, 1954.
(32) S. D. Mandamadiotis, Thesis, Carnegie Institute of Technology, Pittsburgh, Pennsylvania, 1954.
(33) A. W. Francis, *Ind. Eng. Chem.*, **35**, 442 (1943).
(34) A. W. Francis, *ibid.*, **36**, 256 (1944).

atoms. M. L. Huggins[35–37] adapted the method to the molal volume and the molal refraction. An incremental method involving short range interaction terms was employed by Taylor, Pignocco and Rossini[38] in correlating the isomeric variation in the values of the molal volume, molal refraction and normal boiling point. H. Weiner[39–41] presented a method of correlation based upon a two parameter equation which was remarkably successful in correlating the isomeric increments for a number of physical and thermodynamic properties. J. R. Platt[42,43] suggested another incremental method based upon short range interactions and presented an analysis of the Wiener parameters.

A number of other investigators[44–47] have employed correlation methods involving the interrelationships between various properties, utilizing at the same time various structural parameters.

2. Recommended Equations.—Following a series of preliminary studies, a set of equations based upon a modification of the Wiener–Platt correlation was adopted. This section includes the presentation of those equations and a discussion of their use and range of validity. A review of their development will be deferred to the following section.

The recommended equations are

Variation in molal volume in 25°:

$$V^{25} = M/d^{25}$$

where d^{25} is the density at 25° and M is the molecular weight (C = 12.010, H = 1.008), in milliliters per mole

$$V^{25}(\text{isomer}) - V^{25}(\text{normal}) = 0.439C_3 + 0.578C_4 - 1.993\Delta P_3 - 4.410\Delta W/(n^2 - n) - 3.68P'_4 \quad (1)$$

Variation in molal refraction at 25°:

$$R^{25}{}_D = V^{25}[(n^{25}{}_D)^2 - 1]/[(n^{25}{}_D)^2 + 2]$$

where $n^{25}{}_D$ is the refractive index for the sodium-D line at 25°, in milliliters per mole

$$R^{25}{}_D(\text{isomer}) - R^{25}{}_D(\text{normal}) = 0.017C_3 + 0.047C_4 - 0.121\Delta P_3 \quad (2)$$

Variation in boiling point at 10 mm., BP_{10} in °C.:

$$BP_{10}(\text{isomer}) - BP_{10}(\text{normal}) = -12.27C_3/n^{1/2} - 24.18C_4/n^{1/2} + 5.33\Delta P_3/n^{1/2} + 22.49\Delta W/(n^2 - n) \quad (3)$$

Variation in boiling point at 760 mm., BP_{760}, in °C.:

$$BP_{760}(\text{isomer}) - BP_{760}(\text{normal}) = -4.50C_3/n^{1/2} - 5.72C_4/n^{1/2} + 15.87\Delta P_3/n^{1/2} + 72.93\Delta W/(n^2 - n) + 10.6P'_4 \quad (4)$$

Variation in standard heat of formation of the liquid at 25°, ΔHf^0, in kcal./mole:

$$\Delta Hf^0(\text{isomer}) - \Delta Hf^0(\text{normal}) = -0.351C_3 - 1.057C_4 + 0.975\Delta P_3 + 9.427\Delta W/(n^2 - n) + 1.978P''_4 + 5.19P'_4 \quad (5)$$

Variation in standard heat of vaporization at 25°, ΔHv^0, in kcal./mole

$$\Delta Hv^0(\text{isomer}) - \Delta Hv^0(\text{normal}) = 0.118C_3 - 0.307C_4 + 0.164\Delta P_3 + 3.081\Delta W/(n^2 - n) \quad (6)$$

Values of the variables appearing in the preceding equation will be simply defined here. An interpretation of their physical significance in each of the above properties may be found in the section on interpretation.

C_3 is the no. of tertiary carbon atoms in the isomer

C_4 is the no. of quaternary carbon atoms in the isomer

$\Delta P_3 = P_3(\text{isomer}) - P_3(\text{normal})$, where P_3 is the total no. of pairs of carbon atoms three bonds apart

$\Delta W = W(\text{isomer}) - W(\text{normal})$, where W, the "Wiener" number, is the total no. of bonds between all pairs of carbon atoms

n is the total no. of carbon atoms

P'_4 is the no. of quaternary carbon pairs separated by one carbon atom in the isomer

P''_4 is the no. of pairs consisting of one quaternary and one tertiary carbon atom separated by one other carbon atom

The coefficients of equations 1 were obtained from a least-squares fit of selected experimental values for 104 compounds in the range C_5 to C_{30}. All of the values employed for this and all other equations received equal weight in the least-squares determination of the coefficients. Equation 2 was fitted to 66 compounds in the range C_5 to C_{10}; equation 3 was fitted to 51 compounds in the range C_5 to C_{28}; equation 4 was fitted to 63 compounds in the range C_5 to C_{12}; equation 5 was fitted to 32 compounds in the range C_5 to C_9; and equation 6 was fitted to 27 compounds in the range C_5 to C_8.

The use of equations 1 to 6 in computing the properties of a paraffin isomer may perhaps best be illustrated by an example. Let it be required to compute the density, refractive index, boiling point at 10 mm., normal boiling point, standard heat of formation and standard heat of vaporization of 2,2,3,4-tetramethylpentane.

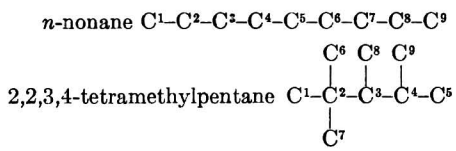

The variables appearing in the equations for the isomeric variations in these properties are n, C_3, C_4, ΔP_3, ΔW, P_4' and P_4''.

n = 9 (there are 9 carbon atoms in 2,2,3,4-tetramethylpentane)

C_3 = 2 (C^3 and C^4 in the isomer are tertiary carbon atoms)

C_4 = 1 (C^2 in the isomer is a quaternary carbon atom)

ΔP_3 = 4[$\Delta P_3 = P_3(\text{isomer}) - P_3(\text{normal})$. There are 10 pairs of carbon atoms 3 bonds apart in 2,2,3,4-tetramethylpentane C^1–C^4, C^2–C^5, C^4–C^6, C^4–C^7, C^2–C^9, C^1–C^8, C^6–C^8, C^7–C^8, C^5–C^8 and C^8–C^9. There are 6 pairs of carbon atoms 3 bonds apart in n-nonane: C^1–C^4, C^2–C^5, C^3–C^6, C^4–C^7, C^5–C^8 and C^6–C^9]

(35) M. L. Huggins, *J. Am. Chem. Soc.*, **63**, 116 (1941).
(36) M. L. Huggins, *ibid.*, **76**, 843 (1954).
(37) M. L. Huggins, *Bull. Chem. Soc. Japan*, **29**, 336 (1956).
(38) W. J. Taylor, J. M. Pignocco and F. D. Rossini, *J. Research Natl. Bur. Standards*, **34**, 413 (1945).
(39) (a) H. Wiener, *J. Chem. Phys.*, **15**, 766 (1947); (b) *J. Am. Chem. Soc.*, **69**, 17 (1947).
(40) (a) H. Wiener, THIS JOURNAL, **52**, 425 (1948); (b) *J. Am. Chem. Soc.*, **69**, 2636 (1947).
(41) H. Wiener, THIS JOURNAL, **52**, 1082 (1948).
(42) J. R. Platt, *J. Chem. Phys.*, **15**, 419 (1947).
(43) J. R. Platt, THIS JOURNAL, **56**, 328 (1952).
(44) M. M. Samygin, *J. Phys. Chem., U.S.S.R.*, **9**, 929 (1937).
(45) T. M. Polonskii, *Nauk. Zapiski Khaikov, Poligraf. Inst.*, **5**, 103 (1940).
(46) M. M. Ventura, Escola agron, Ceara, Publ. Tec. 2A, 1949.
(47) J. C. Chu, M. Dmytryszyn, J. J. Moder and R. L. Overbeck, *Ind. Eng. Chem.*, **41**, 131 (1949).

Note: P(normal) is simply $n - 3$, where n is the number of carbon atoms.

$\Delta W = -34$ [$\Delta W = W$(isomer) $- W$(normal). In 2,2,-3,4-tetramethylpentane the total number of bonds between C^1 and each of the other carbon atoms is $\sum_{n=2}^{9} C^1$ to $C^n = 21$, between C^2 and each of the remaining carbon atoms, $\sum_{n=3}^{9} C^2$ to $C^n = 13$, between C^3 and each of the remaining carbon atoms, $\sum_{n=4}^{9} C^3$ to $C^n = 10$, etc. W(isomer) $= 21 + 13 + 10 + 10 + 13 + 9 + 7 + 3 = 86$. In n-nonane $\sum_{n=2}^{9} C^1$ to $C^n = 36$, $\sum_{n=3}^{9} C^2$ to $C^n = 28$, $\sum_{n=4}^{9} C^3$ to $C^n = 21$, etc. W(normal) $= 36 + 28 + 21 + 15 + 10 + 6 + 3 + 1 = 120$]

Note: a short method for calculating W(isomer), which greatly reduces the computational labors, has been suggested by Wiener.[39b] W may be computed by multiplying the number of C atoms on one side of a bond by the number on the other side and summing the products for all bonds. Thus for 2,2,3,4-tetramethylpentane, the product for bond C^1–C^2 is $1 \cdot 8 = 8$; for C^2–C^5, $8 \cdot 1 = 8$; for C^2–C^7, $8 \cdot 1 = 8$; for C^2–C^3, $4 \cdot 5 = 20$; for C^3–C^8, $8 \cdot 1 = 8$; for C^3–C^4, $6 \cdot 3 = 18$; for C^4–C^9, $8 \cdot 1 = 8$; for C^4–C^5, $8 \cdot 1 = 8$. Therefore W(isomer) $= 8 + 8 + 8 + 20 + 8 + 18 + 8 + 8 = 86$. W(normal), as pointed out by Wiener,[39b] is a simple function of n. W(normal) $= (n - 1)(n)(n + 1)/6$. Thus for n-nonane, W(normal) $= 8 \times 9 \times 10/6 = 120$.

$P'_4 = 0$ (There are no pairs of quaternary carbon atoms in 2,2,3,4-tetramethylpentane)

$P''_4 = 1$ (carbon pair C^2–C^4 in the isomer is a pair consisting of one quaternary carbon, C^2, and one tertiary carbon C^4, separated by one other carbon atom, C^3)

Substituting the preceding values in equations 1 to 6, one obtains

V^{25}(isomer) $- V^{25}$(normal) $= -4.43$ ml./mole
R^{25}_D(isomer) $- R^{25}_D$(normal) $= -0.41$ ml./mole
BP_{10}(isomer) $- BP_{10}$(normal) $= -19.8°$
BP_{760}(isomer) $- BP_{760}$(normal) $= -18.2°$
ΔHf^0(isomer) $- \Delta Hf^0$(normal) $= -0.33$ kcal./mole (liquid at 25°)
ΔHv^0(isomer) $- \Delta Hv^0$(normal) $= -1.34$ kcal./mole (at 25°)

The values of these six properties for n-nonane are

V^{25}(normal) $= 179.67$ ml./mole
R^{25}_D(normal) $= 43.86$ ml./mole
BP_{10}(normal) $= 39.1°$
BP_{760}(normal) $= 150.8°$
ΔHf^0(normal) $= -65.84$ kcal./mole (liquid at 25°)
ΔHv^0(normal) $= 11.10$ kcal./mole (at 25°)

The addition of these values for n-nonane to the corresponding values for the isomeric variation presented above gives for 2,2,3,4-tetramethylpentane

$V^{25} = 175.24$ ml./mole
$R^{25}_D = 43.45$ ml./mole
$BP_{10} = 20.8°$
$BP_{760} = 132.6°$
$\Delta Hf^0 = -66.17$ kcal./mole (liquid at 25°)
$\Delta Hv^0 = 9.76$ kcal./mole (at 25°)

The desired density and refractive index may be computed from the relations defining V^{25} and R^{25}_D

$$V^{25} = M/d^{25} \text{ and } R^{25}_D = \frac{(n^{25}_D)^2 - 1}{(n^{25}_D)^2 + 2} V^{25}$$

therefore

$$d^{25} = M/V^{25} = 0.7319$$

and

$$n^{25}_D = \left[\frac{V^{25} + 2R^{25}_D}{V^{25} - R^{25}_D}\right]^{1/2} = 1.4103$$

Note: values of the above properties for the n-paraffins may be found in the tables of the American Petroleum Institute Research Project 44.[48,49] Values of V^{25}, R^{25}_D and BP_{760} are given through n-tetracontane[48,49]; values of BP_{10} are given through n-eicosane[48,49]; values of ΔHf^0, liq. are given through n-eicosane[49]; and values of ΔHv^0 are given through n-eicosane.[49]

A few specific recommendations in the use of the preceding equations may be noted. The coefficients of equation 1, which was fitted over a large molecular weight range, C_5 to C_{30}, were adjusted to avoid large negative deviations (high molal volumes) for compounds containing long side chains. Accordingly positive deviations (low molal volumes) may be expected for compounds containing chains of intermediate length, *e.g.*, a n-propyl group or two ethyl groups attached to the same carbon atom. The normal boiling point equation 4, on the other hand, was fitted to low molecular weight data and accordingly should only be used with great caution for the prediction of boiling points of high molecular weight paraffins. Equation 3 for the boiling point at 10 mm. does not have the correction term P_4' since the uncorrected equation reproduces the boiling point of 2,2,4,4-tetramethylpentane quite closely. It is to be expected, therefore, that the predicted boiling points for compounds containing unhindered terminal quaternary carbon atoms such as 2,2,5,5-tetramethylhexane will be 5 to 10° too high. Care also should be employed in the use of the calculated values for the 10 mm. boiling point in the C_{10} to C_{11} range since these values have no close experimental support. Equations 5 and 6, which are fitted to the lower paraffins only, should not be extrapolated indiscriminately.

3. Development of the Recommended Equations and Modifications.—Following an unsuccessful search for more fundamental variables the parameters of existing correlations were re-examined. Both the 6 term Taylor, Pignocco, Rossini (TPR) correlations[38] and the 2 term Wiener–Platt correlations[39,40,43] gave satisfactory values for all properties considered over the range C_5 to C_8 for which the numerical coefficients were fitted. All sets of equations extrapolate fairly well to C_{11} or C_{12} with a few compounds showing large deviations, notably those compounds with pairs of quaternary carbon atoms once removed. Inasmuch as the 2 term Wiener–Platt type of formulation seemed to

(48) F. D. Rossini, K. S. Pitzer, R. L. Arnett, R. M. Braun and G. C. Pimentel, "Selected Values of Physical and Thermodynamic Properties of Hydrocarbons and Related Compounds," American Petroleum Institute Research Project 44, Carnegie Press, Pittsburgh, Pa. 1953.

(49) American Petroleum Institute Research Project 44, "Selected Values of Properties of Hydrocarbons and Related Compounds." Carnegie Institute of Technology, Department of Chemistry, Pittsburgh, Pennsylvania.

fit the experimental data for the properties under consideration in the range C_5 to C_{12} nearly as well as the 6 term TPR correlations, and since it seemed somewhat easier to assign a physical significance to the Wiener–Platt variables, possible improvements in this correlation were first investigated.

A factor $1/n^2$ appearing in Wiener's equations was introduced as a damping factor to express the decreasing effect of differences in W upon the value of a property with increasing molecular weight. Platt interpreted $1/n^2$ as a normalizing factor serving to make the term involving ΔW almost independent of molecular weight for a particular isomeric change. Since W is the sum of the number of bonds between all pairs of carbon atoms in the paraffin molecule and since there are $n(n-1)/2$ such pairs, the term $2W/n(n-1)$ may be thought of as an average distance between carbon atoms expressed in terms of carbon–carbon bonds. Accordingly the term $a\Delta W/(n^2-n)$ was adopted in this report as a measure of linear compactness. The factor $1/(n^2-n)$ approached $1/n^2$ for large n, but its use permits a somewhat smaller value of the coefficient a, which is helpful in extrapolation to high molecular weight paraffins with long side chains, as will be discussed later.

The reliability of equations of the Wiener–Platt and TPR types for the prediction of the isomeric variation in the values of properties of high molecular weight paraffins was investigated. A comparison of the calculated values with the experimental data of the American Petroleum Institute Research Project 42 for paraffins in the range C_{13} to C_{28} indicated certain trends in the deviations between observed and calculated values. The majority of the compounds included in this group possessed a long principal chain with one or two side chains, *n*-propyl or longer. Values of the molal refraction calculated from both the TPR and Platt equations agreed quite well with the experimental values for these properties, generally to within ± 0.10 ml./mole and with no observable trends. The values of molal volume, however, did not exhibit a corresponding goodness of fit. Values calculated from the TPR correlation were generally about 2 ml. lower than the observed values, whereas the values from the Wiener–Platt equation were 3 or 4 ml. higher than the experimental quantities, becoming greater as the relative length of the side chains increased. The isomeric variations calculated from the TPR correlation were constant for a given type of local configuration and not dependent upon the length of attached chains provided these chains were ethyl or longer. The isomeric variations calculated from the Wiener–Platt correlations containing the term $a\Delta W/n^2$ are dependent upon the length of attached chains since $\Delta W/n^2$ increases without limit as the chains about a center of branching increase in length in equal increments. The experimental data for the molal volume indicated a dependence upon chain length in the same direction but not nearly of the magnitude of that predicted by the Wiener–Platt equations. Since it was not possible to compare calculated and observed values of the normal boiling point directly for these high molecular weight paraffins, and since experimental values of the boiling point at 10 mm. had been determined for most of these compounds by American Petroleum Institute Research Project 42, the isomeric increment in boiling point at this lower pressure was investigated.

Equations of the Wiener–Platt type gave an adequate fit for the low molecular weight data but boiling points calculated for the C_{13} to C_{28} range were often 15 to 20° lower than the experimental values. The use of the factor $1/(n^2-n)$ in place of $1/n^2$ served to raise the calculated boiling point a few degrees but not nearly enough. A method was sought for decreasing the contribution from the ΔW term for these compounds without sacrificing too much accuracy in the low molecular weight range. If the term $a\Delta W/(n^2-n)$ were to be retained, this necessitated either a reduction in the numerical value of the coefficient "a" by the use of additional terms for chain branching, not dependent upon chain length, or a modification in the way ΔW was to be computed.

The simplest terms expressing the localized effects of chain branching are C_3 and C_4, the numbers of tertiary and quaternary carbon atoms, respectively. These quantities were combined with the terms ΔP_3 and $\Delta W/(n^2-n)$ and fitted to the boiling point at 10 mm.

The damping factor $1/n^{1/2}$ was introduced for the terms C_3 and C_4 and later extended to other combinations of terms. (The term $a\Delta W/(n^2-n)$ approaches zero as a limit as the principal chain length increases without limit providing the lengths of side chains remain constant, and thus it might be advantageous to let the other terms approach zero in a similar manner, so that the predicted isomeric increment for a constant terminal configuration would vanish at infinite chain length.)

It was necessary to add to the equation for the normal boiling point the term P_4', representing the contribution arising from a pair of quaternary carbon atoms once removed, *e.g.*, 2,2,4,4-tetramethylpentane. This is not to imply that the contribution to the boiling point arising from this configuration is absent at 10 mm. It merely indicates that the adjustment of the constants to the 10 mm. data was such that the boiling points of compounds containing unhindered terminal quaternary carbon atoms are apt to be predicted somewhat too high, as indicated in the section on recommended equations.

It was observed that a considerable improvement in the fit of the equation for the standard heat of formation could be obtained by including a term, P_4'', representing the contribution of a quaternary–tertiary carbon pair once removed, as in the compounds 2,2,4-trimethylpentane and 2,2,3,4-tetramethylpentane. The contribution from this configuration had not been apparent in the investigation of the other properties.

4. Physical Interpretation of the Recommended Equations.—The physical significance of the variables employed by Wiener, W and P_3, as reflected in their contributions to the values of various properties, already has been discussed by Platt[43] and will not be repeated in detail here except for some slight modifications in interpretation. Our

approach will generally be much more qualitative.

The two features of molecular structure which seem to play an important role in determining the values of those properties considered in the present investigation are the relative degrees of compactness and steric interference to free rotation present in the various paraffin isomers. The term "compactness," as employed in this discussion, is to be interpreted as a measure of the mean intramolecular distance between the component atoms of an isomer, and is a function of the extent and relative proximity of chain branching.

Increased molecular compactness among a set of paraffin isomers, in the absence of an increase of steric hindrance, seems to lead to an increase in molal volume and a decrease in boiling point. An increase in the degree of steric interference seems to affect these properties in the opposite sense. In interpreting these changes in intermolecular properties, an increase in molecular compactness, *i.e.*, a decrease in the mean internal distance between atoms, may be viewed as increasing the average kinetic volume of the molecules, by the free rotation of unhindered branched chains, and at the same time decreasing the magnitude of the intermolecular forces as a result of the looser arrangement of molecules. The presence of sterically hindered groups would tend to reduce the degree of rotation and lead to a more closely knit arrangement of molecules with greater intermolecular forces.

Those terms appearing in the equations of this investigation which may be considered a measure of molecular compactness are $W/(n^2 - n)$, C_3 and C_4. The term $W/(n^2 - n)$, which is one-half the average distance between pairs of carbon atoms in units of carbon–carbon bonds, may be considered an index of over-all linear compactness, whereas the terms C_3 and C_4, the numbers of tertiary and quaternary carbon atoms, are indices of short range compactness. The failure of equations employing only the term $\Delta W/(n^2 - n)$ as a measure of compactness to give an adequate correlation for compounds possessing long side chains may be due to the unsuitableness of the term for describing distances between atoms in flexible chains. An alternative interpretation is that the index of linear compactness is a good approximation to some more fundamental quantity for molecules with short branches but that it fails as an approximation in the case of molecules with long side chains.

The terms P_3, P'_4 and P''_4 may be considered as measures of the steric hindrance present in the molecular structure. P_3, the number of carbon atoms three bonds apart, may be regarded as the primary steric term, and its contribution appears to be additive and independent of the detailed configuration of the molecule. P'_4 and P''_4 represent interactions between carbon atoms four bonds apart. These may be regarded as secondary steric terms, since they depend upon the detailed molecular configuration, *i.e.*, the nature of intervening atoms. Additional secondary steric terms for carbon pairs four bonds apart seem to be present for such configurations as those occurring in 2,4-dimethyl-3-isopropylpentane and 11-(2,2-dimethyl-*n*-propyl)-heneicosane although these terms were not included in the present correlations.

Inasmuch as the molal refraction is essentially an internal property, depending upon the electronic configuration of the molecule, it is convenient to think of the terms C_3 and C_4 in this case as representing localized changes in the electron pattern rather than indices of short range compactness as was done in the case of the intermolecular properties. The steric term, P_3, is most important in determining the value of this property and may be interpreted as effecting a lengthening of the intermediate carbon–carbon bond and a shift to higher frequency absorption as described by Platt.[43]

The terms appearing in the equation for the standard heat of vaporization may be interpreted in the same manner as the corresponding terms in the boiling point and molal volume equations. The steric terms, P_3, P'_4 and P''_4 appearing in the equation for the standard heat of formation of the liquid may be interpreted as measures of the potential barriers to internal rotation about intermediate carbon–carbon bonds. It is somewhat more difficult to justify the use of the linear compactness term, $W/(n^2 - n)$, in this case. Further studies have indicated that a more plausible approach might be to consider specific carbon–carbon interactions in the manner of the TPR correlation.

II. The Saturated Aliphatic Alcohols

1. Introduction.—One of the purposes of the present investigation was the development of paraffin correlations in such a form that they might be extended to monosubstituted aliphatic compounds with only minor alterations in form. As an example of this class of compounds, the saturated aliphatic alcohols were selected for study. This selection was made for two reasons. In the first place, the experimental values of the physical properties for the lower isomeric alcohols are reasonably accurate and more complete than those for any other set of monosubstituted aliphatics. Secondly, the highly polar nature of this group of compounds offers a severe test to correlations based entirely upon geometric factors. Accordingly the fit of a set of any other monosubstituted aliphatic compounds containing a group of similar size and of equal or less polarity than the hydroxyl group should give a fit comparable to that for the alcohols.

Although a number of equations have been advanced for the normal primary alcohols, correlations in which isomeric variations in the values of properties are considered have been quite limited. Except for a simple recognition of variations introduced by reason of the primary, secondary or tertiary attachment of the hydroxyl group, there appear to be very few detailed analyses of the property-structure relationship for these compounds.

2. Recommended Equations.—A set of equations expressing the isomeric variation in three properties of the saturated aliphatic alcohols was developed through a suitable modification of the corresponding equations for the paraffin hydrocarbons. This section includes the presentation of those equations and a discussion of their use and range of validity. A qualitative interpretation of

TABLE I

SUMMARY OF DEVIATIONS IN THE VALUES OF THE PROPERTIES FOR THE PARAFFIN HYDROCARBONS

Range	No. of compd.	Property	Av. dev.	Stand. dev. (of a single value)	Max. dev.
C_5 to C_{11}	95	Molal vol. at 25°	±0.40 ml./mole	±0.54 ml./mole	1.76 ml./mole
	95	Density at 25°[a]	± .0016 g./ml.	± .0022 g./ml.	−0.0084 g./ml.
	95	Density at 25°[b]	± .0006 g./ml.	± .0008 g./ml.	−0.0045 g./ml.
C_{12} to C_{30}	34	Molal vol. at 25°	± .62 ml./mole	± .83 ml/mole	2.09 ml./mole
	34	Density at 25°[a]	± .0013 g./ml.	± .0018 g./ml.	−0.0044 g./ml.
	34	Density at 25°[b]	± .0005 g./ml.	± .0007 g./ml.	.0019 g./ml.
C_5 to C_{11}	95	Molal refraction at 25°	± .03 ml./mole	± .05 ml./mole	.20 ml./mole
	113	Refractive index at 25°, n_D[c]	± .0008	± .0011	.0038
	95	Refractive index at 25°, n_D[d]	± .0004	± .0005	.003
C_{12} to C_{30}	34	Molal refraction at 25°	± .06 ml./mole	± .08 ml./mole	− .22 ml./mole
	35	Refractive index at 25°, n_D[c]	± .0009	± .0011	− .0026
	34	Refractive index at 25°, n_D[d]	± .0003	± .0005	− .0012
C_5 to C_9	36	Boiling point at 10 mm.	±1.5°	±1.9°	4.9°
C_{10} to C_{30}	31	Boiling point at 10 mm.	±2.8°	±3.6°	−7.4°
C_5 to C_{11}	103	Boiling point at 760 mm.	±1.1°	±1.5°	−5.7°
C_{12} to C_{15}	17	Boiling point at 760 mm.	±2.5°	±3.4°	7.9°
C_5 to C_9	34	Stand. heat of formation of liq. at 25°	±0.35 kcal./mole	±0.53 kcal./mole	−1.89 kcal./mole
C_5 to C_9	30	Stand. heat of vaporization at 25°	±0.06 kcal./mole	±0.07 kcal./mole	0.16 kcal./mole

[a] From calculated value of molal volume. [b] From calculated value of molal refraction using experimental value of refractive index. [c] From calculated value of molal refraction using calculated value of molal volume. [d] From calculated value of molal refraction using experimental value of molal volume.

the physical significance of the equation variables as well as a discussion of the development of the equations will be found in the succeeding section.

The recommended equations are

Variation in molal volume at 25°:

$$V^{25} = M/d^{25}$$

where d^{25} is the density at 25°, and M is the molecular weight (C = 12.010, H = 1.008, O = 16.0000), in milliliters per mole

$$V^{25}(\text{isomer}) - V^{25}(\text{normal}) = 0.493s - 0.192t + 0.196\Delta O_3 - 1.374\Delta P_3 - 5.209\Delta W/(n^2 - n) \quad (7)$$

Variation in molal refraction at 25°:

$$R^{25}{}_D = \frac{(n^{25}{}_D)^2 - 1}{(n^{25}{}_D)^2 + 2} V^{25}$$

where $n^{25}{}_D$ is the refractive index for the sodium-D line at 25°, in milliliters per mole

$$R^{25}{}_D(\text{isomer}) - R^{25}{}_D(\text{normal}) = -0.026s - 0.116t + 0.018\Delta O_3 + 0.017C_3 + 0.047C_4 - 0.121\Delta P_3 \quad (8)$$

Variation in boiling point at 760 mm., BP_{760}, in °C.:

$$BP_{760}(\text{isomer}) - BP_{760}(\text{normal}) = -12.62s - 21.42t - 5.91\Delta O_3 + 4.27\Delta P_3 + 58.30\Delta W/(n^2 - n) \quad (9)$$

Values of the variables appearing in the preceding equations for the saturated aliphatic alcohols are defined as

s is the no. of secondary hydroxyl groups in the isomer
t is the no. of tertiary hydroxyl groups in the isomer
$\Delta O_3 = O_3(\text{isomer}) - O_3(\text{normal})$, where O_3 is the total no. of carbon–oxygen pairs three bonds apart
$\Delta P_3 = P_3(\text{isomer}) - P_3(\text{normal})$, where P_3 is the total no. of carbon–carbon pairs and carbon–oxygen pairs three bonds apart
$\Delta W = W(\text{isomer}) - W(\text{normal})$, where W is the total no. of bonds between all carbon–carbon pairs and all carbon–oxygen pairs
n is the total no. of carbon and oxygen atoms
C_3 is the no. of tertiary carbon atoms in the isomer
C_4 is the no. of quaternary carbon atoms in the isomer

Note: (1) In the monohydric alcohols for which these equations were developed s and t must have either the value one or zero. If the alcohol is primary, $s = 0$ and $t = 0$; if the alcohol is secondary, $s = 1$ and $t = 0$; and if the alcohol is tertiary, $s = 0$, and $t = 1$.

(2) In evaluating the terms ΔP_3 and $\Delta W/(n^2 - n)$, it is convenient to consider the alcohol as a paraffin hydrocarbon in which the attached hydroxyl group becomes a methyl group. The variables P_3, W and n are then determined for this "corresponding" paraffin.

The coefficients of equations 7 to 9 were determined from a least-squares fit of the selected experimental values appearing in the tables of APIRP44[50] for the range C_3 to C_6 and in one case from additional experimental values for the heptanols. All of the values employed received equal weight in the least-squares determinations of the coefficients. The coefficients of equation 7 were determined from 39 values of the molal volume in the range C_3 to C_7. The coefficients of the terms s, t and ΔO_3 in equation 8 were determined from 26 values of the molal refraction in the range C_3 to C_6; the coefficients of the terms C_3, C_4 and ΔP_3 were assigned the values obtained from the fit of equation 2 to values of the molal refraction for the paraffin hydrocarbons. The coefficients of equation 9 were obtained from 27 values of the normal boiling points for the saturated aliphatic alcohols in the range C_3 to C_6.

The use of equations 7 to 9 in calculating the properties of an isomeric alcohol may be illustrated by an example. Suppose that the values of the density, refractive index and normal boiling point of 3,3-dimethyl-2-butanol are desired.

(50) American Petroleum Institute Research Project 44, Carnegie Institute of Technology, Pittsburgh, Pennsylvania, F. D. Rossini, Unpublished.

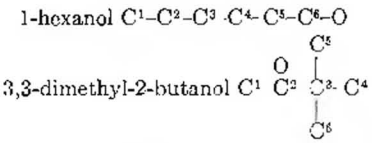

The required variables are s, t, C_3, C_4, ΔO_3, n, ΔP_3 and ΔW.

s = 1 (the oxygen atom in the isomer is attached to a secondary carbon atom, C^2)
t = 0 (the oxygen atom in the isomer is not attached to a tertiary carbon atom)
C_3 = 0 (there are no tertiary carbon atoms in 3,3-dimethyl-2-butanol)
C_4 = 1 (C^3 in the isomer is a quaternary carbon atom)
$\Delta O_3 = 2(\Delta O_3 = O_3(\text{isomer}) - O_3(\text{normal}))$. There are 3 carbon–oxygen pairs 3 bonds apart in 3,3-dimethyl-2-butanol: C^4–O, C^3–O and C^6–O. There is one carbon–oxygen pair 3 bonds apart in n-hexanol: C^4–O

In computing the variables n, ΔP_3 and ΔW, it will be convenient to consider the "corresponding" paraffins n-heptane and 2,3,3-trimethylbutane.

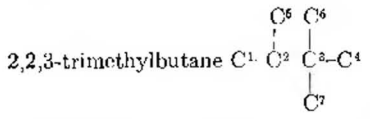

n = 7 (there are 7 carbon atoms in the corresponding paraffins)
$\Delta P_3 = 2(\Delta P_3 = P_3(\text{isomer}) - P_3(\text{normal}))$. There are 6 pairs of carbon atoms 3 bonds apart in 2,2,3-trimethylbutane: C^1–C^4, C^5–C^3, C^1–C^3, C^5–C^3, C^1–C^7 and C^5–C^7. There are 4 pairs of carbon atoms 3 bonds apart in n-heptane: $P_3(\text{normal}) = n - 3 = 7 - 3 = 4$]
$\Delta W = -14$[$\Delta W = W(\text{isomer}) - W(\text{normal})$. Use the method of summing the products of the number of C atoms on one side of a bond by the number on the other side over all bonds. Thus for 2,2,3-trimethylbutane, the product for bond C^1–C^2 is 1·6 = 6; for C^2–C^3, 3·4 = 12; for C^2 C^5, 6·1 = 6; for C^3–C^5, 6·1 = 6; for C^3–C^4, 6·1 = 6; and for C^3–C^7, 6·1 = 6. Therefore W(isomer) = 6 + 12 + 6 + 6 + 6 + 6 = 42. Use the formula

$$W(\text{normal}) = \frac{(n-1)(n)(n+1)}{6}$$

$$W(\text{normal}) = \frac{6 \times 7 \times 8}{6} = 56$$

Substituting the preceding values in equations 7 to 9, one obtains

$$V^{25}(\text{isomer}) - V^{25}(\text{normal}) = -0.13 \text{ ml./mole} \quad (7)$$
$$R^{25}\text{D}(\text{isomer}) - R^{25}\text{D}(\text{normal}) = -0.19 \text{ ml./mole} \quad (8)$$
$$\text{BP}_{760}(\text{isomer}) - \text{BP}_{760}(\text{normal}) = -35.3° \quad (9)$$

The values of these three properties for 1-hexanol are

V^{25}(normal) = 125.28 ml./mole
R^{25}D(normal) = 31.44 ml./mole
BP_{760}(normal) = 157.1°

The addition of these values for 1-hexanol to the corresponding values for the isomeric variation presented above gives for 3,3-dimethyl-2-butanol

V^{25} = 125.15 ml./mole
R^{25}D = 31.25 ml./mole
BP_{760} = 121.8°

The desired density and refractive index may be computed from the relations defining V^{25} and R^{25}D, $V^{25} = M/d^{25}$ and

$$R^{25}\text{D} = \frac{(n^{25}\text{D})^2 - 1}{(n^{25}\text{D})^2 + 2} V^{25}$$

therefore

$$d^{25} = M/V^{25} = 0.8164$$

and

$$n^{25}\text{D} = \left[\frac{V^{25} + 2R^{25}\text{D}}{V^{25} - R^{25}\text{D}}\right]^{1/2} = 1.4136$$

Note: values of the above properties for the 1-alkanols for the range C^1 to C^{20} may be found in the tables of API R44.[49]

3. Development and Physical Interpretation of the Recommended Equations.—The development of correlations for the isomeric variations in the physical properties of the saturated aliphatic alcohols closely followed the methods adopted for the paraffin hydrocarbons. The terms describing variations in the carbon skeleton were retained and additional factors were introduced to describe interactions between the hydroxyl group and the rest of the molecule. The terms which were devised to express this interaction between the hydroxyl group and the paraffin skeleton included

s, the no. of secondary hydroxyl groups in the isomer
t, the no. of tertiary hydroxyl groups in the isomer
$\Delta O_2 = O_2(\text{isomer}) - O_2(\text{normal})$, where O_2 is the total no. of carbon–oxygen pairs two bonds apart
$\Delta O_3 = O_3(\text{isomer}) - O_3(\text{normal})$, where O_3 is the total no. of carbon–oxygen pairs three bonds apart
$\Delta W_0 = W_0(\text{isomer}) - W_0(\text{normal})$, where W_0 is the sum of the numbers of bonds between the hydroxyl group and all carbon atoms in the molecule

Note: $\Delta O_2 = s + 2t$ and $\Delta W_0/n$ is the average number of bonds between the hydroxyl group and a carbon atom.

These variables were combined with those describing the paraffin portion of the molecule and fitted to experimental values of the isomeric variations in the molal volume, molal refraction and normal boiling point.

The physical interpretation of those terms of paraffinic origin appearing in the recommended equations 7 through 9, *i.e.*, C_3, C_4, ΔP_3 and $\Delta W/(n^2 - n)$, may be considered the same as that given for the corresponding terms in the paraffin correlations. The terms s, t and ΔO_3 may be interpreted as indices of variation in association strength due to steric blocking of the hydroxyl group. For example positive values of s, t and ΔO_3 all lead to a decrease in the calculated value of the normal boiling point. In the corresponding terms for the molal volume, the coefficient of the t term appears to have the wrong sign, indicating a decrease in molal volume in the presence of a tertiary hydroxyl relative to the primary hydroxyl group of the "normal" compound. This anomaly is probably due to the relatively poor fit of other terms in this equation to the molal volume data.

The additive nature of the molal refraction is illustrated by the good fit obtained by retaining the paraffin values of the coefficients for those terms not directly involving the hydroxyl group.

III. Suggestions for Extension to Other Series of Compounds

The various classes of mono-functional saturated aliphatic compounds seem to offer the most direct possibilities for extension of this method. M. L. Huggins[51,52] has proposed correlations for the molal

(51) M. L. Huggins, *J. Am. Chem. Soc.* **76**, 845 (1954).
(52) M. L. Huggins, *ibid.*, **76**, 847 (1954).

TABLE II

SUMMARY OF DEVIATIONS IN THE VALUES OF THE PROPERTIES FOR THE SATURATED ALIPHATIC ALCOHOLS

Range	No. of compd.	Property	Av. dev.	Stand. dev. (of a single value)	Max. dev.
C_3 to C_7	44	Molal vol. at 25°	±0.36 ml./mole	±0.43 ml./mole	0.97 ml./mole
	44	Density at 25°[a]	± .0023 g./ml.	± .0028 g./ml.	− .0057 g./ml.
	39	Density at 25°[b]	± .0009 g./ml.	± .0014 g./ml.	.0051 g./ml.
C_3 to C_7	39	Molal refraction at 25°	± .04 ml./mole	± .05 ml./mole	− .19 ml./mole
	43	Refractive index at 25°, n_D[c]	± .0011	± .0014	.0033
	39	Refractive index at 25°, n_D[d]	± .0005	± .0008	− .0029
C_3 to C_7	50	Boiling point at 760 mm.	±1.4°	±1.8°	−6.8°

[a] From calculated value of molal volume. [b] From calculated value of molal refraction using experimental value of refractive index. [c] From calculated value of molal refraction using calculated value of molal volume. [d] From calculated value of molal refraction using experimental value of molal volume.

refraction and molal volume for a number of such substituted paraffins. The correlations developed for the aliphatic alcohols in this investigation constitute an example of such an extension. It will be recalled that in this set of compounds the straight chain primary alcohols were selected as the "normal" series from which isomeric variations in properties were computed. The variables P_3 and $W/(n^2 - n)$ were evaluated by considering the hydroxyl group as equivalent to a methyl group, and three additional variables s, t and O_3 were selected to express the effects of the functional group upon the isomeric increment in properties. However, only in the case of the molal refraction was it possible to retain the same numerical coefficients for the terms of paraffinic origin, C_3, C_4, ΔP_3 and $\Delta W/(n^2 - n)$, as were obtained in the least-squares fit for the properties of the paraffin hydrocarbons. This variation in numerical values was ascribed to a more complex effect of association upon the intermolecular properties of molal volume and boiling point than exists for the intramolecular property of molal refraction. This effect is to be expected in other highly associated classes of compounds, *e.g.*, in the carboxylic acids.

Li *et al.*,[50] have found independently that certain simplifications may be introduced in the treatment of those aliphatic compounds containing less highly associated functional groups. In the case of the saturated aliphatic sulfides and mercaptans, it was possible to eliminate all variables relating to the paraffin skeleton of the molecule by correlating the increment in property relative to the paraffin hydrocarbon of corresponding structure rather than relative to the "normal" sulfide or mercaptan. With this simplification the only variables required are a group contribution term for the functional group and rather simple interaction terms expressing modifications in the contribution of the functional group due to the presence of neighboring carbon atoms.

In those instances where it is applicable, the use of the corresponding paraffin as a reference compound possesses two distinct advantages over the use of a normal series reference. The first is the forementioned simplification in the number and complexity of the terms required for the empirical correlation of properties. The second is the greater confidence with which extrapolations often may be made. In many instances the data on physical or thermodynamic properties for a particular class of aliphatic compounds are quite meager and reliable values exist only for a few compounds of low molecular weight. Thus it becomes almost impossible to obtain numerical coefficients of skeletal parameters which will give dependable values for compounds of higher molecular weight. This difficulty is avoided if the skeletal parameters can be eliminated through the use of a paraffin reference.

The properties of polyfunctional aliphatic compounds may ostensibly be correlated by the method of isomeric increments, although the practical difficulties which may be encountered have not been investigated. If the paraffin of corresponding structure may be used as a reference compound, variables will be needed to express the group contribution of each functional group modified perhaps by reason of its attachment at a primary, secondary or tertiary carbon atom, and terms expressing the interaction of the functional groups with each other and with the carbon skeleton. The use of a normal series reference seems to be limited for practical purposes to compounds containing two functional groups. Probably the most convenient reference series would be that in which the functional groups were attached to either end of a normal carbon chain. This would minimize the effects of functional group interactions in the reference series.

Another class of compounds for which the present method seems to hold some promise is the monoölefin hydrocarbons. The most detailed correlation based upon structural parameters which has been proposed for the monoölefins seems to be that of Taylor, Pignocco and Rossini.[38] Their correlation employs the paraffin of corresponding structure as a reference compound and the terms of the equation are accordingly of the functional group contribution and interaction type. The olefinic group, C=C, may be linked to the paraffinic skeleton of the molecule, (designated as R) in any one of six different ways

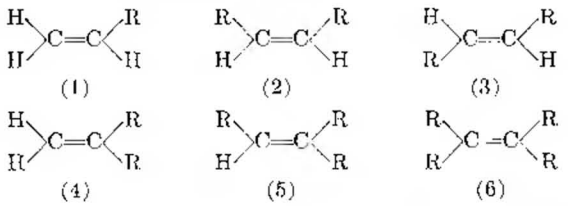

(1) (2) (3) (4) (5) (6)

with additional variations in forms (5) and (6) if the R groups are different. Taylor, Pignocco and Rossini combined forms (2) and (3), disregarded the possible variations in forms (5) and (6) and were

left with five forms each of which was regarded as making a unique functional group contribution to the increment in properties. A further refinement, analogous to the interaction terms of the present investigation, was the introduction of terms specifying the number of primary, secondary, tertiary and quaternary carbon atoms adjacent to the olefinic group. One variable was found to be redundant and the resulting equation possessed eight terms. This equation when fitted to the increments in molal volume, molal refraction and normal boiling point gave average deviations of approximately three to five times those obtained for the paraffin hydrocarbons using a six term equation. Refinements to the Taylor, Pignocco, Rossini correlation (designated as TPR) might proceed along two lines. First a more detailed analysis of the steric interference terms could be made after the manner of the present investigation, and in which *cis* and *trans* isomers were distinguished. As an example, consider the three di-*t*-butylethylenes

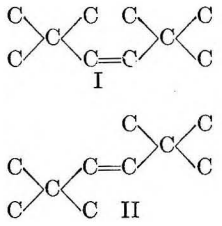

I

II

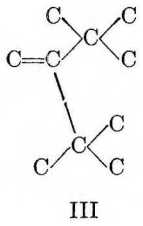

III

The TPR correlation does not distinguish between forms I and II, and form III is only distinguished by a different functional group classification. Yet each compound differs markedly in its compactness and degree of steric interaction, and accordingly in the values of its physical properties. A possible solution is to consider two types of steric interference induced by the valence angles of the olefinic group, 1-*cis*-2, occurring in compound I and 1-1, occurring in compound III. The maximum interference in these compounds does not occur between carbon atoms three bonds apart as in the paraffin hydrocarbons, but between carbon pairs 5 bonds apart in (I) and 4 bonds apart in (III) (*cf.*, 2,2,4,4-tetramethylpentane). It probably will be necessary, therefore, to consider interactions of the 1-*cis*-2 and 1-1 types between carbon pairs 3, 4 and 5 bonds apart. The magnitudes of some of these interactions undoubtedly will be dependent on over-all structure and not directly proportional to the number of carbon pairs (*cf.* the four bond steric term in the paraffins).

A second possibility is the use of the straight chain 1-monoölefins as a reference series in place of the paraffin of corresponding structure and the introduction of a new compactness term. In the development of this term the average distance between carbon pairs would be modified by the fixed angles at which the paraffinic portions of the molecule are joined to the olefinic group.

FLAT FLAME STUDIES ON ETHYLENE GLYCOL DINITRATE. I. TEMPERATURE PROFILES

BY R. STEINBERGER AND V. P. SCHAAF

Hercules Powder Company, Allegany Ballistics Laboratory, Cumberland, Md.

Received June 26, 1957

A method has been developed for stabilizing a stationary flat flame of a liquid monopropellant, using a fritted disk burner. The low-pressure flame of ethylene glycol dinitrate, stabilized in this manner, has been probed with fine-wire thermocouples. The resulting temperature profile, analyzed in terms of the volumetric heat release rate, shows the presence of two distinct reaction zones which can be correlated with the visible features of the flame.

In attempting to study the combustion of double-base propellants, the major difficulty has been the inability to stabilize a stationary laminar flame. Success has been achieved in slowing down or stopping the motion of the burning front sufficiently to allow spectroscopic examination[1,2] and probing[3] of the rather broad "dark" and "flame" zones. However, the initial reaction, which takes place at the propellant surface in a turbulent region called the "foam" zone, has not been susceptible to detailed study.

Since the principal reasons for this experimental impasse are physical, it has been found possible to make progress by changing the physical nature of the material, *i.e.*, by using liquid nitrate esters as models for the solid propellants. The burning characteristics of these compounds have been found to be quite comparable to those of the solids. It may be presumed, therefore, that any conclusions regarding burning mechanism derived from studying liquids may be applied directly to the solids. Several investigations have been reported[4-7] on the detailed structure of the reaction zone in liquid nitrate esters. The most advanced work is that of Needham and Powling[7] who established a stationary flat flame of ethyl nitrate at atmospheric pressure and measured temperature and composition profiles through the flame. Unfortunately this flame was not stable enough in space to allow analysis of the initial reaction zone, which extends no

(1) (a) R. G. Rekers and D. S. Villars, *Rev. Sci. Instr.*, **25**, 424 (1954); (b) R. G. Rekers and D. S. Villars, *J. Opt. Soc. Am.*, **46**, 534 (1956).

(2) A. D. Dickson, D. L. Rotenberg and B. L. Crawford, *Ind. Eng. Chem.*, **48**, 759 (1956).

(3) C. A. Heller and A. S. Gordon, THIS JOURNAL, **59**, 773 (1955).

(4) D. L. Hildenbrand, A. G. Whittaker and C. B. Euston, *ibid.*, **58**, 1130 (1954).

(5) D. L. Hildenbrand and A. G. Whittaker, *ibid.*, **59**, 1024 (1955).

(6) R. Steinberger and K. E. Carder, *ibid.*, **59**, 255 (1955).

(7) D. P. Needham and J. Powling, *Proc. Roy. Soc., London*, **A232**, 337 (1955).

more than 0.5 mm. from the liquid surface.

In the present work an attempt has been made to penetrate this early reaction zone, to measure accurately the temperature distribution within it, and to derive a heat release pattern from these data. The experimental approach involved the use of a fritted glass disk as a "wick," thus eliminating even minor fluctuations of the liquid surface. The model compound used was ethylene glycol dinitrate, which produced a stable flame on the fritted disk at a pressure as low as 50 mm. At this pressure the primary reaction zone was found to be sufficiently lengthened, *ca.* 4 mm., to allow detailed exploration with fine-wire thermocouples. Work now in progress is designed to yield composition profiles through this flame.

In separate experiments the final products of combustion were analyzed. A flame temperature was calculated on the basis of these analyses and was used to establish radiation corrections for the thermocouple readings.

Experimental

Materials.—Ethylene glycol dinitrate was prepared by mixed acid nitration of ethylene glycol. Nitrogen analysis by $FeCl_2$ reduction followed by $TiCl_3$ titration of the liberated Fe^{+3} gave, for different batches, 18.41 to 18.44% N (theory 18.42% N). The liquid was degassed before each experiment by evacuating for at least one hour at 60°.

Oxygen, nitrogen and propane were commercial products, not further purified. The propane was the C.P. grade (The Matheson Co., Inc.)

Reagents for the gas analyses were 37% KOH for the absorption of CO_2, a mixed acid of 98% concentrated H_2SO_4 and 2% concentrated HNO_3 for NO,[8] and freshly prepared acid Cu_2Cl_2 for CO.[9]

Flat Flame Studies

Apparatus.—As shown in Fig. 1, the apparatus included a burner tube located within a combustion chamber. Equipment was designed to feed in fuel, maintain constant pressure, ignite the fuel and measure the temperature at specific positions in the flame.

Burner Tube.—Combustions were carried out on a 33-mm.-diam. Pyrex fritted disk, porosity F (pore size 4–5.5 μ) ground flat on optical grinding machinery. The space beneath the disk was packed in order to avoid the accumulation of gas pockets and also to conserve fuel. A combination of 33-mm.-diam. Pyrex beads and fine sand was satisfactory for this purpose. However, a packing of lead shot and granular tin was preferred because it could be degassed more easily. Both packings were used during the course of experimentation. The fuel supply, 50 g. per experiment, was kept in a barricaded reservoir and admitted through a pneumatically operated pinch valve to a small reservoir attached to the burner tube (see Fig. 1). The flame was shielded by means of a 1-inch-long Pyrex cylinder (see Fig. 1), slotted to admit the thermocouple lead tube. A stainless steel screen, generally 14-mesh but variable during the course of experimentation, was supported in the cylinder approximately 12 mm. from the fritted glass disk.

Combustion Chamber.—The burner tube was cemented into a four-sided, four-windowed combustion chamber with an inside bore of 3 inches. Suitable connections were provided for fuel inlet, thermocouple leads and nitrogen inlet (for flushing). Evacuation was carried out through the lid, a vacuum seal being provided between the lid and chamber by means of a rubber gasket and silicone grease. The exit gases passed through a series of traps, ice, Dry Ice and liquid nitrogen (2 traps), before reaching the manostat and pumps. The manostat was the Cartesian diver type, Emil Greiner Style 8, modified by inclusion of a 3-way set valve to provide smoother action. Pressure was read on mercury manometers connected to the nitrogen inlet of the

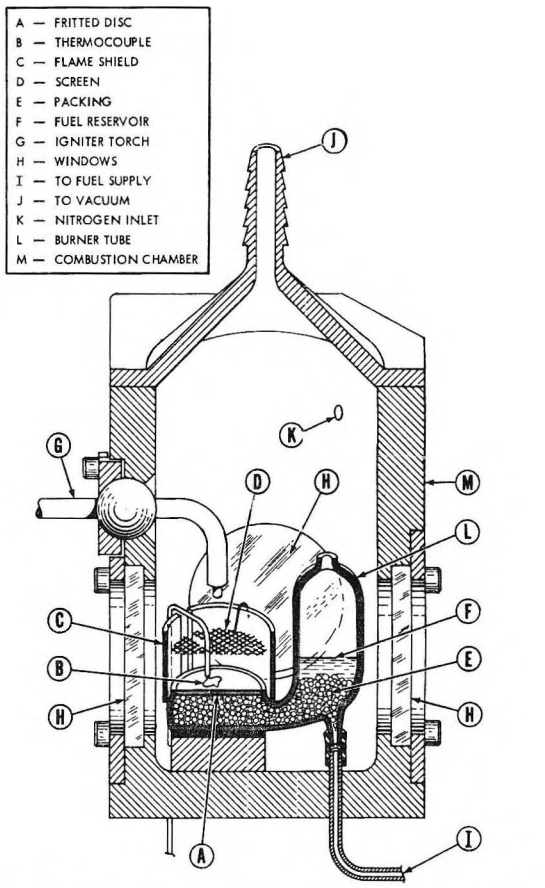

Fig. 1.—Flat flame burner tube and combustion chamber.

combustion chamber and thus outside the gas flow during an experiment. Evacuation was done by means of two mechanical oil pumps connected in parallel.

A small torch, burning propane–oxygen, was used to ignite the liquid fuel. The torch was freely movable inside the combustion chamber by means of a ball and socket joint with an O-ring seal inside the ball to allow sliding of the igniter tube.

During operation the combustion chamber was placed behind an explosion screen with 1/2-inch-thick "bullet-proof" glass windows.

Thermocouple.—Platinum and platinum–10% rhodium were used as the thermocouple materials. The leads were encased in "Ceramo" tubing (Thermo Electric, Inc.) which consists of an Inconel tube in which the wires are packed in a ceramic powder. The "Ceramo" tubing was brought into the combustion chamber through a packing gland. The tube was bent in such a way as to line up the thermocouple with the center of the disk and to allow the tube to be moved up and down in the slot of the shielding cylinder. On emerging from the "Ceramo" tube the thermocouple wires were bent parallel to the fritted disk and fused to short sections of thinner wires grading down to the final junction wire size. In the early stages of the work, 0.0003-inch-diam. wires were used for the junction. However, these were found to give erratic results, and 0.0001-inch-diam. wires were used in the final work. The thermal junction and all exposed wires were coated with NBS ceramic slip A-417 (samples graciously supplied by National Bureau of Standards and by Ceramic Color and Chemical Co.). The output of the thermocouple was recorded on the X-scale of an X-Y recorder (Brown Instrument Company).

The thermocouple was moved up and down slowly by means of a screw drive powered by a reversible clock motor. The position of the thermal junction was observed continually during an experiment through the telescope of a cathetometer (Gaertner Scientific Corp. Cat. No. M930-342). The motion of the traveling screw of the cathetometer was recorded on the Y-scale of the X-Y recorder by way

(8) C. L. Johnson, *Anal. Chem.*, **24**, 1572 (1952).

(9) V. J. Altieri, "Gas Analysis and Testing of Gaseous Materials," Am. Gas Assoc., New York, N. Y., 1945, p. 104.

of a helipot and bridge circuit. Illumination for this observation was provided by the beam of a microscope illuminating lamp passing through a 10-inch focal length double convex lens. No disturbance of the flame was noted as a result of the presence and motion of the thermocouple.

Flat Flame Combustion Procedure.—The fuel was degassed by heating to 60° under vacuum reflux conditions. Sufficient fuel to fill the bottom of the burner tube was then allowed to flow into the tube, and evacuation proceeded for one hour.

Ignition involved lighting the propane–oxygen torch at atmospheric pressure, closing the system by putting on the combustion chamber lid, and reducing the pressure slowly to $^1/_2$ atmosphere by manipulation of the manostat set valve. The propane flow was continually adjusted to maintain a stable flame. The torch was then played over the surface of the burner disk through the openings of the stabilizing screen. After the fuel ignited, the propane torch was turned off and the pressure was slowly reduced to the desired value, usually 53.0 ± 0.5 mm.

The initial position of the thermocouple was 4–5 mm. from the burner disk. After the flame was stabilized at the desired pressure, the thermocouple was driven down slowly (0.53 mm. per minute) toward the disk. As it moved, the cross hairs of the cathetometer telescope were kept trained on the thermal junction.

Fuel was allowed to flow into the small reservoir by intermittent (remote) operation of the pneumatic pinch valve. The liquid level in the small inside reservoir was maintained between the level of the disk and $^1/_2$ inch above it. The exact position of the liquid level was unimportant, inasmuch as the major driving force for liquid flow was the capillary action of the porous disk, rather than the liquid head in the reservoir. The chamber pressure was maintained constant within a ±0.5-mm. range by minor adjustments of the manostat. An experiment was stopped when the thermocouple reached the disk or when the 50-g. fuel supply was exhausted. The duration of an average run was 10 minutes.

Combustion Products

A separate combustion technique, utilizing a simple glass apparatus was employed to collect combustion products samples suitable for analysis.

Apparatus.—The fuel was contained in a tube, 16 mm. i.d., for runs at atmospheric pressure and 22 mm. i.d. for runs at reduced pressure. Ignition was provided by an electrically heated platinum wire, 0.024-inch diam., coated with A-417 ceramic slip. A pre-evacuated bulb of 1150 cc. volume was used to withdraw gas samples. The apparatus could be opened to the nitrogen supply or exhausted to the atmosphere or to the pumping system which was used in the flat flame setup. In experiments run for the determination of the amount of H_2O, a series of four liquid-nitrogen-cooled traps was incorporated in the system.

Combustion Procedure.—The fuel sample was degassed in its combustion tube by evacuation for 1–2 hours in a vacuum desiccator. The apparatus, except for the evacuated sample bulb, was flushed several times with N_2 and then filled with N_2 to a pressure slightly greater than atmospheric. The igniter wire was heated by connection to a 30-volt source. After ignition the gases were allowed to escape to the atmosphere for runs at atmospheric pressure or to the manostat and pumping system for runs at reduced pressure. In the latter case the pressure was slowly decreased to the desired value, usually 60–70 mm., by adjustment of the manostat. In the runs made for water analysis the combustion procedure was altered for the low-pressure runs to the extent of igniting at the desired final pressure rather than at atmospheric pressure, so that the entire combustion took place at constant pressure. After smooth, stable combustion conditions had been attained, the stopcock to the sample bulb was opened slowly, so as to induce a minimum of pressure disturbance. After the bulb had sufficient time to fill, its stopcock was closed, and the fuel sample was allowed to burn to completion.

Analytical Procedure.—The gas samples were analyzed in a standard Orsat-type apparatus. For runs at atmospheric pressure, the gas sample was transferred directly to the gas analysis apparatus, one sample being sufficient for four or more analyses. Samples obtained at reduced pressure were first concentrated to a 125-cc. volume by means of a Toepler pump and were sufficient for only one analysis.

Analyses for water were made by weighing the fuel before combustion and then the material caught in the four liquid-nitrogen-cooled traps after these had been allowed to warm to room temperature.

Analysis for formaldehyde, which was encountered only in the low-pressure runs, was carried out by adding excess 2,4-dinitrophenylhydrazine reagent to the liquid caught in the runs for water analysis and weighing the precipitate. This derivative had a melting point of 162–164°. After two recrystallizations it melted at 165–166° (literature value for the 2,4-dinitrophenylhydrazone of formaldehyde 166°). The water analyses were then corrected for the amount of formaldehyde found.

Treatment of Data

The general scheme of interpreting the temperature profiles obtained in this study is patterned after that used by Friedman and Burke[10] in their investigation of propane–air flames.

The raw data were first corrected for radiation errors by use of the equation

$$\Delta T = \Delta T_{max} \left(\frac{T + 273}{T_{max} + 273} \right)^4 \qquad (1)$$

where ΔT is the correction applied to the temperature T(°C.), and ΔT_{max} is the difference between the maximum observed temperature T_{max} and the theoretical flame temperature, 1377°, calculated on the basis of the analysis of the combustion products. For the runs reported here ΔT_{max} varied between 136 and 310°. Temperatures were read off the recorder trace at 0.1-mm. intervals, corrected according to the above equation, and replotted. A smooth curve was then drawn through these points and values of dT/dx determined from the curve by means of a Gerber Derivimeter (The Gerber Scientific Instrument Co.). The volumetric heat release rate Q was then calculated by use of the equation

$$Q = v\rho C_p \, dT/dx - d/dx \, (\lambda \, dT/dx) \qquad (2)$$

the second term on the right being determined by a process similar to that used for dT/dx. Here v is the linear burning rate of the fuel, which was determined by independent means to be 0.0026 cm./sec. at 53 mm.; ρ is the density of the fuel, 1.48 g./cm.^{3}; C_p is the heat capacity of the gas; x is the distance normal to the fritted disk; and λ is the conductivity of the gas. Since the gas is a mixture of unknown composition, and since this composition changes as a function of x, no precise values of the parameters C_p and λ can be assigned. As a first approximation, the gas was assumed to be triatomic with a molecular weight of 32. This represents an average between the final composition, in which the average molecular weight is 26 and the average atomicity is 2.4, and a hypothetical original composition ($NO_2 + CH_2O$) with a molecular weight of 38 and an atomicity of 3.5. The values tabulated for CO_2[11] were therefore used after correction for a molecular weight of 32.

Results

Appearance of Flame.—The ethylene glycol dinitrate flame has been described previously by Belajev[12] and our observations are in accord with his. The visible part of the flame is orange in color

(10) R. Friedman and E. Burke, *J. Chem. Phys.*, **22**, 824 (1954).

(11) "Tables of Thermal Properties of Gases," Nat. Bur. Standards (U. S.), Circ. 564, Nov. 1, 1955.

(12) A. F. Belajev, *Acta Physicochim. U.R.S.S.*, **14**, 523 (1941).

and is separated from the liquid surface by a nonluminous zone. At 53 mm. pressure the thickness of the dark zone is approximately 2 mm. The luminous zone is also approximately 2 mm. thick, but its upper edge is quite diffuse. No other visible features have been noted.

Stability of Flame.—When burning as a free liquid surface in a 20-mm. i.d. glass tube, the flame is stable down to a pressure of 40 mm., and linear burning rate measurements have been made from this pressure up to 1 atmosphere. However, stability on the fritted glass burner is not as good, and it has not been found possible to maintain a stable flame at pressures below 50 mm. In order to provide a margin of safety, actual experiments were performed at 53 mm.

It was of interest to determine whether the flame as stabilized on the fritted disk is equivalent to that on a free liquid surface. To this end the linear burning rate was measured in the flat flame apparatus by measuring the volumetric consumption rate and dividing by the area of the fritted disk; the rate was found to be 0.0025 cm./sec. at 53 mm. This is in good agreement with the value of 0.0026 cm./sec. found for a free surface at the same pressure.

Effect of Screen.—The stainless steel screen suspended at some distance from the burner disk in order to help stabilize the flame has a definite effect on the flame structure. This is shown in Fig. 2, where the normal curve (screen-to-disk distance 12 mm.) is compared to the curves obtained when the screen-to-disk distance was 6 and 9 mm. The curve obtained at a distance of 9 mm. shows differences from the normal but is similar enough to it to indicate that the 12 mm. distance approximates infinity.

It is clear that even at the 12 mm. distance the screen has some effect on the flame, since without it the flame becomes unstable. The exact function of the screen is not known, but it may help to dampen out flow disturbances, as postulated in other flat flame work.[13] In addition it can convey a small amount of heat to the burner disk by radiation.

Temperature Profiles.—The early work was done with 0.0003-inch-diam. thermocouple wires and with a thermocouple arrangement in which the heavier lead wires came down from the lead-in tube in a loop, the last 2 mm. of lead wire being approximately parallel with the flame. The records resulting from this arrangement were marked by a lack of reproducibility and by an excessively steep temperature gradient covering approximately one-third the total rise. This sharp gradient was aggravated by shortening the final small thermocouple wires and was eliminated by lengthening them. It was concluded that conduction of heat along the thermocouple assembly was responsible.

The thermocouple arrangement was then changed to use 0.0001-inch-diam. wires and to allow all of the lead wire loop to lie in the plane of the flame. The resulting curves were smooth and free of excessively steep gradients.

It was not found possible, however, to obtain results which were as reproducible as might be desired. This fact is illustrated in Fig. 3, in which the dotted and dashed curves represent different experiments under supposedly identical conditions of room temperature (28–29°), pressure (53 ± 0.5 mm.) and distance between fritted disk and stabilizing screen (12.0 ± 0.1 mm.). It is believed that the differences between curves are due to slight variations in pressure, which can be very important under these near-quenching conditions. The solid curve represents the average of the other three.

(13) R. Friedman, "Fourth Symposium on Combustion," The Williams and Wilkins Company, Baltimore, Md., 1953, p. 260.

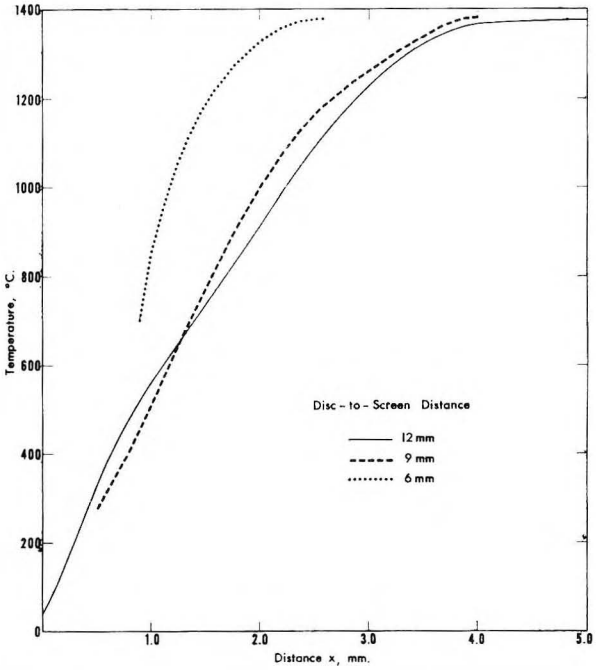

Fig. 2.—Variation of temperature profiles with disc to screen distance.

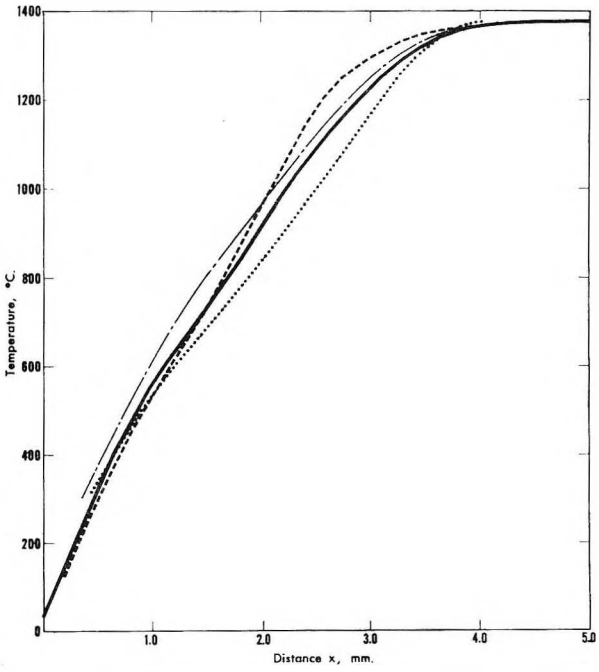

Fig. 3.—Variation of temperature profiles under supposedly identical conditions.

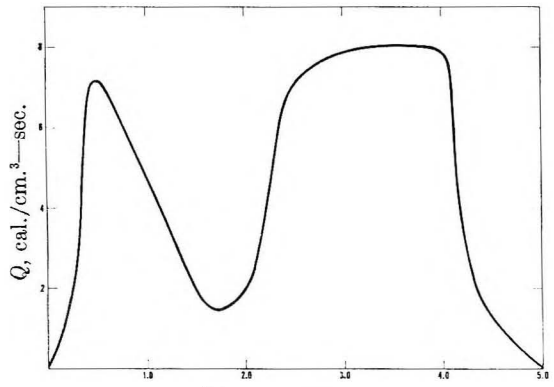

Fig. 4.—Heat release pattern.

In another set of experiments special attention was paid to the temperature at the fritted disk, which represents the liquid–gas interface. This measurement is difficult to make because the thermocouple lead wires interfere with the close approach of the junction to the disk. Most runs in which the approach was close enough to make extrapolation meaningful indicated that the surface temperature was essentially room temperature. In one experiment, in which the final thermocouple wires were 0.0003-inch diameter and made a 90-degree angle at the junction which pointed toward the disk, the temperature recorded as the junction touched the disk was 153°. The thermocouple was then driven down further, causing the thermal junction to slide along the disk and the immediately adjacent wires to lie on the disk essentially in an isothermal environment. The lowest temperature recorded in this manner was 29°. Aside from showing that the temperature at the liquid surface is not appreciably higher than room temperature, this experiment emphasizes the importance of conduction errors in these measurements.

On the basis of these special runs, the average curve of Fig. 3 has been extended to a surface temperature ($x = 0$) of 29°. The curve was then used to calculate the heat release pattern given in Fig. 4. In view of the limited precision of the data and the simplifications made in the calculations, this curve cannot be regarded as more than a first approximation. Nevertheless the distinct separation into two reaction zones appears to be beyond experimental uncertainty.

An internal check of the calculations is provided by integrating eq. 2 to get

$$\int Q\,dx = v\rho \int C_p\,dT - \lambda\,dT/dx \Big|_{x=0}^{x=0.5\text{ cm.}} \quad (3)$$

The first term on the right-hand side was found by stepwise integration to be 2.07 cal./cm.²-sec. The second term is zero at the upper limit, where $dT/dx = 0$, and has the positive value 0.20 cal./cm.²-sec. at $x = 0$. Thus the left-hand term is 2.27 cal./cm.²-sec., in good agreement with the value of 2.32 found by graphical integration of the Q *vs.* x curve (Fig. 4).

Composition of Products.—The composition of the combustion products is given in Tables I and II. It may be noted that each value represents the average of several determinations. Table I includes some values which were obtained with an uncoated igniter wire. As was to be expected, due to the catalysis by Pt of the reduction of NO,[14] these samples contained more CO_2 and N_2, and less NO, CO and H_2 than those obtained with a coated wire.

The analytical values were used to compute a decomposition equation for ethylene glycol dinitrate at both pressures

(1 atm.) $C_2H_4(ONO_2)_2 \longrightarrow 1.93NO + 0.06N_2 + 1.58CO + 0.38CO_2 + 0.32H_2 + 1.77H_2O$ (1)

(60–70 mm.) $C_2H_4(ONO_2)_2 \longrightarrow 1.95NO + 0.014N_2 + 1.51CO + 0.38CO_2 + 1.68H_2O + 0.19H_2 + 0.13CH_2O$ (2)

The slight deviations from correct stoichiometry represent experimental error. It may be seen that the change in products as a function of pressure is very slight, the most prominent feature being the small amount of formaldehyde appearing at the low pressure.

TABLE I

PRODUCTS OF COMBUSTION—GAS SAMPLES

Product	Mole %: 740–750 mm. bare igniter[a]	740–750 mm. coated igniter[b]	60–70 mm. coated igniter[c]
CO_2	11.6	8.8	9.1
NO	42.6	45.4	49.9[d]
CO	35.4	37.1	36.3
H_2	6.8	7.4	4.4
N_2[e]	3.6	1.4	0.3

[a] Average of 17 analyses of 4 samples. [b] Average of 8 analyses of 3 samples. [c] Average of 4 analyses of 4 samples. [d] Includes CH_2O. [e] By difference.

TABLE II

PRODUCTS OF COMBUSTION—TRAP CONTENTS

Pressure, mm.	Trap products[a]	Weight % CH_2O	H_2O
742–747	21.0	0.0	21.0
58–72	25.2	2.58[b]	22.6

[a] Average of 4 analyses at each pressure. [b] Average of 4 analyses.

Examination of the gas samples by infrared spectroscopy revealed no products except those included in the analytical scheme.

Flame temperatures were calculated from the above compositions, using a heat of explosion of 266.5 kcal./mole,[15] standard heats of formation, heat capacities for CO, CO_2, N_2 and H_2 from tabulated values[11] and for the other constituents from empirical equations compiled by Spencer.[16,17] The calculated heats of reaction are 95.9 and 92.1 kcal./mole and the flame temperatures are 1710 and 1650°K. at atmospheric pressure and 60–70 mm., respectively. No allowance was made in these calculations for dissociation. However, this is thought to be insignificant at the temperatures under consideration.

The analytical results and the flame temperatures are in substantial agreement with the values reported by Belajev.[12]

(14) R. Klein, M. Mentser, G von Elbe and B. Lewis, THIS JOURNAL, **54**, 877 (1950).

(15) W. H. Rinkenbach, *Ind. Eng. Chem.*, **18**, 1195 (1926).

(16) H. Spencer, *J. Am. Chem. Soc.*, **64**, 2511 (1942).

(17) H. Spencer, *Ind. Eng. Chem.*, **40**, 2152 (1948).

Discussion

Significance of Temperature Profiles.—In the present work it has been necessary to use the most stringent conditions deemed practical in order to get useful results. The thermocouple wires (0.0001-inch diam.) were the finest obtainable. Their length could not be increased appreciably without inviting undue loss due to breakage, warping, etc. It was not possible, therefore, to check the validity of the data by the usual method of applying more stringent conditions to see whether comparable results could be obtained. This is especially unfortunate in view of our inability to obtain greater precision. However, even the general shape of the temperature profile and of the derived heat release pattern are significant, especially when compared with similar data for a propane–air flame.[10] Thus it may be seen that the over-all reaction zone thickness is considerably less in the present case and the temperature gradient correspondingly steeper (maximum dT/dx is 5900°/cm. as compared to 1200°/cm. for a propane–air flame at slightly lower pressure and flame temperature). Moreover, the heat release pattern shows two peaks of comparable magnitude in place of the single major peak of the propane–air flame. The preheat zone observed in the latter flame is also completely absent here. The significance of these observations with respect to combustion mechanism must remain the subject of speculation for the time being.

The most feasible method for deriving greater meaning from this work appears to involve analysis of the flame gases as a function of distance. Experiments in this direction, using fine quartz probes and infrared and gas-chromatographic techniques, are now underway. Knowledge of the composition will allow more accurate calculation of the heat release pattern, because C_p and λ will be known more precisely. It should also be possible to determine the chemical reaction sequence and this should be correlatable with the heat release pattern.

Significance of Dark Space.—Belajev,[12] on observing the gap between liquid surface and luminous flame, concluded that the fuel vaporizes and is preheated in this dark space and then burns in the visible flame zone. The present data are at variance with this view. The visible flame begins approximately at the start of the second heat release peak (see Fig. 4). However, there is considerable heat production in the first (dark) zone also and the value of Q is always positive, rather than negative as would be expected for a vaporization and preheating process. Therefore the dark zone must be regarded as a reaction zone as well.

The question of vaporization at the liquid–gas interface was discussed in a previous paper[6] in which it was shown that, if the temperature gradient is assumed to be continuous across the interface, the gradient is much too small to provide heat for vaporization at the required rate. This conclusion was challenged by Hildenbrand,[18] who pointed out that the heat flow rather than the temperature gradient is continuous, so that the assumption regarding the gas phase temperature gradient was not justified. Temperature data for the gas phase adjacent to the surface were not available at that time, so that the situation could not be evaluated experimentally. The present data are appropriate, however, for such an evaluation, and a simple calculation has been made using the same relationships as before. The experimental temperature gradient is 5900°/cm. and the heat conductivity of ethylene glycol dinitrate vapor is estimated to be 3.7×10^{-5} cal./cm.^{2}-deg.-sec. Therefore the heat which could be transferred through the layer of vapor next to the surface is 0.22 cal./cm.^{2}-sec. In addition, as much as 0.10 cal./cm.^{2}-sec. could be transferred to the disk by radiation from the screen, this figure being based on a measured screen temperature of 530°. The heat necessary for vaporization, on the other hand, is 0.45 cal./cm.^{2}-sec., based on a heat of vaporization of 17,870 cal./mole[19] and a linear burning rate of 0.0026 cm./sec. Thus the heat necessary for vaporization at the burning rate is 50% greater than the heat which could be transferred by conduction and radiation. However the difference is not very great and may be coming dangerously close to experimental error. Therefore, the previous conclusion of "no vaporization" can no longer be stated with any degree of certainty.

Conclusion

By the use of a fritted glass burner it has been found possible to stabilize a stationary flat flame of ethylene glycol dinitrate at pressures as low as 50 mm. Temperature traverses have been made through this flame with 0.0001-inch-diameter thermocouples. The flame has been found to consist of two physically separate reactions. Further work now in progress involves analysis of the flame gases as a function of distance.

(18) D. L. Hildenbrand, THIS JOURNAL, **59**, 672 (1955).

(19) T. E. Jordan, "Vapor Pressure of Organic Compounds," Interscience Publishers, Inc., New York, N. Y., 1954, p. 189.

THE SIMULTANEOUS MEASUREMENT OF DISTRIBUTION COEFFICIENTS AND HYDROLYSIS RATES

BY ELIAS KLEIN, JOHN B. MCKELVEY AND BEVERLY G. WEBRE

Southern Regional Research Laboratory,[1] *New Orleans, Louisiana*

Received August 12, 1957

When butadienediepoxide is reacted with cotton cellulose in the presence of aqueous sodium hydroxide a three-phase reaction system is involved. Two of the important parameters are the distribution of the reagent between the organic and aqueous phases, and the rate of hydrolysis of the reagent in the latter. Consequently, a technique which would allow the measurement of the distribution coefficient and the hydrolysis rate as a function of base strength was highly desirable.

The measurement of heterogeneous hydrolysis involving two phase systems was first treated by Goldschmidt and Messerschmidt[2] who studied the hydrolysis of an ester distributed between an aqueous acid solution and benzene. Their method took into consideration the distribution coefficient of the ester, but required an independent measurement for the determination of its value and a total ester analysis.

The case of a reversible reaction of an olefin distributed between the gas and aqueous phases has been described by Levy, *et al.*[3] The distribution coefficient in this instance was determined from the slope of an appropriate experimental pressure plot. In a recent publication Larsson[4] has derived a simpler method for calculating from appropriate measurements the distribution coefficient and rate constant for a solute distributed between two phases, in one of which it reacts. His method, however, involves the analysis of the solute concentration in the reacting phase in the presence of its own reaction product; this leads to severe analytical complications in many cases. Consequently, we have arrived at an analogous equation involving the change with time of the solute concentration in the inert phase; extension of this idea to a system involving a gas phase leads to the determination of the Henry's law constant. This differs from the results of Levy, *et al.*,[3] in that it is derived for an irreversible first-order reaction.

We define the symbols

$(A)_o$ and $(A)_w$	= concn. in moles/l. of the solute in the organic and aqueous phases, resp.
V_o and V_w	= vol. in l. of the organic and aqueous phases, resp.
k	= reaction rate constant of the solute in the aqueous phase leading to the first reaction product
(A'')	= dimeric form of the solute
p	= partial pressure of the solute in equilibrium with a soln. of the solute
t	= time
K	= distribution coefficient between the organic and aqueous phases

If the concentration of the solute decreases in the aqueous phase by a first-order kinetic mechanism described by $(A)_w \longrightarrow (P)_w$ where P is the first reaction product, then

$$d(P)_w/dt = -d(A)_w/dt = K(A)_w \qquad (1)$$

By reasoning similar to Larsson[4] one can derive a relationship between the variables based on solute analyses in the inert phase

$$\ln (A)_o^0 - \ln (A)_o = \frac{kV_w}{KV_w + V_o} t \qquad (2)$$

where $(A)_o^0$ is the concentration of the solute in the organic phase after distribution has occurred, but before hydrolysis. Except in the case of very slow reactions this value cannot be measured with any degree of accuracy.

A plot of $\ln (A)_o$ *versus* time then yields a slope involving both the rate and distribution constants; by the solution of simultaneous equations utilizing two ratios of V_o/V_w these constants can be evaluated.

In the case of a gaseous solute, the same technique leads to an equation in terms of the partial pressure of the solute

$$\ln p^0 - \ln p = t \frac{kRTV_w}{K'V_o + RTV_w} \qquad (3)$$

where p^0 is the initial pressure of the solute after distribution has occurred, and K' is the Henry's law constant. The same method can then be used to treat the slope values to determine the constants.

If the kinetics follow a self-collision process, a parallel derivation leads to an equation in terms of $1/(A)_o$ and $1/p$.

For those solutes which associate in the organic phase the derivation is complicated by the fact that only the monomeric species is involved in the phase equilibria, but both monomeric and associated solute species must be considered in the analysis of the inert phase.

By defining an association constant in the inert phase

$$a = (A'')_o/(A')_o^2 \qquad (4)$$

the total concentration of the solute in the organic phase at any time t can be expressed by

$$(A)_o = (A')_o + 2(A'')_o = (A')_o + 2a(A')_o^2 \qquad (5)$$

In order to solve for $(A')_o$ for subsequent use in the distribution and kinetic relationships the coordinates are transposed and one obtains

$$(A')_o = 1/4a \times [(8a(A)_o + 1)^{1/2} - 1] \qquad (6)$$

Equation 6 may then be used in deriving the desired relationships using the same reasoning as employed for eq. 2, with the restriction now that the distribution coefficient involves only the monomeric species; *i.e.*, $K = (A')_o/(A)_w$. The resulting equation is

(1) One of the laboratories of the Southern Utilization Research and Development Division, Agricultural Research Service, United States Department of Agriculture.

(2) H. Goldschmidt and A. Messerschmidt, *Z. physik. Chem.*, **31**, 235 (1899).

(3) J. B. Levy, R. W. Taft, Jr., D. Aaron and L. P. Hammett, *J. Am. Chem. Soc.*, **73**, 3792 (1951).

(4) L. Larsson, *Acta Chem. Scand.*, **10**, 1071 (1956).

TABLE I

1 NaOH, N	2 Vol. CCl_4, ml.	3 Vol. H_2O, ml.	4 Slope $\times 10^3$	5 Error of the slope $\times 10^4$	6 k, $min.^{-1}$	7 NaOH activity coefficient γ	8 k/activity OH^-
0.5015	25.00	25.00	−2.478	0.82	0.00861	0.693	0.0248
0.5015	15.00	40.00	−3.140	1.71			
1.0030	25.00	25.00	−4.518	1.04	.01624	.679	.0232
1.0030	15.00	40.00	−5.827	1.85			
1.4840	25.00	25.00	−6.413	0.74	.03013	.683	.0297
1.4840	15.00	40.00	−9.412	2.98			
2.054	25.00	25.00	−7.828	1.54	.04078	.701	.0283
2.054	15.00	40.00	−12.320	1.94			

$$\frac{V_w u^{1/2}}{V_o} + \left[\frac{V_w}{V_o} + \frac{1}{K}\right] \ln (u^{1/2} - 1) = \frac{-kt}{K} + \text{Constant} \qquad (7)$$

where

$$u = 8a(A)_o + 1 \qquad (8)$$

If the association constant a is determined from independent data, such as freezing point depressions, the value of u can be calculated. Because of the appearance of K on the left side of equation 7 no direct plot is applicable, but a method of successive approximations can be used to determine K and k.

Experimental

Materials.—The butadienediepoxide was obtained from Union Carbide and Carbon Chemical Co.[5] and was used without further purification. The carbon tetrachloride was Reagent Grade. The NaOH solutions were prepared from the reagent grade material and analyzed with standardized HCl.

Procedure.—The kinetic runs were carried out in water-jacketed solubility burets having a 60-ml. capacity. The procedure was as follows: the water jackets of the burets were filled with water from the constant temperature bath maintained at 25.00 ± 0.01° and the lower outlet of the jacket clamped off so that the jacket remained full during the loading process. A fixed volume of standardized NaOH solution was then pipetted into the inner chamber of the buret; following this a fixed volume of 0.1997 M solution of butadienediepoxide in CCl_4 was added by pipet. The time at which half of the second pipet had emptied into the reaction chamber was taken as the starting time of the measurement. The pipet was then agitated immediately and placed into a tumbling rack in the constant temperature-bath. After a predetermined time interval the pipet was removed from the bath with the water jacket filled and the phases separated. The concentration of the diepoxide in the CCl_4 was then determined on a 10.00-ml. titer using the method of Durbetaki.[6] The HBr reagent was standardized periodically between samples.

Results

The log of the remaining diepoxide concentration in the CCl_4 layer was plotted against the reaction time, and the slope of the line determined by the method of least squares. The error σ associated with the slope determination[7] also was calculated for each run. The values of the slopes calculated for two series utilizing varying ratios of V_o/V_w were then used to calculate the distribution coefficient K and the hydrolysis rate constant k. It must be emphasized that in this instance k represents the rate constant for the hydrolysis of the first oxirane ring, since this removes the butadienediepoxide from participation in the phase distribution equilibria. Since the two oxirane rings are equivalent, this does not present any complications.

Table I presents a summary of the data obtained; the first column gives the concentration of the NaOH in the aqueous phase; the following two columns give the volumes of the organic and aqueous phases, respectively; the fourth column gives the slope of the log $(A)_o$ *versus* time plot as determined from the least squares equation; the fifth column shows the error σ_b associated with this slope determination and the sixth column gives the calculated values of k. In addition we have shown the activity coefficients of the NaOH solutions (on a molarity basis) as estimated from interpolation of data given by Harned and Owen[8] and finally the ratio of the experimentally determined value of k to the activity of the NaOH.

If one may assume that the uncatalyzed hydrolysis of butadienediepoxide is very slow compared to the base-catalyzed reaction, the rate of the hydrolysis may be expected to follow an equation of the type

$$\text{rate} = k^0 (\text{activity of } OH^-)(\text{activity of epoxide}) \qquad (9)$$

Under the experimental conditions employed this reduces to a pseudo-first-order reaction which may be expressed as

$$\text{rate} = k (\text{activity of epoxide}) \qquad (10)$$

where

$$k = k^0 (\text{activity of } OH^-)$$

The last column in Table I gives the ratio k/(activity of OH^-); for the concentration range employed the constancy of this ratio is acceptable, indicating a direct relationship between the reaction rate constant and the OH^- activity. This relationship also has been found to hold for the base-catalyzed hydrolysis of diacetone alcohol.[9]

The results do not lend themselves to interpretation on the basis of the transition state theory both because of the high ionic strengths involved, and because of the accuracy limitations.

The average rate constant, 26.5×10^{-3} l. $mole^{-1}$ $min.^{-1}$ for the alkaline hydrolysis of butadienediepoxide found in this investigation is in harmony with the values reported by Hansson[10] for the alkaline hydrolysis of ethylene oxide, propylene

(5) The mention of trade names and firms does not imply their endorsement by the Department of Agriculture over similar products or firms not mentioned.

(6) A. J. Durbetaki, *Anal. Chem.*, **28**, 2000 (1956).

(7) M. Ezekiel, "Methods of Correlation Analysis," 2nd ed., John Wiley and Sons, New York, N. Y. 1947, p. 315.

(8) H. S. Harned and B. B. Owen, "The Physical Chemistry of Electrolytic Solutions," 2nd Ed., Reinhold Publ. Corp., New York, N. Y., 1950.

(9) G. Akerlof, *J. Am. Chem. Soc.*, **49**, 2955 (1927).

(10) J. Hansson, *Svensk. Kem. Tidschr.*, **66**, 351 (1954).

TABLE II

NaOH, N	Distribution coefficient K
0.5015	0.509
1.003	0.561
1.484	1.040
2.054	1.166

oxide, glycidol and epichlorohydrin: 6.88×10^{-3}, 6.31×10^{-3}, 6.9×10^{-3} and 23.5×10^{-3} l. mole^{-1} min.$^{-1}$, respectively.

Table II lists the values of K, the distribution coefficient for the various NaOH concentrations. Since activity coefficients of butadienediepoxide in aqueous solutions are not available, no relationship has been found between the distribution coefficient and the salt strength of the aqueous layer.

THE SELF-DIFFUSION COEFFICIENT OF STRONTIUM AS COUNTERION TO POLYSTYRENE SULFONIC ACID[1]

BY J. P. DUX AND J. STEIGMAN[2]

Contribution from the Department of Chemistry, Polytechnic Institute of Brooklyn, Brooklyn, New York

Received August 14, 1957

The self-diffusion coefficients of strontium as a counterion to the strong electrolyte polystyrene sulfonic acid in dilute aqueous solution were measured at 25°. The coefficients were independent of the time of diffusion, pointing to an exchange between free and bound strontium which is more rapid than the diffusion process. For a low molecular weight polyelectrolyte the diffusion coefficient of the strontium was independent of the degree of neutralization. For a higher molecular weight material the coefficient dropped markedly after about 35% of the acid had been neutralized. These results are interpreted in terms of a preferential neutralization of low molecular weight material. Barium replaced strontium with difficulty in these solutions. The exchange rate between barium and strontium was more rapid than the diffusion.

I. Introduction

There is not yet available a completely satisfactory theory which explains the behavior of polyelectrolyte solutions. However, there has emerged in recent years[3-7] a qualitative picture of such solutions which has been generally accepted. The polyions are regarded as volume elements of high charge density in the solution. The counterions are grouped about them in a distribution described by a Poisson–Boltzmann function. The counterions would thus have a high concentration in or near the volume occupied by the polyions, with their density decreasing gradually with distance. Wall, Huizenga and Grieger[5] have further simplified this picture by dividing the counterions into two groups—those which travel with the mobility of the polyion, and those which are "free" —*i.e.*, move essentially independently of the polyion. This simplification is certainly not true in a rigorous sense. However, it is a useful concept for the interpretation of transport phenomena in polyelectrolyte solutions.

This paper describes the self-diffusion of strontium ions as counterions to polystyrene sulfonic acid, interpreted in terms of the simplified division of these ions into "free" and "bound" particles. The treatment which is developed for this case resembles that of Wang,[8] which was applied to the self-diffusion of water in protein solutions.

(1) From a thesis submitted by James P. Dux to the Graduate School of the Polytechnic Institute of Brooklyn in partial fulfillment of the requirements for the degree of Doctor of Philosophy.

(2) To whom inquiries should be addressed.

(3) R. Fuoss and J. Cathers, *J. Polymer Sci.*, **4**, 121 (1949).

(4) G. Kimball, M. Cutler and H. Samelson, THIS JOURNAL, **56**, 57 (1952).

(5) J. Huizenga, P. Grieger and F. Wall, *J. Am. Chem. Soc.*, **72**, 2636, 4228 (1950).

(6) F. Osawa, I. Nobuhisa and I. Kagawa, *J. Polymer Sci.*, **13**, 93 (1954).

(7) R. Fuoss, *Disc. Faraday Soc.*, **11**, 125 (1951).

(8) J. H. Wang, *J. Am. Chem. Soc.*, **76**, 4755 (1954).

II. Theory

Consider a solution of a polyelectrolyte, composed of γ different types of polyions, where γ refers to the degree of polymerization. There will also be present a sufficient number of counterions to ensure electroneutrality. Some of the counterions are considered to be bound to the polyions, and some are free of them. The latter are moving with a diffusion coefficient which depends only upon the counterion and the solvent.

By way of definition let

C_A = concn. of free counterions
C_n = concn. of counterions bound to the polyion of degree of polymerization n (*i.e.*, the nth polyion)
D_A = diffusion coefficient of the free counterions
D_n = diffusion coefficient of the nth polyion
C_T = total concn. of counterions = $C_A + \sum_n C_n$
f_A = fraction of counterions which are free = C_A/C_T
f_n = fraction of counterions bound to nth polyion = C_n/C_T
f_P = total fraction of bound counterions = $\sum_n f_n$
g_n = fraction of bound counterions bound to nth polyion = $\dfrac{C_n}{\sum_n C_n}$

It is assumed that the exchange rate between free and bound counterions is much more rapid than the rate of diffusion for either species. The question of exchange rate has been considered by Wall and his co-workers.[9] They have concluded that in sodium polyacrylate solution there are two rates of exchange for the sodium ions—one instantaneous, and the other rapid, but finite. Similar considerations have been advanced by Fuoss and Cathers[3] and by Kagawa and his co-workers.[6] The assumption that the rate of exchange between free and bound counterions is faster than the dif-

(9) F. Wall, P. Grieger, J. Huizenga and R. Doremus, *J. Chem. Phys.*, **20**, 1200 (1952).

fusion rates is equivalent to the assumption that an effective equilibrium is maintained between the free and the bound counterions at all points along the diffusion path. We may thus write

$$K_n = \frac{C_n}{C_A} \tag{1}$$

where K_n is the equilibrium constant governing the exchange. The further assumption is made that the polyions exchange their bound counterions only by way of the free counterions. This assumption is described by the equation

$$\frac{\partial f_A}{\partial t} = -\sum_n \frac{\partial f_n}{\partial t} \tag{2}$$

in which t is the time. This states that a change in the concentration of counterions bound to a given polyion produces an equal and opposite change in the concentration of free counterions. The assumption on which the equation is based is probably true only in dilute solution.

On the basis of equation 2, one may write

$$\frac{\partial C_T}{\partial t} = \frac{\partial C_A}{\partial t} + \sum_n \frac{\partial C_n}{\partial t} \tag{3}$$

Applying Fick's second law of diffusion, assuming linear diffusion in the x direction, it follows that

$$D\frac{\partial^2 C_T}{\partial x^2} = D_A\frac{\partial^2 C_A}{\partial x^2} + \sum_n D_n\frac{\partial^2 C_n}{\partial x^2} \tag{4}$$

From the definition

$$C_T = C_A + \sum_n C_n$$

we may write

$$\frac{\partial^2 C_T}{\partial x^2} = \frac{\partial^2 C_A}{\partial x^2} + \sum_n \frac{\partial^2 C_n}{\partial x^2} \tag{5}$$

From equation 1 it follows that

$$\frac{\partial^2 C_n}{\partial x^2} = K_n\frac{\partial^2 C_A}{\partial x^2} \tag{6}$$

By means of equations 5 and 6, it is possible to eliminate $\partial^2 C_A/\partial x^2$ and $\partial^2 C_n/\partial x^2$ from equation 4, to yield

$$D\frac{\partial^2 C_T}{\partial x^2} = \left(\frac{D_A + \sum_n K_n D_n}{1 + \sum_n K_n}\right)\frac{\partial^2 C_T}{\partial x^2} \tag{7}$$

and

$$D = -\frac{D_A + \sum_n K_n D_n}{1 + \sum_n K_n} \tag{8}$$

Equation 8 shows a relation between the observed diffusion coefficient D, and the diffusion coefficients D_A (of the free counterions) and D_n (of the counterions) bound to the different polyions. This equation can be transformed by replacing K_n by the term f_n/f_A, to yield

$$D = f_A D_A + \sum_n f_n D_n \tag{9}$$

Equation 9 states that the observed diffusion coefficient is the weighted mean of the diffusion coefficients of the different species of counterions present in the solution, where the weighting factors are the distribution of the counterions among the free ions and the various polyions. It is convenient to define a diffusion coefficient D_p in the following fashion

$$f_p D_p = \sum_n f_n D_n \tag{10}$$

and this leads to

$$D_p = \sum_n g_n D_n \tag{11}$$

The term D_p hence represents the weighted mean diffusion coefficient of the bound counterions. Equation 9 now becomes

$$D = f_A D_A + f_p D_p \tag{12}$$

According to equation 12, the diffusion coefficient D is a constant whose value depends only on the solution composition and the individual diffusion coefficients. In particular, it should be independent of the time of diffusion, since there are no time dependent quantities in the equation. This would not be true if exchange between free and bound counterions were slow compared to diffusion. With slow exchange, the faster (free) ions would diffuse out first, followed by the slow-moving (bound) ions. If an appreciable fraction of counterions were found, the observed diffusion coefficient should be a function of the time of diffusion. Since the polyelectrolyte which was studied is a strong one (highly charged in solution), and since the counterion is divalent, an appreciable fraction of the counterions should be bound. Hence, one indirect test of the validity of the assumption of rapid exchange in equation 1 is the study of the experimental diffusion coefficient as a function of time of diffusion.

This paper describes the behavior of a divalent cation, strontium, as counterion to a strong polyelectrolyte, polystyrene sulfonic acid, in dilute aqueous solution. The counterion behavior was investigated through a study of its self-diffusion coefficient in various solutions.

The work which is reported here includes the measurement of the tracer diffusion coefficient of strontium ions in solutions of hydrochloric and sulfuric acids, the measurement of self-diffusion coefficients of strontium ions in solutions of both low and high molecular weight sulfonated polystyrenes which are neutralized to differing extent, the variation in time of the self-diffusion coefficient, and the effect on the coefficient of an added barium salt.

Experimental

Materials.—Solutions of barium chloride, hydrochloric acid, sulfuric acid and strontium hydroxide were prepared from reagent grade materials.

Polystyrene (High Molecular Weight).—A sample obtained from the Dow Chemical Company was fractionated by precipitation from benzene by methanol. Viscosity measurements of the three resulting fractions were performed in toluene[10] and yielded a weight average molecular weight of 32,500.

Polystyrene (Low Molecular Weight).—Styrene monomer was polymerized with benzoyl peroxide in dilute carbon tetrachloride solution according to the method of Mayo.[11]

(10) R. H. Boundy and R. F. Boyer, Styrene, A.C.S. Monograph, Chap. 9, Reinhold Publ. Corp., New York, N. Y., 1950.

(11) F. R. Mayo, *J. Am. Chem. Soc.*, **70**, 3689 (1948).

A sample of the resulting polymer was fractionated by precipitation from dioxane solution by the addition of water. Eight fractions were obtained. Chlorine analysis for seven of these fractions permitted calculations of their molecular weights. The weight average molecular weight of the material was 1230. Its number average molecular weight was 1040.

Polystyrene Sulfonic Acid.—Sulfonation of both the higher and lower molecular weight polymers was performed according to the procedure developed by Bachman.[12] Approximately 400 mg. of polymer was heated in a test-tube together with 4 ml. of concentrated sulfuric acid at a temperature of 160° for four hours. The resulting dark, almost opaque solution was diluted with water, and passed through a Dowex II anion-exchange column in the hydroxyl state, in order to remove sulfate ion. Solutions for the diffusion experiments were prepared by dilution from analyzed stock solutions. The polyelectrolyte originating from the low molecular weight material was analyzed by precipitating the insoluble barium salt from a solution of a known weight of previously dried acid, igniting it, and converting it to barium sulfate. The molar ratio of sulfonic acid to barium was 2.27. The polysulfonic acid derived from the higher molecular weight material was analyzed by titrating aliquots of a solution containing a known weight of dried polymer, using 0.05 *N* sodium hydroxide. The calculated degree of sulfonation was 1.05, on the assumption that there was one molecule of water associated with each sulfonic acid group in the dried solid.

Diffusion Measurements.—The measurement of strontium diffusion was made by the open-ended capillary technique devised by Anderson and Saddington[13] and developed by Wang,[14] Kennedy,[15] Hoffmann[16] and others. The apparatus was similar to those described by Wang[14] and Hoffmann.[16] The diffusion cells had an inside diameter of approximately 1 mm., and were about 2.6 cm. long. One end was sealed flat by cementing to it a small piece of microscope slide glass by means of a thin film of Araldite CN 502 epoxy resin (Ciba Company). Before sealing, the length of the capillary was measured with a micrometer. After sealing, its volume was determined by filling it with mercury which was subsequently weighed.

One liter of a solution of the polystyrene sulfonic acid was prepared by dilution of an aliquot of a stock solution. This solution was partially or completely neutralized by adding the required amount of a saturated solution of strontium hydroxide from a microburet. It was then filtered through a sintered-glass funnel into a three-necked flask. The flask was immersed in a constant-temperature-bath at 24.6 ± 0.005°. A 10-ml. portion was withdrawn, centrifuged for a half-hour, and transferred to a clean, dry 10-ml. volumetric flask. By means of a small loop in a nichrome wire, a very small drop (0.01 ml. or less) of a radioactive, carrier-free Sr^{90}-Y^{90} solution was transferred to the 10-ml. aliquot. The specific activity of the resulting solution was enough to give about 2,000 counts per minute when a volume corresponding to that of an average capillary cell was dried on a cupped aluminum planchet, and counted under an end-window Geiger–Müller tube.

The tracer diffusion measurements in hydrochloric and sulfuric acid solutions were carried out in essentially the same way, except that the only strontium in such experiments was the very small drop of carrier-free Sr^{90}-Y^{90} transferred to the 10-ml. aliquot.

By means of micro-pipets, four capillaries were filled with the radioactive solution, attached to glass rods in the side necks of the three-necked flask, and immersed until the top of each capillary was just above the surface of the surrounding (non-radioactive) solution. They were maintained in this position for at least an hour to ensure thermal equilibration and then gently submerged to a level one to two inches below the surface. The time of submersion was recorded, stirring at 60 r.p.m., was started, and after a suitable diffusion period had elapsed the capillaries were removed. They were emptied onto aluminum planchets, washed twice with distilled water, filled with 1:1 HCl solution, allowed to stand one hour to clean adsorbed activity from the walls, and again washed twice with distilled water. The HCl solution and its washings were emptied on a second planchet. The initial activities of the capillaries, which were determined before each diffusion run, were measured in the same manner.

Adsorption.—Toward the end of this research it was discovered that some of the activity was being absorbed on the walls of the capillaries. The effect in general was quite small, changing the diffusion coefficient by less than 5%. The extent of adsorption was determined by treating each capillary with concentrated HCl, after the active solution had been removed. Where it was noted the diffusion coefficient was appropriately corrected. Such corrections were applied to the high molecular weight sulfonic acid.

Radioactive Counting.—Aluminum cupped planchets contained the solutions from the capillaries. These were evaporated to dryness and counted with a Geiger–Müller end-window tube and a standard scaling circuit. At least 5000 counts were recorded for each planchet. Because of the presence of yttrium-90, a 65-hour daughter of the 25-year strontium-90, the planchets were allowed to stand until radioactive equilibrium was established, which required four to five days.

Calculations.—The solution of Fick's law for the boundary conditions of these experiments is given[13] by the equation

$$\gamma = 8/\pi^2 \sum_{n=0}^{n=\infty} 1/(2n+1)^2 \exp\left(-\frac{(2n+1)^2\pi^2}{4l^2} D t\right) \quad (13)$$

in which γ is the ratio of the final to the initial activities in the capillary, D is the diffusion coefficient, t represents the time of diffusion, and l is the length of the capillary. This series converges very rapidly, and if the quantity Dt/l^2 is greater than 0.2, only the first term is considered, yielding

$$\gamma = 8/\pi^2 \exp(-\pi^2 Dt/4l^2) \quad (14)$$

from which the diffusion coefficient is calculated easily. However, it was found desirable to use more than the first term of the sum for short diffusion times and for small diffusion coefficients. The first four terms of the sum were therefore calculated for various assumed values of the ratio Dt/l^2 and the corresponding values of γ were plotted against the values of the ratio. The value of the ratio corresponding to a particular experimental value of γ could then be read from the graph, and the diffusion coefficient D could be calculated. Four terms of the sum were sufficient for all diffusion runs which were conducted in this work. This is equivalent to all values of the ratio which are greater than 0.02, or all values of γ which are less than 0.841.

IV. Experimental Results and Conclusions

A. Tracer Diffusion Coefficients in H_2SO_4 and HCl–NaCl Solutions.—The tracer diffusion coefficients of strontium ion were determined in sulfuric and hydrochloric acid solutions of varying concentrations. The time of diffusion was approximately 48 hours in all cases. All values reported are the average of at least three determinations, and usually four, run simultaneously in the same solution. The results are given in Tables I and II.

TABLE I

TRACER DIFFUSION COEFFICIENT OF Sr^{++} IN HCl–NaCl SOLUTIONS: COMPOSITION OF SOLUTION

HCl, moles/l.	NaCl, moles/l.	$D \times 10^5$, cm.²/sec.
9.5×10^{-4}	5.0×10^{-4}	0.681 ± 0.027
9.5×10^{-3}	5.0×10^{-3}	.809 ± .014
4.75×10^{-2}	2.5×10^{-2}	.797 ± .014
9.5×10^{-2}	5×10^{-2}	.750 ± .013
4.7×10^{-1}	2.5×10^{-1}	.739 ± .026

(12) G. B. Bachman, *et al.*, *J. Org. Chem.*, **12**, 108 (1947).
(13) J. S. Anderson and K. Saddington, *J. Chem. Soc.*, S381 (1949).
(14) J. H. Wang, *J. Am. Chem. Soc.*, **73**, 4181 (1951); **74**, 1183 (1952); **75**, 1768 (1953); **76**, 1528 (1954).
(15) J. W. Kennedy and R. Mills, *ibid.*, **75**, 5696 (1953).
(16) R. F. Hoffmann, *J. Chem. Phys.*, **30**, 1567 (1952).

TABLE II

TRACER DIFFUSION COEFFICIENT OF Sr^{++} IN H_2SO_4 SOLUTIONS

H_2SO_4, moles/l.	$D \times 10^5$, cm.²/sec.
9.57×10^{-4}	0.677 ± 0.012
9.57×10^{-3}	.658 ± .005
4.78×10^{-2}	.698 ± .031
9.57×10^{-2}	.713 ± .027
4.78×10^{-1}	.644 ± .012
9.57×10^{-1}	.623 ± .018

It can be seen that while there are some differences in the effects of the two anions, particularly at higher ionic strengths, the coefficients in the most dilute solutions are quite close, and tend toward a value of approximately 0.7×10^{-5} cm.²/sec.

B. Diffusion Coefficient and Time of Diffusion.—The self-diffusion coefficients of strontium ions were measured in two solutions for increasing periods of time. The first solution was composed of the high molecular weight material neutralized to the extent of 43.0% with strontium hydroxide; its concentration was 1.67×10^{-4} *M* before neutralization. The second solution was 8.43×10^{-5} *M* in low molecular weight acid, which was 58.2% neutralized. The results are shown in Table III.

TABLE III

STRONTIUM DIFFUSION COEFFICIENTS IN POLYION SOLUTIONS AS A FUNCTION OF TIME

Time of diffusion (hr.)	$D \times 10^5$ (cm.²/sec.) High mol. wt.	Low mol. wt.
43	0.518 ± 0.033	
67	.525 ± .024	0.519 ± 0.024
90	.....	.536 ± .008
91	.516 ± .026	
115	.....	.551 ± .022
139	.526 ± .043	

It can be seen that the self-diffusion coefficients are essentially constant for different times of diffusion. These results support the hypothesis implicit in equation 1, that the exchange rate between bound and free ions is faster than the diffusion process.

It can also be seen that the values of the diffusion coefficients are significantly lower than the values for the tracer diffusion coefficients in Tables I and II. This would indicate that some fraction of the strontium ions are bound to the polyanion, and diffuse with it. No distinction is made here between ionic binding and the time of relaxation effect, because no present theory permits quantitative estimation of the latter in the case of polyelectrolytes.

C. Effect of Barium Salts on Strontium Diffusion.—A solution of the sulfonic acid prepared from the high molecular weight polystyrene was completely neutralized by strontium hydroxide. Its concentration was 1.67×10^{-4} *M* in sulfonic acid. The self-diffusion coefficient of strontium was determined for this solution. Increasing quantities of barium chloride were added to aliquots of this solution, and the strontium diffusion coefficients were measured after each addition. In one additional experiment an aliquot of acid was completely neutralized with barium hydroxide, and a quantity of strontium chloride equivalent to the barium chloride of an earlier run was added. The results are reported in Table IV.

TABLE IV

BARIUM–STRONTIUM EXCHANGE

Ratio $(Ba^{++})/(Sr^{++})$	Sr. $D \times 10^5$ (cm.²/sec.)
0.0	0.440 ± 0.021
0.2	.450 ± .014
0.5	.511 ± .033
1.0	.451 ± .013
11.0	.646 ± .009
1.0 (Sr added to Ba)	.500 ± .008

It will be noted that the strontium diffusion coefficient is not changed very much by the addition of barium chloride, at least up to a barium–strontium ratio of unity. This incidentally indicates a much stronger interaction between sulfonate ions and strontium than between the polyions and barium, a result in marked contrast to that observed in ion-exchange columns. What is more important here is the question of whether the small effect of added barium is due to a very slow exchange with the bound strontium. Approximately the same coefficient (0.45×10^{-5}) is obtained by adding barium chloride to the polymer which was first neutralized by strontium hydroxide as is obtained by adding strontium chloride to polymer previously neutralized by barium hydroxide (0.50×10^{-5}). With a large excess of barium, the strontium is apparently displaced so that its self-diffusion coefficient approaches the values of Tables I and II in comparable regions of ionic strength. In this system it can again be concluded that the rate of exchange between free and bound ions is faster than the diffusion process.

D. Diffusion Coefficient and Degree of Neutralization.—Table V shows the measured diffusion coefficients of strontium ions in solutions of the polyacid of different degrees of neutralization. The acid concentrations before neutralization were the same as in Table III. In each case the time of diffusion was 67 hours.

TABLE V

% Neutralization	Low mol. wt. $D \times 10^5$ (cm.²/sec.)	% Neutralization	High mol. wt. $D \times 10^5$ (cm.²/sec.)
25.0	0.519 ± 0.024	10.0	0.562 ± 0.044
58.2	.562 ± .029	30.0	.619 ± .026
89.6	.563 ± .023	43.0	.525 ± .024
		57.0	.461 ± .038
		60.0	.411 ± .024
		75.0	.432 ± .032
		90.0	.432 ± .028
		100.0	.411 ± .024

This table shows that the self-diffusion coefficient of strontium ions acting as counterions to the low molecular weight polyelectrolyte is essentially independent of the degree of neutralization. On the other hand, the coefficient observed in solutions of the higher molecular weight material shows a downward trend with increasing neutralization.

A fruitful comparison can be made between these results and those reported by Wall, Huizenga and

Grieger.[5] They studied the diffusion coefficient of sodium as counterion to polyacrylic acid. They found a steady decrease in the coefficient with increasing neutralization from a value of 1.19×10^{-5} cm.^{2}/sec. at 9.6% neutralization to 0.47×10^{-5} at 98% neutralization. This is understandable in terms of the increasing charge on the polyion with increasing neutralization because of the transition from undissociated carboxyl groups to carboxylate ions. In turn, the increasing charge binds a larger proportion of the counterions to the polyion, and the measured sodium ion diffusion coefficient will decrease. In the case of polystyrene sulfonic acid, however, we are dealing with a strong polyelectrolyte, at least in the sense that there is little covalent character in the bond between protons and sulfonates. Increasing neutralization, therefore, should not change the total charge of the polyion, but will result in the replacement of hydronium ions by strontium ions.

One consequence of equation 12 is that any change in the observed diffusion coefficient D must be due to a variation in the diffusion coefficient of the free counterions, D_A, to a variation in the fraction of counterions bound, f_P, to a change in the weighted mean diffusion coefficient of the bound counterions, D_P, or to a combination of such changes. It is unlikely that the diffusion coefficient of the free counterions will change with degree of neutralization of the polyelectrolyte. Hence the observed decrease in diffusion coefficient with increasing neutralization for the high molecular weight material may be attributed to an increasing fraction of bound cations, a decreasing D_P, or both. The absence of such a decrease in coefficient in the case of the low molecular weight material raises the question of possible differences between the two poly-acids. One difference may be that the high molecular weight substance has trapped protons in the interior of the polymer. Mock, Marshall and Slykhouse,[17] in an investigation of polystyrene sulfonic acid have suggested that a certain fraction of the protons in solution remain trapped in the interior of the polyanion, close to the sulfonate groups. It is reasonable to expect that there will be a greater fraction of trapped protons in larger polymers than in small ones. Such trapped protons will be more difficult to displace by strontium ions than protons on the outside of the large polyanion or on a small polyanion. (The presence of low molecular weight material in the larger polyelectrolyte must be considered here because of possible degradation by the sulfuric acid used in the sulfonation. It is, in fact, suggested by the data in Table III. It can be seen that the diffusion coefficient for the strontium is almost the same in partly neutralized solutions of both low and high molecular weight materials.) If the lower molecular weight acids are neutralized first, the bound strontium will be associated with those polyanions. Further neutralization will involve the higher molecular weight materials, causing a redistribution of bound counterions. According to equation 11, the coefficient D_p depends on the diffusion coefficients of the individual polyanions (D_n) and the counterion distribution among them (g_n). A redistribution of the bound counterions to the larger, more slowly moving polyanions will cause a decrease in D_p as neutralization increases. Such a decrease in D_p will result in a decrease in the measured diffusion coefficient D.

One additional possibility must be considered. Trapped protons may tend to shield the polyanion from the solution and, hence, from the free counterions. As these protons are neutralized and replaced by strontium ions, charge shielding may decrease, and a greater fraction of the strontium present may be bound to the polyanion. This will result in an increase in f_p with increasing neutralization, and in turn will cause a decrease in the measured diffusion coefficient. It is possible that both effects—an increase in f_P and a decrease in D_p—are operating here.

Acknowledgment.—This research was supported by the U. S. Army Signal Corps under contract number DA36-039, Sc 5596. We are grateful to Professor F. C. Collins for many helpful discussions. We thank Professor F. Wall for permission to reprint data from one of his papers.

(17) R. A. Mock, C. A. Marshall and T. E. Slykhouse, THIS JOURNAL, 58, 498 (1954).

THE SOLUBILITY AND ENTROPY OF SOLUTION OF IODINE IN n-C_7F_{16}, c-$C_6F_{11}CF_3$, $(C_3F_7COOCH_2)_4C$, c-$C_4Cl_2F_6$, CCl_2FCClF_2 AND $CHBr_3$

BY KŌZŌ SHINODA AND J. H. HILDEBRAND

Contribution from the Department of Chemistry, University of California, Berkeley, California

Received August 27, 1957

The solubility of iodine in six solvents, five of which have very low solubility parameters, has been determined over a range of temperature with the following results, expressed as mole % of iodine, $100x_2$, and $R(\partial \ln x_2/\partial \ln T)_{sat}$ at 25°: in n-C_7F_{13}, 0.01837, 34.4; in c-$C_6F_{11}CF_3$, 0.02101, 31.7; in $(C_3F_7COOCH_2)_4C$, 0.1170, 26.3; in c-$C_4Cl_2F_6$, 0.1241, 26.2; in CCl_2FCClF_2, 0.2447, 24.35; in $CHBr_3$, 6.249, 17.8. Solubility parameters of the solvents calculated from these values of x_2 and the parameter of iodine, 14.1, are less by from 0.2 to 0.4 than those calculated from the heat of vaporization. The points for these additional "poor" solvents fall upon an extension of the straight line when $R(\partial \ln x_2/\partial \ln T)_{sat}$ is plotted against $-R \ln x_2$.

This investigation was undertaken chiefly in order to fill in the long interval in solvent power between 1,1-dimethylbutane and perfluoro-n-heptane shown in Fig. 1 of the paper by Hildebrand and

Glew,[1] and to throw further light upon the factors, especially partial molal and relative molal volumes, that affect the entropy of solution, made strikingly evident in our very recent paper.[2] Bromoform was included in order to extend the range beyond carbon disulfide in the direction of high solubility.

Materials and Procedure.—The f-methylcyclohexane, c-$C_6F_{11}CF_3$, and the *n*-perfluoroheptane, *n*-C_7F_{16}, were purified by the method described by Glew and Reeves.[3] The cyclo-*o*-dichlorohexafluorobutane, c-$C_4Cl_2F_6$, obtained from Peninsular Chem. Research Inc., was dried over silica gel and distilled. The boiling point was constant at 59.4° and 752 mm. The tetraperfluorobutyric ester of pentaerythritol, $(C_3F_7COOCH_2)_4C$, was obtained from Minnesota Mining and Manufacturing Co., through the kindness of Dr. Nelson W. Taylor. It had been vacuum distilled at *ca.* 0.5–2 mm. and 160°. Its refractive index is 1.3340 at 25°. The "Genetron 113," $CCl_2F{\cdot}CClF_2$, obtained from Allied Chemical and Dye Co., was dried over $CaCl_2$ and distilled. The boiling point was 47.5–47.7° at 760 mm. The $CHBr_3$ was Baker "purified" dried over $CaCl_2$ and distilled twice in a stream of argon by Jolley. The iodine, Merck "reagent, resublimed," was resublimed and kept in a desiccator.

The solubility was determined in the apparatus described by Glew and Hildebrand. Saturated solutions of iodine were prepared by continuous stirring of the two-phase mixture in a thermostat, for 72 hr. in the case of $(C_3F_7COOCH_2)_4C$, 24 hr. in the case of $C_6F_{11}CF_3$, *n*-C_7F_{16}, c-$C_4Cl_2F_6$ and CCl_2FCClF_2, and 6 hr. in the case of $CHBr_3$. Further stirring caused no increase in solubility. Solubility in bromoform decreased by about 2% after 4 days at 30°; therefore only fresh solutions were used. Because of the viscosity of the solutions in $(C_3F_7COOCH_2)_4C$, the stirring was interrupted for 2 hours before drawing off samples for analysis in order to allow any fine particles of iodine to settle. The samples were analyzed by titration with thiosulfate, in concentrations appropriate to the widely different solubilities.

Results

The observed results are shown in Table I as mole %, $100x_2$. Each value is the mean of three analyses at each temperature. The root mean square deviation corresponds to about 0.6%. The values in the last column of Table I were calculated by aid of equations in the form $\log x_2 = -A/T + B$, with the following values of A and B

	A	B
n-C_7F_{16}	2240.6	3.7790
c-$C_6F_{11}CF_3$	2066.0	3.2518
$(C_3F_7COOCH_2)_4C$	1715.7	2.8228
c-$C_4Cl_2F_6$	1710.3	2.8305
$CCl_2F{\cdot}CClF_2$	1586.6	2.7100
$CHBr_3$	1157.8	2.6791

Our value for the solubility of iodine in C_7F_{16} at 25° is very close to the figure reported by Glew and Hildebrand, and the temperature dependence is identical. We checked the former work in order to be very sure of the high figure for the entropy of this solution.

Values for the entropy of solution of solid iodine are obtained by aid of the equation

$$\bar{s}_2 - s_2^S = R(\partial \ln x_2/\partial \ln T)_{sat}(\partial \ln a_2/\partial \ln x_2)_T \quad (1)$$

Table II shows, first, values of $R(\partial \ln x_2/\partial \ln T)_{sat}$ corresponding to the slopes, A. The factor $(\partial \ln a_2/\partial \ln x_2)T$, expressing the deviation from Henry's law, is close to unity for nearly ideal and also for very dilute solutions. It can be estimated by aid of the regular solution equation

$$\ln a_2 = \ln x_2 + v_2\phi_1^2(\delta_2 - \delta_1)^2RT \quad (2)$$

giving the values for these solutions shown in Table II. The next to the last column gives the entropies of solution of solid iodine, $\bar{s}_2 - s_2^S$. The figures in the last column represent the entropies of solution of liquid iodine, $\bar{s}_2 - s_2^0$, obtained by subtracting 8.0, the value for the entropy of fusion used in our recent paper. Figure 1 adds these new values to Fig. 1 of that paper.

TABLE I

SOLUBILITY OF IODINE, MOLE %, $100x_2$, AT 25°

Solvent	t, °C.	Measd.	Calcd.
n-C_7F_{16}	20.02	0.01448	0.01444
	28.09	.02183	.02193
	37.11	.03617	.03607
	25.00	....	.01837
	24.89	.01826	.01825[4]
c-$C_6F_{11}CF_3$	18.17	0.01456	0.01446
	20.45	.01634	.01641
	24.30	.02008	.02023
	29.34	.02675	.02641
	34.14	.03360	.03377
	39.98	.04505	.04507
	25.00	....	.02101
$(C_3F_7COOCH_2)_4C$	20.76	0.0961	0.0967
	25.02	.1182	.1171
	31.90	.1581	.1579
	40.50	.2227	.2253
	45.06	.2714	.2699
	25.00	....	.1170
c-$C_4Cl_2F_6$	9.99	0.06147	0.06166
	16.59	.08507	.08464
	25.16	.1245	.1251
	30.29	.1564	.1563
	35.19	.1927	.1922
	25.00	....	.1241
CCl_2FCClF_2	4.86	0.1007	0.1007
	14.95	.1601	.1596
	20.00	.1968	.1986
	25.09	.2474	.2456
	29.97	.2985	.2992
	25.00	....	.2447
$CHBr_3$	11.87	4.145	4.139
	19.02	5.275	5.204
	25.17	6.255	6.281
	30.11	7.259	7.265
	35.27	8.432	8.416
	25.00	...	6.249

TABLE II

ENTROPY OF SOLUTION OF IODINE, 25°

Solvent	$R\left(\frac{\partial \ln x_2}{\partial \ln T}\right)_{sat}$	$\left(\frac{\partial \ln a_2}{\partial \ln x_2}\right)_T$	$\bar{s}_2 - s_2^S$, cal. mole^{-1} deg.$^{-1}$	$\bar{s}_2 - s_2^0$
C_7F_{16}	34.4	0.998	34.3	26.3
c-$C_6F_{11}CF_3$	31.7	.997	31.6	23.6
$(C_3F_7COOCH_2)_4C$	26.3	.999	26.3	18.3
$C_4Cl_2F_6$	26.2	.995	26.1	18.1
CCl_2FCClF_2	24.35	.990	24.1	16.1
$CHBr_3$	17.8	.89	15.9	7.9

We are obtaining values of $(\partial P/\partial T)_v$ for more of these liquids in order to investigate more fully the

(1) J. H. Hildebrand and D. N. Glew, THIS JOURNAL, **60**, 618 (1956).

(2) K. Shinoda and J. H. Hildebrand, *ibid.*, **61**, 789 (1957).

(3) D. N. Glew and L. W. Reeves, *ibid.*, **60**, 615 (1956).

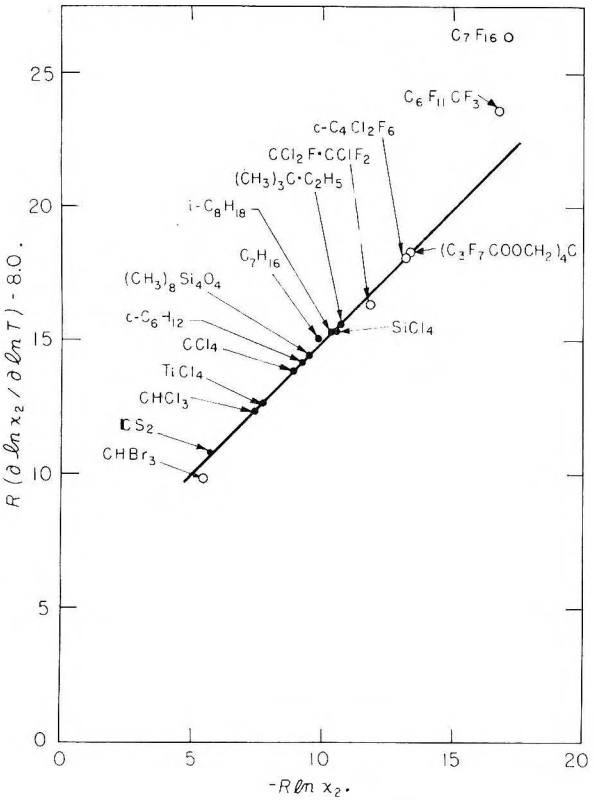

Fig. 1.—Entropy of solution of iodine.

contribution of expansion to the entropy of solution. We are also endeavoring to measure the vapor pressure of iodine over its solutions in CS_2 in order to evaluate $(\partial \ln p_2/\partial \ln x_2)_T$ and avoid the necessity of considering properties of liquid iodine extrapolated 89° below its melting point. Meanwhile, the straight line drawn through the points in Fig. 1 serves well as a norm for the behavior of violet solutions.

Solubility Parameters.—Table III compares solubility parameters for the solvents, δ_1, calculated,

TABLE III

SOLUBILITY PARAMETERS

Solvent	$\delta_2 - \delta_1$ eq. 1	δ_1 if δ_2 = 14.1	$(\Delta E^v/v)^{1/2}$
C_7F_{16}	8.5	5.6	6.0
$C_6F_{11}CF_3$	8.4	5.7	6.1
$(C_3F_7COOCH_2)_4C$	7.4	6.7	..
$C_4Cl_2F_6$	7.3	6.8	7.1
CCl_2FCClF_2	6.6	7.3	7.5
$CHBr_3$	3.9	10.2	10.5

from solubility and from the energy of vaporization, using $\delta_2 = 14.1$ for iodine and 59.0 cc. for v_2^0.

In the absence of values of the heat of vaporization of c-$C_4Cl_2F_6$ and CCl_2FCClF_2, we estimated them from their boiling points by an equation given by Hildebrand and Scott.[4] The fact that δ_1 for bromoform as determined from its solvent power for iodine is 0.3 unit smaller than $(\Delta E^v/v)^{1/2}$ recalls the fact that the same difference occurs in the case of chloroform.[5]

Figure 1 gives the old and new points, the latter in open circles, for $R(\partial \ln x_2/\partial \ln T) - 8.0$ *vs.* $-R \ln x_2$ at 25°.

The following observations are to be noted:

1. The point for $CHBr_3$ is close to that for CS_2, in harmony with their solubility parameters, 10.0 and 10.5, respectively, and the fact the absorption spectrum of the former shows evidence of only minimal solvation.[6] The points for CCl_2FCClF_2 and c-$C_4Cl_2F_6$ fall closely upon the extended straight line. The dipoles present in these molecules are evidently sufficiently buried to exert no significant effect upon their solvent powers for iodine.

The point for $(C_3F_7COOCH_2)_4C$ is exceptionally interesting because the molal volume of this solvent is 540 cc., nine times that of iodine, and if the Flory–Huggins formula applied there would be a large excess entropy, ~2.6 e.u., and the point would fall far above the line. This confirms in even more striking fashion the evidence presented in our recent paper[2] that iodine in octamethylcyclotetrasiloxane, whose molal volume is 312 cc., also shows no F–H excess entropy. The color of our solution was not pure violet; the maximum of the visible band was at 505 μ, which would indicate some reduction of entropy of solution, but hardly so great as to offset the above amount.

The solubility of iodine in c-$C_6F_{11}CF_3$ is only slightly less than it is in n-C_7F_{16} but the entropy of solution in the former is less by 2.7 e.u. We are measuring $(\partial P/\partial T)_v$ for c-$C_6F_{11}CF_3$ in order to compare the contributions to be attributed to expansion. Values of $\bar{v}_2 - v_2$ are reported in the accompanying paper.

We express our appreciation to the Minnesota Mining and Manufacturing Co., for the $(C_3F_7COOCH_2)_4C$, and to the National Science Foundation for support of the work.

(4) J. H. Hildebrand and R. L. Scott, "Solubility of Nonelectrolytes," Reinhold Publ. Corp., New York, N. Y., 1950, p. 427, eq. 12.

(5) J. H. Hildebrand, *Chem. Revs.*, **44**, 37 (1949); also ref. 4, p. 431.

(6) J. H. Hildebrand and D. N. Glew, to be published.

PARTIAL MOLAL VOLUMES OF IODINE IN VARIOUS COMPLEXING AND NON-COMPLEXING SOLVENTS

BY KŌZŌ SHINODA AND J. H. HILDEBRAND

Contribution from the Department of Chemistry, University of California, Berkeley, California

Received August 27, 1957

The partial molal volume of iodine has been measured in 25 solvents at mole fractions less than 0.002. In 10 violet solutions the values range from 60.7 cc. in CS_2 to 81.2 cc. in c-$C_4Cl_2F_6$, increasing smoothly with decreasing solubility. Values are much less, 52.2 to 56.0 cc., in strong complexing ethers and methylnaphthalenes. In benzene and methylated benzenes they are about 62 cc., less than in the comparable non-complexing solvent, cyclohexane, 68.2 cc., but much greater than in the ethers. This may be taken as evidence that these aromatic solvents form weaker "collision complexes," as suggested by Orgel and Mulliken. Further comparisons are considered. The fact that the partial molal volumes are so nearly the same in violet solutions in solvents of very different molal volumes is incompatible with the concept of "holes" in lattice structures.

Hildebrand and Scott,[1] in 1952, showed that the excess of the partial molal entropy of solution of iodine in carbon tetrachloride over the ideal entropy can be largely accounted for by the entropy of expansion, as calculated from the expression $(\bar{v}_2 - v_2^\circ)(\partial P/\partial T)_V$. Hildebrand and Glew[2] showed that this is true also for iodine in perfluoroheptane, where the expansion, $\bar{v}_2 - v_2^\circ$, is amazingly large, 41 cc. per mole of iodine. Reeves and Hildebrand[3] found the same to hold for bromine in f-heptane, where the expansion is 21 cc. per mole. The present authors, in view of the evidently important relation of volume changes to entropy, have determined the partial molal volume of iodine in a number of solvents of different solubility parameters and electron donor strengths. A few of our results were reported in a recent paper.[4]

Experimental

The common method, determining the density of solutions of known composition, requires that both be measured with an accuracy difficult to obtain with volatile components, and that method moreover is very inaccurate when the solute is very dilute (solubility is small). Therefore, we adopted a simple, dilatometric procedure. The dilatometers consisted of cylindrical glass bulbs of 100 to 150-cc. capacity, each containing a large glass ball. The stem is a uniform, calibrated capillary with an internal diameter of 1.8 mm. The bulb is placed in a thermostat at 25° and filled with solvent extending into the lower part of the stem. A weighed amount of iodine is sealed into a long, thin-walled glass capsule, narrow enough to slip down through the stem into the bulb. It is there broken and the iodine is dissolved by twirling the glass ball. The change in the level of the liquid after equilibrium is reached, corrected for the volume of the glass fragments, and divided by the number of moles of iodine dissolved, gives its partial molal volume. Accurate temperature control is of course essential. The fluctuations in this work were within 0.0005°. Three additions of iodine were made in each determination. The mean square deviations of the values of $\bar{v}_2$, the partial molal volume of iodine, were within 0.3 cc. in nearly all cases.

The solvents were all materials of high purity. Many of them had been further purified for other researches.

Results

The results are given in Table I in the first column of figures together with those of other observers for comparison as marked: D for Dawson,[5] all at 18°, instead of 25°; F, Fairbrother;[6] G, calculated from data by Grumert;[7] GH, Glew and Hildebrand;[8] JR, Jepson and Rowlinson.[9] The agree-

TABLE I

PARTIAL MOLAL VOLUME, SOLUBILITY AND "ENTROPY-DEFICIENCY" OF IODINE, 25°

Solvent	$\bar{v}_2$, cc.	$-\log x_2$	$R\frac{\partial \ln x_2}{\partial \ln \bar{v}}$ deficiency
n-C_7F_{16}	100 GH	3.745	
c-$C_4Cl_2F_6$	81.2	2.906	0
CCl_2FCClF_2	67.7	2.611	.4
$SiCl_4$	67.1	2.302	.1
i-C_8H_{18}	66.7	2.270	.2
n-C_7H_{16}	66.3	2.168	− .2
n-C_7H_{16}	63.9 D		
$(CH_3)_8Si_4O_4$	66.6	2.091	.3
c-C_6H_{12}	68.2	2.037	.1
c-C_6H_{12}	67.9 JR		
CCl_4	66.7	1.940	0
CCl_4	65.8 D		
$CHCl_3$	65.6	1.642	0
$CHCl_3$	65.7 G		
CS_2	60.7	1.253	0
CS_2	61.1 D		
CS_2	60.1 G		
C_6H_6	62.4	1.319	2.9
C_6H_6	62.9 JR		
$C_6H_5CH_3$	61.6		
$C_6H_5CH_3$	61.8 D		
p-$C_6H_4(CH_3)_2$	62.5	1.115	4.7
s-$C_6H_3(CH_3)_3$	62.7	0.930	4.9
α-$C_{10}H_7CH_3$	52.2		
1,4-$C_{10}H_6(CH_3)_2$	53.5		
$(C_2H_5)_2O$	49.6 JR		7.4
i-$(C_3H_7)_2O$	50.8		
n-$(C_4H_9)_2O$	56.0		
$(C_2H_5O)_4Si$	60.5	1.240	6.3
C_2H_5OH	60.0	1.327	11.2
C_2H_5OH	59.8 D		
C_3H_7OH	60.6	1.257[a]	
C_4H_9OH	61.0		
$(CH_2OH)_2$	66.6	1.829[a]	
Dioxane	67.8		
Dioxane	64.7 F		
1,2-$C_2H_4Cl_2$	67.1	1.658	0.8

[a] These solubilities were measured in this experiment.

(1) J. H. Hildebrand and R. L. Scott, *J. Chem. Phys.*, **20**, 1520 (1952).

(2) J. H. Hildebrand and D. N. Glew, THIS JOURNAL, **60**, 616 (1956).

(3) J. H. Hildebrand and L. J. Reeves, *ibid.*, **60**, 949 (1956).

(4) K. Shinoda and J. H. Hildebrand, *ibid.*, **61**, 789 (1957).

(5) M. H. Dawson, *J. Chem. Soc.*, **97**, 1041 (1910).

(6) F. Fairbrother, *ibid.*, 1051 (1948).

(7) M. Grumert, *Z. anorg. Chem.*, **164**, 256 (1927).

(8) D. N. Glew and J. H. Hildebrand, THIS JOURNAL, **60**, 616 (1956).

(9) W. B. Jepson and J. S. Rowlinson, *J. Chem. Soc.*, **261**, 1278 (1956).

ment is good in nearly all cases. The fact that Dawson's values were obtained at 18° hardly affects the comparison, since the partial molal volume at high dilution is not very sensitive to temperature. We found practically identical values at 13.8 and 25° in both CS_2 and CCl_4. We found evidence of secondary reactions in a drift with time in the brown solutions of iodine in methyl- and dimethylnaphthalene and in both of the silicones.

The first group of 10 solutions, arranged in order of increasing solubility, are the nearly pure violet solutions, the ones which fall on the line when $R(\partial \ln x_2/\partial \ln T)$ is plotted against $R \ln x_2$ shown in the papers of Hildebrand and Glew[2] and of Shinoda and Hildebrand.[4] The points for solutions in which solvation occurs fall below that line, because of the smaller entropy of solution. The solubility is given as $-\log x_2$ in the second column of figures. In the third is given distance each point falls below the line in cal. deg.$^{-1}$ mole^{-1}. This is essentially the amount by which the entropy of solution is diminished by solvation. We give it in this direct experimental form instead of attempting to convert it to entropy of transfer from hypothetical liquid iodine to solution, $\bar{s}_2 - s_2^\circ$, by applying the factor $(\partial \ln a_2/\partial \ln x_2)_T$, which becomes somewhat uncertain as the solubility increases, as explained in the preceding paper.

The value of $\bar{v}_2$ for all these solutions is greater than 59.0 cc. the (extrapolated) molal volume of liquid iodine at 25°. The connection between contraction and complexing was clearly set forth in the paper by Jepson and Rowlinson.[9] We differ from their interpretations only in one point. They inferred that their value, $\bar{v}_2 = 67.9$ in cyclohexane, the only violet solution they investigated, could be regarded as the normal liquid volume and that anything less indicates complexing. They suggest that pure iodine is not a strictly normal liquid. However, we find $\bar{v}_2 = 60.7$ cc. in CS_2, a pure violet solution. It is to be expected, moreover, that $\bar{v}_2$ would increase with decreasing solubility parameter of the solvent. This is confirmed by the range 60.7 to 100 cc. in the list of violet solutions in Table I.

Contraction is strong in solutions in ethers and in the methylnaphthalenes and, as Jepson and Rowlinson found, in ethyl bromide and iodide, where both solubility and absorption spectra indicate strong complexing.

The partial molal volumes in benzene, toluene, *p*-xylene and mesitylene, approximately 62 cc., are less than in comparable, non-complexing solvents, such as cyclohexane, but larger than in the ethers. This may be interpreted as evidence that the solvation in these aromatics belongs to the class designated by Orgel and Mulliken[10] as "collision complexes," instead of definite stoichiometric complexes.

The large entropy deficiency of solutions in the alcohols is not reflected in small values of $\bar{v}_2$, but this is not to be wondered at, because complexing doubtless occurs at the expense of hydrogen bonds. The reader may make other comparisons.

We offer one final comment. The "violet" solvents in Table I cover a 5-fold range in molal volume. If these liquids were quasi-crystalline lattices, the size of the "holes" they would contain would vary so greatly as to make it inconceivable that the partial molal volumes of dissolved iodine would be so nearly the same as we find them to be.

We gratefully acknowledge the support of this work by the National Science Foundation.

(10) L. E. Orgel and R. S. Mulliken, *J. Am. Chem. Soc.*, **79**, 4839 (1957).

EFFECT OF THERMAL GRADIENTS ON METAL–GAS SYSTEMS[1]

BY GEORGE G. LIBOWITZ

Atomics International, A Division of North American Aviation, Inc., Canoga Park, California[2] and Contribution No. 247 from the Department of Chemistry, Tufts University, Medford, Mass.

Received September 18, 1957

The distribution of a gas dissolved in a metal under a thermal gradient and constant pressure is considered. An expression for the concentration gradient is derived. The effect of compound formation on the distribution and on the shape of pressure–composition isotherms is discussed.

Distribution of Gas in a Single Phase Metal System.—The relation between pressure, temperature and gas content in a metal–gas system exhibiting formation of a non-stoichiometric compound has been derived from statistical mechanical considerations,[3–5] and can be expressed in the form

$$\ln p = \ln p_0 + 2 \ln \frac{n}{s-n} - \frac{4T_c}{T}\left(\frac{2n}{s} - 1\right) \quad (1)$$

where p is the pressure of the gas at any temperature T, and gas concentration n. n is expressed as the atom ratio of gas atoms to metal atoms in the metal; s is the stoichiometric gas to metal ratio in the metal–gas compound; p_0 is the equilibrium pressure of the two-phase region, the two phases being metal saturated with dissolved gas and the non-stoichiometric metal–gas compound; T_c is the critical temperature or the temperature at which the two phases become completely miscible. The equation will hold for the diatomic gas of any element although it is most often used for metal–hydrogen, metal–oxygen and metal–sulfur systems.

Consider a metal bar of uniform density under a temperature gradient ranging from T_0 to T_m. If $n << s$, and is also low enough so that there is no formation of a compound, eq. 1 can be written

(1) This research was supported by the Atomic Energy Commission.
(2) Present address of author.
(3) J. S. Anderson, *Proc. Roy. Soc. (London)*, **A185**, 69 (1946).
(4) A. L. G. Rees, *Trans. Faraday Soc.*, **50**, 335 (1954).
(5) G. G. Libowitz, *J. Chem. Phys.*, **27**, 514 (1957).

$$n = n_g/n_M = s(p/p_0)^{1/2} \exp(-2T_c/T) \qquad (2)$$

where n_g and n_M are the number of gas atoms and metal atoms, respectively, in the bar. p_0 is actually the dissociation pressure of the metal–gas compound and is given by the integrated van't Hoff equation

$$\ln p_0 = A + (2/s)\Delta H/RT$$

where A is a temperature independent constant, ΔH is the heat of formation of the compound, and R is the gas constant. Substituting this into eq. 2 we obtain

$$n_g = n_M s p^{1/2} \exp[(\alpha/T) - (A/T)] \qquad (3)$$

where $\alpha = -(\Delta H/sR) - 2T_c$. This is a positive number since ΔH is negative and $|\Delta H/sR| > |2T_c|$.

For an infinitesimal volume in the metal bar, containing dn_g gas atoms and dn_M metal atoms at an average temperature T, we can write

$$dn_g = dn_M s p^{1/2} \exp[(\alpha/T) - (A/T)] \qquad (4)$$

If the mean free path of the molecules in the gas phase is less than the diameter of the vessel in which the gas is contained, then the pressure of the gas along the metal bar is essentially constant. Assuming a linear gradient from T_0 to T_m, then

$$dn_M = \frac{dT}{T_M - T_c} N_M \qquad (5)$$

since the bar is of uniform density. N_M is the total number of metal atoms in the bar. Putting this into eq. 4 and integrating gives

$$\int_0^{N_g} dn_g = N_g = \frac{N_M s p^{1/2}}{(T_m - T_0)\exp(A/2)} \times \int_{T_0}^{T_m} \exp(\alpha/T)dT \qquad (6)$$

where N_g = total number of gas atoms dissolved in the metal bar. The integral in eq. 6 can be evaluated numerically between definite limits T_0 and T_m, if the heat of formation of the compound, and the critical temperature are known. Denoting the integral by I, the equation can be rewritten

$$p^{1/2} = \frac{N(T_m - T_0)\exp(A/2)}{sI}$$

where $N = N_g/N_M$ = average concentration of gas atoms in the bar. Substituting this into eq. 3 yields

$$n = \frac{N(T_m - T_0)\exp(\alpha/T)}{I} \qquad (7)$$

Equation 7 is an expression for the distribution of dissolved gas along a metal of uniform density under a linear thermal gradient. For gradients other than linear, the expression for the gradient corresponding to eq. 5 is substituted into eq. 4 and a similar analysis can be carried out. Equation 7 holds only for the solution of gas in metal and is no longer valid when the concentration is high enough to form a compound or new phase since eq. 1 is only applicable to one-phase regions.

Distribution of Gas in a Two-phase System.—When the average concentration of gas in the metal exceeds a certain value, the metal–gas compound commences to precipitate at the low temperature end of the bar. In the compound, n is no longer negligible with respect to s, so that an analytical expression for n cannot be obtained from eq. 1. A qualitative consideration of the distribu-

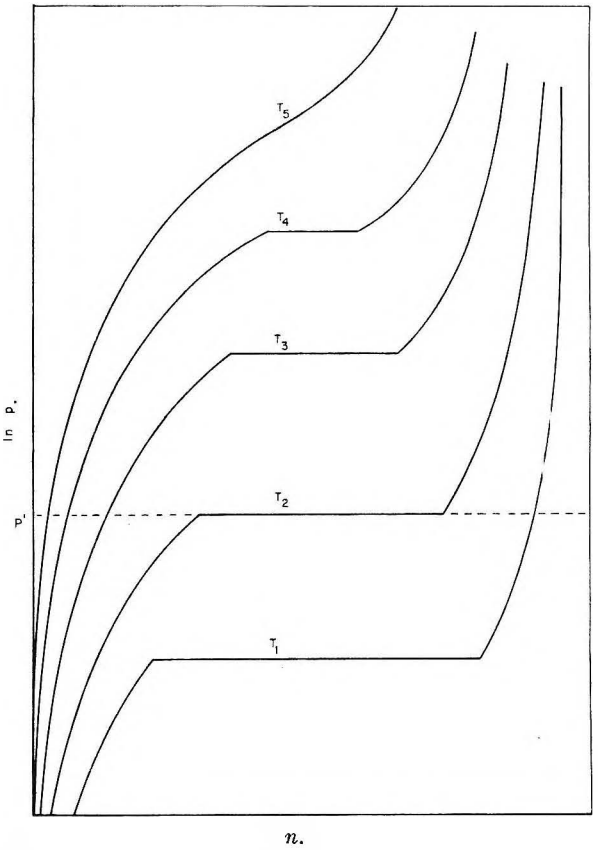

Fig. 1.—Pressure–composition isotherms of metal–gas systems.

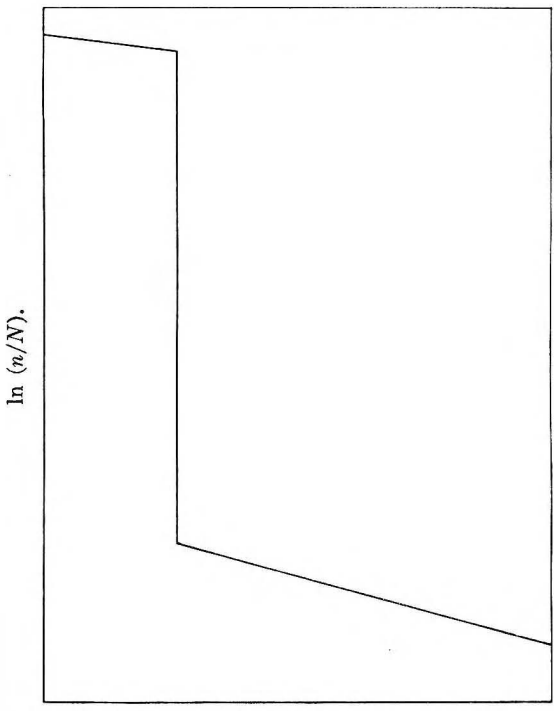

Fig. 2.—Distribution isobar of gas in a two-phase system (metal and metal gas compound) under a thermal gradient.

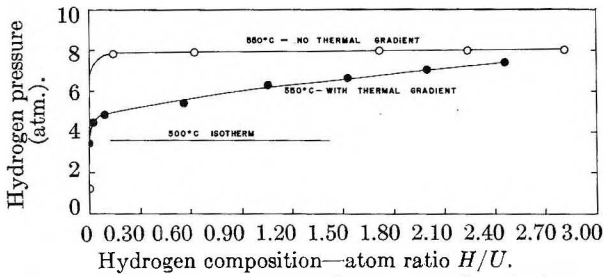

Fig. 3.—Effect of a thermal gradient on uranium–hydrogen pressure–composition isotherms.

tion, however, shows that the bar is divided into two distinct sections, consisting of a metal phase and a compound phase. This can be seen by considering Fig. 1, which is a graphical representation of eq. 1. The set of pressure–composition isotherms shown is characteristic of metal–gas systems exhibiting formation of a compound or a new phase. The regions of sharply rising pressure at the low and high composition ends of the isotherms correspond to single phase metal and single phase nonstoichiometric compound, respectively. The constant pressure portions, or "plateau" regions are characteristic of the coexistence of the two phases in conformity with the phase rule. Consider the constant gas pressure above the metal bar to be P'. In traversing from the high temperature to the low temperature end of the bar, it is seen that the gas composition increases, according to eq. 7, with the bar remaining in the metal phase until the temperature T_2, where the solubility limit in the metal phase is reached. Below this temperature only the compound phase exists. Therefore, both phases coexist only at the sharp boundary line between metal phase and compound phase. The distribution of gas in the bar can then be represented by the isobar shown in Fig. 2.

The minimum over-all content of gas in the metal bar necessary to form the compound phase at the low temperature end can be calculated from eq. 7, if the terminal solubility of gas in the metal is known as a function of temperature. This minimum concentration, N_0, will then be given by the expression

$$N_0 = \frac{n_{T_0} \int_{T_0}^{T_m} \exp(\alpha/T)\, dT}{(T_m - T_0)\exp(\alpha/T_0)}$$

where n_{T_0} is the terminal solubility of gas in the metal at T_0.

Effect on Pressure–Composition Isotherms.—During an investigation of the uranium–hydrogen system[6] in which pressure–composition isotherms were studied, a preliminary series of runs yielded isotherms in which the pressure in the two-phase (U metal and UH_3) region did not remain constant but decreased with decreasing hydrogen composition thus leading to a sloping plateau region. A review of the literature showed that this phenomenon had also been found in the Pd–H,[7–9] Cu–S,[10] Fe–S,[11] Co–S,[12] Ti–S,[13] Zr–H,[14] Th–H,[15] rare earth–hydrogen,[16] and Na–H[17] systems. The sloping plateau regions were ascribed to impurities in some cases,[16] and to the rift theory[18] of hydrides in others.[15]

Further investigation of the uranium–hydrogen system revealed that a thermal gradient of 25° existed along the uranium sample. When this gradient was removed, the pressure in the two-phase region remained constant as shown in Fig. 3. The sloping plateau region was, therefore, a result of the thermal gradient along the sample and can be explained on the basis of the metal to compound phase boundary described above. As hydrogen was added to the uranium metal, it dissolved until the over-all hydrogen content exceeded N_0. Further addition of hydrogen resulted in the formation of uranium hydride at the low temperature end of the sample. The equilibrium plateau pressure is then determined by the temperature at the metal–hydride boundary where the two phases coexist. As additional hydrogen was added to the sample, more metal was converted to the hydride, and the boundary moved toward higher temperatures, thus increasing the equilibrium hydrogen pressure and thereby leading to a "plateau" which sloped upward. Conversely, on dehydriding runs, as hydrogen was removed from the sample the metal–hydride boundary moved toward the cooler end of the sample thus decreasing the equilibrium pressure.

It is quite probable, therefore, that the sloping plateau region in many of the systems mentioned above also may have been due to thermal gradients along the sample during the investigations.

(6) G. G. Libowitz and T. R. P. Gibb, Jr., THIS JOURNAL, **61**, 793 (1957).

(7) C. Hoitsema, *Z. physik. Chem.*, **17**, 1 (1895).

(8) L. J. Gillespie and L. S. Galstaun, *J. Am. Chem. Soc.*, **58**, 2565 (1936).

(9) L. J. Gillespie and W. R. Downs, *ibid.*, **61**, 2496 (1939).

(10) W. Biltz and R. Juza, *Z. anorg. Chem.*, **190**, 173 (1930).

(11) R. Juza and W. Biltz, *ibid.*, **205**, 273 (1932).

(12) O. Hülsmann and W. Biltz, *ibid.*, **224**, 73 (1935).

(13) W. Biltz, P. Ehrlich and K. Meisel, *ibid.*, **234**, 97 (1937).

(14) M. N. A. Hall, S. L. M. Martin and A. L. G. Rees, *Trans. Faraday Soc.*, **4**, 1306 (1944).

(15) M. W. Mallett and I. E. Campbell, *J. Am. Chem. Soc.*, **73**, 4850 (1951).

(16) J. J. Katz and E. Rabinowitch, "The Chemistry of Uranium," McGraw-Hill Book Co., Inc., New York, N. Y., 1951, p. 186.

(17) M. D. Banus, J. J. McSharry and E. A. Sullivan, *J. Am. Chem. Soc.*, **77**, 2007 (1955).

(18) D. P. Smith, "Hydrogen in Metals," University of Chicago Press, Chicago, Illinois, 1948.

THE DEVELOPMENT AND PROPERTIES OF AN ADSORBENT FOR URANIUM[1]

BY LESLIE A. MCCLAINE, PAUL NOBLE, JR., AND EDWARD P. BULLWINKEL

Arthur D. Little, Inc., Western Division, San Francisco, California

Received September 23, 1957

An adsorbent for uranium was developed by placing upon the surface of a porous char an organic substance which has a very low aqueous solubility and a strong tendency to form chelate compounds with uranium under the solution conditions at which uranium adsorption is desired. The quantity of uranium adsorbed from a sulfuric acid solution onto char modified with di-2-ethylhexyl pyrophosphate is on the order of ten times that obtained on unmodified char. Activity and capacity of a modified adsorbent are observed to be dependent on the modifier selected, the surface concentration of the modifier, and the nature of the char adsorbent. The experimental behavior of the modified adsorbents supports the assumption that adsorption occurs by formation of a uranyl chelate compound with the modifier at the surface of the adsorbent and that the adsorptive capacity of the modified adsorbent for uranium is limited by steric considerations determined by the size of the chelate molecule being formed and the pore size distribution of the adsorbent.

Introduction

This paper discusses the preparation and properties of an adsorbent developed specifically for the recovery of uranium from sulfuric acid solutions.

In the sulfuric acid leaching of some uranium ores, slurries are obtained which are extremely difficult to settle or filter. A comparable problem with gold ores was solved by use of a process eliminating the need for separating the slurry of ore and leach solution. This process[2] consists of adding a granular adsorbent which will adsorb the gold values in the leach slurry; the granular adsorbent containing the gold value is then separated from the slurry by use of screens.

In applying such a process to uranium recovery, it was necessary that the uranium adsorbent be of such a particle size that it could be readily separated from the finely ground ore pulp by screening and that it be sufficiently resistant to abrasion so that it would not be rapidly consumed during agitation with the ore pulp. In addition, of course, high selectivity and adsorptive capacity for uranium was desired.

Porous chars, such as those obtained from coconut shell or fruit pits, have these desired physical properties. However, earlier workers[3] had investigated the adsorption of uranium from sulfuric acid solutions by these adsorbents and found little tendency for uranium to be adsorbed at the high acidities and sulfate ion concentrations existing in the leach solutions. No satisfactory uranium adsorbent could be found by the early workers for use in the process.

In our work, therefore, we investigated various methods for increasing uranium adsorption from solution by the porous chars. One approach was to attempt to form a complex uranium species in solution which would be adsorbed by the char. This approach was not successful.

Our second approach was to place upon the surface of the adsorbent, prior to its use, a substance which would bond to the uranium. This substance, termed a modifier, must meet the requirements that it remain on the surface when placed in aqueous solution and that it have sufficient tendency to combine with uranium to enable it to compete with the sulfate ion in solution for the uranium. The organophosphorus compounds which were known to form stable chelates with uranium under the solution conditions were investigated for this purpose. The desired adsorptive capacity and selectivity was obtained using selected organophosphorus compounds as modifiers.

This procedure of modifying the surface of an adsorbent thus provides a general method for producing an active adsorbent for various metal ions. This paper describes the preparation and the properties of the modified adsorbent developed for uranium and outlines the characteristics of modifier and adsorbent which appear to be important in determining adsorptive capacity and selectivity.

Experimental

Materials Used.—The carbons used in the study were steam activated chars manufactured by R. T. Collier Corporation from peach pits. Some pertinent properties of two chars discussed in this paper are outlined in Table I.

TABLE I

CHAR PROPERTIES

Property	Char grade[a] G	SP
Particle size, mesh	−10 +24	−10 +24
Ash, %	6	6
Apparent density, g./ml.	0.35	0 31
Surface area, m.²/g.[b]	1000	1100
Pore vol., ml./g.[c]	*ca.* 0 81	*ca.* 1 1
Absorption		
Butane, ml./g.	0 32	0.35
CCl_4, % by wt.	50	64

[a] R. T. Collier Corp. grading based upon CCl_4 vapor adsorption. [b] As determined by the nitrogen–BET method on single samples. [c] Represents char pore volume which is accessible to water at 1 atm. pressure.

The data were supplied by the manufacturer with the exception of the surface area and the pore volume information. The surface areas were measured for us at Columbia University through the courtesy of Professor M. D. Hassialis and Mr. R. C. Musa. Pore volumes were calculated from the volume of char as determined by mercury displacement minus the volume of char as determined by water displacement.

The phosphorus compounds used in this study were obtained and purified as follows.

1. **Di-2-ethylhexyl Pyrophosphate (OPPA)** $C_8H_{17}OPO(OH)OPO(OH)OC_8H_{17}$.—This compound was obtained from the Victor Chemical Works and used without further purification. This compound is a mixture of both simple and

(1) Work carried out under contract AT(49-6)-923 with the Raw Materials Division, U. S. Atomic Energy Commission.

(2) R. W. Krebs, U. S. Patent 2,476,420 (July 19, 1946).

(3) J. C. Goodrich and R. L. Belcher, "The Adsorption of Uranium from Solutions by Activated Carbon," Battelle Memorial Institute, USAEC Report TID 5101.

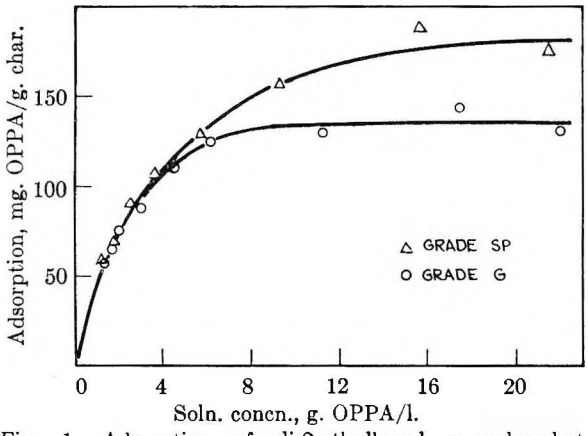

Fig. 1.—Adsorption of di-2-ethylhexyl pyrophosphate (OPPA) from ethanol.

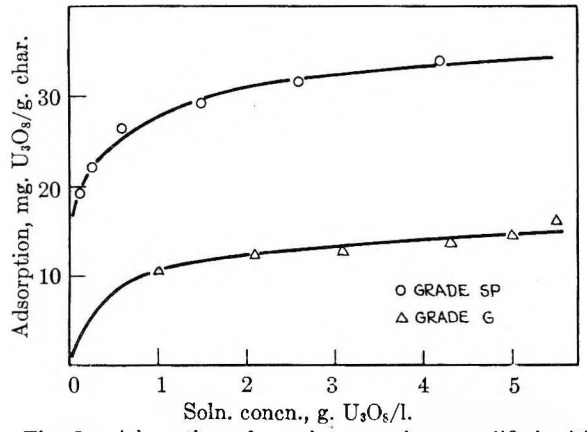

Fig. 2.—Adsorption of uranium on chars modified with 10% di-2-ethylhexyl pyrophosphate from solution containing 100 g. SO_4/l. at *p*H 1.

polymeric esters. A consideration of the reaction used in the preparation of this class of compounds reflects their complexity.[4] Titration with dilute NaOH indicates a substantial contribution from weak phosphoric acids. Cryoscopic molecular weight determination ranged from 460 to 550 for various OPPA samples. Examination of one sample from Victor by the nuclear magnetic resonance spectrum for phosphorus indicated that approximately 65% of the phosphorus was present as pyroester. The remainder was primarily ortho-ester with possibly 5% of the phosphorus present in polymers higher than pyro.

2. **Di-*n*-butyl Pyrophosphate (BPPA)** $C_4H_9OPO(OH)$-$OPO(OH)OC_4H_9$.—This compound was used as received from Victor Chemical Works. It is similar to OPPA.

3. **Di-2-ethylhexyl Orthophosphate** $(C_8H_{17}O)_2PO(OH)$. —This compound was prepared from Tergitol P-28, an aqueous solution of the sodium salt (Union Carbide Chemicals Company) by a method similar to that described by workers at Oak Ridge.[5] Tergitol P-28 (450 ml.) was extracted with 450 ml. of hexane. Three layers separated; the top and bottom layers were discarded. The middle layer containing a mixture of water, Tergitol P-28, and hexane was washed twice with 100-ml. portions of hexane. The upper hexane layer was discarded. The lower phase was acidified with HCl, resulting in the formation of two layers. The upper hexane layer containing the phosphoric acid was washed with three 100 ml. portions of 2 *M* HCl, followed by four portions of distilled water. The hexane layer was then dried over anhydrous Na_2SO_4 and evaporated *in vacuo*.

Anal. Calcd. for $C_{16}H_{35}O_4P$: P, 9.61; equiv. wt., 322. Found: P, 9.64; equiv. wt., 326.

4. **Mono-2-ethylhexyl Orthophosphate (MOPA)** C_8H_{17}-$OPO(OH)_2$.—Mono-2-ethylhexyl orthophosphate was prepared from a mixture of dialkyl and mono-alkyl esters by a procedure described by workers at Dow.[6] The mixed alkyl phosphates were supplied by the Oldbury Electro-Chemical Company. The separation procedure consisted esentially of partition of the alkyl phosphates between 78% methanol and *n*-hexane. The mono-alkyl phosphate extracts into the methanol and the dialkyl into the hexane. Titration with dilute NaOH indicated only a small contribution from any dialkyl acid.

Anal. Calcd. for $C_8H_{19}O_4P$: P, 14.8; equiv. wt., 210. Found: P, 14.71; equiv. wt., 220.

5. **Uranyl Chelate of Di-2-ethylhexyl Orthophosphate.**—To 200 ml. of hexane was added 6.50 g. of di-2-ethylhexyl orthophosphate. This hexane solution was contacted several times with 100-ml. portions of an aqueous solution containing 5 g. of uranyl nitrate hexahydrate. The hexane layer was washed with distilled water and dried over anhydrous Na_2SO_4. This hexane solution of the chelate was used as is.

Anal. Calcd. for $[(C_8H_{17}O)_2P(O)O]_2UO_2$: U_3O_8/PO_4, 1.47. Found: U_3O_8/PO_4, 1.41.

Preparation of Modified Adsorbent.—The modified adsorbent could be prepared by contacting char with either an ethanol solution of the modifier or with a water emulsion of the modifier. The procedure used most frequently for preparing char modified with di-2-ethylhexyl pyrophosphate consisted of agitation of the char with a water emulsion of the chelating agent. The amount of modifying agent added to the emulsion depended upon the loading desired. The following procedure was used to obtain chars analyzing 4.5–5% PO_4. To 400 g. of char was added a suspension of 45 g. of di-2-ethylhexyl pyrophosphate in 1.5 liters of water. This mixture was then agitated 12 to 24 hours. The char was screened, washed well with water, and dried at 50 to 60°.

Determination of Adsorption Isotherms.—Isotherms were determined by equilibrating solutions of known concentration with varying amounts of char. The uranium adsorbed per unit weight of char was calculated from the changes in solution concentration observed. Actual analysis of the carbon was found to agree within experimental error with that determined by decrease in solution concentration.

Determination of Adsorption Activities.—The adsorption of uranium by modified chars as a function of the concentration of modifier on the char was determined for constant solution composition. The hexavalent uranium solution for these determinations analyzed as follows: 1 g. U_3O_8/l., *p*H 1, and 100 g. SO_4/l. The carbon was equilibrated with this solution. The procedure consisted of agitating small amounts of the modified carbon (1–2 g.), contained in small containers constructed of stainless steel screens, with a large quantity of solution (10 liters) for sufficient time to attain equilibria. In this manner the total amount of uranium adsorbed was not sufficient to alter significantly the composition of the solution. By equilibrating several portions of carbon, each having different concentrations of adsorbed chelating agent, data for a typical activity curve were obtained. The adsorbed uranium concentration, as well as that of the modifying agent, was determined by analysis of the char after equilibration. The char was washed well with water and dried prior to analysis. It was found that a sodium peroxide fusion of the char gave the best procedure for obtaining aqueous solutions suitable for U and P analysis.

Results

Adsorption of di-2-ethylhexyl pyrophosphate (OPPA) from ethanol solution is shown in Fig. 1 for grade G and SP chars. Similar curves are obtained using other solvents. The magnitude of the char load for a given solution concentration varies, of course, for various solvents.

(4) G. M. Kosolapoff, "Organophosphorus Compounds," John Wiley and Sons, Inc., New York, N. Y., 1950.

(5) C. A. Blake, K. B. Brown and C. F. Coleman, "The Extraction and Recovery of Uranium (and Vanadium) from Acid Liquors with Di-(2-ethylhexyl)-phosphoric Acid and Some Other Organophosphorus Acids," USAEC Report ORNL 1903, May 13, 1955.

(6) D. A. Ellis, R. R. Grinstead, R. L. Mason, J. E. Magner, R. S. Long and K. G. Shaw, "Recovery of Uranium from Colorado Plateau Ores by Solvent Extraction," USAEC Report DOW 131, July 29, 1955.

The adsorption of uranyl ion from sulfuric acid solutions onto char modified with OPPA is shown in Fig. 2. From spot checks and from isotherms in reference 3 it is known that the adsorption on unmodified char is on the order of one-tenth that shown here. The data for adsorption on modified chars can be expressed by a Langmuir equation. Figure 3 presents Langmuir plots of uranium adsorption on grade SP char modified with various organo-phosphorus esters.

The activity and capacity of a modified adsorbent are dependent on the modifier selected, the surface concentration of the modifier and the nature of the char adsorbent. As shown in Fig. 4, the activity of a modified adsorbent varies directly with the surface concentration of the modifier up to a capacity limit which varies for different grades of char adsorbents. The variation in activity and capacity for several modifiers on grade SP char is indicated in Fig. 5.

The time required to obtain adsorbent loadings in equilibrium with solutions decreases with increasing solution concentration, indicative of a diffusion limited process. The times required to attain equilibrium vary from 2 to 3 hours for a solution analyzing 2 g./l. U_3O_8 to 50–100 hours for one analyzing 0.02 g./l. U_3O_8.

The adsorption of uranium from sulfate solution increases by a factor of 1.4 on increasing *p*H from 1 to 2.5. It has been observed that at constant *p*H the adsorption of uranium is decreased by increasing the sulfate ion concentration or by adding phosphate ion. For example, in a solution at *p*H 1 uranium loadings were 1.5 times greater from a solution containing 20 g. SO_4 per liter than from a solution containing 200 g. SO_4 per liter. This effect is, of course, explained by UO_2^{++} complexing with these ions.

The effect of adding other cations to the solution is dependent on the nature of the cation, the modifier used, and the solution conditions. For the purpose of the process development for which these studies were made the selectivity of the modified adsorbent for uranium was more favorable at *p*H 1 than at higher *p*H and was sufficiently great to provide a feasible separation process.

Desorption of Uranium.—The uranium adsorption is reversible. Thus, uranium can be removed by sufficient washing with sulfuric acid solutions or phosphoric acid solutions. In process development studies, use has been made of the fact that uranium forms a stable complex with carbonate to remove it with solutions of this reagent.

Life of Modified Absorbent.—Process studies have shown that the life of the modified adsorbent is limited only by the slow hydrolysis of the organophosphorus ester. The loss of the di-octyl pyrophosphoric acid ester observed over several hundred hours of acid contact and 80 adsorption–desorption cycles averaged less than 0.1% per hour of acid contact. In process use a periodic replacement of the modifier lost by hydrolysis would maintain the adsorption activity of the modified adsorbent at a high level.

Discussion

The data obtained to date can be correlated by

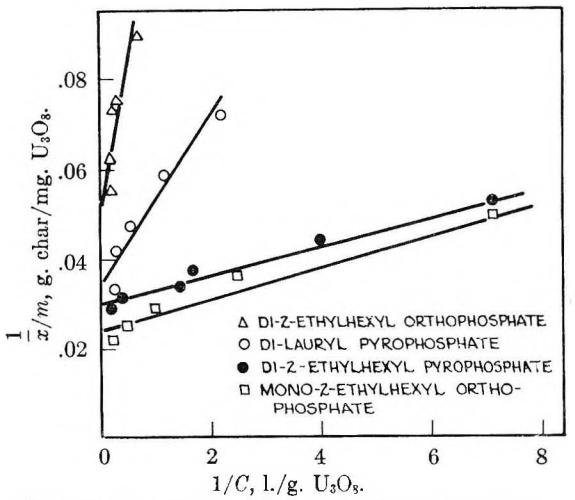

Fig. 3.—Uranium adsorption on grade SP char as a function of phosphate ester on the char: char, ester concentration on surface equivalent to 5% PO_4 by weight; solution, 100 g. SO_4/liter *p*H 1.

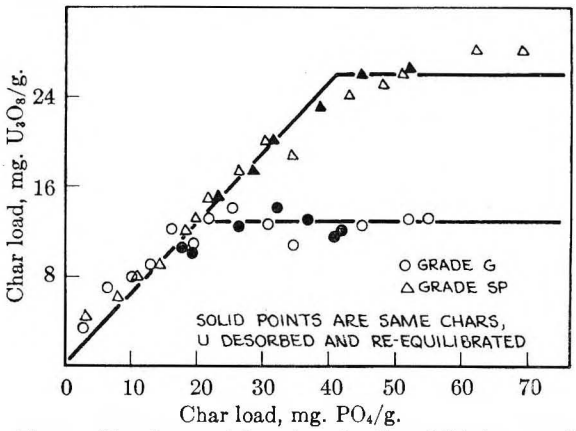

Fig. 4.—Uranium activity of grades G and SP chars modified with di-2-ethylhexyl pyrophosphate as a function of phosphate load.

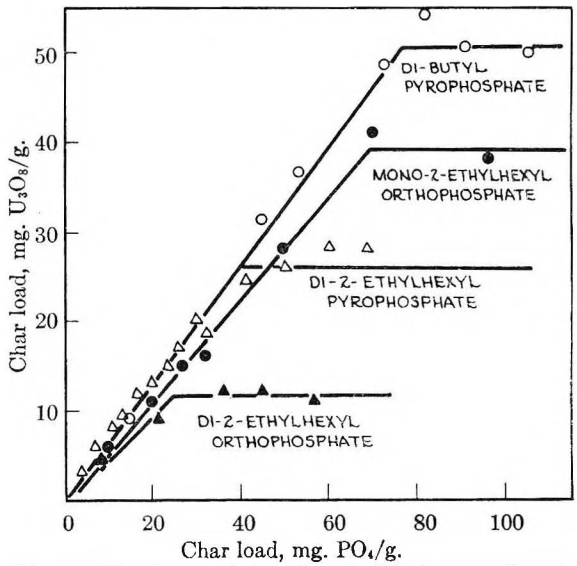

Fig. 5.—Uranium activity of grade SP char as a function of the nature and concentration of phosphate ester on the surface. Data obtained from equilibration of modified char with uranium solution containing 1 g. U_3O_8/liter and 100 g. SO_4/liter at *p*H 1.

the assumptions (a) that the over-all reaction occurring between the aqueous and surface phases for a system using a di-alkyl pyrophosphate ester ($R_2P_2O_7H_2$) is

$$UO_2^{+2}(aq) + R_2P_2O_7H_2(surface) = UO_2R_2P_2O_7(surface) + 2H^+(aq)$$

and (b) that the adsorptive capacity of the modified adsorbent for uranium is limited by steric considerations determined by the size of the chelate molecule being formed and the pore size distribution of the adsorbent.

It is evident from a consideration of the equation for the over-all reaction that distribution of uranium to the surface phase would be favored by decreasing aqueous acidity, by increasing the ester concentration on the surface, and by decreasing the concentration in aqueous solution of ions tending to complex uranyl ion. This indicated behavior is in accord with experimental evidence.

A quantitative relationship between the uranium distribution and the total ester concentration on the surface can be derived from the equation given above for the over-all reaction. The equilibrium expression for this reaction is

$$K = \frac{(UO_2R_2P_2O_7)_s(H^+)^2_{aq}}{(R_2P_2O_7H_2)_s(UO_2^{+2})_{aq}}$$

while the total ester on the surface (represented by $\Sigma R_2P_2O_7H_2$) is equal to the sum of the complexed and uncomplexed ester concentrations

$$\Sigma R_2P_2O_7H_2 = (UO_2R_2P_2O_7)_s + (R_2P_2O_7H_2)_s$$

From these relationships, we obtain the expression

$$\frac{(UO_2R_2P_2O_7)_s}{(UO_2^{+2})_{aq}} = \frac{K}{(H^+)^2_{aq} + K(UO_2^{+2})_{aq}} (\Sigma R_2P_2O_7H_2)$$

Thus, at constant solution conditions of acidity and uranyl ion concentration the uranium adsorbed should be directly proportional to the total ester concentration on the adsorbent. The data of Figs. 4 and 5 show this linear dependency up to a point at which a saturation loading is attained. It can be shown that when comparable calculations are made for a di-alkyl orthophosphate, a linear dependency is not indicated. To explain the fact that a linear dependence is shown experimentally for di-2-ethylhexyl orthophosphate (see Fig. 5), we must assume that this compound exists as a dimer on the surface.

If we substitute into the equilibrium expression for the over-all reaction letting

$$(UO_2R_2P_2O_7)_s = \frac{x}{m}$$

and

$$(UO_2^{+2})_{aq} = kC$$

and

$$(R_2P_2O_7H_2)_s = \left(\frac{s}{m} - \frac{x}{m}\right)$$

where s/m represents the uranium loading per gram of modified adsorbent at saturation and x/m represents the loading in equilibrium with a solution concentration C, then we obtain the expression

$$\frac{1}{\frac{x}{m}} = \frac{1}{K'\frac{s}{m}C} + \frac{1}{\frac{s}{m}}$$

which is the form of the Langmuir equation. In this derivation, we are assuming that the uranyl ion concentration is directly proportional to the total uranium concentration in solution and that the acidity and sulfate ion concentration are maintained constant. As is shown in Fig. 3, the data obtained fit a Langmuir plot reasonably well.

It is instructive to obtain the expression for the distribution coefficient of uranium between surface and aqueous phases from the expressions for the separate equilibria involved in the over-all reaction. Assume that the over-all reaction is a combination of the following reactions with their corresponding equilibrium constants

$$R_2P_2O_7H_2(surface) = R_2P_2O_7^{-2}(surface) + 2H^+(surface) \qquad K_1$$

$$R_2P_2O_7^{-2}(surface) + UO_2^{+2}(surface) = UO_2R_2P_2O_7(surface) \qquad K_2$$

$$UO_2^{+2}(aqueous) = UO_2^{+2}(surface) \qquad K_3$$

$$H^+(aqueous) = H^+(surface) \qquad K_4$$

By definition

$$D^{surface}_{aqueous} = \frac{(UO_2R_2P_2O_7)_s}{(UO_2^{+2})_{aq}}$$

and by substitution

$$D^{surface}_{aqueous} = \frac{K_1K_2K_3(R_2P_2O_7H_2)_s}{K_4^2(H^+)^2_{aq}}$$

From this expression we observe that the distribution of uranium should be proportional to the dissociation constant of the organophosphorus acid and to the stability constant of the chelate. It is interesting to observe in Fig. 5 that greater distribution coefficients are obtained for the pyrophosphate than for the orthophosphate esters. This behavior is in accord with that expected on the basis that the initial acid dissociation constant for the pyrophosphate esters would be expected to be greater than those for the ortho esters and that the pyrophosphate esters offer the possibility of six-member chelate ring formation with the uranium which, other factors being equal, is generally accepted to produce a more stable ring configuration than a four-member ring which would be formed with the orthophosphate esters.

Thus, it is evident from the above discussion that the general chemical behavior can be correlated with the reactions outlined. However, from the data in Figs. 2, 3, 4 and 5, it is evident that the nature of the base adsorbent in conjunction with the modifier selected is an important variable in determining the ultimate adsorptive capacity for uranium. The factors in char and modifier which determine the adsorptive capacity are discussed next.

The surface areas of grade G and SP char differ by about 10% as measured by N_2 adsorption (see Table I). Thus, it is not surprising that the isotherms for adsorption of di-2-ethylhexyl pyrophosphate from ethanol (as shown in Fig. 1) indicate about 20% difference between the two chars in surface area available to OPPA if we assume similar surface concentrations at saturation. However, as shown in Fig. 2, uranium adsorption on the modified adsorbents differ by a factor of two. This appears surprising in view of the indicated difference in surface area of only about 20%. Pore volume measurements on the chars showed that there was es-

sentially no change from the values listed in Table I on adding modifier and adsorbing uranium. Thus, the formation of hydrophobic pores upon modification resulting in a large change in area available to the uranium solution apparently cannot account for the effect.

The fact that uranium loadings at low modifier concentrations are identical for the two chars (as shown in Fig. 4) also indicates that the total surface available to OPPA is available to uranium solution. It is to be expected that the uranium loadings will be proportional to the number of molecules of ester exposed to solution; if for one char a large fraction of the ester modifier were on surface not available to uranium solution, then different uranium loadings would be obtained at the same loading of modifier.

From the above considerations we are led to believe that the twofold difference in capacities of the chars must be related to the size of the uranium chelate and some property of the chars which prevents similar packing of the chelate on the two surfaces. It is evident from the data shown in Fig. 5 for di-butyl as compared with di-2-ethylhexyl pyrophosphate that size of the ester is important in determining the adsorptive capacity. A consideration of the surface area and pore volume information for the two chars given in Table I indicates that grade G char has a lower average pore diameter. Therefore, this variation in pore size distribution could readily be the property of the char which affects the surface packing of the uranium chelate.

Figure 6 presents the isotherms obtained for the adsorption of the di-2-ethylhexyl orthophosphate chelate of uranium on grade G and grade SP char. The adsorption isotherms obtained differ much more than those obtained with OPPA (presented in Fig. 1). These results further indicate that the surface area available is closely related to the size of the molecule being adsorbed. Again such behavior can be explained readily on the basis of a difference in pore size distribution for the two chars.

Thus, on the basis of the evidence available at this time, we conclude that the adsorptive capacity of modified adsorbents is related to the size of the chelate formed and the pore size distribution of the char adsorbent.

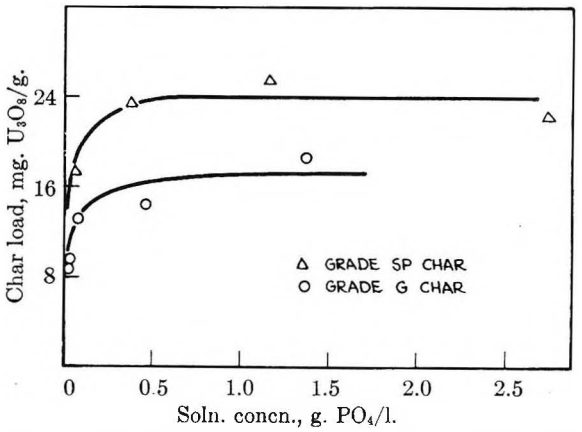

Fig. 6.—Adsorption from hexane of the uranyl di-2-ethylhexyl orthophosphate chelate.

Conclusions

It is evident that such a procedure for achieving an adsorbent for a given cation is not limited to uranium. From a consideration of the expression for $D_{\text{aqueous}}^{\text{surface}}$ it readily can be recognized that by suitable combination of chelating agent on the base adsorbent and complexing agents in solutions, highly specific metal separations can be achieved. Some preliminary work along this line has been carried out and modified adsorbents for metals other than uranium have been developed.

It is believed that further development work would produce adsorbents with a more favorable pore distribution and chelating agents with more ideal properties. The combination should yield modified adsorbents with much higher adsorptive capacity for uranium or other metal ion.

MEASUREMENT OF THE TRANSFERENCE NUMBERS OF AQUEOUS CUPRIC SULFATE SOLUTIONS BY THE MOVING BOUNDARY METHOD

BY J. J. FRITZ AND C. R. FUGET

Department of Chemistry, The Pennsylvania State University, University Park, Pennsylvania

Received September 23, 1957

Techniques have been developed for measurement of the transference numbers of aqueous copper sulfate solutions by the moving boundary method. Copper acetate is used as the indicator substance. The methods have been tested rigorously by standard methods. The results are in agreement with the (rather inaccurate) values obtained many years ago by the Hittorf method.

Introduction

The only reported measurements of the transference numbers of aqueous copper sulfate solution are those of Jahn,[1] by the Hittorf method, later reported in smoothed form in the International Critical Tables.[2] In view of the recent controversy over the transference numbers of $ZnSO_4$[3-7] it seemed desirable to check the transference numbers of copper sulfate solutions. The moving boundary method was chosen for the determinations because

(1) H. Jahn, *Z. physik. Chem.*, **37**, 673 (1901).

(2) K. G. Falk, "International Critical Tables," Vol. VI, McGraw-Hill Book Co., New York, N. Y., 1929, p. 310.

(3) G. M. Wolten and C. V. King, *J. Am. Chem. Soc.*, **71**, 576 (1949).

(4) E. P. Purser and R. H. Stokes, *ibid.*, **73**, 5650 (1951).

(5) R. E. Lang and C. V. King, *ibid.*, **76**, 4716 (1954).

(6) R. H. Stokes, *ibid.*, **77**, 3219 (1955).

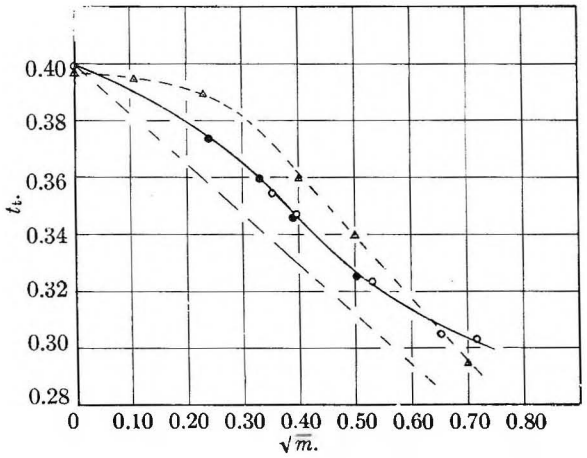

Fig. 1.—Positive transference number of $CuSO_4$ and $ZnSO_4$ solutions: ○ $CuSO_4$ at 25°, this research; ● $CuSO_4$ at 18°, I.C.T.; ▲ $ZnSO_4$ at 25°, ref. 6.

of its directness and its natural precision.

A literature search failed to reveal previous investigation of copper sulfate or any other divalent sulfate by the moving boundary method. Preliminary investigations disclosed that there was considerable difficulty in finding a suitable "indicator" solution, due to the low mobility of copper ion. (At the higher concentrations even sulfates of complex monovalent ions were unsuitable. Other transition group sulfates were tried unsuccessfully; the failure of these as indicator salts was probably due to the fact that their densities and mobilities were too near those of copper sulfate for stability of the boundary.) However, copper acetate solution proved suitable for following the sulfate ion, and formed stable boundaries with copper sulfate solutions. This salt therefore was used as the indicator solution in all the experiments.

Experimental

The moving boundary cell consisted of a 5 cm. length of 4 mm. i.d. precision bore tubing, with larger tubing attached at each end. Copper electrodes were inserted in electrode chambers sealed on the sides of the large tubing. The cross-sectional area was determined by weighing the volume of mercury required to fill a carefully determined length.

A falling boundary was used in all experiments. The acetate solution was carefully floated on top of the sulfate solution. Once a stable rate of motion of the boundary had been established, the times at which the boundary passed a series of 8 engraved marks were observed optically. The current was controlled by an electronic constant-current device and was observed potentiometrically. The current used ranged between 5 and 20 milliamperes. The cell was maintained in a thermostat at 25 ± 0.01°. Copper sulfate solutions used were analyzed electrolytically, and copper acetate solutions were analyzed by determination of their densities at 25°.

The reliability of determination of transference numbers was evaluated as follows:

1. The extent of the "plateau" region within which the observed transference number was unaffected by change in indicator concentration was determined for all solutions investigated. The plateau generally extended over 5 to 10% range of indicator concentration. Only those measurements were used which were safely within the plateau region.

2. In each experiment the rate of motion of the boundary was observed in at least six separate sections of the calibrated tube. The total time required to pass through five of these sections was used as a basis for calculation of the transference number. A small fraction of experiments in which the rate of motion varied from section to section were discarded.

3. The effect of current upon observed transference number was determined for each copper sulfate solution, and the currents used for the final determinations were selected from the region where current variation did not affect the observed result.

4. In several instances the boundary was deliberately destroyed during an experiment by temporary reversal of the current. In all cases the boundary rapidly re-formed and returned to its proper rate of motion.

All measurements were corrected for the small effect of volume changes at the lower electrode by use of tabulated densities, using a method essentially the same as that of Lewis.[7]

Results and Discussion

The results of measurements at five concentrations of copper sulfate are listed in Table I. The precision of each measurement is estimated as ±0.001; an extra figure is given in each case for internal consistency. The results are shown graphically in Fig. 1, where the transference member of the copper ion is plotted against the square root of the molarity (moles/liter). The curve is extended to the limiting value calculated from ion conductances.[8] For comparison the smoothed results of Jahn[2] at 18° are also plotted.[9] The solid line is drawn through our experimental points; it will be observed that the results of Jahn fall upon this curve. The light broken line represents values calculated from the Onsager equation. It will be observed that the present values show a slight levelling above 0.7 molal and are in all cases above the values calculated from the Onsager equation.

TABLE I

TRANSFERENCE NUMBERS IN AQUEOUS COPPER SULFATE SOLUTIONS AT 25°

Concn. of $CuSO_4$, moles/l.	*p*H	Transference no. of sulfate ion	Transference no. of positive ion[a]
0.0000		(0.5970)	(0.4030)
.1249	4.15	0.6452	0.3548
.1557	4.00	.6528	.3472
.2801	3.79	.6763	.3237
.4230	3.69	.6945	.3055
.5131	3.47	.6960	.3040

[a] In a separate set of experiments, the *p*H was varied by addition of sulfuric acid. Extrapolation of these results to a region of negligible hydrogen ion concentration reduced the positive transference numbers by about 0.001. The values reported in Table I are for the normal *p*H of aqueous $CuSO_4$ solutions.

The results of Stokes[6] for $ZnSO_4$ are also plotted in Fig. 1. These results are higher and show more curvature at low concentrations than those for $CuSO_4$, although the limiting transference number of Zn^{++} is slightly lower than that of Cu^{++}.

(7) G. N. Lewis, *J. Am. Chem. Soc.*, **32**, 862 (1910).

(8) For a table of these, see H. S. Harned and B. B. Owen, "Physical Chemistry of Electrolytic Solutions," Reinhold Publ. Corp., New York, N. Y., 1950, p. 172.

(9) Only those results of Jahn above 0.05 molar are included. Although all his results are all a marvel of consistency, the accuracy falls rapidly at lower concentrations, and the results do not extrapolate to the proper limiting transference number.

MULTI-BARRIER KINETICS. NUCLEATION[1]

BY J. CALVIN GIDDINGS AND HENRY EYRING

University of Utah, Salt Lake City, Utah

Received September 25, 1957

A great number of problems in chemical kinetics involve the passage of a point in configuration space over a series of successive free-energy barriers. Examples of this general process are nucleation, membrane permeability, diffusion-controlled reactions, unimolecular reactions and chain reactions. It is our purpose here to indicate a general solution for the steady-state rate of such processes, and to show certain approximations that greatly simplify some of the problems. Insofar as it is possible, the approximate and exact expressions will be compared. Certain problems in nucleation are discussed in terms of the theory.

A theoretical analysis of the transport of ions through membranes has been presented by Parlin and Eyring.[2] Their equation for ion transport is valid for any problem in multi-barrier kinetics involving only single-step transfer processes from a given energy minimum to an adjacent minimum. The general problem of multi-barrier kinetics, where transfer can be made from a given energy minimum to a distant minimum, in a single step, is formulated in a later section.

The Parlin–Eyring equation for the steady-state flux of particles, by a single-step mechanism, over a series of n free-energy barriers, is

$$Q = \frac{\lambda_0 k_0 c_0 - \lambda_n k_n' c_n \dfrac{k_1' k_2' \ldots k_{n-1}}{k_1 k_2 \ldots k_{n-1}}}{1 + \dfrac{k_1'}{k_1} + \dfrac{k_1' k_2'}{k_1 k_2} + \ldots \dfrac{k_1' k_2' \ldots k_{n-1}'}{k_1 k_2 \ldots k_{n-1}}} \quad (1)$$

In this expression, c_i is the concentration at the ith minimum, and λ is the distance between the two adjacent maxima. The k's are the unimolecular rate constants, or the number of jumps per second over the barriers as indicated in Fig. 1. The first term in the numerator is the flux of particles passing from left to right, and the second term is the flux of those passing from the right to the left boundary. The sum is the net flux, Q.

The flux of particles passing from left to right may be written as

$$q = \lambda_0 k c_0 \quad (2)$$

where, for simplicity, the series of n barriers is considered as a single potential barrier, with an effective rate constant k. This expression must equal the first term of equation 1, so that we obtain

$$k = 1/\left(\frac{1}{k_0} + \frac{k_1'}{k_0 k_1} + \frac{k_1' k_2'}{k_0 k_1 k_2} + \ldots + \frac{k_1' k_2' \ldots k_{n-1}'}{k_0 k_1 k_2 \ldots k_{n-1}}\right) \quad (3)$$

This expression for k may be simplified by substituting the absolute reaction rate expression for the individual rate constants

$$k_i = \mathcal{K}_i \frac{kt}{h} \exp\left(-\frac{\Delta F_i^{\ddagger}}{kT}\right)$$

$$k_i' = \mathcal{K}_i' \frac{kT}{h} \exp\left(-\frac{\Delta F_i'^{\ddagger}}{kT}\right) \quad (4)$$

where each term has its usual meaning. Using these values, the reciprocal of the $(i+1)$th term in the denominator of equation 3 becomes

$$\frac{k_0 k_1 k_2 \ldots k_i}{k_1' k_2' \ldots k_i'} = \frac{\mathcal{K}_0 \mathcal{K}_1 \mathcal{K}_2 \ldots \mathcal{K}_i}{\mathcal{K}_1' \mathcal{K}_2' \ldots \mathcal{K}_i'} \frac{kT}{h} \exp\left[-\frac{(\Delta F_0^{\ddagger} + \Delta F_1^{\ddagger} + \ldots + \Delta F_i^{\ddagger} - \Delta F_1'^{\ddagger} - \ldots - \Delta F_i'^{\ddagger})}{kT}\right] \quad (5)$$

The transmission coefficient, $\mathcal{K}_i$, from equilibrium considerations, equals that of the reverse reaction, $\mathcal{K}'_{i+1}$. Hence the term involving the product of transmission coefficients reduces simply to $\mathcal{K}_i$. The free energy terms may be broken down as follows: $\Delta F_0^{\ddagger}$ is the free energy change in passing from the initial state to the top of the first barrier; $\Delta F_1^{\ddagger} - \Delta F_1'^{\ddagger}$ is the additional free energy, over and above that of the first barrier, needed to reach the second. Thus all the free energy terms appearing in the exponent of equation 5 add up to the difference in free energy of the $(i+1)$th barrier, and the initial equilibrium state. This sum may be abbreviated as $\Delta G_i^{\ddagger}$. The entire expression, (5), is the rate constant for passage from the initial state over the $(i+1)$th barrier, providing they were adjacent. This rate constant, k_{0i}, equals

$$k_{0i} = \mathcal{K}_i \frac{kT}{h} \exp(-\Delta G_i^{\ddagger}/kT) \quad (6)$$

For most processes, $\mathcal{K}_i$ may be set equal to unity.

The various k_{0i}'s can be substituted back into equation 3, giving

$$k = 1/\left(\frac{1}{k_{00}} + \frac{1}{k_{01}} + \frac{1}{k_{02}} + \ldots \frac{1}{k_{0(n-1)}}\right) = \left(\sum_0^{n-1} \frac{1}{k_{0i}}\right)^{-1} \quad (7)$$

The free energies of activation, $\Delta G_i^{\ddagger}$, were not restricted solely to chemical energy. If the transport of an ion is to be described, and a potential gradient exists, then the free energy change is (except for strong fields) the sum of chemical and electrical changes in free energy.

Equation 1 was derived using the steady-state assumption for the concentrations at the different energy minima, and this restriction is sometimes important in the application of (7). A given set of energy barriers has a certain relaxation time, after which the steady-state assumption is valid. For a single barrier the relaxation time is negligible, being about 10^{-13} second.

In physical examples of multibarrier kinetics, $\Delta G_i^{\ddagger}$ may depend upon i in a number of ways. An important example involves transport through a uniform membrane where all free-energies are equal. From equation 7 we see that

$$k = k_0/n \quad (8)$$

(1) The research reported in this paper has been sponsored by the Geophysics Research Directorate of the Air Force Cambridge Research Center, Air Research and Development Command, under Contract No. AF 19(604)-2057.

(2) R. B. Parlin and H. Eyring, "Ion Transport Across Membranes," Academic Press, Inc., New York, N. Y., 1954, p. 103.

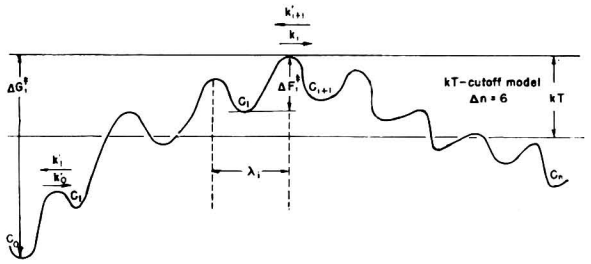

Fig. 1.—Schematic energy profile for multi-barrier kinetics.

where k_0 is the rate constant for any of the n equal barriers.

It is a more common physical occurrence for $\Delta G_i^{\pm}$ to pass through a maximum with increasing values of i. This occurs in all nucleation problems as well as with certain problems in chemical kinetics. For these examples we have introduced a kT-cutoff model for the approximate description of k. It can be seen from equations 6 and 7 that if $\Delta G_m^{\pm} - \Delta G_i^{\pm} > kT$ (where $\Delta G_m^{\pm}$ is the maximum value for the activation free energy), then k_{0i} makes only a small contribution to the over-all rate constant, k. However, when $\Delta G_m^{\pm} - \Delta G_i^{\pm} < kT$, the contribution of k_{0i} and of k_{0m} to k are approximately the same. We have thus assumed that every problem is analogous to the uniform membrane example, (8), where the rate constant k_{0m} must be reduced by an effective number of barriers, Δn, to give the true rate constant.

$$k = k_{0m}/\Delta n \qquad (9)$$

From the above discussion it is clear that, as an approximation, Δn may be set equal to the number of barriers that possess a free energy within kT of the highest free energy. The method is illustrated diagrammatically in Fig. 1.

We have used two specific expressions for the dependence of $\Delta G_i^{\pm}$ on i to assess the accuracy of the kT-cutoff model. First is the linear case, which represents, among other things, an ion moving through a uniform membrane with the addition of an applied potential gradient.

$$\begin{aligned} \Delta G_i^{\pm} &= \Delta G_m^{\pm} + i\epsilon \quad i \lesseqgtr 0 \\ \Delta G_i^{\pm} &= -\infty \quad i > 0 \end{aligned} \qquad (10)$$

The choice of $-\infty$ for $i > 0$ simply indicates that the contribution of k_{0i} to k is negligibly small for this range of i. When these values are substituted into (6) and (7), and compared to equation 9, we find

$$\begin{aligned} \Delta n &= \sum_i \exp\left(\frac{\Delta G_i^{\pm} - \Delta G_m^{\pm}}{kT}\right) \\ &= 1 + \exp\left(-\frac{\epsilon}{kT}\right) + \exp\left(\frac{-2\epsilon}{kT}\right) + \ldots = \\ &\qquad \frac{1}{1 - \exp\left(\frac{-\epsilon}{kT}\right)} \end{aligned} \qquad (11)$$

where, for each i, $\mathcal{K}_i = 1$. Δn differs considerably from unity only when $kT >> \epsilon$. Under these circumstances

$$\Delta n = kT/\epsilon \qquad (12)$$

This result may be compared with that of the kT-cutoff model. From (10), the free energy of each barrier is a value ϵ less than the following one in the region $i \leq 0$. Thus kT/ϵ barriers lie between the maximum one, and that one with a free energy kT less than the maximum. In this case, the model yields the same result as the exact calculation, (12).

The second expression follows from a Taylor's expansion of $\Delta G_i^{\pm}$ about its maximum value. This expression can be used in the description of nucleation processes

$$\Delta G_i^{\pm} = \Delta G_m^{\pm} + \tfrac{1}{2}\left(\frac{d^2\Delta G_i^{\pm}}{di^2}\right)_m (i - m)^2 \qquad (13)$$

Proceeding as before, we find

$$\Delta n = \sum_i \exp\left[\frac{\left(\frac{d^2\Delta G_i^{\pm}}{di^2}\right)_m (i - m)^2}{2kT}\right] \qquad (14)$$

This sum may be replaced by an integral when $kT >> \tfrac{1}{2}(d^2\Delta G_i^{\pm}/di^2)_m$. The result is

$$\Delta n = \int_{-\infty}^{\infty} (\,)\, di = \left[\frac{2\pi kT}{-\left(\frac{d^2\Delta G_i^{\pm}}{di^2}\right)_m}\right]^{1/2} \qquad (15)$$

From equation 13 we can see that the number of barriers with free energy within kT of the highest value is

$$\Delta n = \left[\frac{8kT}{-\left(\frac{d^2\Delta G_i^{\pm}}{di^2}\right)_m}\right]^{1/2} \qquad (16)$$

The kT-cutoff approximation, (16), is too large by a factor of only $(8/2\pi)^{1/2} \cong 1.13$. Both of the previous examples indicate the model to be an excellent approximation to multi-barrier kinetics.

Nucleation.—The above methods for problems in multi-barrier kinetics are useful in nucleation theory, both in clarifying certain aspects of the classical theories of homogeneous nucleation, and in presenting a method for the treatment of more complicated problems, particularly nucleation at oriented interfaces.

The free energy for the formation of a phase B embryo within a phase, A, is

$$\Delta G_i = i\Delta G_\infty + \sigma(6\pi^{1/2} iv)^{2/3} \qquad (17)$$

where i is the number of molecules contained in the embryo, ΔG_∞ the corresponding free energy change, per molecule, where each phase is of macroscopic extent, σ is the surface free energy (for unit area), and v is the volume occupied by a single molecule in the B phase. As emphasized by Turnbull,[3] an activation energy for diffusion must be added to ΔG_i in any study involving the kinetics of the embryo's growth and decay. When the phase, A, is a pure substance, the additional free-energy term involves the activation energy for reorientation and slight displacement at the interface. Whatever the nature of this term, it is designated by $\Delta G_D^{\pm}$. Thus the kinetic problem again involves a series of maxima, with quasi-equilibrium states between. The free energy at a given maximum is

$$\Delta G_i^{\pm} = \Delta G_i + \Delta G_D^{\pm} \qquad (18)$$

The problem of interest arises when B is the stable phase ($\Delta G_\infty < 0$). Under these circumstances, $\Delta G_i^{\pm}$ passes through a maximum. The number of molecules in this so-called critical nucleus, is

$$m = \frac{-32\pi\sigma^3 v^2}{3(\Delta G_\infty)^3} \qquad (19)$$

(3) D. Turnbull, "Solid State Physics," Vol. III, Academic Press, Inc., New York, N. Y., 1956, p. 225.

The theoretical treatment of Volmer and Weber[4] assumes that passage over the single highest barrier controls the rate of nucleation. Equation 7 shows, however, that the rate constant, k_{0m}, for passage over the highest barrier contributes simply the largest term to a series of term, involving the rate constants for passage over neighboring barriers. Further, the rate depends only on the magnitude of the contributing terms, and does not depend upon their position in the sequence. Thus an energy barrier beyond the maximum barrier contributes exactly the same as an equal one preceding the maximum. It is sometimes erroneously assumed that passage over the highest barrier (along with its precursors) is tantamount to the completion of the multibarrier process. If the barriers are distributed symmetrically about the highest barrier, this assumption leads to a result twice as large as it should be. The kT-cutoff model reflects this property of equation 7; the contribution of a given barrier depends only upon its free energy, and not upon its position.

The problem of nucleation can be greatly simplified, providing we can expand $\Delta G_i^{\mp}$ around m, retaining no terms above the square. The problem is then equivalent to the one set out in equation 13. Thus Volmer's rate constant, k_{0m}, must be divided by Δn, equation 15. This is evaluated with the aid of (17) and (19), and we have

$$\Delta n = \left(\frac{G\pi mkT}{-\Delta G_\infty}\right)^{1/2} \qquad (20)$$

The result, of course, is similar to that of Becker and Döring[5] and subsequent workers.[3,6] The number of molecules in the critical nucleus, m, is usually of the order of 100, and Δn is several times less than this.

When nucleation involves growth on oriented surfaces (either in certain cases of heterogeneous nucleation, or where the new embryo itself has certain structural features), the free-energy changes cannot be described by a simple expression such as (17). In such cases, the classic problem of nucleation of new surface layers is superimposed on ordinary nucleation theory. This results since only through the addition of successive oriented layers is the nucleus able to grow.

So far we have not discussed the question as to how many active nuclei, N_a, are present in the steady state. The rate of growth of crystals should be proportional to N_a. Suppose the total number of possible sites, N_0, for such growth structures is $N_0 = N_a + N_i$, where N_i is the number of inactive centers. From equilibrium consideration we write $N_i/N_a = K$. Hence $N_0 = N_a + KN_a$ or $N_a = N_0/(1 + K)$. Multiplying the number of active nuclei N_a by the rate of growth per barrier (see equations 1 and 9) we obtain for the total rate of crystal growth, r, the equation

$$r = \frac{N_0}{1+K}\,\frac{(k_{0m} - k_{0b})}{\Delta n} \qquad (21)$$

Here k_{0b} takes care of the back reaction when there is one. An article by Manson, Cagle and Eyring[7] develops the significance of the term $N_0/(1 + K)$.

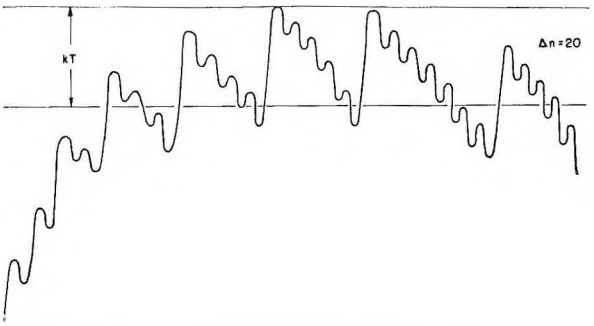

Fig. 2.—Free-energy profile for oriented-interface nucleation.

The free-energy profile for oriented-interface nucleation cannot be generally written down, since the structural aspects of the problem are not well understood. However, a profile like that in Fig. 2 is expected. Once the profile is obtained for any particular case, the kT-cutoff model provides a simple method for determining the rate of nucleation.

Chemical Kinetics.—Multi-barrier processes are not restricted by the condition that energy barriers must be crossed singly. In some cases, a contribution arises from transfer across several barriers. Thus in nucleation, two or more molecules may simultaneously and coöperatively effect phase change. Similar considerations, to be discussed presently, arise in the study of chemical kinetics. The general problem is formulated in the following discussion.

Suppose $p_{ij}dt$ is the probability that in the time element, dt, a system initially in the ith state (minima) undergoes transition to the jth state. (In this nomenclature, the k_i of the preceding sections becomes $p_{i,i+1}$, and k_i' becomes $p_{i,i-1}$). The flux of particles across the ith barrier (or, more generally, through the transition region between the ith and $i + 1$th state) is

$$Q_i = \sum_{\substack{k \leq i \\ l > i}} (n_k p_{kl} - n_l p_{lk}) \qquad (22)$$

where n_k is the number of systems in the kth state. The elements of the transformation matrix between Q and n consist of sums of p_{kl} terms. The steady-state condition requires that all the Q_i's be equal. The set of linear equations, (22), can be handled by the standard methods.

The general formulation, (22), can be used to treat problems in chemical kinetics (including the non-steady state), once the potential energy profile is known. However, simple kinetic problems (involving, say, passage over a single barrier) do not need such elaboration. We will discuss briefly some of the problems to which the above formulation applies.

The problem of unimolecular reactions involves transition through successive vibrational states in the vicinity of the activated complex. The problem has been discussed by Zwolinski and Eyring[8] and by Hirschfelder.[9] The latter treats only the cases for which the energy between successive states

(4) M. Volmer and A. Weber, *Z. physik. Chem.*, **119**, 277 (1925).
(5) R. Becker and W. Döring, *Ann. Physik*, **24**, 719 (1935).
(6) J. Frenkel, "Kinetic Theory of Liquids," Dover Publications, Inc., New York, N. Y., 1955, Chapter 7.
(7) J. E. Manson, F. W. Cagle and H. Eyring, to be published.
(8) B. J. Zwolinski and H. Eyring, *J. Am. Chem. Soc.*, **69**, 2702 (1947).
(9) J. O. Hirschfelder, *J. Chem. Phys.*, **16**, 22 (1948).

is equal to or greater than kT, stating that for smaller energy differences, the motion becomes classical. In this case, energy jumps still occur with changes of the order of kT. Thus the latter problem involves simultaneous transition through several states. It is expected that even with the larger energy differences, these higher order transitions will be important, since non-linear terms contribute so heavily to the potential energy in the neighborhood of the activated complex. For either small or large energy differences, it appears that Δn is of order unity, and the problem can be treated to a good degree of approximation as one involving transfer across a single barrier.

A great number of kinetics problems involve several mechanisms by which a single product can be reached. In many cases where radical-chain reactions are involved, there is a simultaneous molecular mechanism yielding the same product. The chain mechanism proceeds through several successive kinetic steps, and is described by equation 7, with only slight modification. When the molecular mechanism is also important, the more general formulation, equation 21, must be used for the total rate of reaction. The various transition probabilities, p_{Ri}, are then written in terms of reaction rate constants, and the concentrations of the various species involved.

ELECTROPHORESIS OF PROTEINS AT LOW *p*H IN AMINO ACID BUFFERS

By E. F. Woods

Biochemistry Unit, Wool Textile Research Laboratories, Commonwealth Scientific and Industrial Research Organization, Parkville, Victoria, Australia

Received October 1, 1957

Bovine serum albumin gave two moving boundaries on electrophoresis in buffers of amino acid hydrochlorides at *p*H values between 2 and 3, and only one moving boundary in all other buffer mixtures studied. The ascending and descending patterns in the amino acid hydrochloride buffers were non-enantiographic but this appeared to be unrelated to heterogeneity of the protein or to the physico-chemical changes which occur at low *p*H values. From a study of the electrophoresis of bovine serum albumin in glycine hydrochloride under various conditions of *p*H, ionic strength and protein concentration, it is concluded that the faster moving descending boundary and the slower moving ascending boundary appearing between *p*H 2 and 3 are false boundaries. The behavior of these boundaries does not fit the requirements of a false boundary of the Svensson[10] type. A qualitative explanation of the electrophoretic patterns is suggested in terms of the moving boundary theory for weak electrolytes. Non-enantiographic electrophoretic patterns between *p*H 2 and 3 in amino acid buffers were also obtained with egg albumin, lysozyme, bovine γ-globulin, bovine fibrinogen, a water-soluble gelatin and poly-L-lysine. It is concluded that amino acid hydrochlorides either alone or in conjunction with a neutral salt are unsuitable as electrophoresis buffers for the examination of the heterogeneity of proteins or polyelectrolytes at low *p*H.

On moving boundary electrophoresis at *p*H values below the iso-electric point serum albumin appears heterogeneous and the rising and descending boundaries are non-enantiographic.[1-4] It has been suggested that serum albumin consists of an equilibrium mixture of proteins, the equilibria prevailing in the body of the protein solution being continually adjusted in the boundary layers as electrophoretic separation occurs.[1,3] More recently Phelps and Cann[5] have shown that the complex electrophoretic patterns between *p*H 4.0 and 4.7 in buffer mixtures of acetate and chloride are influenced by the buffer composition, mainly the acetate concentration. They concluded that bovine serum albumin is an equilibrium mixture of components, the equilibrium composition depending on the composition of the supporting medium. Similar results were obtained with γ-globulin and ovalbumin. Aoki and Foster[6,7] using serum albumin concentrations of 0.2% and *p*H values between 4.6 and 3.5 obtained enantiographic patterns in 0.02 ionic strength HCl–NaCl and have postulated that the protein is reversibly isomerized in this *p*H range. At protein concentrations above 0.2% enantiography was lost.

At *p*H values below 3.5 a single moving boundary has been observed for serum albumin in HCl–NaCl of ionic strengths between 0.01 and 0.10.[6-8] However Singer and Campbell[9] noticed the presence of a fast moving peak in addition to the main protein boundary in the descending limb for bovine serum albumin, γ-globulin, β-lactoglobulin and ovalbumin at *p*H 2.3 in 0.1 ionic strength glycine hydrochloride. They considered this faster moving boundary to be due to the fact that the hydrogen ion constituent attains an electrophoretically significant concentration in this buffer. The fast moving descending boundary in glycine hydrochloride at 0.1 ionic strength[9] was not observed by Schlessinger[8] but at 0.01 ionic strength he reported false moving boundaries of the type predicted by Svensson.[10] Non-enantiographic electrophoretic patterns in glycine hydrochloride buffers were also observed by Longsworth for ovalbumin.[11]

We have noticed the effect described by Singer and Campbell[9] in glycine hydrochloride at 0.1 ionic strength, but in addition have found two moving boundaries in the ascending limb of the electropho-

(1) L. G. Longsworth and C. F. Jacobsen, This Journal, **53**, 126 (1949).

(2) R. A. Alberty, *ibid.*, **53**, 114 (1949).

(3) R. A. Alberty and H. H. Marvin, *ibid.*, **54**, 47 (1950).

(4) A. Saifer and H. Corey, *Proc. Soc. Exp. Biol. Med.*, **86**, 46 (1954). This paper contains many earlier references to the electrophoretic heterogeneity of the serum albumins.

(5) R. A. Phelps and J. R. Cann, *J. Am. Chem. Soc.*, **78**, 3539 (1956).

(6) K. Aoki and J. F. Foster, *ibid.*, **78**, 3538 (1956).

(7) K. Aoki and J. F. Foster, *ibid.*, **79**, 3385 (1957).

(8) B. S. Schlessinger, Thesis, University of Wisconsin, September, 1955.

(9) S. J. Singer and D. H. Campbell, *J. Am. Chem. Soc.*, **77**, 3504 (1955).

(10) H. Svensson, *Arkiv. Kemi., Mineral. Geol.*, **22A**, 1 (1946).

(11) L. G. Longsworth, *Ann. N. Y. Acad. Sci.*, **41**, 285 (1941).

resis tube. The patterns were non-enantiographic. This behavior may be related to the physico-chemical changes that have been found to occur in serum albumin at low *p*H.[12-18] In this paper a detailed study of the electrophoresis of bovine serum albumin in various buffer mixtures has been made in the *p*H range 1.5–3.0. It was found that the observed heterogeneity occurred only when amino acids were used as buffers. Similar results were obtained with other proteins and poly-L-lysine. An attempt is made in this paper to account for the electrophoretic behavior in terms of the moving boundary theory for weak electrolytes.[19-21]

Experimental

Materials.—The bovine serum albumin was a product of Armour laboratories, Lot No. M66909, and was used without further purification. The concentration of bovine serum albumin was determined before electrophoresis by measuring its ultraviolet absorption at 280 mμ with a Beckman spectrophotometer. A value of 6.6 for $E^{1\%}_{1cm}$ was determined and is in agreement with previously reported values. When submitted to electrophoresis at a concentration of 0.6% in 0.1 ionic strength veronal buffer of *p*H 8.6 the mobility was $6.6_8 \times 10^{-5}$ cm.^{2}volt^{-1} sec.$^{-1}$ and more than 98% of the protein migrated as a single boundary (3.5 hours at 6.5 volt cm.$^{-1}$). There was no change in the electrophoretic pattern or the mobility at *p*H 8.6 after the protein had stood in acid buffer of *p*H 2.0 for 5 days at 2°. In the ultracentrifuge in 0.2 *M* NaCl the protein sedimented as a single peak with a very slight shoulder toward the leading edge. Egg albumin, lysozyme, bovine γ-globulin and bovine fibrinogen were products of Armour laboratories. The water-soluble low molecular weight gelatin was prepared by the action of anhydrous hydrofluoric acid on gelatin.

The author is indebted to Dr. J. A. Maclaren for the preparation of poly-L-lysine. Poly-ε-carbobenzoxy-L-lysine was prepared by the method of Becker and Stahmann[22] and was decarbobenzoxylated with anhydrous HBr in acetic acid. The poly-L-lysine hydrobromide contained a considerable proportion of low molecular weight material which was removed by dialysis through cellophane. The hydrobromide was exhaustively dialyzed against the buffer to be used for electrophoresis to remove the bromide ion.

Several brands of glycine were used without further purification except drying—they were L. Light & Co., Pfanstiehl, and B. D. H. laboratory reagent. The results were independent of the glycine used. The alanine was a product of L. Light & Co.

Sarcosine (N-methylglycine) was prepared by Dr. J. M. Swan by the method of Schütte.[23]

Triethylamine hydrochloride was prepared from triethylamine and HCl. The maleic acid was B.D.H. laboratory reagent. All other reagents were of A.R. quality.

Methods.—The protein solutions were dialyzed at 2° for 3 days against two changes of buffer before electrophoresis at a temperature of 1°. Conductivities were measured at 0°. *p*H values were measured with a glass electrode assembly at 20°.

Electrophoresis was carried out in a standard Tiselius apparatus (L.K.B., Sweden) using the combined Schlieren and Rayleigh interference optics for observation of the boundaries.[24] The centroidal ordinates of the gradient curves were used for calculating mobilities.[25] The field strength was calculated from the specific conductance of the protein solution, hence only the displacement of the fastest moving descending boundary is a true mobility. The boundary displacements were not corrected for volume changes around the electrodes since an open electrode system was used. The proportions of the total refractive increment under each peak were estimated by counting the number of Rayleigh fringes between successive minima; in some cases the gradient curves were traced and the areas estimated by planimetry. In many cases one of the ascending boundaries was so sharp that the fringes were not resolved and the contribution of this boundary to the refractive increment was estimated by taking the total number of fringes from the descending side. If the boundaries were well separated the fringes could be resolved by allowing the boundaries to diffuse after the current was switched off. The percentage of the total refractive increment contributed by each boundary was calculated excluding the ε and δ boundaries. In all experiments in this paper the displacement of each boundary was linear with time and the displacement per coulomb was independent of current strength; the refractive increments were also independent of current strength and time.

Results

Electrophoresis of Bovine Serum Albumin in Glycine Hydrochloride. Effect of Protein Concentration.—In glycine hydrochloride at *p*H 2.3 and ionic strength 0.1 two moving boundaries were observed in both limbs of the electrophoresis tube at all protein concentrations studied with the exception of the lowest concentration (0.16%) where there was incomplete separation in the ascending limb (Table I). The faster descending boundary had a higher rate of movement than both ascending boundaries in nearly every experiment and as the protein concentration was increased there was an increased separation of the two moving bound-

TABLE I

ELECTROPHORESIS OF SERUM ALBUMIN AT VARIOUS PROTEIN CONCENTRATIONS IN GLYCINE HYDROCHLORIDE AT *p*H 2.30; IONIC STRENGTH 0.1

Protein concn., %	Apparent mobilities[a] × 10^5 Descending	Ascending	Areas, % Faster desc.	Slower asc.
0.16	8.8, 10.9	9.5	13	18
.37	8.4, 12.1	8.6, 9.9	17	30
.57	8.2, 12.3	8.5, 10.3	14	38
.68[b]	7.9, 12.3	8.2, 10.6	16	36
.68	8.0, 12.2	8.3, 10.7	19	36
.88	7.5, 12.4	7.9, 10.7	17	35
.91[c]	7.5, 12.6	8.0, 10.8	18	37
1.02	7.7, 13.0	7.7, 11.0	21	38
1.48	7.2, 12.3	7.1, 11.4	25	25
1.91	6.6, 11.3	5.9, 11.7	35	18
2.56	6.4, 14.1	6.7, 12.6	19	29

[a] The apparent mobilities are given in cm.^{2}volt^{-1}sec.$^{-1}$. Since the conductivity of the protein solution at 0° was used to calculate the field strength in this and subsequent tables, only the displacement of the faster descending boundary represents a true mobility. The values indicate however the relative separation of the boundaries. [b] This protein was isolated from an electrophoretic fractionation experiment and represents the slower descending layer. [c] The faster ascending layer from a fractionation experiment.

(12) (a) H. Gutfreund and J. M. Sturtevant, *J. Am. Chem. Soc.*, **75**, 5447 (1953); (b) J. T. Yang and J. F. Foster, *ibid.*, **76**, 1588 (1954).

(13) M. E. Reichmann and P. A. Charlwood, *Can. J. Chem.*, **32**, 1092 (1954).

(14) H. A. Saroff, G. I. Loeb and H. A. Scheraga, *J. Am. Chem. Soc.*, **77**, 2908 (1955).

(15) P. Bro, S. J. Singer and J. M. Sturtevant, *ibid.*, **77**, 4924 (1955).

(16) C. Tanford, S. A. Swanson and W. S. Shore, *ibid.*, **77**, 6416 (1955).

(17) M. J. Kronman, M. D. Stern and S. N. Timasheff, THIS JOURNAL, **60**, 829 (1956).

(18) W. F. Harrington, P. Johnson and R. H. Ottewill, *Biochem. J.*, **62**, 569 (1956).

(19) H. Svensson, *Acta Chem. Scand.*, **2**, 841 (1948).

(20) R. A. Alberty and J. C. Nichol, *J. Am. Chem. Soc.*, **70**, 2297 (1948).

(21) R. A. Alberty, *ibid.*, **72**, 2361 (1950).

(22) R. R. Becker and M. A. Stahmann, *ibid.*, **74**, 38 (1952).

(23) E. Schütte, *Z. physiol. Chem.*, **279**, 61 (1943).

(24) H. Svensson, *Acta Chem. Scand.*, **5**, 1301 (1951).

(25) L. G. Longsworth and D. A. MacInnes, *J. Am. Chem. Soc.*, **62**, 705 (1940).

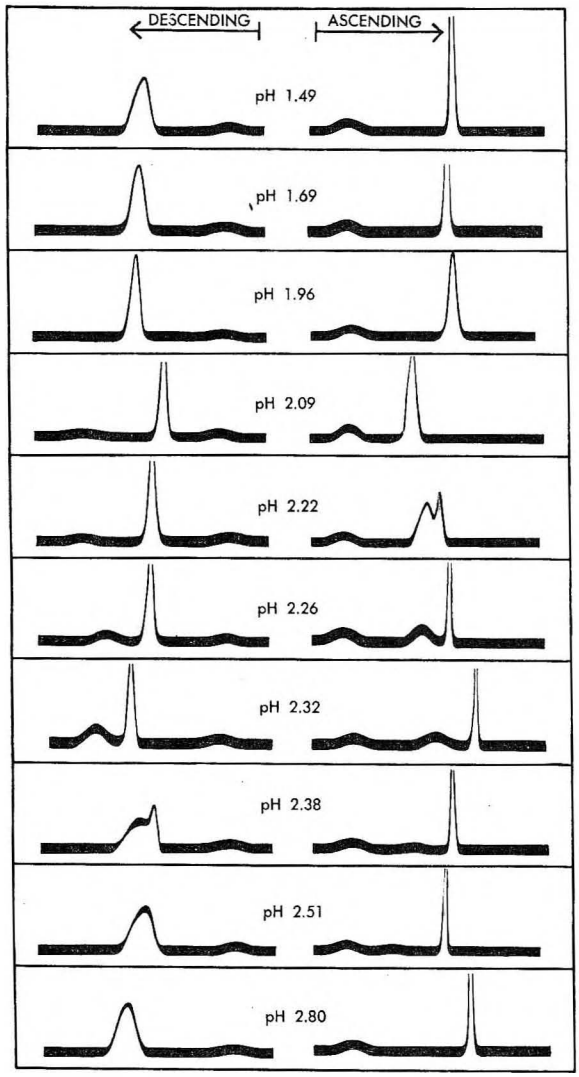

Fig. 1.—Electrophoresis of bovine serum albumin at various *p*H values in glycine hydrochloride of 0.1 ionic strength. Field strengths between 3.0 and 3.8 volt cm.$^{-1}$. Time of electrophoresis 180 min. in all cases except *p*H 2.09 (121 min.), and *p*H 2.22 (150 min.). The apparent mobilities and relative areas of each boundary are given in Table II.

aries. Enantiography between the ascending and descending limbs was absent in all cases. There does not appear to be any clear relation between protein concentration and the areas of the faster descending and slower ascending boundaries. This section of the work was carried out before it was realized that the area under each peak was extremely sensitive to slight variation in *p*H.

The slower descending and the faster ascending layers were isolated in several experiments using short intermediate cells. These electrophoretic fractions were dialyzed, freeze dried, then resubmitted to electrophoresis in glycine hydrochloride at *p*H 2.30. They gave patterns almost identical with the original protein and there was no difference in the mobilities or relative areas under the two peaks (Table I).

Effect of *p*H at Constant Ionic Strength.—Figure 1 shows how the patterns change as the *p*H is raised from 1.5 to 3.0 in glycine hydrochloride, ionic strength 0.1 at a protein concentration of 0.8%. The details of the changes in mobility and areas of the boundaries are given in Table II. At *p*H 1.5 only one moving peak was observed in ascending and descending limbs. At higher *p*H values a very small fast moving peak split off from the descending boundary. With increase of *p*H its relative area increased and its mobility decreased and at *p*H 2.5 only one moving boundary was obtained. In the ascending limb the sharp boundary observed at low *p*H showed increased spreading as the *p*H was raised and splitting into two between 2.1 and 2.2. The slower moving ascending boundary decreased in area and mobility with increase of *p*H and at *p*H 2.8 only one peak was observed in the ascending side. The faster moving boundary in the descending limb was diffuse, and the slower boundary was quite sharp, whereas in the ascending side the faster boundary was sharp and the slower one diffuse.

TABLE II

ELECTROPHORESIS OF 0.85% SERUM ALBUMIN IN GLYCINE HYDROCHLORIDE OF 0.1 IONIC STRENGTH AT VARIOUS *p*H VALUES

*p*H	Apparent mobilities × 10^5 Descending	Ascending	Areas, % Faster desc.	Slower asc.
1.49	8.2	9.8	..	..
1.69[a]	8.3	9.7	..	..
1.96	8.1, 23.8	9.8	4	..
2.09	7.9, 21.0	9.2	5	..
2.22	7.5, 17.4	9.4, 11.0	8	73
2.26	7.6, 12.1	7.8, 10.7	20	33
2.32	7.5, 10.9	7.0, 10.6	32	22
2.33	7.1, 9.8	6.4, 10.4	43	16
2.38	7.3, 8.8	5.0, 9.9	64	9
2.50	8.3	3.1, 9.4	..	4
2.80	8.2	9.2	..	..

[a] A fast moving boundary appeared on the descending side in this experiment but was too small to be measured.

Effect of Ionic Strength at Constant *p*H.—Table III summarizes the results of experiments in which the ionic strength was changed by increasing the quantity of glycine hydrochloride in the buffer.

TABLE III

ELECTROPHORESIS OF 0.85% SERUM ALBUMIN AT VARIOUS IONIC STRENGTHS IN GLYCINE HYDROCHLORIDE, *p*H 2.27

Ionic strength[a]	Apparent mobilities × 10^5 Descending	Ascending	Areas, % Faster desc.	Slower asc.
0.025[b]	8.5, 26.1	12.9, 24.8	10	69
.050	8.4, 18.2	9.4, 15.1	18	44
.075	7.6, 13.3	7.7, 11.3	19	39
.10	7.4, 12.6	8.0, 10.7	17	42
.15	6.9, 8.3	5.7, 8.8	52	8
.20	7.2	8.5[c]	..	2

[a] Refers to the ionic strength of the buffer solution. In this and subsequent tables the contribution of the protein to the ionic strength was not taken into account. [b] A small descending boundary of apparent mobility 13.4 × 10^{-5} cm.^{2}volt^{-1}sec.$^{-1}$ also appeared in this experiment and contributed 5% of the refractive increment across the moving boundaries. [c] The small slow-moving boundary was too diffuse for its displacement to be measured.

Increase of ionic strength caused decreased resolution in both limbs as is normally found in the electrophoresis of protein mixtures. However the

reduction in mobility and corresponding increase in area of the faster descending boundary is greater than would be expected from the usual effect of ionic strength on electrophoretic patterns. Similarly the displacement and proportion of the slower ascending boundary showed a marked reduction with increase of ionic strength. At 0.2 ionic strength one boundary was observed in the descending limb and the slower ascending boundary was reduced to 2% of the total.

Table IV shows the effect of adding sodium chloride to a 0.1 ionic strength glycine hydrochloride buffer. It is seen that the effects are similar to those reported in Table III where only glycine·HCl was used but they are not equivalent. At 0.2 ionic strength in glycine hydrochloride–NaCl with 50% of the ionic strength contributed by NaCl, there were still two boundaries in the descending limb, whereas in 0.2 ionic strength glycine hydrochloride alone only one boundary was observed. At the lowest ionic strength studied (0.025) three moving boundaries were observed in the descending limb.

TABLE IV

ELECTROPHORESIS OF 0.85% SERUM ALBUMIN AT VARIOUS IONIC STRENGTHS AND CONSTANT *p*H IN GLYCINE HYDROCHLORIDE–NaCl

*p*H	Ionic strength	Apparent mobilities × 10^5 Descending	Apparent mobilities × 10^5 Ascending	Areas, % Faster desc.	Areas, % Slower asc.
2.21	0.1 (glycine·HCl)	7.5, 15.2	9.4, 10.9	8	27
2.21	.2 (glycine·HCl–NaCl)[a]	6.7, 8.2	6.1, 8.6	19	17
2.26	.1 (glycine·HCl)	7.6, 12.1	7.8, 10.7	20	33
2.26	.2 (glycine·HCl–NaCl)[a]	6.9, 8.1	6.7, 8.0	28	16

[a] Half of ionic strength contributed by NaCl.

Effect of Replacing Glycine Hydrochloride by NaCl at Constant Ionic Strength (Table V).—As the proportion of NaCl in the mixture increased with glycine hydrochloride–NaCl buffer the resolution of both ascending and descending boundaries decreased but there was no clear trend in the relative refractive increments across the faster descending or slower ascending boundaries. When 80% of the ionic strength was contributed by NaCl two boundaries were still observed in either limb although there was only partial resolution of the descending boundaries.

TABLE V

ELECTROPHORESIS OF 0.85% SERUM ALBUMIN IN GLYCINE HYDROCHLORIDE–NaCl MIXTURES OF VARYING COMPOSITION AT IONIC STRENGTH 0.1 AND *p*H 2.34

Buffer composition *N* HCl, ml./l.	Glycine, g./l.	NaCl, g./l.	Apparent mobilities × 10^5 Descending	Apparent mobilities × 10^5 Ascending	Areas, % Faster desc.	Areas, % Slower asc.
100	14.10	..	7.5, 10.0	6.2, 10.3	44	16
66.7	8.50	1.95	7.5, 10.7	7.9, 10.4	27	29
50.4	6.73	2.90	7.3, 9.7	7.7, 10.2	36	23
33.3	4.05	3.90	7.4, 9.4	8.2, 10.2	44	20
20	2.15	4.68	7.6, 9.3	8.8, 10.0	36	20
6	...	5.50	8.5	9.9	..	..

Electrophoresis in Other Buffers.—Patterns similar to those obtained in glycine hydrochloride were observed in alanine or sarcosine hydrochlorides and these are shown in Fig. 2.

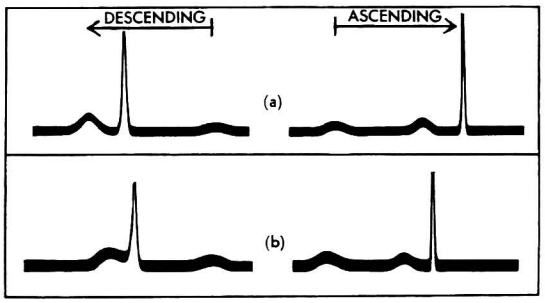

Fig. 2.—Electrophoresis of bovine serum albumin in 0.1 ionic strength buffers. (a) Alanine hydrochloride *p*H 2.30, 150 min. at 4.50 volt cm.$^{-1}$. Apparent mobilities: descending boundaries, 7.3 and 10.6 × 10^{-5} cm.^{2}volt^{-1}sec.$^{-1}$, ascending boundaries, 6.6 and 10.2 × 10^{-5} cm.^{2}volt^{-1} sec.$^{-1}$ (b) Sarcosine hydrochloride *p*H 2.12, 150 min. at 3.96 volt cm.$^{-1}$. Apparent mobilities: descending boundaries, 7.2 and 9.7 × 10^{-5} cm.^{2} volt^{-1} sec.$^{-1}$, ascending boundaries, 7.2 and 10.2 × 10^{-5} cm.^{2} volt^{-1} sec.$^{-1}$

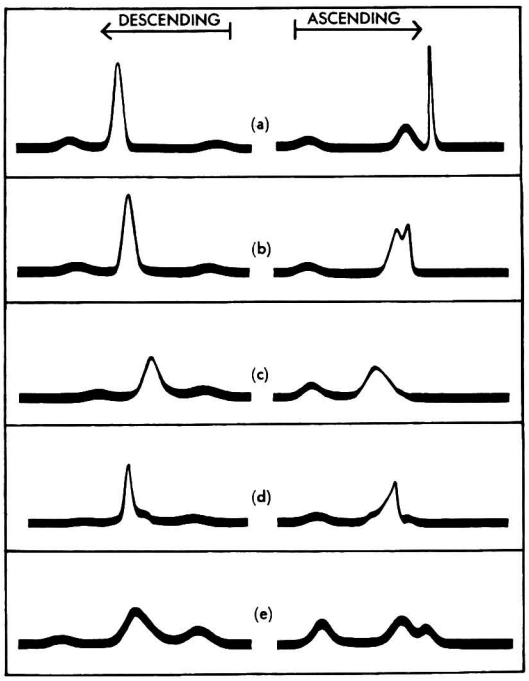

Fig. 3.—Electrophoresis patterns of various proteins in glycine hydrochloride of 0.1 ionic strength at *p*H 2.25: (a) lysozyme; (b) egg albumin; (c) γ-globulin; (d) fibrinogen; (e) degraded gelatin; (a), (b) and (e) 150 min. at 4.25 volt cm.$^{-1}$, (c) and (d) 120 min. at 4.25 volt cm.$^{-1}$.

In all other buffer mixtures studied a single moving boundary was observed between *p*H 2 and 3 at 0.1 ionic strength. Table VI gives the descending mobilities and the shapes of the boundaries which were observed to vary with the buffer used. Serum albumin gave more symmetrical boundaries in triethylamine hydrochloride–HCl and LiCl–HCl than in NaCl–HCl. There also appears to be a definite variation in mobility, depending on the anion and cation in the buffer mixture. The mobility was markedly reduced in sodium maleate–maleic acid and this is taken to indicate that the maleate ion is bound to the protein to a greater extent than either chloride or phosphate. Since chloride ions are known to be bound to serum albumin at this *p*H, phosphate ions must also be bound to approximately the same extent as judged from

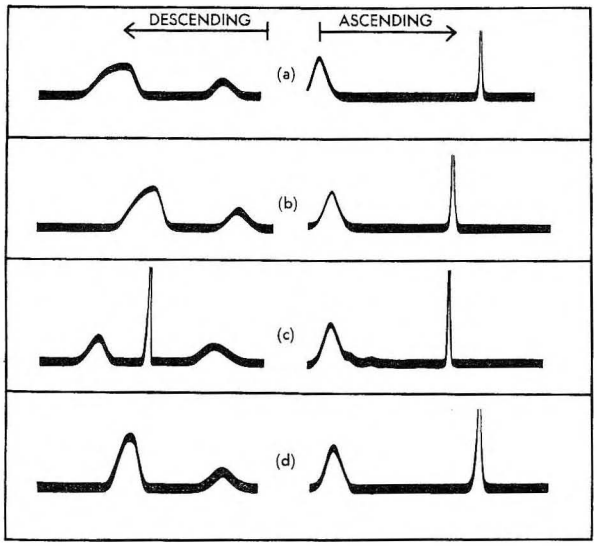

Fig. 4.—Electrophoresis of poly-L-lysine in 0.1 ionic strength buffers. (a) Sodium acetate *p*H 5.10, 120 min. at 3.6 volt cm.$^{-1}$. Descending mobility: 13.2×10^{-5} cm.^{2}-volt^{-1}sec.$^{-1}$ (b). Sodium phosphate *p*H 2.28, 150 min. at 2.9 volt cm.$^{-1}$. Descending mobility: 15.1×10^{-5} cm.^{2}-volt^{-1}sec.$^{-1}$. (c) Glycine hydrochloride *p*H 2.29, 150 min. at 2.2 volt cm.$^{-1}$. Mobility of faster descending boundary: 19.2×10^{-5} cm.^{2}volt^{-1}sec.$^{-1}$ (d) Glycine hydrochloride *p*H 2.90, 153 min. at 2.0 volt cm.$^{-1}$. Descending mobility: 14.1×10^{-5} cm.^{2}volt^{-1}sec.$^{-1}$

the electrophoretic mobilities. There appears to be no significant effect of the presence of un-ionized acetic acid on the electrophoretic pattern or mobility in NaCl–HCl.

TABLE VI

ELECTROPHORESIS OF 0.85% SERUM ALBUMIN IN 0.1 IONIC STRENGTH BUFFER MIXTURES AT LOW *p*H

Buffer	*p*H	Descending mobility $\times 10^5$	Shape of descending boundary
NaCl–HCl	2.32	8.58	Very skew
LiCl–HCl	2.32	8.29	Fairly symmetrical
Triethylamine–HCl	2.36	8.25	Fairly symmetrical
NaCl–HCl–HAc	2.33	8.47	Skew
NaH_2PO_4–H_3PO_4	2.30	8.21	Fairly symmetrical
NaH_2PO_4–H_3PO_4	2.07	8.28	Fairly symmetrical
Maleic acid–NaOH	2.33	6.03	Symmetrical
Maleic acid–NaOH–NaCl[a]	2.30	8.07	Skew

[a] 4/5 of ionic strength contributed by NaCl.

Electrophoresis of Other Proteins in Glycine Hydrochloride.—Figure 3 gives the electrophoretic patterns of other proteins which were investigated in 0.1 ionic strength glycine hydrochloride buffer at *p*H 2.25. Of these lysozyme, egg albumin and the water soluble gelatin gave non-enantiographic patterns similar to those of serum albumin. In the case of lysozyme the separation of the peaks and their relative areas were almost identical with serum albumin at the same protein concentration and *p*H. Bovine fibrinogen and bovine γ-globulin showed a small descending peak, which moved faster than any peak in the ascending limb.

Electrophoresis of Poly-L-lysine.—Figure 4 gives the patterns and mobilities of poly-L-lysine in several buffers. At *p*H 2.29 in glycine hydrochloride and 0.1 ionic strength two moving boundaries were present in the descending limb, and the faster boundary contributed 46% of the total refractive increment. A slow moving boundary in the ascending limb appeared to be unstable. In the following 0.1 ionic strength buffers a single moving boundary was observed in each limb of the electrophoresis tube: glycine hydrochloride *p*H 2.90, sodium phosphate–phosphoric acid *p*H 2.28, and sodium acetate–acetic acid *p*H 5.10. The descending boundaries in phosphate and acetate buffers were very diffuse.

Discussion

The results will be considered first in terms of buffer ion interaction and heterogeneity of the proteins. Interaction of buffer ions with the protein would not be expected to show the behavior described in this paper. Where the protein combines with an ion in the buffer and is in rapid equilibrium with it a single moving boundary is observed in either limb, the rate of movement being modified by the combination. This is the case for example in the maleic acid–sodium maleate buffers where the mobility of serum albumin is considerably less than in chloride or phosphate buffers in this *p*H range (Table VI) due to the greater combination of the maleate ion with protein.

Non-enantiographic electrophoretic patterns[26] are observed when two components, A and B, interact and are in rapid equilibrium according to the equation $A + B \rightleftarrows AB$. The electrophoretic patterns of serum albumin in the *p*H range 4.0–4.6 have been explained in this way,[3] A and B representing two types of albumin molecule. In order to explain the fact that the mobility of the faster descending boundary is greater than the ascending, it was assumed that the mobility of the complex, u_{AB}, was greater than either u_A or u_B. If $u_A > u_B$ then the faster descending boundary would yield the constituent mobility of A and the slower boundary would move with the mobility of free B ions. In the ascending limb the faster boundary would yield u_A, and the slower boundary would be a constituent B boundary. In such a system isolation of the slower descending boundary by electrophoretic fractionation should give component B and the faster ascending boundary should yield component A. Electrophoretic fractionation of bovine serum albumin in glycine hydrochloride at *p*H 2.30 gave fractions indistinguishable in electrophoretic behavior from the original protein (Table I), suggesting that rapidly adjusted equilibria in the protein solution were not responsible for the non-enantiographic patterns. This is further confirmed by the appearance of these patterns only in buffers containing an amino acid hydrochloride and the similar behavior of a number of proteins. It seems unlikely that all the proteins consist of two kinds of molecules which interact to give a complex in rapid equilibrium, and it is difficult to see how the behavior of poly-L-lysine could be explained in this way. It is therefore concluded that the observed patterns are not explained by heterogeneity or rapidly adjusted

(26) L. G. Longsworth and D. A. MacInnes, *J. Gen. Physiol.*, **25**, 507 (1942).

equilibria prevailing in the protein preparation. If the proteins consisted of interacting components and the rate of equilibrium was slow compared with the time of electrophoresis then normal electrophoretic separations would take place. Equilibrium reactions whose rate of adjustment is comparable to the time of electrophoretic separation cannot explain the results since the separations obtained were independent of field strength and time, and in many cases the gradient curves returned to the base line between the peaks.

Although proteins are weak electrolytes, it has been found that the theory of moving boundaries for strong electrolytes[10,27] gives a reasonable quantitative interpretation of their behavior.[28,29] According to the moving boundary theory of Dole[27] and Svensson[10] a system that contains n ions will in general form a maximum of $n - 1$ boundaries one of which is stationary if relative ion mobilities are assumed constant. In the amino acid hydrochloride buffers there are three positive ions, hydrogen, amino acid cation and protein, and one negative ion, chloride. It is usual to neglect the hydrogen ion as a constituent of the system when assessing the number of possible boundaries but at the pH values considered in this work its concentration is high enough to make an appreciable contribution to the conductivity of the solutions. Hence two boundaries with positive velocities are possible and one stationary boundary. One of these moving boundaries would be a true boundary and will give the correct mobility of the protein ion, the other would be a false boundary the mobility of which would not correspond to any ion in the system. Svensson[10] has discussed the occurrence of false moving boundaries and why they are so rarely observed. He studied a false moving boundary in the system: gum arabic–lithium barbiturate–lithium chloride, and found that its mobility varied with the ratio between the two anions. The boundary mobility was found to agree with that theoretically predicted for a three ion system. Hence in the glycine–HCl–protein system we may expect a boundary moving with a mobility between that of the hydrogen ion and the glycine cation. The mobility of the hydrogen ion[30] at 0° is 217.8 × 10^{-5} cm.^{2} volt^{-1} sec.$^{-1}$ and the positive mobility of the glycine ion[32] at 0° is 15.6 × 10^{-5} cm.^{2} volt^{-1} sec.$^{-1}$. It is seen from Table II that the mobility of the fast descending boundary decreases as the pH increases and does not always lie between the mobilities of the hydrogen and glycine ions, becoming less than that of the glycine ion at about pH 2.25.

Figure 5 compares the curve relating pH and the mobility of the faster descending boundary with that calculated for a false moving boundary from Svensson's equation[10]

$$U = -\frac{C_{Cl}u_Hu_G + C_Hu_Gu_{Cl} + C_Gu_{Cl}u_H}{C_{Cl}u_{Cl} + C_Hu_H + C_Gu_G} \quad (1)$$

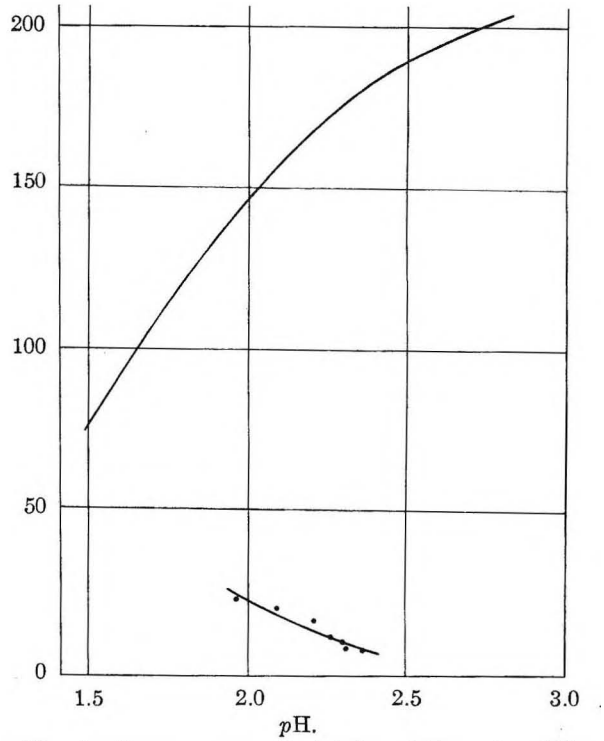

Fig. 5.—Upper curve, calculated variation of mobility with pH for false boundary in glycine hydrochloride 0.1 ionic strength using equation 1, lower curve, observed variation in mobility with pH for fast descending boundary in glycine hydrochloride.

for the conditions given in Table II. In this equation G is the glycine cation, and all the concentrations and mobilities are signed quantities. The above equation was derived for the case where three ions are present on both sides of the boundary and should be a close approximation in the present instance even though no allowance is made for the presence of the protein ions. It is seen that the mobility of the faster descending boundary does not agree with the theoretical predictions for a false boundary of the Svensson type. Equation 1 also predicts an increase in mobility with increased ionic strength at constant pH for the data of Table III, whereas the reverse occurs in the present investigation. The boundaries observed by Schlessinger[9] at slightly higher pH values in 0.01 ionic strength glycine hydrochloride also showed a decrease of mobility with increase of pH and seem to be similar to the boundaries observed in this work.

Besides failing to describe the pH–mobility relationship of the faster descending boundary and its ionic strength dependence, the moving boundary theory for strong electrolytes does not account for the presence of the slower ascending boundary. The slower ascending boundary and the faster descending boundary are considered to be false boundaries since their displacements are very pH dependent. Considerable refractive increments occur across these false boundaries and in some cases it is difficult to determine which moving boundary is due to the protein. The migration rates of the false boundaries in either limb decrease as both the pH and ionic strength is increased (Tables II and III). In glycine hydrochloride at constant ionic

(27) V. P. Dole, *J. Am. Chem. Soc.*, **67**, 1119 (1945).

(28) L. G. Longsworth, *ibid.*, **67**, 1109 (1945).

(29) L. G. Longsworth, THIS JOURNAL, **51**, 171 (1947).

(30) Calculated from the conductivity of 0.1 *N* HCl at 0° assuming additivity of ion conductances and taking the mobility of the chloride ion[31] as 37 × 10^{-5} cm.^{2} volt^{-1} sec.$^{-1}$.

(31) J. C. Nicol, *J. Am. Chem. Soc.*, **72**, 2367 (1950).

(32) R. A. Alberty, "The Proteins," Ed. Neurath and Bailey, Vol. 1A, 1953, p. 461.

strength the *p*H is varied by adding differing amounts of neutral glycine to 0.1 *N* HCl; at constant *p*H the ionic strength is varied by altering both the amount of glycine and HCl in the system. Hence it appears that the total glycine concentration (*i.e.*, cationic form + neutral glycine) is a determining factor in the variation of mobility and the refractive increments across the false boundaries. Another interesting fact is that with few exceptions whenever the refractive increments across the faster descending boundary increase, the increments across the slower ascending boundary decrease. Moreover if mobilities are calculated from the first moment of the entire gradient curve the values for serum albumin from either side of the channel seem to agree with those in other buffers where only single boundaries were observed. This is found also with poly-L-lysine.

It may be more appropriate to describe the system in terms of the theory of moving boundary systems for weak electrolytes formulated by Alberty[20,21] and Svensson.[19] The permissible number of boundaries in such systems[33] is $N - 2$ where N is the number of constituents contained in the system. If relative ion mobilities are assumed constant throughout the system one of the boundaries will be stationary. For protein dissolved in glycine hydrochloride there are five constituents: protein, glycine, Cl, H, OH, hence two moving boundaries are possible. The mobility of a false buffer boundary would be expected to be determined by the constituent concentrations of the ions,[34] although Svensson[10] found that the mobility of the false barbiturate–chloride boundary was unaffected by the addition of free barbituric acid. For the amino acid hydrochloride systems in this work it appears that changes in the glycine concentration cause a marked change in the electrophoretic patterns. The data of Table II can be qualitatively explained in terms of the constituent mobilities of hydrogen and glycine, both of which decrease as the *p*H is raised, the mobility of the fast descending boundary lying between these two mobilities. At constant *p*H with increasing ionic strength (Table III) the hydrogen and glycine constituent mobilities decrease. Increase of ionic strength by the addition of NaCl at constant *p*H causes smaller changes in the hydrogen constituent mobility (Table IV) and does not change the electrophoretic patterns as much as increase of ionic strength by glycine hydrochloride alone (compare 0.1 and 0.2 ionic strengths in Tables III and IV). At constant ionic strength and *p*H and with varying amounts of glycine (Table V) the glycine constituent mobility is the same at all glycine concentrations but as the glycine concentration is increased the hydrogen constituent mobility decreases but not as rapidly as in Table II or III.

After electrophoresis of bovine serum albumin at *p*H 2.35 in glycine hydrochloride of 0.05 ionic strength the boundaries were sufficiently separated to withdraw the phases between the boundaries and measure their *p*H values. The results, being the mean of two independent experiments, were as follows, the nomenclature of the phases being that of Longsworth[29]

Descending: δ(buffer)::$\gamma \rightarrow \beta \rightarrow \alpha$(buffer, protein)

*p*H	2.35	2.30	2.25	2.38

Ascending: α(buffer, protein)::$\beta \rightarrow \gamma \rightarrow \delta$ (buffer)

*p*H	2.38	2.45	2.57	2.35

In these experiments the apparent mobilities of the descending boundaries were 8.6 and 20.1 $\times 10^{-5}$ cm.^{2} volt^{-1} sec.$^{-1}$, the faster boundary being 12.5% of the total refractive increment; the apparent mobilities of the ascending boundaries were 10.2 and 15.6 $\times 10^{-5}$ cm.^{2} volt^{-1} sec.$^{-1}$, the slower boundary being 59% of the total refractive increment. Corresponding to the large changes in *p*H value across the moving boundaries there must be considerable changes in the ratio of the cationic to the zwitterionic forms of glycine and hence in the conductivities of the various phases. The conductivity of the α-phase in the descending limb would be expected to be less than that of the β-phase, and this would be expected to cause increased spreading of the α,β-boundary. The β,γ-boundary in the descending limb would, on the other hand, be sharpened by the conductivity effect and this is in agreement with experiment. In the ascending limb the γ,δ-boundary would be expected to be sharp and the β,γ-boundary more diffuse, as observed experimentally. The effect of *p*H on the shape of the boundaries is opposed to the conductivity effect, but would be small since there is no great change in the ionization of the protein in this region.

Dismukes and Alberty[33] studied the electrophoresis of aspartic acid in a sodium acetate buffer and under certain conditions found two moving boundaries in addition to the stationary boundary. The conditions were derived under which only one moving boundary was obtained, that is when all ions were diluted to the same extent across the stationary boundaries. They predicted that a second moving boundary would be formed if the hydrogen ion was not diluted to the same extent as other ions across the stationary boundaries. They found experimentally that two boundaries appeared as expected when the calculated difference in flow of hydrogen ions was large. Although it has not been possible to demonstrate this in the glycine hydrochloride–protein system or to define precisely the starting conditions under which more than one moving boundary is formed, the system seems to be best treated by weak electrolyte moving boundary theory.

Glycine has been recommended as a standard electrophoresis buffer[32,35] in the *p*H range 2–3, but

(33) E. B. Dismukes and R. A. Alberty, *J. Am. Chem. Soc.*, **76**, 191 (1954).

(34) The constituent mobility for a constituent R is defined as[19,21]

$$\bar{u}_R = \sum_{i=1}^{n} u_i C_i \Big/ \sum_{i=1}^{n} C_i$$

where C_i represents one of the n species in solution which comprise the R constituent.

$$\sum_{i=1}^{n} C_i$$

therefore represents its constituent concentration.

(35) G. L. Miller and R. H. Golder, *Arch. Biochem.*, **29**, 420 (1950).

it is apparent that it is unsuitable either alone[36] or in conjunction with a neutral salt such as NaCl. In all the other buffer mixtures only one moving boundary was observed although two are theoretically possible. The first three buffer salt mixtures in Table VI contain no weak acid, and false boundaries if formed would be expected to move between the mobilities of the hydrogen ion and the cation of the salt used. The phosphate and maleate buffers are uncharged acid type buffers whereas glycine hydrochloride is of the uncharged base type and the *p*H changes across the moving boundaries should be reversed. If the mobilities of false buffer boundaries are modified by the presence of uncharged acid or base then the formation of constituent boundaries with mobilities close to that of the protein could complicate the examination of the heterogeneity of proteins by moving boundary electrophoresis. It is possible that such effects may contribute to the complexity of the electrophoretic patterns observed in bovine serum albumin and other proteins in acetate buffers at higher *p*H values.[38]

Acknowledgment.—The author wishes to acknowledge the assistance of Miss B. F. Greening with the experimental work.

(36) Glycine–NaOH buffers of 0.1 ionic strength appeared to behave satisfactorily for the electrophoresis of bovine serum albumin in the *p*H range 9–11 although an extensive investigation has not been made. In the electrophoresis of some soluble wool proteins in glycine–NaOH at *p*H 11 a fast moving descending boundary has been frequently observed.[37]

(37) J. M. Gillespie and E. F. Woods, unpublished.

(38) Since completion of this manuscript papers by Cann and Phelps[39] have appeared dealing with the electrophoresis of proteins in dilute buffers at *p*H 4. Many of their results are similar to those described in this paper for amino acid hydrochloride buffers. The conclusion of Cann and Phelps that the electrophoretic patterns are a result of equilibria prevailing in the protein solutions does not appear likely in amino acid buffers at lower *p*H values since poly-L-lysine also gives abnormal patterns. The author considers that a complete explanation of the electrophoretic patterns of proteins in acidic media will be possible only when the moving boundary equations for weak electrolytes are solved for these systems. In a supporting medium containing only one salt anion at *p*H 4 as used by Cann and Phelps[39] two moving boundaries will be permissible according to the moving boundary theory for weak electrolytes[33] and this could account for one of the three moving boundaries observed in some of their experiments. The situation is so complicated that one simple explanation does not appear to cover the whole range of phenomena and as pointed out by Cann and Phelps[39] some caution is needed in interpreting electrophoretic experiments designed to test the homogeneity of protein preparations.

(39) J. R. Cann and R. G. Phelps, *J. Am. Chem. Soc.*, **79**, 4672, 4677 (1957).

REACTION OF ACETYLACETONE WITH METALLIC IRON IN THE PRESENCE OF OXYGEN

By Robert G. Charles and Sidney Barnartt

Westinghouse Research Laboratories, Pittsburgh 35, Pennsylvania

Received October 2, 1957

At room temperature metallic iron reacts with pure acetylacetone in the presence of oxygen to give a solution of iron(III) acetylacetonate. The solution also contains two acidic by-products formed simultaneously. These are acetic acid and, in smaller quantities, a stronger acid which appears to be pyruvic acid. Since acetic acid was found as a by-product also when iron(II) acetylacetonate was oxidized in the presence of acetylacetone, the ferrous compound is suggested as an intermediate in the oxidation reaction. The principal gaseous by-product of the reaction is carbon dioxide; smaller amounts of carbon monoxide were also found. The rate of reaction at 30.2° in the absence of oxygen was found to be extremely small compared with that in the presence of oxygen.

Introduction

The reaction of acetylacetone (2,4-pentanedione) with a metallic element has been used as a method of preparing the acetylacetonates of a number of metals including aluminum,[1] copper,[2] lead,[3] magnesium,[4] potassium[4] and sodium.[4,5] Copper reacts readily with pure acetylacetone at 50° in the presence of oxygen.[2] In the absence of oxygen, magnesium reacts vigorously at 60–70° with acetylacetone dissolved in ethanol, with simultaneous evolution of hydrogen.[4] These two types of reactions may be written in the general forms

$$M + x CH_3COCH{=}COHCH_3 + \frac{x}{4} O_2 \longrightarrow M\left(\begin{array}{c} O{=}C{-}CH_3 \\ \diagup \quad \diagdown \\ CH \\ \diagdown \quad \diagup \\ O{-}C{-}CH_3 \end{array}\right)_x + \frac{x}{2} H_2O \quad (1)$$

I

(1) F. Gach, *Monatsh.*, **21**, 98 (1900).

(2) B. Ciocca, *Gazz. chim. ital.*, **67**, 346 (1937).

(3) R. C. Menzies, *J. Chem. Soc.*, 1755 (1934).

(4) L. F. Hatch and G. Sutherland, *J. Org. Chem.*, **13**, 249 (1948).

(5) L. E. Marchi, "Inorganic Syntheses," Vol. II, Maple Press, York, Pa., 1946, p. 14.

$$M + y CH_3COCH{=}COHCH_3 \longrightarrow M\left(\begin{array}{c} O{=}C{-}CH_3 \\ \diagup \quad \diagdown \\ CH \\ \diagdown \quad \diagup \\ O{-}C{-}CH_3 \end{array}\right)_y + \frac{y}{2} H_2 \quad (2)$$

No investigation into the mechanisms of these reactions at metal surfaces has been reported heretofore.

A study of the reaction of pure acetylacetone with metallic iron is reported in this paper. The experiments to be described are concerned with the effect of oxygen on the reaction rate at room temperature, and with the mechanism of the reaction in the presence of oxygen. The reaction was followed principally by allowing the three substances to react in a closed system for a given length of time, then determining the decrease in gas pressure, the weight loss of the iron, and the concentrations of the products in the solution and gas phases.

Experimental

Materials.—The iron test specimens used in this study were all cut from a single sheet of pure (99.9%) iron, 0.045 cm. thick, which had been rolled smooth and annealed at 850° in argon. Just before use each specimen was etched

for 3 minutes in 3 *M* HCl, then rinsed with distilled water and redistilled acetone.

Acetylacetone was purified in the following manner. Concentrated NaOH solution was added in an amount equivalent to twice the acetic acid content as determined by titration. After filtration the liquid was treated with anhydrous calcium sulfate, filtered and fractionally distilled. The final product was stored in a glass-stoppered bottle in a dry box; $d^{30.2}_4$ 0.9630 (±0.0001) and $n^{25}D$ 1.4494.

Oxygen was commercial 99.5+% grade, dried by passage through a column of anhydrous calcium sulfate.

Iron(III) acetylacetonate was prepared from an aqueous solution of ferric chloride, acetylacetone and sodium acetate.[6] It was recrystallized from a water–methanol solution; m.p. 182–183°.

Iron(II) acetylacetonate (hydrate) was prepared by the method of Emmert and Jarczynski.[7] It was dried in a vacuum desiccator which had been previously flushed with nitrogen.

Reaction Rates.—The influence of oxygen on the rate of reaction of iron metal in acetylacetone was determined at 30.2° in a dual-compartment Pyrex vessel.

For the reaction in the absence of oxygen, the metal specimen was placed in one compartment and 25.0 ml. of acetylacetone placed in the other, and nitrogen gas (from liquid nitrogen) was passed through both compartments for 10 minutes to sweep oxygen out of the system. The acetylacetone was then transferred to the compartment containing the metal to begin the reaction. At the end of the reaction time, 100 hours, the liquid was transferred back to the other compartment to isolate it from the metal. The apparatus was opened to air and the liquid was removed quickly, diluted with de-oxygenated acetylacetone, and analyzed spectrophotometrically for iron(III) acetylacetonate at 434 mμ (the absorption maximum). Hydrogen peroxide was then added to oxidize any ferrous chelate present, and the analysis for the ferric compound repeated.

The reaction rate in the presence of oxygen was determined by immersing the metal specimen in 25.0 ml. of acetylacetone and bubbling oxygen around it at a rate of 0.2 liter/min. At the end of the reaction time (5 hours) the metal specimen was washed with acetone and its weight loss measured.

Oxygen Absorption Measurements.—For the reaction in the presence of oxygen, the ratio of iron dissolved or reaction product formed to oxygen absorbed was measured in a simple gas-absorption apparatus.[8] A strip of the metal 5 × 1 cm. was covered with a thin layer of the liquid (10.0 ml.), in a flask containing a known volume of pure oxygen (*ca.* 115 ml.) and connected to a mercury manometer. After a given absorption period the decrease in gas pressure was measured, and the metal reacted was determined by the loss in weight of the specimen. In some experiments the solution was analyzed by titration and by visible absorption spectrum, and in other experiments the gas phase was analyzed with a mass spectrometer.

Titrations.—A 5-ml. aliquot of the reaction solution was added to 50 ml. of water and stirred for 20 minutes. During this time a portion of the iron(III) acetylacetonate precipitated from the solution. The mixture was then titrated with standard aqueous sodium hydroxide, using a Precision-Dow recording titrator.

Visible Absorption Spectra.—Absorption spectra were determined by accurately diluting aliquots of the reaction solution with pure acetylacetone to a concentration of about 1.5×10^{-4} g. atoms Fe/l. and measuring the optical densities of the resulting solutions against acetylacetone as the blank. A Beckman DU spectrophotometer was used, with a tungsten light source and 1 cm. quartz cells. The molar extinction coefficient ϵ was calculated from the relation

$$\epsilon = \frac{1}{c}(\log_{10} I_0/I)$$

where $\log_{10} I_0/I$ is the optical density and c the molar concentration of the solution.

(6) A. Hantzsch and C. H. Desch, *Ann.*, **323**, 1 (1902).

(7) B. Emmert and R. Jarczynski, *Ber.*, **64**, 1072 (1931).

(8) L. L. Davis, B. H. Lincoln, G. D. Byrkit and W. A. Jones, *Ind. Eng. Chem.*, **33**, 339 (1941).

Results and Discussion

Reaction Rates.—In the presence of oxygen, iron was found to react readily with acetylacetone at room temperature to produce a red solution of iron(III) acetylacetonate (cpd. I, M = Fe, x = 3). The iron surface remained clean and metallic. The average dissolution rate at 30.2° was found to be 135 micrograms cm.$^{-2}$hr.$^{-1}$ over the 5-hour reaction time. In the absence of oxygen very little reaction occurred. The average rate at 30.2° was found to be 0.55 microgram cm.$^{-2}$hr.$^{-1}$ over the 100-hour period.

It was found that neither of the rate values given was reproducible to better than a factor of 2 or 3. The above value in the absence of oxygen, although small, is considered to be too high because complete absence of oxygen in the nitrogen atmosphere was not assured by the experimental procedure followed. The reasons for the poor reproducibility of the rate in the presence of oxygen remain to be clarified.

Ratio of Iron Reacted to Chelate Produced.—In the presence of oxygen the product of the reaction was identified as iron(III) acetylacetonate from its visible absorption spectrum. The extinction coefficient was determined for several reaction solutions as a function of wave length over the range 400 to 540 mμ, and the curves obtained agreed within experimental error with that for a synthetic solution prepared from pure, recrystallized iron(III) acetylacetonate. It is noteworthy that the reaction solutions obtained from the experiments in the "absence" of oxygen also contained all of the iron in the oxidized form, as iron(III) acetylacetonate. This was shown by rapidly measuring the optical absorption at 434 mμ, then adding hydrogen peroxide and repeating the measurement. The peroxide did not increase the amount of iron(III) acetylacetonate. Presumably there was sufficient oxygen contamination in the reaction vessel to allow the minute amount of iron which reacted to dissolve in accordance with equation 1.

The product iron(III) acetylacetonate was further identified by diluting with water one of the reaction solutions produced in the presence of oxygen. The red substance which precipitated was shown by mixed melting point to be identical with an authentic sample of the iron(III) chelate. Additional evidence that this chelate was the only iron-containing product was obtained by paper chromatography of a sample from one of the reaction solutions. Elution with *n*-hexane, or with xylene, resulted in only a single colored spot.

By-products. A. Density Measurements.—Definite evidence was found for the presence of by-products which contained no iron. All of the experiments to be described below were carried out in the presence of oxygen. Figure 1 shows the increase in density, determined pycnometrically, as a function of iron content for reaction solutions produced at 30.2°. Also shown are the densities of synthetic solutions made from recrystallized iron (III) acetylacetonate and acetylacetone. For the same iron content the reaction solution had an appreciably higher density. The difference in density could not be attributed entirely to the water pro-

duced during the reaction (reaction 1); it was estimated, from density measurements on solutions of water in acetylacetone, that the water produced accounted for only one-sixth of the observed density difference. Since this density difference increased as the reaction proceeded, side reactions were indicated.

B. Titrations.—Since one of the possible side reactions is oxidation of acetylacetone to form organic acids, 5-ml. aliquots of the reaction solution were diluted with 50 ml. of water and titrated. In Fig. 2, curve 1 shows the titration curve for a typical reaction solution. Curve 2 of Fig. 2 refers to a 0.17 M[9] synthetic solution of pure iron(III) acetylacetonate in acetylacetone; the titration curve of acetylacetone alone was identical with curve 2. Comparison of these two curves indicated that the reaction solution contained two substances more acidic than acetylacetone.

Curve 3 of Fig. 2 refers to a 0.17 M[9] synthetic solution of acetic acid in acetylacetone. The pK value for acetic acid from this curve is 4.70. For the weaker of the two additional acids in the reaction mixture, the value $pK = 4.73 \pm 0.08$ was obtained from curve 1 and similar curves. From the good agreement between these two pK values, it was concluded that acetic acid was the primary acidic by-product of the reaction.

For the stronger acid by-product, a rough value $pK = 2.7$ was estimated from the titration curves. This by-product could be pyruvic acid, for which $pK = 2.49$.[10] Small amounts of pyruvic acid would occur if the primary side reaction were the oxidation of acetylacetone to acetic acid plus pyruvic aldehyde, with subsequent oxidation of the aldehyde at least partially to pyruvic acid and possibly further oxidation to CO_2 plus acetic acid

$$CH_3COH{=}CHCOCH_3 + O_2 \longrightarrow CH_3CO_2H + CH_3COCHO \quad (3)$$

$$2CH_3COCHO + O_2 \longrightarrow 2CH_3COCO_2H \quad (4)$$

$$CH_3COCHO + O_2 \longrightarrow CH_3CO_2H + CO_2 \quad (5)$$

The ratio of the weaker acid by-product (acetic) to the stronger acid was found from the titration curves to be close to 4.0 to 1.

Experiments were carried out to determine whether these two acids are produced (a) only during the reaction with metallic iron, or (b) by oxidation of acetylacetone itself or of dissolved iron(III) acetylacetonate in the bulk of the solution. The latter possibility was negated by measurements on the rates of oxygen absorption by pure acetylacetone alone and by solutions of iron(III) acetylacetonate in acetylacetone—these rates were negligible, less than 1% of the rate of oxygen absorption by iron plus acetylacetone under the same conditions.

Thus the acid by-products occurred only when the iron metal reacted. Catalytic oxidation of acetylacetone at the iron surface was indicated. The possibility remained, however, that the intermediate compound iron(II) acetylacetonate was formed and dissolved from the surface, then oxidized further in the bulk of the solution, the by-products being formed during the last step. To test this possibility, oxygen was bubbled through a suspension of freshly-prepared iron(II) acetylacetonate (hydrate) in acetylacetone at room temperature. The ferrous chelate oxidized rapidly to yield a deep red solution of the ferric chelate within 10 minutes; the oxygen flow was continued for an additional three hours to ensure complete oxidation. A 5-ml. aliquot of the resulting solution was diluted and titrated by the standardized procedure, and yielded curve 4 of Fig. 2. It is evident that acetic acid was formed during oxidation of the ferrous chelate. The stronger acid by-product may have formed also, but because of the relatively low concentration of by-products in this case it is not identifiable from the titration curve.

The ratio of acetic acid to iron(III) chelate produced during the oxidation of iron(II) acetylacetonate was found to be roughly half of the value ob-

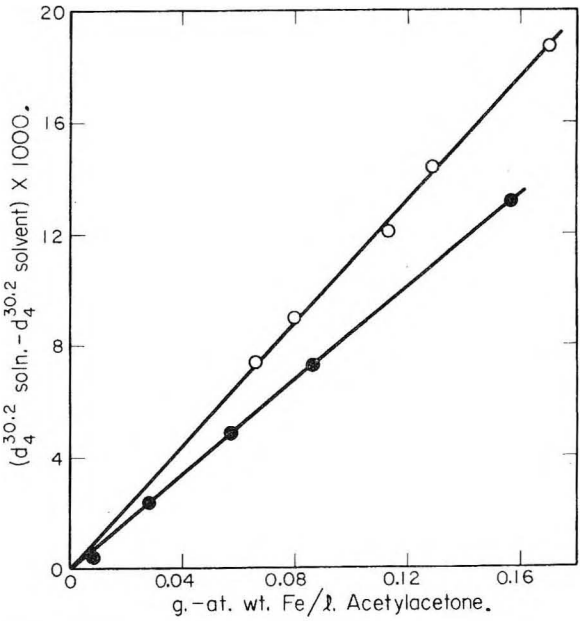

Fig. 1.—Density as a function of iron concentration: ○, reaction mixtures of iron with acetylacetone; ●, pure iron-(III) acetylacetonate in acetylacetone.

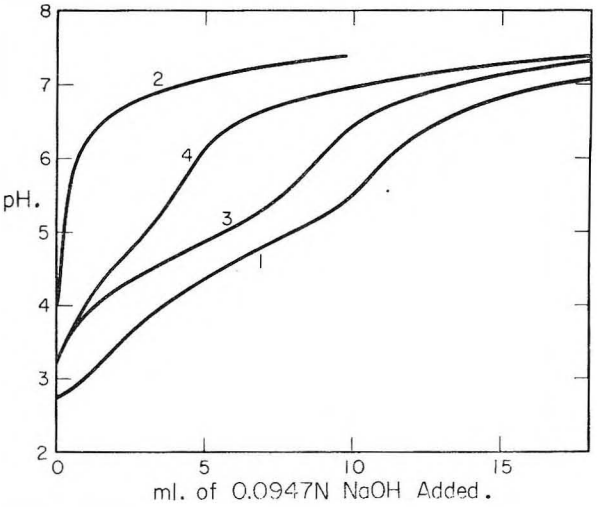

Fig. 2.—Titration curves of acetylacetone in which was dissolved reacted Fe (curve 1), Fe(III) acetylacetonate (curve 2), acetic acid (curve 3), or reacted Fe(II) acetylacetonate (curve 4).

(9) These molarities refer to the solutions before dilution with water.

(10) K. J. Pedersen, *Acta Chem. Scand.*, **6**, 243 (1952).

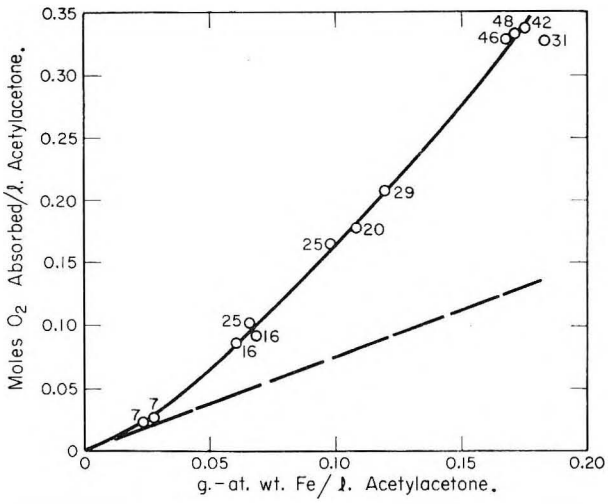

Fig. 3.—Oxygen consumed during reaction of metallic iron with acetylacetone at 25°: solid line, experimental; broken line, calculated from reaction 1. Numbers adjacent to points indicate reaction time in hours.

tained when metallic iron reacted with acetylacetone. Because the nature of the reaction of the ferrous chelate powder is different from, and faster than, that at the metal surface, it is not surprising that different quantities of by-products were found.

Other evidence that side reactions occur during the oxidation of iron(II) acetylacetonate is provided by the work of Emmert and Jarczynski.[7] These authors found that the amount of oxygen consumed when this compound is converted to the ferric chelate in an alcoholic solution is greater than the theoretical requirement. The by-products, however, were not investigated.

From the above evidence it is suggested that iron(II) acetylacetonate is an intermediate in the reaction of iron metal with acetylacetone and oxygen to form iron(III) acetylacetonate. At least a portion of the acid by-products (acetic and probably pyruvic) are formed during the further reaction of this intermediate with oxygen and acetylacetone. The possibility that by-products are produced also by catalytic oxidation of acetylacetone at the metal surface, by a mechanism not involving the ferrous chelate, cannot be ruled out on the basis of the above experiments.

C. Analysis of the Gas Phase.—In three of the oxygen-absorption experiments the gas phase in equilibrium with the reaction mixture was analyzed mass-spectrometrically at the conclusion of the reaction. Carbon dioxide was the principal gaseous by-product found. Small quantities of carbon monoxide also were found. The data are given in Table I. These data were used to calculate the number of moles of oxygen absorbed from the total pressure decrease during the reaction.

Figure 3 shows the calculated oxygen absorption per Fe reacted. Each point represents a separate experiment, the duration of which in hours is indicated by the number adjacent to the point. Incidentally, the latter numbers serve to illustrate the poor reproducibility of the reaction rates. The broken line in Fig. 3 is the relationship calculated from reaction 1. It is seen that the fraction of the oxygen absorbed which is used up in side reactions is initially small, and increases continuously with increasing extent of reaction.

TABLE I

GASEOUS BY-PRODUCTS EVOLVED AND OXYGEN CONSUMED DURING DISSOLUTION OF IRON IN ACETYLACETONE, 25°

Fe dissolved in 10 ml. acetylacetone g. at. wt. × 10³	CO_2 evolved, moles × 10³	CO evolved, moles × 10³	O_2 consumed, moles × 10²	Molar ratios CO_2/Fe	CO/Fe	O_2/Fe
0.61	0.03	0.008	0.83	0.05	0.01	1.36
1.19	.16	.05	2.08	.13	.04	1.75
1.75	.26	.05	3.35	.15	.03	1.91

The experimental data obtained do not fix unequivocally the side reaction by which CO_2 was produced. The over-all reaction represented by reactions 3 and 5, however, is not an unlikely source.[11] Assuming that reactions 1, 3, 4 and 5 apply, one can calculate the amount of oxygen equivalent to the experimental quantities of iron dissolved and of the major by-products formed (acetic acid, pyruvic acid and CO_2). Table II presents a comparison of this calculated oxygen requirement with the measured oxygen consumption for two experiments. There remains about 20% of the total measured oxygen absorption available for other side reactions not yet considered. A discussion of possible side reactions that would yield minor quantities of carbon monoxide would be purely speculative. It is, however, unlikely that one-fifth of the observed amount of oxygen absorbed would be used up in producing the small quantity of this gas found. Thus it appears likely that by-products were formed in addition to those revealed by the above experiments.

TABLE II

OXYGEN CONSUMPTION EQUIVALENT TO THE MAJOR REACTION PRODUCTS

Reaction time, hr.	46	48
Major reaction products, moles/10 ml. acetylacetone × 10³		
Fe(III) acetylacetonate	1.67	1.71
Acetic acid	1.18	1.17
Pyruvic acid	0.30	0.29
Carbon dioxide	0.25	0.25
Calcd. oxygen equiv. of above major products (reactions 1, 3, 4, 5)	2.58	2.60
Measured oxygen absorption	3.20	3.30
Ratio: $\frac{\text{oxygen equivalent}}{\text{oxygen measured}}$	0.81	0.79

Acknowledgments.—The writers are indebted to Dr. W. M. Hickam for mass spectrometer analyses and to Miss M. I. Mistrik for assistance in obtaining the titration data.

(11) H. Wieland, A. Wingler and H. Rau, *Ann.*, **434**, 185 (1924).

THE VAPOR PRESSURES OF ZIRCONIUM TETRACHLORIDE AND HAFNIUM TETRACHLORIDE[1]

BY A. A. PALKO, A. D. RYON AND D. W. KUHN

Chemistry Division, Oak Ridge National Laboratory, Oak Ridge, Tenn.

Received October 7, 1957

The vapor pressures of zirconium and hafnium chlorides were determined over the solid range up to the melting points, and in the case of $ZrCl_4$, vapor pressures in the liquid region also were obtained. Melting points for the two chlorides were determined. $ZrCl_4$ melts at 437° and $HfCl_4$ at 434°. Equations for the vapor pressure curves were calculated by a method of least squares in the solid region for both chlorides and in the liquid region for $ZrCl_4$. $HfCl_4$ (from 476 to 681°K.) $\log_{10} p_{mm.} = -5197/T + 11.712$; $ZrCl_4$ (from 480 to 689°K.) $\log_{10} p_{mm} = -5400/T + 11.766$; $ZrCl_4$ (from 710 to 741°K.) $\log_{10} p_{mm.} = -3427/T + 9.088$. From the slopes of these curves, the following physical constants have been calculated: heat of sublimation for $HfCl_4$, 23.8 + 0.3 kcal./mole (95% C.I.); heat of sublimation for $ZrCl_4$, 24.7 ± 0.3 kcal./mole (95% C.I.); heat of vaporization for $ZrCl_4$, 15.7 ± 0.9 kcal./mole (95% C.I.); heat of fusion for $ZrCl_4$ (by difference), 9.0 ± 0.9 kcal./mole (95% C.I.); vapor pressure for $ZrCl_4$ at m.p. 14,500 mm.; vapor pressure for $HfCl_4$ at m.p., 23,000 mm.

Introduction

The investigation of methods for separating zirconium and hafnium includes the possibility of fractional distillation of the metal chlorides. For this work it was desirable to have vapor pressure data for these salts above their melting points. Three different static methods were used to measure the vapor pressure over the range from 10 to 30,000 mm. The lower pressures (10–1000 mm.) were measured in a diaphragm-type apparatus. The higher pressures were obtained using a modification of the capillary "bridge" apparatus which was used by the U. S. Bureau of Mines[2] in their extensive investigation of the vapor pressures of common metal chlorides. At pressures above 10,000 mm., the capillary became clogged due to condensation of chloride vapors. Consequently, another method, involving a molten tin manometer, was used at higher pressures.

Experimental

Materials.—The charge materials were prepared from oxides obtained from De Rewal International Rare Metals Company. According to the manufacturer, the ZrO_2 contained less than 0.1% Hf, and the HfO_2 contained 0.3% Zr. The oxides contained traces of impurities such as iron, titanium and calcium, so they were purified by the following method. Each oxide was chlorinated with CCl_4 at 500° and the chloride was dissolved in 6 *N* HCl. The metal was precipitated as the mandelate from a solution 3 *N* in HCl and containing 5% excess mandelic acid.[3] The precipitate was washed thoroughly and ignited to oxide which according to spectrographic analysis was quite pure. The final charge material was made by chlorination of the oxide followed by double sublimation in a nitrogen atmosphere to remove traces of CCl_4.

Temperatures were measured by means of a Leeds and Northrup type K-1 potentiometer using chromel–alumel thermocouples with 0° reference junctions. The couples were calibrated and checked periodically against the melting points of tin, cadmium and zinc. Temperature readings were taken at approximately 5° increments with the temperature maintained at each point until the pressure was constant.

Care was taken in handling and loading the samples into the apparatus to ensure absence of moisture. Once loaded, the apparatus and charge were completely outgassed at approximately 180° for several hours. The chamber was then closed and vapor pressure measurements were made.

Diaphragm Apparatus.—The diaphragm apparatus was made of nickel, following the design of K. O. Johnsson[4] of this Laboratory and the modifications by J. H. Junkins and R. L. Farrar of the K-25 laboratories.[5] It consists essentially of a sample chamber bounded on one side by a flexible diaphragm which can be distorted inward or outward, depending upon whether the pressure inside the chamber is less than or greater than the pressure applied to the outer side of the diaphragm. To obtain the vapor pressure of the sample at a given temperature, the pressure of an inert gas on the external side is adjusted until the diaphragm assumes its balance position, as indicated by a contact rod which completes an electrical lighting circuit, at which time the pressure of the inert gas is measured on a mercury manometer.

The apparatus was heated in a five-inch tube furnace with copper conductors and magnesia insulators placed so that both ends of the chamber were slightly hotter than the center section. This was necessary to prevent condensation of vapors on these parts. The temperature of the coldest portion of the chamber was taken as the equilibrium temperature.

Capillary "Bridge" Apparatus.—In this method, the sample was placed in a capsule connected by a small capillary to a pressure balancing and measuring system. The apparatus is shown in Fig. 1. The volume of the capsule was large compared with that of the capillary. In addition to the sample, a quantity of inert gas was introduced into the capsule to reduce to a minimum the expansion of the vapors into the cold section of the capillary where they could condense and plug the capillary. With the volume of the mixture of vapors and inert gas maintained constant, the pressure that was measured at the end of the capillary was equal to the sum of the pressure of the confined inert gas and the vapor pressure of the sample. The method of balancing the external pressure against the vapor pressure of the sample was the major modification needed to adapt the U. S. Bureau of Mines apparatus for high pressure measurements. The Bureau of Mines investigators[2] used a small mercury manometer at the end of the capillary to confine the sample and applied a sufficient pressure of nitrogen on the other side to keep the manometer balanced.

Because of the difficulty in balancing a gas system at high pressure with a small manometer, the apparatus was modified so that no manometer was used. The outside pressure was obtained by a hydraulic system which was filled with oil up to a mark on the cold section of the capillary tube. The oil was maintained at this mark throughout the experiment so that the volume of gases in the capsule remained constant.

The capsule and capillary were made of quartz. The "U" tube and expansion bulb were built in the capillary to prevent accidental displacement of oil into the capsule. The connection of the quartz to the copper tubing was effected by means of a packing gland packed with rubber, with a bulb on the end of the capillary to hold the end thrust at high pressure. The pressure gauge was a 500 p.s.i. strain gauge made by the Baldwin Locomotive Company. This gauge was found to be accurate within 0.4% at 500 p.s.i. The power source for the gauge was two cells of a

(1) This paper is based on work performed for the U. S. Atomic Energy Commission by Union Carbide Nuclear Company.

(2) C. G. Maier, "Vapor Pressures of the Common Metallic Chlorides and a Static Method for High Temperatures," U. S. Bureau of Mines, Technical Paper 360, 1925.

(3) C. A. Kumins, *Anal. Chem.*, **19**, 375 (1947).

(4) K. O. Johnsson, "The Vapor Pressure of Uranium Tetrafluoride," Y-42, Oct. 20, 1947. Decl. Dec. 7, 1955.

(5) Private communication.

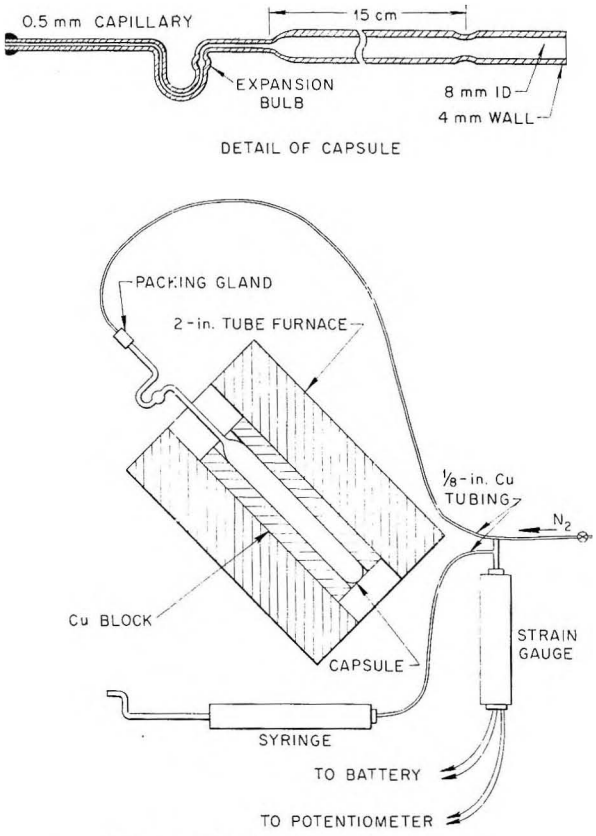

Fig. 1.—Capillary "bridge" apparatus.

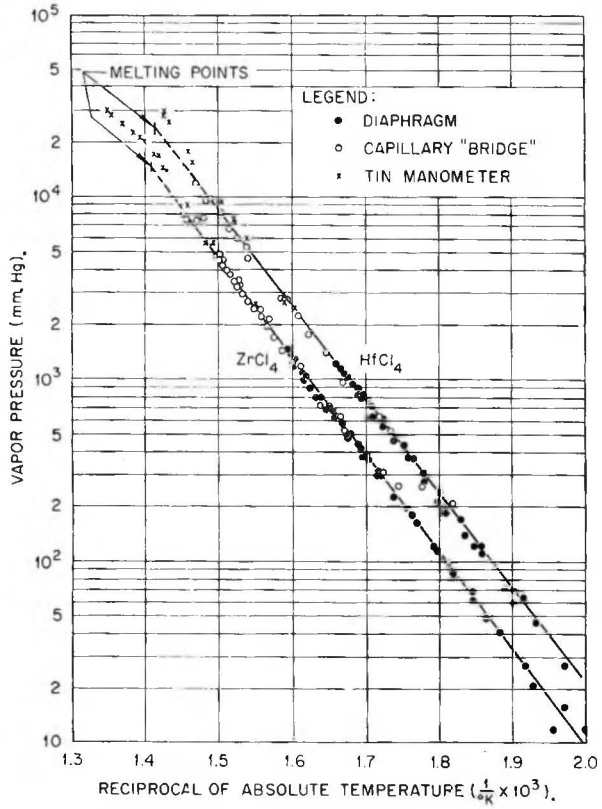

Fig. 2.—Vapor pressure of $ZrCl_4$ and $HfCl_4$.

storage battery and the output was measured on a K-1 potentiometer. At the top of the gauge one hydraulic line was connected to a threaded piston-cylinder arrangement which was used to maintain the oil level at a constant position and to compensate for any leakage in the system. Another line was connected at the gauge to admit the desired initial pressure of nitrogen to the capsule. The capsule and capillary were inclined at a 45° angle to help prevent diffusion of the vapors into the capillary. The capsule was heated in a heavy copper block placed in the center of a two-inch tube furnace with insulation arranged so that the closed end of the capsule was slightly cooler than the rest of the tube.

After the capsule was charged, sealed off, and the sample outgassed, the syringe and connecting line were filled with oil up to the tee at the gauge. Then the capsule was attached, the desired pressure of nitrogen was admitted, and the shut-off valve closed. Finally, the oil was forced carefully into the capillary up to the mark at the bottom of the expansion bulb. Then the apparatus was heated slowly and pressure readings taken at the desired temperature intervals.

The calculation of the results involved correction of the pressure readings for the partial pressure of nitrogen at the given temperatures. The pressures measured at temperatures below 200° were due essentially to the nitrogen alone since the vapor pressure of the chlorides was less than 10 mm. at these temperatures. The ratio of pressure to temperature was found constant in this range, indicating the absence of volatile impurities in the charge. This ratio was used to calculate the partial pressure of nitrogen at higher temperatures which was subtracted from the measured pressure to obtain the vapor pressure.

Despite the fact that the volume of the capsule was about 200 times as large as that of the capillary, at high pressures the capillary became plugged with condensed salt vapors. It was possible to extend the pressure range somewhat by introducing a high pressure of nitrogen at the beginning of the run, but the practical limit was about ninety pounds per square inch.

Tin Manometer Apparatus.—In this method the sample was confined in a chamber by molten tin in a small manometer which was maintained at the same temperature as the charge, and the vapor pressure was balanced by applying a pressure of nitrogen on the other side of the manometer. The pressure of nitrogen was measured with the strain gauge described above. A large enough volume of nitrogen was confined between the tin and the hydraulic fluid to permit operation from atmospheric pressure up to 800 p.s.i. without forcing the oil into the heated portion of the apparatus. The measured pressure was the sum of the nitrogen pressure and the vapor pressure of the metallic chloride. The initial pressure of nitrogen confined with the sample was determined by observing the pressures at three or four temperatures above the melting point of tin and subtracting from these pressures the known vapor pressures of $ZrCl_4$ or $HfCl_4$, as determined by the previous methods. Having once established the partial pressure due to nitrogen, vapor pressures at higher temperatures could then be calculated by correcting the total pressure for the pressure of nitrogen.

Results with the tin manometer method deviated from the results obtained by the other two methods at higher pressures as shown in Fig. 2. The reason for these deviations was not determined, and for this reason the data were not used in the derivation of the solid vapor pressure equations. The tin manometer points shown in Table I, part C were used in the calculation of the liquid region vapor pressure equation for $ZrCl_4$.

Determination of Melting Points.—The apparatus was of the type used for organic melting point determinations. Samples were sealed in 2 mm. heavy-wall quartz capsules and placed in a large aluminum block which was heated by Nichrome wire wound on the outside. A small transverse port hole was used to observe the samples which were placed in two small adjacent wells in the center of the block. The temperature was measured with calibrated chromel–alumel thermocouples located near the samples. The apparatus was heated at the rate of about 0.1° per minute and the first appearance of liquid was taken as the melting point.

Results and Discussion

The vapor pressure data for $ZrCl_4$, as determined by the three methods, are presented in Table I, parts A, B and C. Here the data are presented in the same heating and cooling sequence as recorded. Similarly, vapor pressure data for $HfCl_4$

are shown in Table II. The vapor pressure curves for both salts are shown in Fig. 2.

TABLE I

VAPOR PRESSURE OF $ZrCl_4$

PART A. DIAPHRAGM APPARATUS

Temp. (°K.)	Pressure (mm.)	Temp. (°K.)	Pressure (mm.)
503.5	6	462.0	4
511.5	12	479.5	5
519.0	21	500.5	12
536.5	49	507.5	16
541.5	61	521.5	27
556.5	114	549.5	86
567.5	181	582.5	297
582.5	310	595.5	479
586.5	363	597.0	505
591.5	439	603.0	619
595.5	503	610.0	794
599.5	578	615.5	900
602.0	630	619.0	975
603.5	670	624.0	1175
604.5	699	627.0	1461
605.0	703	625.5	1391
595.0	502	623.5	1281
590.5	425	619.0	1081
587.5	388	618.0	1041
581.0	300	611.5	798
569.0	197	606.5	680
565.0	164	604.0	617
557.5	122	589.5	372
542.0	69	582.0	300
531.0	41	575.0	227

PART B. CAPILLARY "BRIDGE" APPARATUS

580.0	310	551.5	100
598.0	520	573.0	310
610.0	720	600.0	620
618.0	980	619.5	1190
624.0	1240	637.0	2120
630.6	1450	653.5	3460
634.7	1710	665.5	4860
638.6	1960	675.0	7650
642.0	2220		
645.5	2430	602.5	670
648.8	2690	627.0	1450
652.1	2950	642.0	2430
655.0	3210	654.0	3360
657.3	3460	663.0	4500
659.8	3720	671.5	5690
662.0	3980	680.0	7390
664.0	4190	686.5	7450
665.8	4450	689.0	7910
667.7	4710		

PART C. TIN MANOMETER APPARATUS

714.1	19700	730.0	24700
717.9	20500	737.8	27700
722.7	22100	741.0	29200

The equations for the vapor pressure curves using the diaphragm and capillary bridge data have been determined by the method of least squares. The treatment in this manner results in weighting the points as though the per cent. error in pressure measurement were constant. Points below $p = 20$ mm. were rejected. The equations are

TABLE II

VAPOR PRESSURE OF $HfCl_4$

PART A. DIAPHRAGM APPARATUS

Temp. (°K.)	Pressure (mm.)	Temp. (°K.)	Pressure (mm.)
476.5	6	507.5	27
481.0	10	517.5	46
485.0	11	522.0	64
496.5	19	526.0	70
526.0	59	538.5	123
529.0	71	546.5	172
538.0	112	555.0	240
541.0	123	561.5	309
545.0	140	566.0	368
552.5	185	570.5	431
556.0	214	580.0	610
561.5	273	584.5	715
569.0	372	587.0	781
575.0	459	589.0	823
580.0	544	591.5	895
584.0	621	593.5	939
590.0	785	596.0	1019
590.5	805	598.0	1079
591.0	810	600.0	1149
		602.0	1214

PART B. CAPILLARY "BRIDGE" APPARATUS

649.7	5330	550.2	210
627.5	2740	576.5	520
606.7	1400	598.3	980
581.5	620	616.5	1760
562.3	260	630.5	2790
		649.0	4600
621.6	2220	661.0	6620
655.0	5950	673.2	9410
665.1	8220		
671.0	9670		
680.8	11600		

$HfCl_4$ (from 476 to 681°K.) $\log_{10} p_{mm.} = \frac{-5197}{T} + 11.712$ (1)

$ZrCl_4$ (from 480 to 689°K.) $\log_{10} p_{mm.} = \frac{-5400}{T} + 11.766$ (2)

For $ZrCl_4$ vapor pressures in the liquid region, the following equation applies

$ZrCl_4$ (from 710 to 741°K.) $\log_{10} p_{mm.} = \frac{-3427}{T} + 9.088$ (3)

The precision of the pressure measurements may be indicated by the 95% confidence interval calculated from the data used.

	Table I, A, B	Table II, A, B	Table I, C
95% C.I. $(p)/p$	0.144	0.131	0.021

From the slopes of these curves, the following physical constants have been calculated

Heat of sublimation for $HfCl_4$	23.8 ± 0.3 kcal./mole (95% C.I.)
Heat of sublimation for $ZrCl_4$	24.7 ± 0.3 kcal./mole (95% C.I.)
Heat of vaporization for $ZrCl_4$	15.7 ± 0.9 kcal./mole (95% C.I.)
Heat of fusion for $ZrCl_4$ (by difference)	9.0 ± 0.9 kcal./mole (95% C.I.)

The data of this report are in good agreement

with the results obtained at the Ames Laboratory[6] where vapor pressures in the range 30–700 mm. were measured.

The melting point of $ZrCl_4$ is 437° and of $HfCl_4$ is 434°. Calculated from equations 1 and 2 above, the vapor pressure of $ZrCl_4$ at its melting point is 14,500 mm., and the vapor pressure of $HfCl_4$ at 437° is 24,700 mm. The separation coefficient for a single plate as given by the ratio of the vapor pressures at 437° is 1.70 as compared with 1.14 for the coefficient of the phosphorus oxychloride complexes of zirconium and hafnium.[7]

(6) B. A. Rogers, *et al.*, Iowa State College Progress Report in Metallurgy, ISC-45, June 9, 1949; (b) W. K. Plunknett, R. S. Hansen and F. R. Duke, Iowa State College Progress Report in Physical and Inorganic Chemistry, ISC-51, July 14, 1949.

(7) D. M. Gruen and J. J. Katz, "Separation of Hafnium and Zirconium by a Fractional Distillation Procedure," AECD-2584, March 29, 1949, decl. May 10, 1949.

THE EFFECT OF PRESSURE ON THE INTERFACIAL TENSION OF THE BENZENE–WATER SYSTEM

BY R. R. HARVEY

Research and Development Dept., Phillips Petroleum Co., Bartlesville, Oklahoma

Received October 8, 1956

Using the pendant drop method, the effect of pressure on the interfacial tension for the benzene–water system has been measured at pressures of 68–1360 atm., temperatures of 31.90, 49.88, 75.19 and 95.19. Interfacial tension values varied only 2–3 dynes/cm. over this range of pressure, showing a minimum at 340 atm. at 31.90, a slight maximum at 540 atm. at 49.88 and a regular decrease with increasing pressure for the two higher temperatures.

I. Introduction

The porous nature of an oil reservoir leads to a distribution of fluids which presents a large and varied surface area. It is apparent that any description of such a system cannot be complete without some information on the interfacial properties of the various reservoir phases. Although reservoir surface properties have been studied for many years, the conclusions reached have been inferred largely from measurements made under atmospheric pressure. An exception to this has been the recent work of Hough, Rzasa and Woods[1] in which the interfacial tension of the methane–water system was measured from atmospheric pressure to 1000 atm. Hassan, Nielsen and Calhoun[2] have also measured the interfacial tension of a series of paraffin hydrocarbons against water at pressures up to 200 atm.

The present apparatus has been designed to measure interfacial tensions involving reservoir materials at pressures up to 1360 atm. over a range of temperature from 25–150. As part of the initial work on this equipment the interfacial tension of the benzene–water system was measured at pressures from 68–1360 atm. at four temperatures. This system was chosen for several reasons: first, reasonably reliable data existed over part of the range of pressure to provide a method of checking the accuracy of the equipment; second, the benzene–water system is of sufficient theoretical interest to justify extending the interfacial tension measurements to 1360 atm.; and finally, the two liquids were readily obtainable in a very pure state. This system previously has been studied by Michaels and Hauser[3] at pressures from atmospheric to 700 atm. and by Hassan, *et al.*,[2] up to 200 atm.

(1) E. W. Hough, M. J. Rzasa and B. B. Woods, *Trans. A.I.M.E.*, **192**, 57 (1951).

(2) M. E. Hassan, R. F. Nielsen and J. C. Calhoun, Jr., *ibid.*, **198**, 299 (1953).

(3) A. S. Michaels and E. A. Hauser, THIS JOURNAL, **55**, 408 (1951).

II. Experimental

Materials.—Merck "Reagent Grade Thiophene Free" benzene was used. The surface tension of this was checked independently by tensiometer measurements and gave a value of 28.90 dynes/cm. at 20°. This is in agreement with the value given in the International Critical Tables.[4] Laboratory distilled water was further purified before use by passing it through a commercial ion-exchange resin demineralizer. The surface tension of this water gave a tensiometer reading of 71.57 dynes/cm. at 26.5°. This differs from the literature[4] value of 71.74 dynes/cm. by 0.24% or within the accuracy of the tensiometer. Although designed specifically to remove inorganic impurities, such ion-exchange beds also act as effective filters for small amounts of organic contaminants and when properly prepared and washed should introduce no impurities themselves. However, to check further for any impurity a sample of this ion-exchange water was redistilled from a neutral $KMnO_4$ solution in an all Pyrex apparatus. A center cut of this distillation gave a value of 71.66 dynes/cm. at 26.0°. This differs by 0.22% from the reported[4] value. Surface tension measurements of other cuts from this distillation gave nearly identical values. The interfacial tension between benzene and water also was measured independently on a tensiometer. This value was 34.20 dynes/cm. at 26.5° which is only about 0.4 dyne/cm. lower than the value given in the International Critical Tables.[4]

This value remained constant with time and together with the other tests this was considered sufficient evidence of the absence of interfacially active components in either phase. In carrying out the tensiometer measurements all the precautions and corrections previously outlined by Harkins[5] were observed.

Apparatus.—The equipment uses the pendant drop method of interfacial tension measurement. It consists of a pressure generating system, a means of transmitting the pressure to the fluids to be studied, a double-windowed observation cell, a light source and a camera to record the drop profiles. Pressure is generated by an air-operated hydraulic pump having a multiplication factor of 200:1. Close adjustment of pressure is achieved with a hand operated pump which may be used independently after the approximate pressure has been reached. Hydraulic pressure is read directly on a Heise gauge, accurate to ±0.68 atm., over the range of measurement. Mineral oil is used as the hydraulic fluid.

(4) "International Critical Tables," Vol. IV, McGraw-Hill Book Co., Inc., New York, N. Y., 1928.

(5) W. D. Harkins, "Physical Methods of Organic Chemistry," Part One, Interscience Publishers Inc., New York, N. Y., 1949, p. 382.

Pressure is transmitted from the oil to the fluids being studied by two "O" ring sealed floating pistons.

The observation cell is a four inch diameter Monel metal cylinder four inches long with a 1.25 inch bore. It is fitted at each end with plate glass windows one-half inch thick. All entrances to the cell are made at one end with the exception of the dropper tip assembly. This contains a needle valve for controlling drop formation and a means for raising or lowering the dropper tip within the field of vision. All seals are made by "O" rings.

The pressure transfer vessels are Monel lined steel cylinders with Monel pistons and end plugs. All valves and connecting lines are of stainless steel. Teflon seals are used throughout the entire apparatus.

The cell is surrounded by a cylindrical air-bath maintained within $\pm 0.1°$ by a mercury thermoregulator. The cell and air-bath temperatures are measured by Western Electric 14-A thermistors. Due to the large heat lag in the metal cell, temperatures within the fluid under study can be held to $\pm 0.05°$.

For interfacial tension measurements the drops are illuminated by collimating the light from a 100 watt zirconium arc lamp, and photographs are made on 3.25×4 inch Kodak contrast lantern slide plates in a Bausch and Lomb Model L photomicrographic camera. Drop profiles obtained with the benzene–water system were quite sharp and free from distortion. Since the glass cell windows are the only part of the optical system subjected to the extremes of pressure and temperature the chance for any distortion is slight. However, one of the most revealing features was the appearance of diffraction lines, in most cases to the fourth order, around the dropper tip and drop edge. These were quite sharp and regular and could be seen at any position over the field of view at all pressures and temperatures. The regularity of these patterns appeared to preclude the presence of any short range distortions. Finally, the constancy of the dropper tip dimensions under a variety of temperatures and pressures and over the entire field of vision gave assurance of the absence of any long range distortions.

The choice of the dropper tip size was quite critical since the range of stable and measurable drops is determined by both the nature of the fluids and the diameter of the tip from which the drop is suspended. Early in the investigation it was noted that outside this range one could obtain apparently stable drops, some of which were measurable, but all of which would give rise to erroneous interfacial tension values. Niederhauser[6] studied the range of stable drops as a function of the radius of the dropper tip, the nature of the fluids involved and the shape of the drops. On the basis on these studies a dropper tip 0.2972 cm. in diameter was chosen which produced stable drops of suitable size over the entire range of investigation. This tip was measured on a linear comparator and its diameter was known to ± 0.001 mm. With a 158 mm. E.F. photomicrographic lens placed about 25 cm. from the drop an image of adequate magnification (about $6\times$) was obtained at the camera. Exposure time was about $^1/_5$ second, chosen as the optimum value from a study of drop measurement reproducibility as a function of exposure time.

A series of measurements of the interfacial tension of benzene–water at 27.0° and atmospheric pressure gave an average value of 34.32 dynes/cm. with an average deviation of about two parts per thousand. This compared favorably with the literature[4] value of 34.59 dynes/cm.

A consideration of all possible sources of error (most of which lie in the drop measurement) leads to an expected total random error in the instrument of not over 1%.

Procedure.—Photographs of benzene drops in water were taken at 68 atm. intervals from 68–1360 atm. at 31.90 49.88, 75.19 and 95.19°. It was necessary to discontinue measurement on the 31.90° isotherm at 748 atm. because the high viscosity of the benzene at this pressure made drop formation excessively slow.[7]

Photographs were made only of equilibrium drops; an excess of benzene was kept in the cell and the cell was rocked as the pressure was increased to keep the water saturated. The drop when originally formed was pure benzene but studies of the variation of interfacial tension with time indicated that solution equilibrium within the drop is reached very quickly, in most cases within the first minute after formation. One half hour was allowed after each pressure change to allow the system to return to equilibrium and five minutes after the formation of each drop.

To assure that the liquids did not suffer any contamination during the course of a run, preliminary checks were made by recording two separate sets of data, one with increasing pressure and the other with the pressure decreasing. No differences between these series were noted larger than the ordinary instrument error. This precaution not only assured the continuing purity of the liquids but indicated that the proper amount of time had been allowed to achieve equilibrium.

Drop profile photographs were measured on a modified Gaertner comparator microscope which could be read to 0.00025 cm. on both horizontal and vertical scales. In all, 206 separate drop photographs were made, at least two at each pressure and temperature and in some cases as many as eight.

III. Results and Discussion

Calculation of d_e^2/H.—The equation used to calculate the interfacial tension from pendant drop measurements is given[8] as

$$\gamma = \frac{\sigma g d_e^2}{H}$$

where

σ = difference in density between the drop and the surrounding phase
g = acceleration of gravity
d_e = maximum or equatorial diameter of the drop
H = a value, independent of the system, obtained by soln. of the drop profile eq.

Values of H have been tabulated by Niederhauser and Bartell,[9] Fordham[10] and Mills[11] in terms of the ratio, S, of two easily measured drop dimensions, d_s and d_e where d_e has the meaning given above and d_s is the drop diameter at a selected plane the distance d_e above the base of the drop. Figure 1 presents the variation of d_e^2/H with pressure for the four temperatures investigated.

Agreement within all sets of the data but one is within 1.0% and in the majority of cases within 0.5%. The average deviation of points from the smooth curves is 0.5%.

Density Data.—Since d_e^2/H was measured at equilibrium conditions, for a rigorous calculation of the interfacial tension, σ in the drop equation should be the density difference between the two mutually saturated phases. Such data were not available over the pressure range studied here, nor was it possible to make even a partial correction due to the lack of solubility data at elevated pressures. It is expected that such a correction would be nearly negligible except at high temperatures and pressures and small even there due to the low density difference between the two liquids. This low density difference, however, makes it very important that accurate density values be known for the water and benzene since an error in these quantities may give rise to an error nearly ten times as large in σ.

Keenan and Keyes[12] have measured the specific

(6) D. O. Niederhauser, Ph.D. Thesis, Univ. of Michigan, 1947.

(7) Benzene solidifies at 884 atm. at this temperature.

(8) J. M. Andreas, E. A. Hauser and W. B. Tucker, THIS JOURNAL, **42**, 1001 (1938).

(9) D. O. Niederhauser and F. E. Bartell, "Fundamental Research on the Occurrence and Recovery of Petroleum," American Petroleum Institute, 1948–1949, p. 114.

(10) S. Fordham, *Proc. Roy. Soc. (London)*, **A194**, 1 (1948).

(11) O. S. Mills, *Brit. J. Appl. Phys.*, **4**, 247 (1953).

(12) J. H. Keenan and F. G. Keyes, "Thermodynamic Properties of Steam," John Wiley and Sons, Inc., New York, N. Y., 1936.

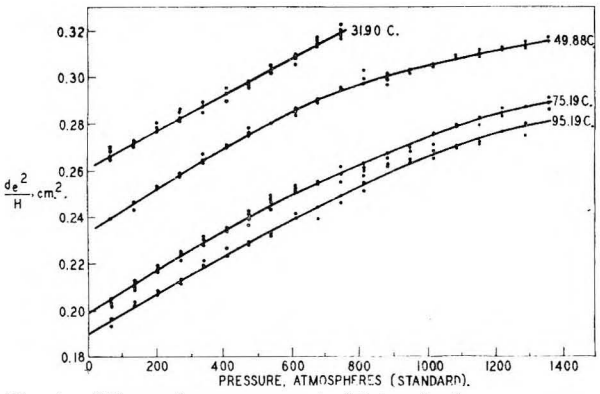

Fig. 1.—Effect of pressure on d_e^2/H for the benzene–water system.

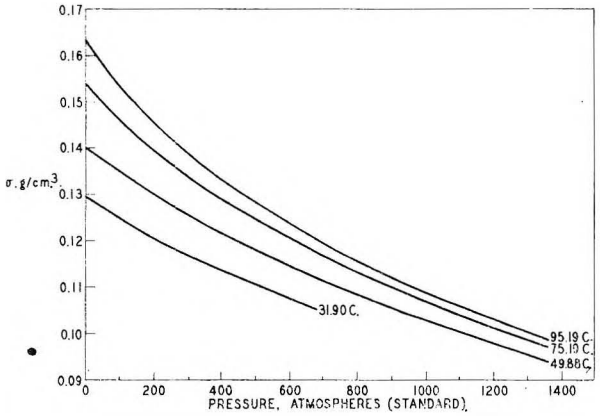

Fig. 2.—Effect of pressure on phase density difference for the benzene–water system.

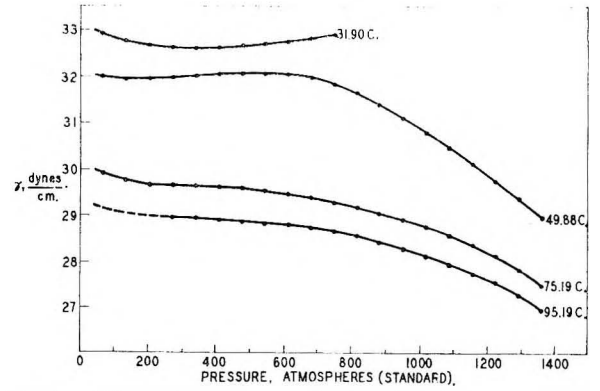

Fig. 3.—Effect of pressure on the interfacial tension for the benzene–water system.

volume of water at several temperatures and pressures up to 408 atm. and Bridgman[13] has extended these data up to pressures of 11,000 kg./cm.^{2} (10,600 atm.). These data yield a smooth relationship for water over the desired range. The data of Glanville and Sage[14] on benzene, when combined with those of Bridgman,[13] failed to give as good relationship because the data could not be joined smoothly. This difficulty, however, could be removed by smoothing out the anomalous hump which appeared in the density difference curves.

(13) P. W. Bridgman, *Proc. Am. Acad. Arts Sci.*, **66**, 185 (1931).

(14) J. W. Glanville and B. H. Sage, *Ind. Eng. Chem.*, **41**, 1272 (1949).

The resultant variation of σ with pressure for the four temperatures is shown in Fig. 2.

Interfacial Tension.—Following the technique used by Michaels and Hauser, the values of d_e^2/H read from the smoothed curves of this quantity *versus* pressure have been used together with the density difference curves to calculate variation of interfacial tension with pressure at the four temperatures shown in Fig. 3. Values of d_e^2/H used here are about 5% higher initially and increase slightly faster with increasing pressure than those of Michaels and Hauser over the pressure range to 700 atm. This difference is reflected in the interfacial tension curves which are initially about 0.5–1.5 dynes/cm. higher and decrease more slowly with increasing pressure. While Michaels and Hauser had reported a slight increase in interfacial tension with pressure at their lowest temperature, the maximum in the 49.88° curve shown here is without precedent. No ready explanation for this behavior presents itself and, while such a slight peak could be due to a slight error in density, the remarkable similarity shown in the curves at the two higher temperatures makes this doubtful.

A partial explanation for the difference between the present data and those of Michaels and Hauser may lie in the departure of their empirically determined relationship of S *versus* $1/H$ from that determined by solution of the drop equation. This departure, while in the correct direction, cannot be quantitatively determined without complete knowledge of the individual drop sizes used by the above investigators. A more striking indication of the source of error lies in the fact that the benzene–water interfacial tension at 23° given by Michaels and Hauser is 2.1 dynes/cm. lower than that given by the International Critical Tables and 1.7 dynes/cm. lower than this work.

In the curve for interfacial tension *versus* pressure at 95.19° the experimental points have been omitted over the initial portion of the curve. Subsequent investigation of these measurements showed that the diameter from which the drops were suspended gave rise to S values lying slightly outside the stable region as indicated by the data of Niederhauser.

IV. Conclusion

In summary the results of this investigation indicate that: 1. The pendant drop method is entirely satisfactory for interfacial tension measurements at elevated pressures and temperatures but is highly dependent on the possession of accurate equilibrium density values for the liquids composing the systems studied.

2. For accurate interfacial tension data by this method under any conditions it is extremely important that drop sizes are chosen which lie within the range of true stability. Quasi-stable drops may be obtained which will almost certainly lead to spurious though often self-consistent results.

3. The apparatus constructed for the present work is capable of yielding reliable values of interfacial tension at pressures up to 1360 atm. and temperatures at least as high as 100° within the limits of the above paragraphs.

4. The interfacial tension of the benzene–water system decreases only slightly with increasing pressure and shows slight though definite increases at low temperatures over the low pressure ranges.

HEATS OF FORMATION OF α-PHASE SILVER–CADMIUM ALLOYS

BY RAYMOND L. ORR,* ALFRED GOLDBERG† AND RALPH HULTGREN*

* *Minerals Research Laboratory, University of California, Berkeley, California, and the*
† *U. S. Naval Postgraduate School, Monterey, California*

Received October 11, 1957

Heats of formation at 308°K. were determined by liquid tin solution calorimetry for a series of alloys covering the α-phase of the Ag–Cd alloy system. The results are in good agreement with previously reported values obtained from vapor pressure measurements and serve to fix the heats of formation of the phase as a function of composition to within ±50 cal./g. atom. The data are well represented by a regular solution equation with an added short-range order term except near the α-phase boundary where there is a positive energy effect which may be due to the filling of high electronic energy levels of the first Brillouin zone.

Introduction

Attempts to elucidate the nature of atomic bonding in alloys have emphasized the need for accurate thermodynamic data for alloy systems. This in turn has stimulated considerable interest in the study of alloy thermochemistry. Heat of formation studies have been undertaken by the authors because the data provide a direct measure of the difference between the total bonding energy in an alloy and that in the pure metals of which it is composed. From such data for representative alloy systems, it is hoped to deduce the effect upon intermetallic behavior of such factors as differences in electronegativity, differences in atomic size, and the electron to atom ratio. The α-phase Ag–Cd alloys offer the opportunity of determining a possible effect of the filling of the first Brillouin zone upon the bonding energy of the phase.

Experimental

Seven Ag–Cd alloys containing 10, 20, 30, 34, 36, 38 and 40 atomic % Cd were prepared by melting the pure metals together in sealed evacuated quartz tubes and homogenizing about 50° below the respective solidus temperatures for two weeks. The compositions were verified by X-ray precision lattice constant measurements which agreed well with published data.[1] The homogeneity of the alloys was indicated by the sharpness and good resolution of the back-reflection diffraction lines.

The liquid tin calorimeter and experimental procedures used for the heat of formation determinations have been described in detail elsewhere,[2] hence only a brief description will be given here. The calorimeter consists basically of a stirred bath of approximately 250 grams of liquid tin contained in a molybdenum crucible and surrounded by a heavy copper jacket. The jacket is heated by a resistance heating element, and externally caused drifts or fluctuations in the jacket temperature are kept within less than 0.001° by means of a sensitive resistance thermometer temperature controller. The temperature difference between the jacket and crucible is measured by means of a copper–constantan differential thermocouple, and the jacket temperature is measured separately by a calibrated platinum–platinum +10% rhodium couple. The calorimeter is contained in an evacuated chamber which also contains the specimen dispenser unit.

When the calorimeter has reached a steady state, the specimen temperature is recorded and it is dropped into the tin bath. Readings of the differential and jacket temperatures are then taken at frequent intervals. The total heat effect after the reaction is complete is evaluated from the change in the differential temperature, the measured heat capacity of the calorimeter, and a correction for the heat transfer between the jacket and crucible. The heat capacity of the calorimeter is determined from the temperature drop accompanying the addition of a specimen of solid tin, using the known heat content data for tin.[3] The heat transfer correction for the reaction period is evaluated by established methods based on Newton's law of heat transfer.

The magnitude of the heat transfer correction and the measured heat effect are reduced by using the balanced heat effect method, described previously.[2] Spherical specimens, about 5.5 mm. in diameter and containing about 0.005 gram atom of solute metals, were prepared by enclosing cuttings of the samples in gold capsules along with excess gold, which dissolves exothermically, to balance the endothermic effect of Ag, Cd and the alloys. In order to reduce vaporization of cadmium from the tin-bath, the temperature of the liquid tin was held at the low value of 517°K., only about 10° above the melting point of tin. The tin-bath was replaced before the total concentration of solute metals reached 2.5 atomic %, reducing possible concentration effects to less than could be detected by the measurements. The specimen temperature was 305–311°K.

Results

Results for the pure metals evaluated at the solution temperature are given in Table I. Since the measurements were made in dilute solution, the values listed approximate the relative partial molal heat contents of Au, Ag and Cd in infinitely dilute solution in liquid tin at 517°K. with respect to the solid metals at that temperature, *i.e.*, $(\bar{H} - H^0)_{517°K.,x_{Sn}=1}$.

TABLE I

HEATS OF SOLUTION OF PURE METALS AT 517°K.

Run no.	Metal	ΔH_{soln} cal./g. atom	Run no.	Metal	ΔH_{soln} cal./g. atom
10-2	Au	−5,939	10-4	Ag	3,443
10-3	Au	−5,918	10-6	Ag	3,510
11-2	Au	−5,952	15-3	Ag	3,590
11-3	Au	−5,927	16-2	Ag	3,562
15-2	Au	−5,905			
			Av.	Ag	3,526 ± 50
Av.	Au	−5,928 ± 14	11-5	Cd	3,240
			12-4	Cd	3,240
			16-3	Cd	3,235
			Av.	Cd	3,238 ± 2

The results show good agreement for Au and Cd,

(1) W. Hume-Rothery, G. F. Lewin and P. W. Reynolds, *Proc. Roy. Soc. (London)*, **A157**, 167 (1936).

(2) R. L. Orr, A. Goldberg and R. Hultgren, *Rev. Sci. Instr.*, **28**, 767 (1957).

(3) K. K. Kelley, U. S. Bureau of Mines Bull. 476, 1949.

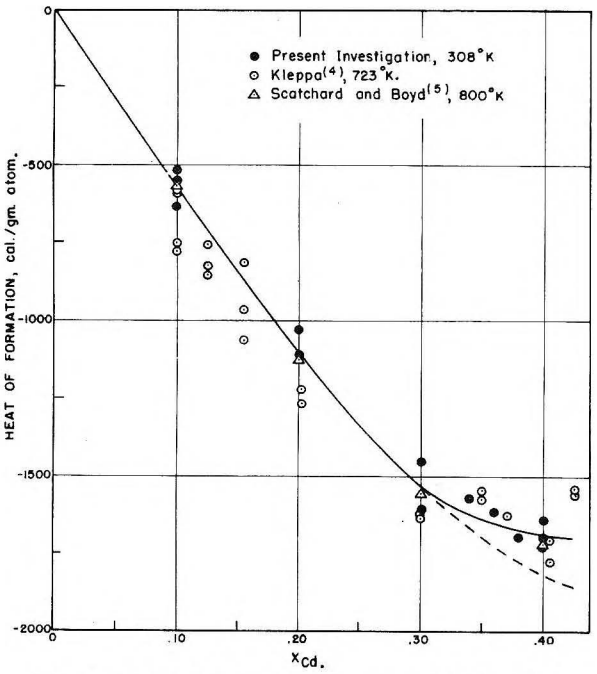

Fig. 1.—Heats of formation of α-phase Ag–Cd alloys.

which dissolved rapidly in liquid tin at this temperature, in about eight and two minutes, respectively. The considerably higher scatter in the values for Ag probably resulted from the longer time required for its solution, about 25 minutes.

The results for the alloys are given in Table II.

TABLE II

HEATS OF FORMATION OF Ag–Cd ALLOYS AT 308°K.

Run no.	x_{Cd}	T_i,[a] °K.	T_f,[b] °K.	ΔH_{soln} cal./g. atom	$\Delta H_{formation}$ 308°K., cal./g. atom
8-6	0.10	310.7	515.9	5,290	− 518
10-10	.10	307.2	516.3	5,431	− 637
10-11	.10	307.5	516.2	5,343	− 549
7-10	.20	310.3	515.6	5,780	−1,029
11-7	.20	306.3	516.5	5,893	−1,111
11-8	.30	305.6	516.5	6,217	−1,453
15-6	.30	308.4	520.6	6,381	−1,607
15-7	.34	308.4	520.6	6,335	−1,570
15-8	.36	309.2	520.4	6,369	−1,614
12-8	.38	307.4	516.4	6,432	−1,697
11-9	.40	305.7	516.5	6,380	−1,638
12-7	.40	308.2	516.4	6,455	−1,729
12-9	.40	307.5	516.4	6,429	−1,698

[a] T_i = initial specimen temperature. [b] T_f = final solution temperature. ΔH_{soln} = total heat effect for solid alloy at T_i going to solution in liquid tin at T_f.

The heats of formation of the alloys at 308°K., the average value of T_i, are evaluated from the reactions

$$Ag_{(s,T_i)} = Ag\ (\text{in Sn})_{(l,T_f)},\ \Delta H_1 \quad (1)$$

$$Cd_{(s,T_i)} = Cd\ (\text{in Sn})_{(l,T_f)},\ \Delta H_2 \quad (2)$$

$$Ag_{1-x}Cd_{x(s,T_i)} = (1-x)Ag\ (\text{in Sn})_{(l,T_f)} + x\text{Cd}\ (\text{in Sn})_{(l,T_f)},\ \Delta H_3 \quad (3)$$

The measured reactions are combined to yield the heat of formation of the alloy at T_i

$$(1-x)Ag_{(s,T_i)} + xCd_{(s,T_f)} = Ag_{1-x}Cd_{x(s,T_i)} \quad (4)$$

$$\Delta H_{\text{formation},T} = (1-x)\Delta H_1 + x\Delta H_2 - \Delta H_3 \quad (5)$$

It should be noted that the final solution temperature does not enter into the evaluation provided it is the same for reactions 1, 2 and 3, and no assumptions regarding changes in heat content for the alloys between T_i and T_f are made.

The heat of formation values are shown plotted in Fig. 1 together with the data of Kleppa[4] and of Scatchard and Boyd.[5] Kleppa measured, by liquid tin calorimetry, the heats of formation at 723°K., referred to solid silver and liquid cadmium. His values have been recalculated to refer to superheated solid cadmium at 723°K., using 1450 cal./g. atom for the heat of fusion of cadmium.[3] The plotted values of Scatchard and Boyd were calculated by Anderson[6] from the $\Delta\bar{F}_{Cd}$ and $\Delta\bar{S}_{Cd}$ data obtained from their vapor pressure measurements, and refer to solid silver and superheated solid cadmium at 800°K.

Discussion

The presently reported data and those of Scatchard and Boyd are in good agreement. The solid curve shown in Fig. 1 was drawn giving major weight to these two sets of data and is believed to represent the heats of formation to within ±50 cal./g. atom. The scatter shown by the present values is somewhat greater than has been found in studies on other alloy systems such as Ag–In, Ag–Au and Au–Cu. This is thought to be partly due to the long times required for the alloys to go into solution, usually of the order of 60 minutes or more, the slight amount of vaporization of Cd from the solution during the long runs, and a possible small dependence of the heats of solution on solute concentration. The larger scatter shown by Kleppa's data may have resulted from an increased amount of Cd vaporization at his higher solution temperature, 723°K. The good agreement found between the present values obtained at 308°K. and those of Scatchard and Boyd and Kleppa obtained at much higher temperatures indicates that ΔC_p for the α-phase alloys is negligible in this temperature range. This has been confirmed by unpublished heat capacity measurements in this Laboratory.

The heat of formation curve from $x_{Cd} = 0$ to 0.30 is fitted with a high degree of precision by the equation

$$\Delta H = -5500x_{Ag}x_{Cd} - 8600(x_{Ag}x_{Cd})^2 \quad (6)$$

Equation 6, obtained from quasi-chemical theory, represents the heat of formation of a regular binary solution with an added term to correct for short-range order.[7] Above $x_{Cd} = 0.30$ the experimental heats of formation become less exothermic than the values given by equation 6 which are represented by the dashed curve in Fig. 1. Some of this deviation may be due to the first-order approximations involved in the derivation of equation 6. It is believed, however, that the rather sharp change in slope of the heat of formation curve at about 30 atomic % Cd is due at least in part to a

(4) O. J. Kleppa, THIS JOURNAL, **60**, 846 (1956).

(5) G. Scatchard and R. H. Boyd, *J. Am. Chem. Soc.*, **78**, 3889 (1956).

(6) P. D. Anderson, M.S. Thesis, University of California, 1957.

(7) A. W. Lawson, *J. Chem. Phys.*, **15**, 831 (1947).

Brillouin zone effect which forces the additional valence electrons into higher energy levels after the first zone boundary is touched, thus decreasing the exothermic heat of formation of the alloys. Theoretical calculations show that for face-centered cubic phases at 0°K. the Fermi surface touches the first Brillouin zone at an electron to atom ratio of 1.36.[8] For Ag–Cd this occurs at 36 atomic % Cd; however, the thermal energy of the electrons at the temperature of measurement may well account for the initiation of the effect at the lower concentration of Cd.

Acknowledgments.—The authors wish to express their appreciation to the Office of Ordnance Research, United States Army, under whose sponsorship this investigation was conducted.

(8) W. Hume-Rothery, "Atomic Theory for Students of Metallurgy," Second Edition, The Institute of Metals, London, 1952.

DIFFERENTIAL CALORIMETER FOR HEATS OF FORMATION OF SOLID ALLOYS. HEATS OF FORMATION OF ALLOYS OF THE NOBLE METALS[1]

BY R. A. ORIANI AND W. K. MURPHY

General Electric Research Laboratory, Schenectady, New York

Received October 15, 1957

A twin, differential, high-temperature calorimeter for the measurement of the enthalpy of formation of solid alloys is described. The principle and the various methods of operation are discussed. Experimental results for the enthalpy of formation of solid Ag–Au, Au–Cu and Ag–Cu alloys are presented. The accuracy of a heat of formation is estimated as ±2% or ±20 cal./g. atom, whichever is larger.

Perusal of a critical compilation, such as that by Kubaschewski and Caterall[2] quickly shows how scarce are reliable data on the energy of formation of solid metallic solutions. Such data are a necessary prerequisite toward the goal of understanding interactions in alloy systems. Indeed, enthalpy values are of more interest than are free energy values, because theories of solutions are usually more sensitive toward the enthalpy than toward the free energy. At the present time there exist more numbers for the enthalpy of formation of solid alloys obtained by equilibrium techniques (*i.e.*, based on the temperature variation of a vapor pressure, or a ratio of gaseous components, or an e.m.f. of a galvanic cell) than those obtained by direct calorimetry. However, it is often very difficult, when equilibrium techniques are used, both to obtain accurate values for the enthalpy of formation and to establish the degree of accuracy. Not only are the experimental approaches difficult, but also the algebraic manipulations introduce further error, since the difference of large numbers must be taken and graphical integration of the Gibbs–Duhem equation is necessary.

Direct calorimetry offers the best possibility for the precise determination of heats of formation of alloys. Unfortunately, however, for solid alloys calorimetry also is not very straightforward, since the two pure solid components cannot be directly combined while the heat of reaction is measured, as is the case for liquid alloys from liquid components.[3] In the case of solid alloys the intermediacy of a solvent liquid is needed in order to reduce both the alloy and a mechanical mixture of the pure solid components to the same physical and energetic state. Therefore, one has the problem of obtaining the difference between two numbers, one for the dissolution of the alloy in the solvent liquid and the other for the dissolution of the mechanical mixture, each of which must be measured with great accuracy so that their difference may be significant.

The principle of the present calorimeter is that of using a liquid metal as solvent, and our design has profited from the earlier work of Ticknor and Bever[4] and of Kleppa.[5] Our design is predicated on the desirability of electrical calibration and of a large temperature range of operation. The ability to hold the alloy and mixture at elevated temperatures before they are dropped into the dissolving medium is important since this feature enables one to measure the variation of the enthalpy of formation with temperature, a quantity of importance in the evaluation of the non-configurational entropy of formation of the alloy. Lastly, the desire to avoid the subtraction of two large numbers led to a twin, differential design of the calorimeter. This advantage of a differential design is more illusory than real, since in effect, the apparatus carries out the differencing operation with the same errors as are involved in the arithmetic difference of two numbers individually measured. Nevertheless, the differential design has certain advantages, as will be described below. To the authors' knowledge the only other differential calorimeter for measurements of heats of formation of solid solutions is that developed by Nurmia[6] for ionic salts.

Description of Apparatus.—The calorimeter consists of several units, each of which will be briefly described in turn. These units are the two calorimetric cells, the temperature signal system, the recording wattmeter, and the furnace and temperature controller.

Each of the two calorimeter cells is composed of a large silica tube (see Fig. 1) which is coupled to a Pyrex dome by means of an O-ring seal. The silica tube supports a silica cup, fitted with three short legs, which contains the liquid tin used as the solvent. Into the liquid tin dip a silica ther-

(1) This work was done under contract No. W-31-109-Eng. 52 for the U. S. Atomic Energy Commission.

(2) O. Kubaschewski and J. A. Caterall, "Thermochemical Data of Alloys," Pergamon Press Ltd., London and New York, 1956.

(3) R. A. Oriani and W. K. Murphy, THIS JOURNAL, **62**, 199 (1958).

(4) L. B. Ticknor and M. B. Bever, *J. Metals*, **4**, 941 (1952).

(5) O. J. Kleppa, THIS JOURNAL, **59**, 354 (1955).

(6) M. J. Nurmia, Dissertation, Univ. of Helsinki, 1956.

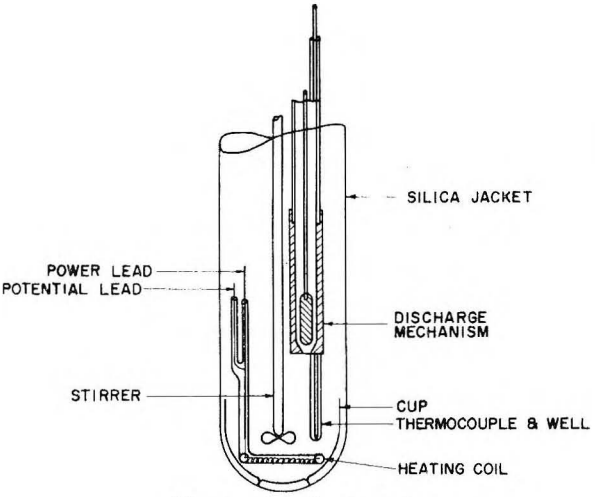

Fig. 1.—Calorimeter cell.

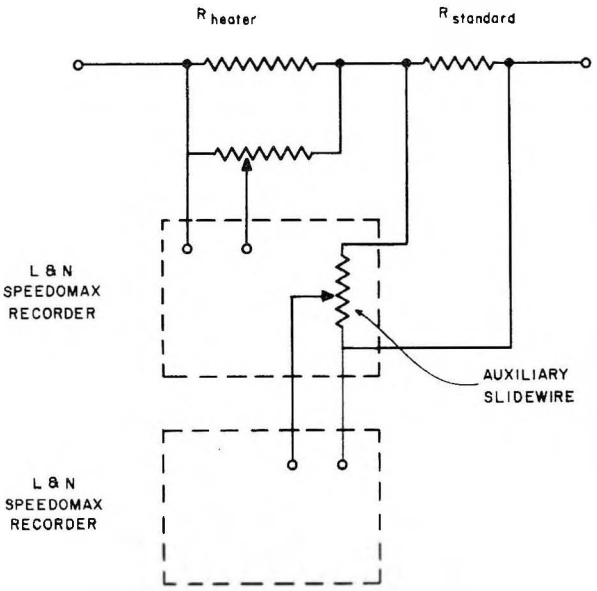

Fig. 2.—Schematic of recording wattmeter.

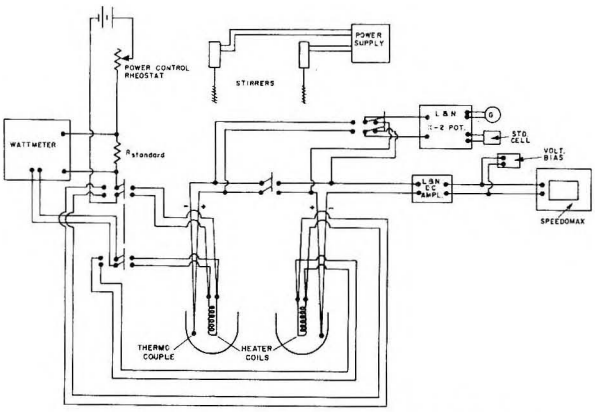

Fig. 3.—Schematic of measuring circuits.

mocouple well, a spiral silica tube which contains a tungsten spiral wire used for electrical calibration, and a silica stirrer. All these objects are supported from the Pyrex-silica grades. The Pyrex dome connects to the vacuum system by a large-bore tube. Rising vertically from the dome is a tube to which are attached six sample holders; these can be rotated about tapered joints in order to introduce the samples into the discharge mechanism of the calorimeter without disturbing the vacuum within. The bulb of an ionization vacuum gage is sealed to the top of the column of sample holders.

The Pyrex dome also supports the brass housing of the rotor of the induction motor which drives the stirrer. The base of the housing seals to the housing by an O-ring; the base is soldered to a Fernico tube which itself is sealed to the large vertical Pyrex tube coming from the dome. The rotor is moved by the rotating magnetic field induced in the stator coils surrounding the brass housing; a variable frequency power supply is used for the stirrer motors. Motion is transferred by means of universal joints lubricated by Octoil-S, and by a Fernico seal graded to a silica shaft; this rotates in a graphite bushing within a silica bearing attached to the support of the discharge mechanism.

Also supported by the Pyrex dome is the graphite discharge mechanism for holding metal samples until thermal equilibration is achieved (see Fig. 1). The discharge of the small pieces of metal into the liquid tin is accomplished by raising a graphite valve from its seat by means of a solenoid above the Pyrex dome. The solenoids of both calorimetric cells are actuated at the same instant.

The calibrating, or heater, coil is a spirally wound, 0.006″ tungsten wire of about 2 ohms resistance at room temperature, enclosed in a circular tube of thin-walled silica. The tungsten wire is sealed in with an atmosphere of argon in order to improve the heat conductivity. Two wires make contact to each end of the heater coil: a heavy 0.040″ wire to carry the heating current, and a finer, 0.010″ wire by which the voltage drop across the heater coil is fed to the wattmeter. The contact between the power lead and the heating coil is at a point below the level of the molten tin in the cup in order that all the joulean heat generated be received by the tin.

The direct current received by the heater coil is passed through a standard resistor, the voltage drop across which is fed to the wattmeter. This instrument, designed and assembled with the help of Mr. J. Groves and Mr. F. Ludwig, General Engineering Laboratory, records the power delivered to either one of the calorimeter cups with an overall accuracy of 0.5%. Its design is schematized in Fig. 2, and its relation to the calorimeter is shown in Fig. 3. The response time of the recording wattmeter is 1 sec. for full scale deflection; graphical integration of the recorded curve yields the total energy delivered. The d.c. power supplied to either of the heaters is supplied by a large storage battery and is controlled by a simple rheostat.

The temperature-sensing elements that have been used are of two kinds: resistance elements and thermocouples. The resistance elements are tungsten filaments enclosed in silica tubules, one within each calorimeter cup, and both having the same resistance at room temperature. These filaments constitute portions of arms of a Wheatstone bridge, the off-balance of which is either measured by an electronic galvanometer, or else amplified by a Leeds–Northrup d.c. amplifier, and then recorded by a Leeds–Northrup Speedomax. The Wheatstone bridge was so designed that a very high sensitivity was obtained. However, it has proven impossible so far to obtain a signal from the Wheatstone bridge that is free of electrical noise, probably because of poor electrical connections due to difficulties in the fabrication methods. Since the inherently high sensitivity is partially nullified by the noise, thermocouple signals have been employed in the work reported in this paper. However, it is intended to continue to try to learn how to fabricate such resistance elements for noise-free operation, because of the much higher sensitivities possible.

The thermocouples are made of chromel and constantan wires, and have been checked against a platinum platinum–rhodium thermocouple. The signal of any one thermocouple, or of the opposed thermocouples may be measured by a potentiometer, or recorded after amplification. It has been found impractical to employ multi-junction thermocouples in an effort to increase the sensitivity, because vibration from the stirrers produces variable contact between the several junctions and the walls of the well, leading to variable thermal contact and hence to signal noise.

Both calorimeter cells are enclosed by a furnace of very large thermal capacity, and of large zone of temperature homogeneity. Both cells occupy the same heated zone, *i.e.*, both are surrounded by one and the same set of heating coils. Hence, both cells will experience the same residual temperature fluctuations and the signal of the opposed ther-

mocouples will be only little affected by variations in the furnace. On the other hand, one cell is isolated from the other by a septum of insulation between the two cells; hence, a reaction in one cell does not affect the other.

The furnace is powered through voltage stabilizers and the temperature is controlled by a resistance element, the temperature variation of which is used to adjust the firing of a thyratron. Because there is much lagging between the furnace windings and the cells, a temperature fluctuation at the winding is much attenuated at the position of the cells. Since the furnace winding is of nichrome, the maximum safe operating temperature is about 1000°, and the calorimeter has been designed for that top temperature. The controlled alternating current is rectified before it enters the furnace winding because it was found that without this provision the circuit of the temperature controller was perturbed by sixty-cycle pick-up, making it impossible to maintain the temperature sufficiently constant. Elaborate electrical shielding had to be provided for the resistance probe and the various circuit elements of the temperature controller before sufficiently good temperature stability could be attained.

Operation of the Calorimeter.—Almost 700 g. of tin of 99.998% purity are used in each cup of the calorimeter. The metal is melted into the cups under vacuum, and the solidified ingots are adjusted so that their weights do not differ by more than 10 mg. The alloy and pure metal samples are weighed and placed individually in the sample holders. The calorimeter is assembled, the tin melted and freed of oxide by a high-temperature hydrogen treatment, and then the apparatus is evacuated to 10^{-5} mm. After the calorimeter attains constant temperature, it is ready for use.

The calibration of the recording wattmeter is accomplished by means of standard resistors and a Leeds–Northrup K-2 potentiometer. Its calibration is known to an accuracy of ±0.8%, and the circuitry is so arranged that the calibration at any setting of its sensitivity may be measured at any time.

Electrical calibration of each calorimeter is accomplished by passing electrical power through the heating coil of that calorimeter, recording the power and time on the wattmeter, and recording the amplified e.m.f.–time curve of the opposed thermocouples. This curve is analyzed by a procedure described below. The results of the electrical calibrations at 418° are 0.353 cal./chart division ±0.4% for one calorimeter cell, and 0.350 cal./div. ±0.3%. Hence, the limitation, arising solely from all calibration operations, upon the accuracy of a measurement is ±1.2%.

A method of calibration that has been used by other workers is to drop into the molten tin at a known temperature some cold metal at room temperature. One can use solid tin added to pure liquid tin in the calorimeter, or solid tungsten added to the liquid tin of whatever solute content, since the tungsten does not dissolve in the tin, at least at moderate temperatures. We have used solid tin; the enthalpy change undergone by the tin is obtained from data in the literature, and the decrease in temperature of the calorimeter cell is recorded. The tin calibrations at 418° yielded 0.357 cal./div. ± 1.4% for one cell and 0.355 cal./div. ± 1.4% for the other. The fact that these numbers are somewhat larger than those obtained by electrical calibration is consistent with the small and irreproducible increase of temperature that the tin must suffer during its drop through the body of the calorimeter. For this reason, the electrical calibrations are preferable and are used in this work.

The e.m.f.-time curve reveals that at 418° the heat transfer from the calorimeter cell to its surroundings is somewhat different from Newtonian. We find that the cooling is adequately described by $d\Delta T/dt = -k(1 - at)\Delta T$, where ΔT is the instantaneous difference of temperature between the cell and its surroundings at time t, and k and a are parameters to be determined experimentally. Then, the corrected temperature difference ΔTc is given by

$$\Delta Tc = \Delta T(t') - k\int_0^{t'} \Delta T\, dt + ak\int_0^{t'} t\,\Delta T dt$$

where t' is any time after reaching the pseudo-Newtonian cooling region. A check of the adequacy of this approach is obtained by finding that the ΔTc is the same whatever value of t' is chosen.

For the measurement of enthalpy of formation of a solid alloy there are three ways of operating this calorimeter. The first way is to use each of the two calorimeter cells individually as a separate apparatus. One dissolves the alloy first and measures its heat of dissolution, and then at a subsequent time one dissolves either the same weight of mechanical mixture or proper weights of the pure components separately. One calculates the heat of formation from the separate measurements, using the measured calibration factor of the calorimeter. The difficulty here is that one must empirically ascertain that the energies of dissolution of metals into the tin are not affected by differences in solute content of the tin.

This difficulty is immediately obviated by the second method of operation, whereby one dissolves simultaneously the alloy in one cup and the same weight of mechanical mixture in the other cup. The temperature–time curve that results is a function of the rate of dissolution of each of the two components and of the alloy, and may be quite complex. In principle, this complexity is of no consequence, but in practice, it may be difficult to ascertain the point at which all dissolution processes have ceased. The heat of formation of the alloy is at once obtainable from ΔTc of the differential curve and from the calibration factor of the apparatus.

When the rates of dissolution of the components or of the alloy are very slow, accuracy of such measurements is much decreased. In this circumstance, a third method of operation is available. One dissolves alloy and mixture simultaneously as in the second method, but one furnishes metered electrical power to the cup which at any one instant is the cooler in order to maintain the observed temperature difference between the two cups at any time the same as it was prior to the dissolutions. The graphical integration of the recorded power–time wattmeter curve, with due regard to the signs of the areas, leads at once to the energy of formation of the alloy, without the need of a calibration factor of the calorimeter. This factor must be known, however, in order to apply a correction for the sequence of deviations from zero instantaneous temperature differences that may be recorded as the run progresses. Clearly, in any specific case, some combination of these three basic methods of operation will be best.

The alloys are made with great care to avoid contamination and to achieve homogeneity of composition. The alloys are chemically analyzed to an accuracy such that the inaccuracy in the chemical analysis does not cause an inaccuracy in the measured heat of formation greater than 2%. The alloys and the pure components are drawn to wire of 0.040″ diameter and are cut into 0.040″ lengths for use in the calorimeter.

Experimental Results

A. Energy of Dissolution of Metals into Liquid Tin.—An excellent way of checking the operation of the calorimeter, because it is the most direct measurement one can carry out, is to measure the energy of dissolution of very small amounts of pure metals in the liquid metal in the calorimeter cups. Figure 4 exhibits the limiting heat of dissolution of solid gold and of solid copper, individually added in very small amounts (less than 0.01 g. atom of solute), to about 4 g. atoms of liquid tin. It is seen that the present results agree very well with those of Ticknor and Bever[4] and of Hultgren, *et al.*,[7] but disagree with those of Kleppa.[8] The authors do not know the cause of the systematic error that appears to have occurred in Kleppa's work. The present measurements lead to $\overline{\Delta H}_{Au}$ of −5197 cal./g. atom ± 0.3% for the addition of solid gold to liquid tin, both at 418°, and to $\overline{\Delta H}_{Cu}$ of 2816 cal./g.

(7) (a) R. L. Orr, A. Goldberg and R. Hultgren, Institute of Engineering Research Report, Univ. of California, Berkeley, Series No. 76, Issue No. 1, 1955; (b) R. L. Orr and R. Hultgren, Institute of Engineering Research Report, Univ. of California, Berkeley, Series No. 76, Issue No. 2, 1956.

(8) O. J. Kleppa, THIS JOURNAL, **60**, 842 (1956).

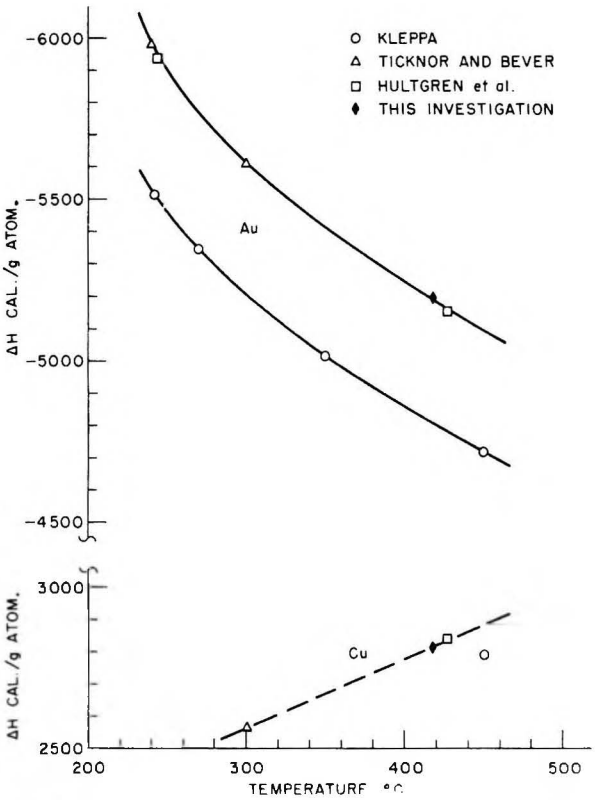

Fig. 4.— Limiting heat of solution of solid Au and solid Cu into liquid Sn, cal./g. atom.

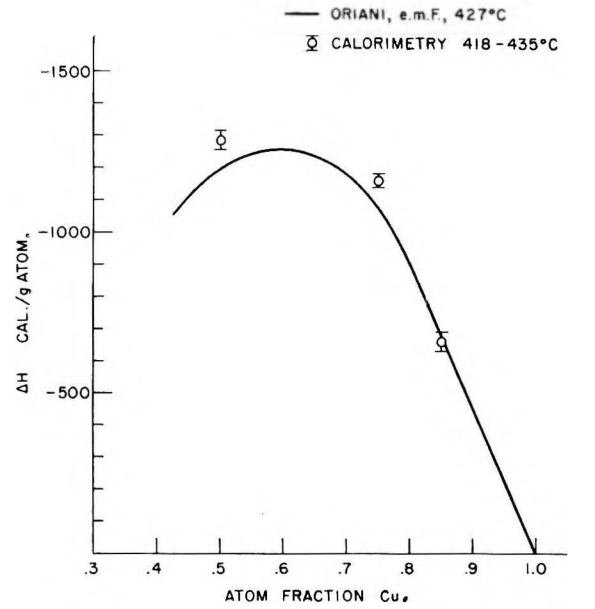

Fig. 5.—Heat of formation of solid, disordered Au–Cu alloys, cal./g. atom.

atom ± 0.5% for the corresponding process for copper. The per cent. figures indicate reproducibility only; the absolute accuracy of these numbers is estimated at ±1.2% from the uncertainties in the calibrations of the calorimeter and of the wattmeter.

B. Solid Silver–Gold Alloy.—The present work on the solid solution $Ag_{0.394}Au_{0.606}$ has been carried out as a further check on the over-all operation of the calorimeter, since this alloy system is rather well characterized after many independent investigations. The two most recent critical compilations give the following values for the ΔH_f of this alloy from the pure solid components: Kubaschewski and Caterall,[2] −1020 cal./g. atom; Hultgren,[9] (−1050 ± 40) cal./g. atom at 800° K. The present result is −1090 cal./g. atom at 423°, with a reproducibility figure of ±1.6%. These experiments were done by simultaneously dissolving the mechanical mixture and the alloy, and recording the resulting output of the differential thermocouple.

C. Solid Gold–Copper Alloys.—Figure 5 shows a curve for the ΔH_f at 427° of solid disordered gold–copper alloys derived from the galvanic cell measurements of Oriani.[10] Also shown are the present calorimetric results for three alloy compositions; it is seen that the agreement is very good.

The alloy $Au_{0.15}Cu_{0.85}$ was measured at 418° in three sets of determinations. One set of four runs was carried out differentially, that is, by simultaneous dissolution of alloy and mechanical mixture, and yielded ΔH_f = (−665 ± 38) cal./g. atom. A second set, comprising four individual dissolutions of the alloy, and using measured heats of dissolution of pure copper and of pure gold, led to (−659 ± 31) cal./g. atom. A third set, of four differential runs, yielded (−658 ± 32) cal./g. atom. Despite the good agreement, the differential runs are to be preferred. It has been found that the heat of dissolution of the pure copper, and also of the alloy, into the liquid tin, is a function of the existing solute content in the tin. Therefore, in carrying out non-differential runs it is necessary to measure the energy of dissolution of the components and of the alloy into the tin, all at the same solute concentration in the liquid tin. This requirement is automatically satisfied in the differential method of operation. The present value of ΔH_f for $Au_{0.15}Cu_{0.85}$ is to be compared with −710 cal./g. atom obtained by Hultgren, *et al.*,[7b] at 50°.

The composition $Au_{0.25}Cu_{0.75}$ was examined at 420° by a differential measurement which yielded ΔH_f = −1150 cal./g. atom, and by two non-differential runs, yielding (−1170 ± 15) cal./g. atom. These numbers are to be compared with that of Hultgren, *et al.*,[7b] of (−1179 ± 34) cal./g. atom for this disordered alloy at 50°, and with the value of (−1124 ± 55) cal./g. atom at 0° obtained by Rubin, Leach and Bever.[11]

The alloy $Au_{0.500}Cu_{0.500}$ was disordered at 435° and its heat of formation was measured at the same temperature by two differential runs. The result is ΔH_f = (−1285 ± 31) cal./g. atom, which disagrees strongly with the number of Hultgren, *et al.*,[7b] of −1630 cal./g. atom for the disordered alloy at 50°. However, recent work by Hultgren[12] in which the alloy was dropped into liquid tin from 700° K., has yielded results in close agreement with the galvanic cell values.[10] It is supposed that the high value obtained by Hultgren's earlier work[7b] is the result of a

(9) R. Hultgren, "Selected Values, Thermodynamic Properties of Metals and Alloys," Minerals Research Laboratory, Univ. of California.

(10) R. A. Oriani, *Acta Met.*, **2**, 608 (1954).

(11) L. R. Rubin, J. S. L. Leach and M. B. Bever, *J. Metals, Trans. A.I.M.E.*, **203**, 421 (1955).

(12) R. Hultgren, private communication.

partial ordering undergone by the alloy either during the quench from the disordering temperature of 873° K., or during its dissolution period in the liquid tin. The reason for the latter possibility is that in Hultgren's earlier work, the quenched alloy at 50° is dropped into liquid tin at 427°, so that as the alloy is dissolved into the tin at any one moment the as yet undissolved alloy is being heated through a range of temperatures at which the rate of ordering is rapid.[13]

Although Hultgren's earlier data for the heat of formation of disordered $Au_{0.5}Cu_{0.5}$ are not correct, there is no reason to suspect his value of ΔH_f for the ordered (face-centered tetragonal) $Au_{0.5}Cu_{0.5}$ of -2150 cal./g. atom. Hence, if we use his value for the ordered alloy and the present value for the disordered alloy, we find an energy of ordering of (-865 ± 40) cal./g. atom. However, it is not known how this energy is apportioned between the two reactions that occur at this composition, namely, disordered alloy $\rightleftarrows$ orthorhombic superlattice $\rightleftarrows$ f.c. tetragonal superlattice. It is intended to examine this situation in detail.

D. Solid Silver–Copper Alloys.—For the measurement of the enthalpy of formation of solid silver–copper alloys it was found necessary to operate the calorimeter at a higher temperature than for the alloys already discussed, because the mutual solubility at lower temperatures is quite limited. A temperature of 622° was chosen, even though this permits the investigation of only a small range of composition, in order to avoid whatever troubles may arise at higher temperatures as yet unexplored by this calorimeter. The results of a series of differential determinations are listed in Table I, and are shown in Fig. 6. There do not exist any other data with which to compare these results except the point on Fig. 6 by Hultgren and Orr[14] with which the present data are consistent.

(13) G. J. Dienes, *Acta Met.*, **3**, 549 (1955).

(14) R. Hultgren and R. L. Orr, private communication.

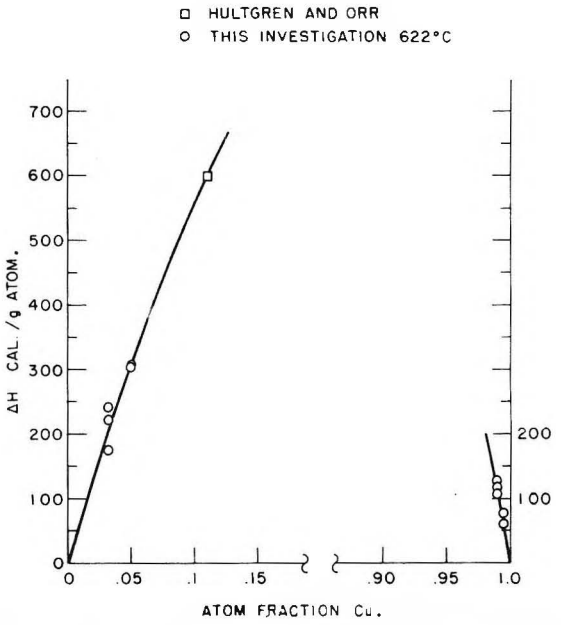

Fig. 6.—Heat of formation of solid Ag–Cu alloys, cal./g. atom.

It may also be pointed out that the curve for the enthalpy of formation of liquid Ag–Cu alloys from the liquid components[3] is superimposable upon the present data for the corresponding solid alloys; this fact demonstrates the smallness of the influence of the rigidity of the lattice upon the energetics of the formation of the solid alloy for this system.

TABLE I

ENTHALPY OF FORMATION OF SOLID SILVER–COPPER ALLOYS, 622°

Composition	ΔH_f, cal./g. atom
$Ag_{0.006}Cu_{0.994}$	76.2, 59.0, 77.4
$Ag_{0.011}Cu_{0.989}$	115, 126, 106
$Ag_{0.968}Cu_{0.032}$	222, 242, 174
$Ag_{0.950}Cu_{0.050}$	307, 304

THE EXPLOSIVE OXIDATION OF PENTABORANE

BY HARRY C. BADEN, WALTER H. BAUER AND STEPHEN E. WIBERLEY

Walker Laboratory, Rensselaer Polytechnic Institute, Troy, New York

Received October 17, 1957

The explosive reaction of pentaborane and oxygen has been investigated. The lower explosion limit for mixtures of pentaborane and oxygen on rapid mixing was studied as a function of mixture composition at 15 and 21.5° and from 1 to 90 mm. pressure of pentaborane. Explosion pressures increased with decrease in temperature when clean vessels were used. Limits were found to be higher in vessels coated with oxidation products than in clean vessels. In coated vessels the explosion limit was lowered with increased vessel size, but no temperature dependence was found for such vessels. Addition of nitrogen lowered the pressures at which spontaneous explosion took place, while addition of diborane slightly inhibited the reaction. When carbon monoxide was added, erratic inhibition of the explosion occurred. Addition of 1% of iron carbonyl to pentaborane caused total inhibition of the oxidation at 25°. When 0.1% of iron carbonyl was added to the pentaborane, both lower and upper temperature–pressure explosion limits were found for pentaborane and oxygen mixtures.

Because of the high energy release, the rapidity of reaction and the high flame speeds developed on oxidation, the boron hydrides offer a fruitful field for study. Since pentaborane, the most stable of the volatile boranes, is a liquid at room temperature and soluble in hydrocarbons, it has advantages for practical applications. However, there are some properties of this compound which have limited its use. Pure pentaborane may ignite spontaneously on mixing with air under some conditions.[1] A study of the kinetics and mechanism of the oxidation of pentaborane was undertaken in

(1) D. T. Hurd, "An Introduction to the Chemistry of the Hydrides," John Wiley and Sons, Inc., New York, N. Y., 1952.

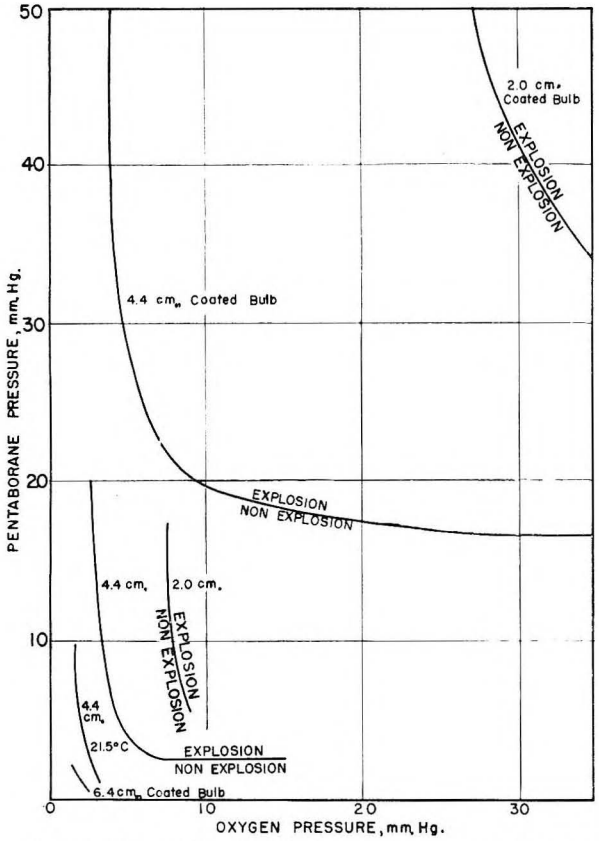

Fig. 1.—Composition explosion limits for pentaborane–oxygen mixtures in clean vessels and in vessels coated with reaction products, at 15° except as noted otherwise.

the hope that conditions could be established for the most efficient use of this reaction. Simultaneously, a study of the explosive oxidation of diborane was undertaken[3,4] in order to gain some knowledge of the mechanism of boron hydride combustion in general.

A kinetic study of the pentaborane–oxygen system[4] showed the existence of an explosion limit at very low pressures and at room temperature, implying the presence of a branching chain reaction. Investigations of flame spectra in the oxidation of pentaborane were made by Berl and co-workers,[5] showing the presence of B_2O_3 in the explosion diffusion flame.

Experimental

Materials.—Pentaborane was prepared by the pyrolysis of diborane.[6-8] After purification, various batches were assayed, by the cryoscopic method,[9] to be 99.7 to 99.9% pure. The main pentaborane supply was maintained at −20°, except for short periods of time when small amounts were transferred to a vacuum line. These portions were kept frozen by Dry Ice slush, in a storage limb off the vacuum manifold. Infrared and mass spectrographic analysis of this material failed to indicate the presence of any impurities.

Matheson prepurified oxygen was used throughout the course of the study. The gas was admitted to the vacuum line and was condensed in a trap at liquid nitrogen temperature. The middle third fraction of the liquid oxygen was allowed to vaporize and kept in a two-liter storage bulb for subsequent use in the oxidation experiments.

Iron pentacarbonyl was obtained from the General Aniline and Film Corporation. A small amount of the liquid was introduced to the vacuum line, and alternately distilled and frozen three times before being frozen in a limb off the manifold. This limb was wrapped with black paper to exclude all light.

Apparatus.—A Pyrex glass vacuum system was employed for handling and storing materials. The vacuum manifold was fitted with gas storage bulbs, freeze-out limbs for holding pentaborane, and taps for the inlet of gases and for drying cleaned explosion bulbs. All joints and stopcocks were greased with Apiezon N, except those in the explosion apparatus where Dow Corning Silicon High Vacuum Grease was used. The reactants were mixed in spherical Pyrex explosion bulbs 2.0, 4.4 or 6.4 cm. in diameter similar to those used by Price.[4] These bulbs were fitted with a capillary stopcock and standard taper joint to allow rapid exchange of used bulbs for clean bulbs. The explosion apparatus consisted of the explosion bulb, connected through a ground joint to a small calibrated volume, and a measuring pipet. Capillary lines led to the measuring manometer and manifold, the Bodenstein gauge, the measuring pipet, and through a capillary leak to the vacuum manifold.

The explosion apparatus could be completely submerged in a constant temperature-bath, which could be raised and lowered as desired. By means of this bath, the temperature of the reactants could be maintained to ±0.1° in the range −10 to 100°.

Operating Procedure.—When an explosion test was made, the constant temperature-bath was raised around the explosion apparatus, and pentaborane was introduced to the explosion bulb and to the line to the manometer. The pressure was recorded, the stopcock to the bulb closed, and the excess pentaborane re-collected in the storage freeze-out limb. The measuring pipet and connecting lines were then evacuated and a pressure of oxygen sufficient to give the final desired pressure of this component in the explosion bulb was allowed to enter the pipet and the line to the measuring manometer. The oxygen pressure was recorded, the stopcock to the pipet closed, and the apparatus again evacuated. The stopcock connecting to the manifold was then closed and the stopcock to the pipet opened. Manipulation of the air pressure above the mercury well compressed all the oxygen into the small calibrated volume above the explosion bulb.

The stopcock on the explosion bulb was then opened to the calibrated volume, allowing oxygen to enter the bulb. As the pressure of oxygen was always much greater than the pressure of the pentaborane in the bulb, entry and mixing were very rapid. When explosion occurred, a bright flash, easily visible through the transparent-bath, was seen.

Experimental Results

First Explosion Limit at Room Temperature.—When oxygen was added rapidly to pentaborane at 21.5°, explosion resulted above low critical pressures. Results obtained with an explosion bulb of 4.4 cm. diameter, show limits falling between those obtained for bulbs of 3.7 and 6.62 cm. diameter by Price,[4] at higher pressures of pentaborane. At lower pressures, below 2 mm. of pentaborane, the pressure limit curve obtained crossed that found by Price. Since the pressures involved in the explosion range studied by Price were so low, below 5 mm., the temperature at which explosion tests were made was lowered to 15°.

Composition Limits at 15°.—When oxygen and pentaborane were mixed rapidly at 15°, the explosion region was shifted to higher pressures as shown in Fig. 2. Results of a typical set of explosion tests are plotted in Fig. 3 in detail. Al-

(2) W. Roth and W. H. Bauer, "Fifth Symposium on Combustion," Reinhold Publ. Corp., New York, N. Y., 1955.
(3) W. Roth and W. H. Bauer, THIS JOURNAL, **60**, 639 (1956).
(4) F. P. Price, *J. Am. Chem. Soc.*, **73**, 2141 (1951).
(5) W. G. Berl, E. T. Gayhart, H. L. Olsen, H. P. Broida and K. E. Shuler, *J. Chem. Phys.*, **25**, 797 (1956).
(6) L. V. McCarty and P. A. DiGiorgio, *J. Am. Chem. Soc.*, **73**, 3138 (1951).
(7) A. Stock, "Hydrides of Boron and Silicon," Cornell University Press, Ithaca, N. Y., 1933.
(8) A. Burg and H. Schlesinger, *Chem. Revs.*, **31**, 13 (1942).
(9) P. D. Zemany, *Anal. Chem.*, **24**, 348 (1952).

though explosive and non-explosive regions were clearly defined, occasional erratic results were obtained. The shift of the explosion limit with increasing vessel size reported for room temperature in clean bulbs was also found at 15°. However, the limit was found to be temperature sensitive. The limits were shifted to higher pressures with decreasing temperature, as shown in Fig. 1.

Effect of Oxidation Product Coating.—The explosion of pentaborane–oxygen mixtures produces a deposit on the vessel surface. When repeated explosions were made in a single vessel, it was found that the pressure explosion limit curve was shifted to higher pressures. Reproducible limits were found which were shifted to much higher component pressures than those found in clean vessels of the same size, as is seen in Fig. 2. The limits obtained in coated bulbs also exhibited dependence on vessel diameter, but no temperature dependence was observed.

Effect of Iron Pentacarbonyl on Explosive Reaction of Pentaborane and Oxygen.—It was concluded from the existence of a clearly defined lower explosion limit that the oxidation of pentaborane was initiated by a chain mechanism, as was found to be the case for diborane. Chain-breaking additives might therefore be expected to exist. It was found that addition of diborane inhibited the explosion only slightly, and that carbon monoxide produced an erratic inhibition of the explosion.

Since it has been reported that iron pentacarbonyl, when added to liquid pentaborane, inhibited the tendency of the borane to ignite spontaneously on exposure to air, the effect of this carbonyl on the composition limits was investigated. The iron pentacarbonyl was added to pentaborane in a storage bulb, at a concentration of 1% by volume, and samples of this mixture were transferred to the explosion bulb. Oxygen was then added and the result noted. These determinations were made at 24 ± 1°. No explosions were found in clean bulbs of either 4.4 or 6.4 cm. diameter with partial pressures of up to 140 mm. for pentaborane and 80 mm. for oxygen.

When the concentration of iron pentacarbonyl was decreased to 0.01% of the pentaborane, explosions occurred at this concentration of additive when oxygen was added. Although the experiments with added carbonyl were made at room temperature, the pressures required for explosion were only slightly higher than those in the same bulbs at 15° with no additive.

A concentration of 0.1% added iron pentacarbonyl was selected for a more intensive survey of the effect of this additive. It was discovered that warming a bulb containing the unexploded mixture of oxygen, pentaborane and iron pentacarbonyl was sufficient to cause explosion. This phenomenon suggested the possible existence of a set of pressure–temperature explosion limits; therefore, a constant-temperature hot oil-bath was introduced to the system to determine these limits. All tests in the study of this limit were made in clean bulbs 4.4 cm. diameter, and with a ratio of $3O_2$ to $1B_5H_9$ by volume. Mixtures were made at room temperature, and the temperature was increased until explosion occurred. Pressure was followed by means of a Bodenstein quartz spiral gauge. The results of this study, given in Fig. 3, show the presence of an upper and lower explosion limit for pentaborane–oxygen mixtures in the presence of iron pentacarbonyl. The lower limit changes very little with tempera-

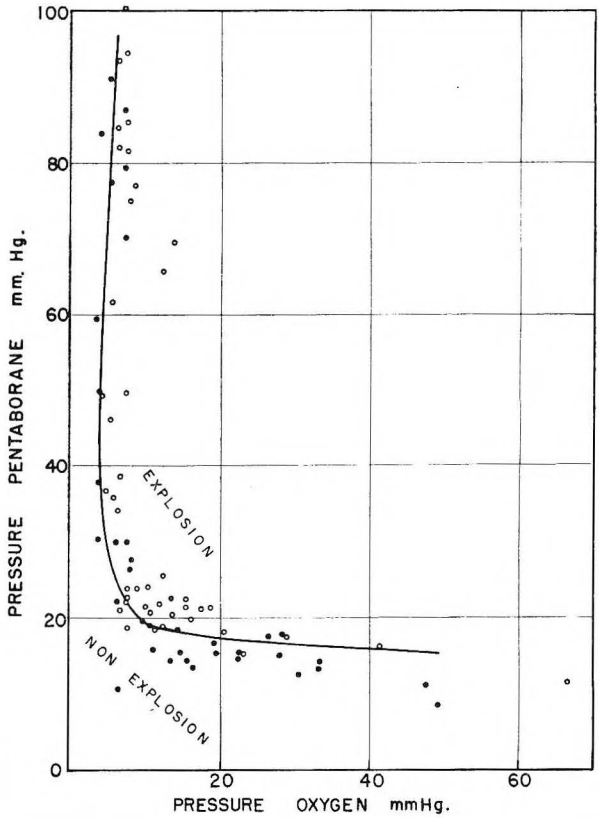

Fig. 2.—Typical composition explosion limit data at 15° for pentaborane–oxygen mixtures in 4.4 cm. Pyrex bulb coated with reaction products.

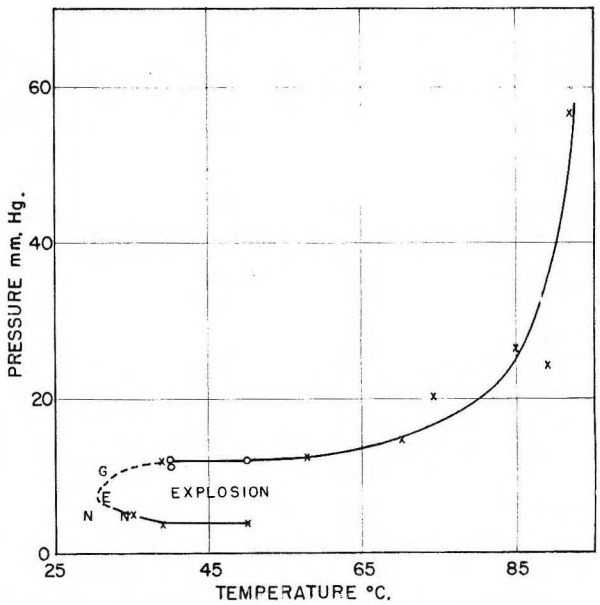

Fig. 3.—Temperature–pressure explosion limits for pentaborane–oxygen, mixture ratio 1 to 3, with 0.1% iron carbonyl, in clean Pyrex bulbs 4.4 cm. in diameter: x, explosion on heating; o, explosion on withdrawal; G, glow on mixing; E, explosion on mixing; and N, no reaction on mixing.

ture. The upper limit is more temperature sensitive, rising slowly at first, but becoming almost vertical between 85 and 95°. At approximately 30° and at mixture pressures near 10 mm., a glow reaction was noted, similar to that described by Price[4] for mixtures of pentaborane and oxygen without iron pentacarbonyl.

Discussion

The results of this investigation support the conclusion of Price[4] that the reaction of pentaborane and oxygen is of the branched chain type. No chain carrying intermediate has been isolated but the inhibiting effect of small amounts of iron carbonyl clearly indicates that oxygen atoms may be involved in the chain mechanism. The well defined lower composition explosion limit is sensitive to both vessel diameter and coating with reaction products. As the limit is found at very low pressures in clean vessels, the glass must have a comparatively low chain-breaking efficiency. In coated vessels, the limit occurs at considerably higher component pressures, indicating a greater capacity for chain breaking. Although the addition of nitrogen gas had little effect on the limit observed in clean bulbs, in coated vessels the addition of nitrogen lowered the explosion limit pressures. This would be expected if the nitrogen molecules hindered diffusion of chain carriers to the surface, thus decreasing the rate of destruction. The solid coating formed on explosion varied from a brown color when pentaborane rich mixtures were exploded to a white color when oxygen rich mixtures were used. All white solids were soluble in methanol or ethanol. While the brown solid was not completely soluble in these solvents, it did dissolve in either dilute or concentrated nitric acid. Infrared analysis showed only the presence of boric acid. Some boron hydride polymers are yellow solids or oils, which may account for the yellow coloration observed in some experiments. The major portion of the brown solid is believed to consist of elemental boron and boric acid.

The total inhibition of the spontaneous explosion of pentaborane at room temperature is notable. Iron carbonyl is presumed to inhibit oxidation chain reactions by the destruction of active oxygen species.[10] Whether these are oxygen atoms or oxygen-containing intermediates was not determined. The upper temperature–pressure explosion limit exhibited when only 0.1% of iron carbonyl is present is thought to be due to increase of chain breaking in the gaseous phase at higher pressures, sufficient to lead to inhibition of the explosion when combined with the action of iron pentacarbonyl. The failure to thus far locate an upper temperature–pressure explosion limit for pure pentaborane–oxygen mixtures need not eliminate the possibility of existence of such a limit. The method of test used by Price, and in this investigation, involves high flow gradients and high concentration gradients during the sudden mixing of oxygen with pentaborane. An upper limit may well be located under different experimental conditions. The partial oxidation of pentaborane on slow addition of oxygen[11] indicates that speed of mixing may be an important factor in the initiation of explosive conditions.

Acknowledgment.—Acknowledgment is made to Dr. C. C. Clark for helpful advice and suggestions. This work was carried out under the sponsorship of the Olin Mathieson Chemical Corporation.

(10) B. Lewis and G. von Elbe, "Combustion, Flames and Explosions of Gases," Academic Press, Inc., New York, N. Y., 1951.

(11) H. C. Baden, S. E. Wiberley and W. H. Bauer, THIS JOURNAL, 59, 287 (1955).

MOLECULAR STRUCTURE AND MOTION IN IRRADIATED POLYETHYLENE[1]

BY W. P. SLICHTER AND ELAINE R. MANDELL

Bell Telephone Laboratories, Inc., Murray Hill, New Jersey

Received October 28, 1957

Molecular structure and motion have been studied in polyethylene subjected to high-energy irradiation from an atomic pile and from electrons. Measurements involved X-ray diffraction and proton magnetic resonance spectroscopy. Contrary to earlier findings, it is shown that high-energy irradiation inflicts change concurrently in the crystalline and the amorphous regions. Lattice defects are introduced into crystallites. The characteristic separations between chains are altered in both the crystalline and the amorphous regions, and the two regions merge at higher dosages. With increasing dosage, the irradiation causes progressively greater constraint to even small-scale motions.

1. Introduction

It is well known that the physical and chemical properties of polyethylene are markedly changed by high energy irradiation. These changes occur from bombardment in nuclear reactors, from high energy electrons, and from γ-rays. Evidently the changes involve several processes, including cross-linking, chain scission and double bond formation, for which mechanisms have been proposed by a number of authors. Earlier studies dealt with highly branched polyethylenes. This paper reports on additional studies of the morphology of irradiated polyethylene, both branched and linear, and of the extent of chain motion in irradiated polyethylene. Two ranges of dosage were used: comparatively light dosage, of the sort which is of interest in polymer technology; and very extensive irradiation, which so thoroughly changes the mate-

(1) Presented at the 132nd Meeting of the American Chemical Society, New York, September 9, 1957.

rial that the word "polyethylene" is something of a misnomer.

2. Experimental

The experiments involved X-ray diffraction, nuclear magnetic resonance spectroscopy and measurements of polymer density. The X-ray measurements made use of crystal-monochromatized copper K_α radiation and a flat plate camera. The studies were confined to unit cell dimensions, with no effort at determination of atomic coördinates. The diffraction studies were performed at room temperature. The nuclear resonance experiments were carried out over a temperature range of 80 to about 400°K. The apparatus is described elsewhere.[2] Densities were found by a flotation method.

Polyethylenes were irradiated in the atomic pile at Harwell, England, or else in a Van de Graaff generator. The polymer bombarded in the pile had been made by Imperial Chemical Industries, Ltd., using high-pressure methods, and was presumed for the purposes of these studies to be typical of branched polyethylene. Two kinds of polyethylene were irradiated in the Van de Graaff generator. One was a typical branched polyethylene, made by the Bakelite Division, Union Carbide and Carbon Corp., and designated DYNH by the manufacturer. The other was a typical linear polyethylene, Marlex 50, made by the Phillips Petroleum Co.

The exact conditions of pile irradiation are not known, but presumably they resemble those used in other studies.[3,4] The dosages ranged up to 1.49×10^{19} slow neutrons/cm.^{2}, with associated fast neutrons and γ-particles. As expressed by Charlesby,[3,4] this maximum dosage was 149 units, where one unit is 10^{17} slow neutrons/cm.^{2}. Expressed in terms of roentgens equivalent physical (rep), these dosages ranged up to 5.7×10^{10} rep. The conversion from neutron dosage to rep has been made on the basis of Charlesby's calculations[3] of the energy absorption in polyethylene; but several considerations, including the question of the contribution from fast neutrons and γ-radiation under the circumstances of the experiment, lead to uncertainties amounting to a factor of three or more.[5-8] For the purpose of the present paper, this uncertainty in the conversion of dosage units is not too serious.

There is no information as to the pile temperature used for these samples, though typically[4] the temperature lies between 70 and 80°. It has been reported[9] that a variation of a few degrees in the irradiation temperature has a marked effect on the ultimate degree of crystallinity. Some effects of progressively higher dosages on the appearance and physical properties of polyethylene which has undergone drastic irradiation have already been described.[3-5,10]

The Van de Graaff generator was operated at 700 kv. To prevent oxidation or undue temperature rise, a steady stream of nitrogen was blown across the samples during the irradiation. Although the sample temperature was not measured, it is believed, on the basis of rough estimates of thermal conduction and heat dissipation, that the temperature did not exceed 60°. The radiation doses ranged up to 7.5×10^9 rep. The uncertainty in the irradiation dosage is estimated at no more than about 25%. Some of the samples for electron irradiation were in the form of compression molded sheets. Fibers of Marlex 50, which had been cold-drawn at a rate of 1 inch/minute to a thickness comparable to the unoriented specimens, were also irradiated. The sample thicknesses were 50 mils or less, and hence were well below the depth of maximum penetration of the electrons.

(2) D. W. McCall and W. P. Slichter, *J. Polymer Sci.*, **26**, 171 (1957).

(3) A. Charlesby, *Proc. Roy. Soc. (London)*, **A215**, 187 (1952).

(4) A. Charlesby and M. Ross, *ibid.*, **A217**, 122 (1953).

(5) A. Charlesby, *ibid.*, **A222**, 60 (1954).

(6) M. Dole, C. D. Keeling and D. G. Rose, *J. Am. Chem. Soc.*, **76**, 4304 (1954).

(7) M. Dole and W. H. Howard, THIS JOURNAL, **61**, 137 (1957).

(8) "Reactor Handbook: Physics," U. S. Atomic Energy Commission, McGraw-Hill Book Co., Inc., New York, N. Y., 1955.

(9) R. A. V. Raff and J. B. Allison, "Polyethylene," Interscience Publishers, Inc., New York, N. Y., 1956, p. 152.

(10) A. Charlesby and N. H. Hancock, *Proc. Roy. Soc. (London)*, **A218**, 245 (1953).

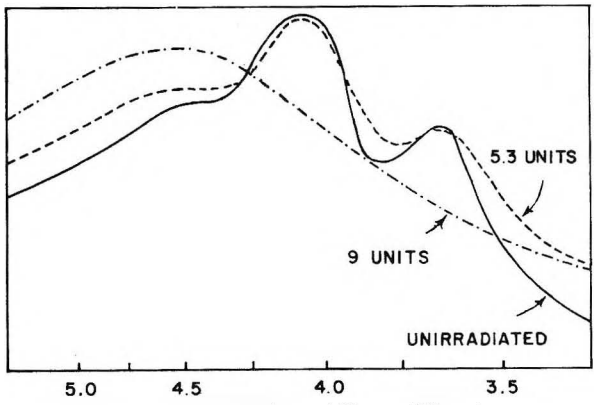

Fig. 1.—Photometer tracings of X-ray diffraction patterns for unoriented branched polyethylene irradiated in atomic pile. The scale of Bragg spacings is shown in abscissa. (Curves are smoothed somewhat from photometer data. Sample thicknesses and exposure times were the same in all cases.)

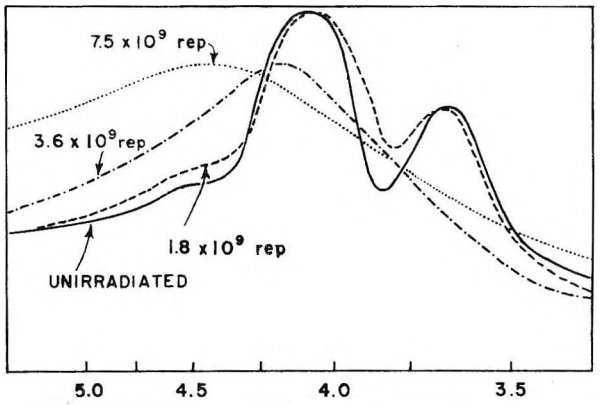

Fig. 2.—Photometer tracings of X-ray diffraction patterns for unoriented linear polyethylene irradiated by electrons. The scale of Bragg spacings is shown in abscissa. (Curves are smoothed somewhat from photometer data. Sample thicknesses and exposure times were the same in all cases.)

3. Structural Changes

It is plain from the outward appearance of drastically irradiated polyethylene that the crystallinity becomes destroyed, for the substance becomes transparent.[3] Changes in density give a measure of the change in the degree of crystallinity.[4] Charlesby has made X-ray diffraction studies of neutron-irradiated polyethylene,[4,10,11] and has reported that the crystalline X-ray pattern grows weaker but not less sharp as the irradiation dose increases. The weakening of the crystalline pattern is found by Charlesby to correspond to an increase in the intensity of the amorphous halo, but he sees no change in the spacings of the diffractions from the crystalline regions. He finds no evidence that the crystalline lattice becomes distorted and merges into the amorphous. He notes some persistence of a weak but sharp crystalline ring at radiation doses as high as 22 units (22×10^{17} slow neutrons/cm.^{2}).

The observation that the crystalline pattern at elevated dosage stays sharp (even though weakened in intensity) implies that the ordered regions which remain are large in dimension and reasonably free of structural irregularities.[12] This conclusion is

(11) A. Charlesby, *J. Polymer Sci.*, **10**, 201 (1953).

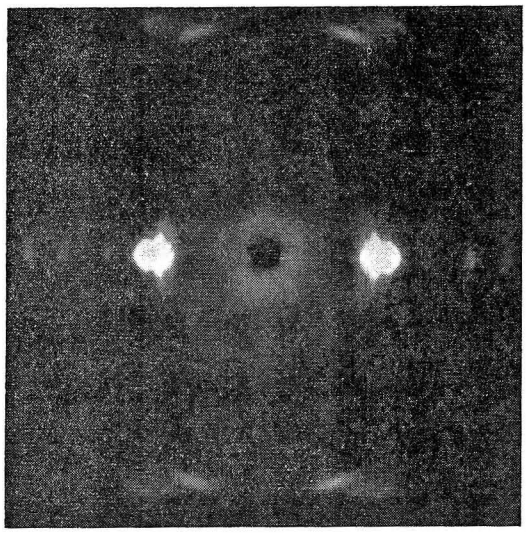

0 rep.

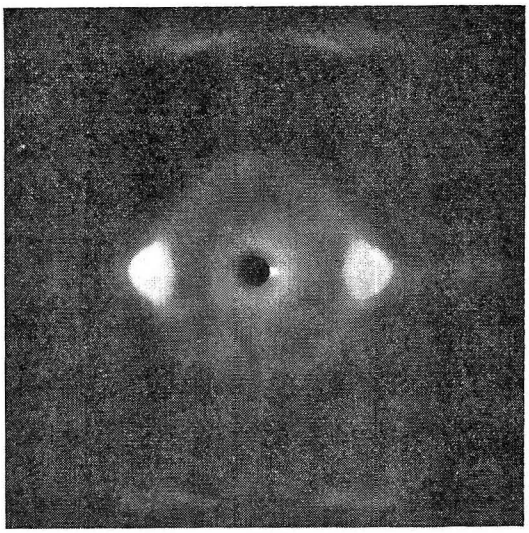

1.8×10^9 rep.

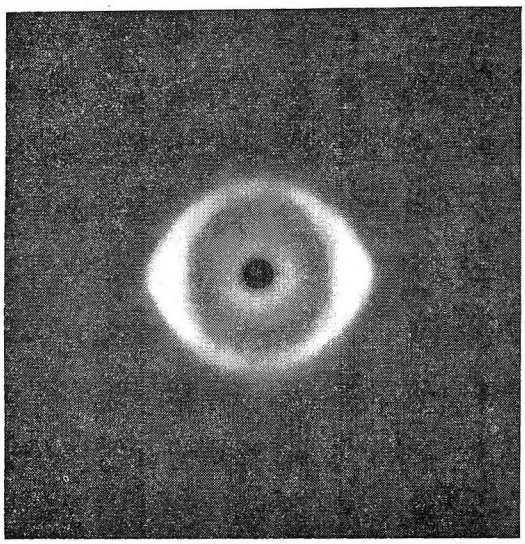

3.6×10^9 rep.

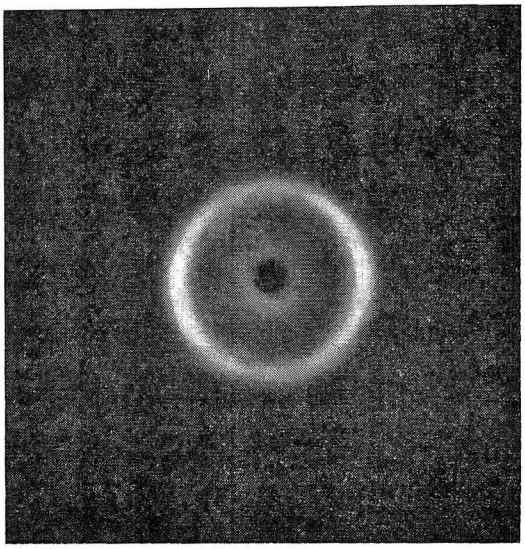

7.5×10^9 rep.

Fig. 3.—X-Ray diffraction patterns for fibers of linear polyethylene irradiated by electrons (fiber axis vertical.)

difficult to accept, for it says that the primary effect of radiation upon the crystalline regions is to diminish their size, while chemical and structural changes (*i.e.*, cross-linking) are peculiar to the amorphous regions.

Our findings agree only in part with those of Charlesby. We note that the amorphous X-ray pattern becomes more prominent, with increasing dosage, at the expense of the crystalline pattern. For the neutron-irradiated polymer, our studies indicate a complete disappearance of crystallinity by a dosage of 9 units, though Charlesby has reported[4] a faint persistence of a crystalline reflection at 22 units. Very likely the disparity here is a measure of the uncertainty in the dosage and the pile temperature. Contrary to Charlesby's conclusions, we find that there are progressive changes in both the sharpness and the spacings of the crystalline pattern as the dosage is increased, for both the branched and the linear polymers. Figures 1 and 2 show the change in the sharpness of the crystalline diffractions, for pile irradiation of branched polyethylene and for electron irradiation of linear polyethylene, respectively. Concurrently there are progressive changes in the orthorhombic crystalline lattice, for the principal spacings describing lateral separations between chains (Table I). The irradiation evidently causes some spreading apart of the chains, through changes in chain structure or through lattice defects. These effects are too small to distort appreciably those spacings which contain a component along the chain direction.

The persistence of the molecular array even at quite high dosages is pointed out in Fig. 3, which shows the response of Marlex 50 fiber to various dosages. Here, although progressively higher irradiation causes the sharp crystalline reflections to become diffuse and ultimately to vanish, there persists even at the highest irradiation studied some evidence of the vestiges of uniaxial order in the molecules.

Irradiation has been shown to affect the density

(12) C. W. Bunn, "Chemical Crystallography," The Oxford University Press, London, 1945, p. 362.

TABLE I

A. LATTICE SPACINGS FOR BRANCHED POLYETHYLENE IRRADIATED IN ATOMIC PILE

Index[13]	Unirradiated, Å.	3.2 Units, Å.	5.3 Units, Å.
110	4.11	4.12	4.17
200	3.70	3.70	3.76
210	2.97	2.98	2.99
020	2.46	2.47	2.49
011	2.25	2.25	2.26
201	2.08	2.08	2.09
211	1.92	1.92	1.93
320, 410, 121	1.72	1.72	1.72

B. LATTICE SPACINGS FOR LINEAR POLYETHYLENE IRRADIATED BY ELECTRONS

Index	Unirradiated, Å.	4.5×10^8 rep, Å.	9.0×10^8 rep, Å.	1.8×10^9 rep, Å.
110	4.12	4.11	4.15	4.21
200	3.70	3.70	3.77	3.82
210	2.96	2.95	2.98	3.07
020	2.47	2.46	2.46	2.49
120	2.35	2.32	2.34	2.36
011	2.27	2.25	2.27	2.27
111	2.17	2.16	2.17	2.17
201	2.09	2.09	2.09	2.10
211	1.93	1.93	1.92	1.94
320, 410, 121	1.71	1.71	1.71	1.73

of polyethylene.[4,7] Figure 4 shows the variation of density (at 25°) and of the Bragg spacing of the principal amorphous halo, as a function of the irradiation dose. The density was measured by a flotation method. The variation in density for pile-irradiated samples compares fairly well with previous findings,[4] Fig. 4a. The decrease in density with increasing dosage in the initial stages is ascribed in part to the progressive disappearance of crystallinity. The density decrease also stems from changes in the amorphous regions, involving expansion of the characteristic distance between chains, up to a certain dosage (see below). The final disappearance of crystallinity and the maximum in the characteristic spacing for the amorphous regions correspond to about the same dosage. At still higher doses the density increases again, the change corresponding to a contraction of the spacings in the amorphous portions, doubtless due to extensive cross-linking. The extrema of density and Bragg spacing in unoriented Marlex 50 (Fig. 4b) occur at comparable dosages to those of the branched polymer which had been exposed to the atomic pile.

The irradiation affects the fiber of Marlex 50 at a lower dosage than it does the unoriented samples (Fig. 4c). Presumably this difference emphasizes some singular features of fibers of highly-crystalline polyethylene. It is believed[14] that the cold-drawing of such polymers, even at quite slow rates (*e.g.*, 1 inch/minute) is a drastic process to which the molecules cannot fully accommodate themselves, and that accordingly voids or dislocations are introduced by the stressing. The alterations manifest themselves by a marked lowering in the density and by evidences, in the X-ray patterns, of disarray in the crystallites. The additional disruption

(13) C. W. Bunn, *Trans. Faraday Soc.*, **35**, 482 (1939).
(14) I. L. Hopkins and W. P. Slichter, unpublished studies.

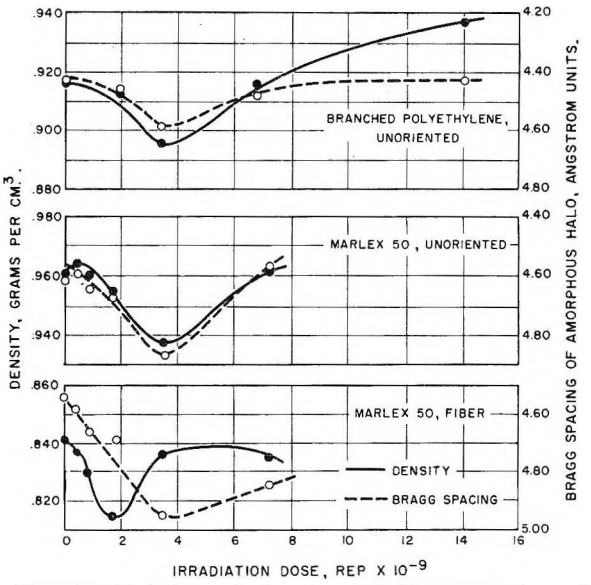

Fig. 4.—Variation of density and Bragg spacing of amorphous halo with irradiation dosage: (a) top, branched polyethylene bombarded in pile; (b) middle, linear polyethylene (unoriented) bombarded with electrons; (c) bottom, linear polyethylene (fiber) bombarded with electrons.

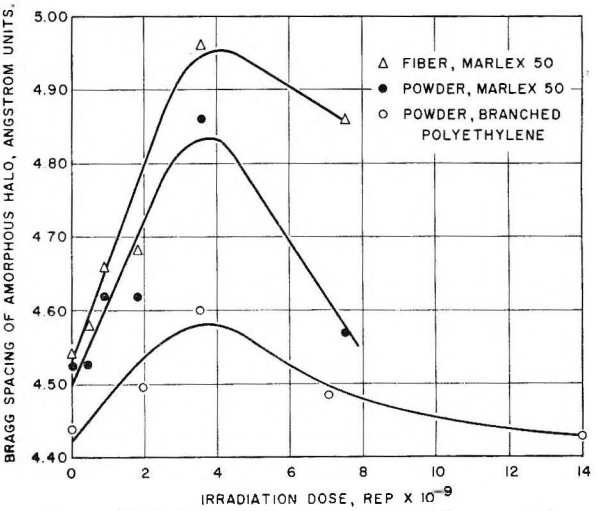

Fig. 5.—Variation of Bragg spacings for amorphous regions with irradiation dose.

of the crystallinity by the irradiation then causes the density to be depressed still further, and at a lower dosage than in the unstressed material.

Figure 5 compares the Bragg spacings in the amorphous regions of the three types of specimen, as a function of dosage. The spacing attributable to a diffuse halo, such as occurs for glassy polymers or for the disordered regions of semi-crystalline polymers, is taken as that which corresponds to the most intense portion of the ring, as one scans along a diameter of the ring. The values in Fig. 5 therefore fail to tell the diffuseness of the ring, *i.e.*, the spread of spacings, though a qualitative notion of this spread may be had from Figs. 1–3. The linear polyethylenes show a narrower distribution of characteristic spacings than do the branched polymers, at every stage of irradiation short of the most drastic. The difference evidently stems from constraints imposed upon the amorphous regions by

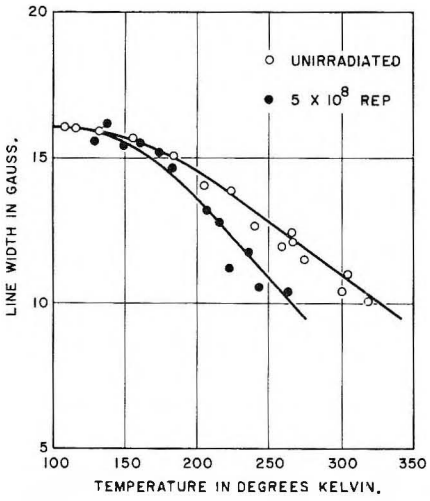

Fig. 6.—Variation of line width in crystalline regions of electron-irradiated, branched polyethylene with temperature.

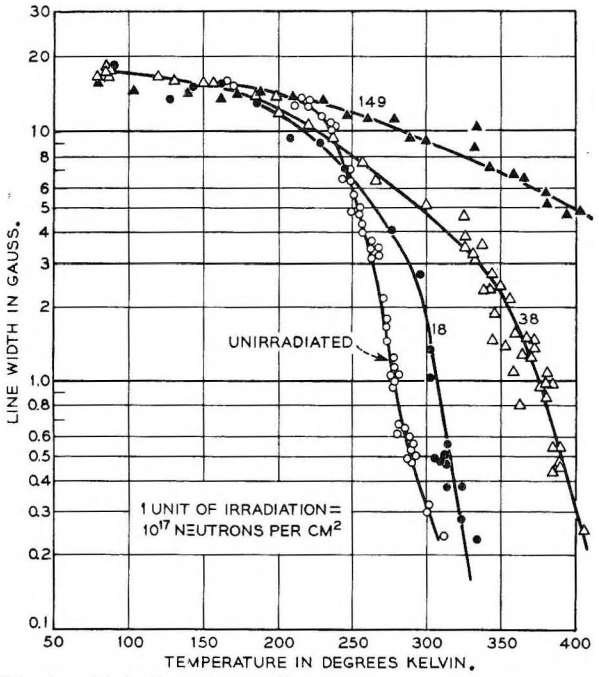

Fig. 7.—Variation of line width with temperature for pile-irradiated polyethylene.

the crystallites,[15] since for a given dosage the degree of crystallinity is greater in linear polyethylene than in branched polyethylene.

Some difficulty attends the measurement of the intensity maximum in the amorphous halo in polyethylene, since this maximum is close to the principal crystalline diffractions (the 110 and 200 reflections). From Fig. 5 and from Table I, it is seen that both the amorphous and the crystalline spacings describing lateral chain separations tend toward greater values with increasing dosage, up to a certain point. The dosage which marks the maxima in the amorphous spacings corresponds approximately to the vanishing of the crystalline diffraction pattern. Perhaps this coincidence is accidental. In any event, the behavior invites further study, for the mechanisms are still obscure. One may postulate that the increase in spacing corresponds to the introduction of voids in the structure, perhaps occasioned by radiation-induced chain branching or by crosslinks which are longer than a single C–C bond. At this point, though, the mechanism for the change in spacings is wholly conjectural. In particular, it is not known why the electron-irradiated samples of linear polyethylene suffer a substantially greater change in the amorphous spacing (Fig. 5) than do the neutron-irradiated samples of branched polyethylene. It would be well to examine closely the effect of irradiation temperature upon the ultimate structure, and to test whether the presence of even small amounts of oxygen affects both the cross-linking[16] and the molecular packing.

At the highest dose in the pile, 149 units (5.7×10^{10} rep, not shown in Figs. 4 and 5) the density of the branched polyethylene rises to 1.018 g./cm.^{3}. On the other hand, the Bragg spacing characteristic of this substance has risen to 4.85Å., a reversal of the trend in Fig. 5. The halo is highly diffuse, though, and there is an extensive amount of incoherent scattering. The seeming contradiction between the high density and the increased spacing no doubt stems from a high degree of short chain branching in the cross-linked network, of which there is evidence from infrared studies.[17]

4. Molecular Motion

As a number of authors have shown, the nuclear magnetic resonance method is valuable for comparisons of the vigor of molecular motion in different substances, particularly in systems which lack permanent electric dipoles and which therefore elude study by dielectric methods. To be sure, the nuclear resonance method suffers from the limitation[18] that the frequencies of motion responsible for the narrowing of the proton resonance line width occur at 10^4 to 10^6 cycles/second, so that the motions accessible to study are circumscribed.[19] The method is also somewhat specialized as a consequence of the rapidity with which the nuclear spin–spin interactions, which are responsible for the line broadening in polymers, fall off with distance between nuclei.

Effectively, this latter point has the result that only those spin–spin interactions which occur within a distance of about 5A. make much of a contribution to the resonance curve. It has already been shown that comparatively light dosages cause marked differences in the solubility[3] and the mechanical properties[10,20] of polyethylene. Evidently, a degree of cross-linking amounting to only one link in about 50 carbon atoms produces significant changes in physical properties. Although such a degree of cross-linking affects the ability of chains to move over large distances, as in tests of solubility

(15) W. P. Slichter, *J. Polymer Sci.*, **21**, 141 (1956).

(16) A. Chapiro, *J. chim. phys.*, **52**, 216 (1955).

(17) A. Brockes and R. Kaiser, *Naturwiss.*, **3**, 53 (1956).

(18) H. S. Gutowsky and G. E. Pake, *J. Chem. Phys.*, **18**, 163 (1950).

(19) The transient ("spin-echo") methods of nuclear resonance are inherently less restricted in this regard.

(20) E. J. Lawton, J. S. Balwit and A. M. Bueche, *Ind. Eng. Chem.*, **46**, 1703 (1954).

or tensile strength, it would not be expected to impart enough stiffness to the chains to quench torsion and rotation, motions which evidently are responsible for most of the proton resonance line narrowing in unirradiated polyethylene at ordinary temperatures.[2] It is not surprising, then, that nuclear resonance studies on samples which have undergone electron irradiation of as much as 1.0×10^8 rep exhibit the same variation of line width with temperature as does the unirradiated polymer.[2] Even at a dosage of 5.0×10^8 rep, the temperature variation of the line width in that part of the resonance curve attributable to the amorphous portions of the polymer[2,21] is indistinguishable from the unirradiated polymer.

Doses of this magnitude have a distinct effect, however, upon the temperature variation of the line width in that part of the resonance curve attributable to the crystalline regions of the polymer. Figure 6 compares the line width as a function of temperature for unirradiated, branched polyethylene and for the same polymer after electron bombardment amounting to 5.0×10^8 rep. In each of these polymers, there is a temperature above which it is no longer possible to resolve the resonance due to the crystalline regions from the more intense contribution from the amorphous regions. As has been pointed out,[22] a factor here is the degree of crystallinity. Thus, the difference in the maximum temperatures at which the crystalline component is discernible (Fig. 6) reflects the difference in the degree of crystallinity between the samples. It is particularly to be noted from Fig. 6, though, that at a given temperature the irradiated polymer shows the narrower line width. That is, the bombardment has reduced the constraints to chain motion within the crystallites. (Although the dosage here is large in terms of the irradiations which are used in polymer technology, it is still well below that which causes disappearance of crystallinity.) It is believed that this effect of irradiation upon chain motion is a consequence of the introduction of defects into the lattice.

Since there is much interest in the effect of radiation upon the degree of crystallinity in the polymer, a comment should be made in passing upon the use of nuclear resonance for a measurement of the crystallinity. It has been suggested[21] that the degree of crystallinity may be found by separating the measured absorption curve (or preferably the derivative of the absorption curve with respect to the applied magnetic field) into two components, one from the amorphous portion and one from the crystalline. It has been pointed out,[22] though, that this measurement is intrinsically a comparison of the vigor of motion in the crystalline and amorphous regions, and that the comparison also serves as a measure of order (crystallinity) only if the chain segments in the crystalline portion are effectively stationary at the same time that the segments in the amorphous regions are engaged in suitably vigorous motion. It does not necessarily follow that such a situation will be realized in a given polymer. Indeed, from Fig. 6 it is evident that a dosage which is by no means drastic leads to considerable chain motion in the crystallites even well below room temperature. At higher dosages the motion would of course be still greater. Hence it seems likely that studies of the degree of crystallinity in irradiated polymers by the nuclear resonance method[23] will prove to be unreliable.

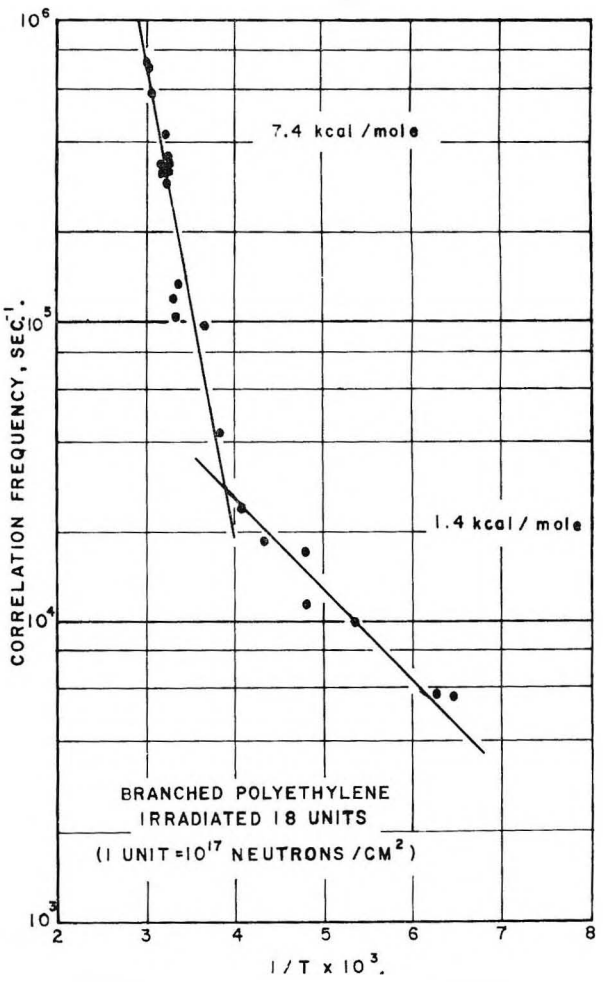

Fig. 8.—Variation of correlation frequency with reciprocal temperature for polyethylene irradiated in atomic pile at 18 units.

When the density of cross-linking becomes great enough to stiffen the chain segments against torsional and rotational motion, one would expect to notice the constraint in nuclear resonance studies. Figure 7 shows the variation of line width as a function of temperature for pile-irradiated samples of branched polyethylene. Specimens irradiated at 18, 38 and 149 units are compared with the unirradiated sample. At these dosages the polymer possesses no crystallinity. At a lower dosage, 9 units (not shown), the line width variation is virtually that of the unirradiated sample. (In the specimens studied, some crystallinity remained at 5 units, but none at 9 units). It is seen from Fig. 7 that as the dosage is increased, the motions which lead to line narrowing become more constrained.

(21) C. W. Wilson, III, and G. E. Pake, *J. Polymer Sci.*, **10**, 503 (1953); *J. Chem. Phys.*, **27**, 115 (1957).

(22) W. P. Slichter and D. W. McCall, *J. Polymer Sci.*, **25**, 230 (1957).

(23) S. Fujiwara, A. Amamiya and K. Shinohara, *J. Chem. Phys.*, **26**, 1343 (1957).

Indeed, in the most densely cross-linked material, there has been comparatively little reduction in line width at temperatures well above the melting point of unirradiated polyethylene.

One is impelled to seek a more detailed description of the molecular motions. As with unirradiated polyethylenes,[2] it may be deduced here that chain motion not far above room temperature assumes a vigor (in samples which have received as much as 18 units of irradiation) greater than that which may be calculated for rotation of all individual chain segments. Hence there exists a significant amount of motion, in terms of the nuclear resonance experiment, which transcends rotation, and which therefore must involve limited translatory movement. At more drastic dosages, the motion is more restricted.

If one assumes that the motion responsible for the line narrowing may be characterized by a single correlation frequency, even though in fact there is a spectrum of motions, then it is possible to relate this frequency to the line width and to obtain an activation energy.[2,18] Though not a precise measure of the motional process, such an activation energy is at least valuable for comparison among samples and among motional processes examined by different methods. Figure 8 shows the variation of the correlation frequency with reciprocal temperature for polyethylene irradiated to a dose of 18 units in the atomic pile. As with unirradiated polyethylene, there appear to be two motional processes, one at low temperature characterized by an activation energy of 1.4 kcal./mole and one at high temperature with an activation energy of 7.4 kcal./mole. A similar situation exists with the other samples described in Fig. 7, giving energies of the order of 1–3 kcal. and 6–8 kcal., with the exception of the sample irradiated at 149 units. In this extreme case only one motional process is identified in the temperature range studied (up to 420°K.); it has an activation energy of 1.8 kcal./mole. As in earlier studies,[2] the low-energy process, which in most samples is manifest only at low temperatures, is ascribed to small-amplitude motion, presumably torsional in character. The process at 6–8 kcal. is ascribed to large-amplitude torsional motion or to rotation and limited translation of chain segments. In the most highly irradiated sample, the molecular segments are so stiff that only the low-energy process can be realized. Indeed, very likely no more vigorous motion can be achieved without bond fracture.

5. Conclusion

It has been found, somewhat at variance to previous studies,[4,10,11] that high-energy irradiation inflicts change concurrently upon the crystalline and the amorphous regions of polyethylene. The characteristic crystalline spacings become altered with increasing dosage, and lattice defects are introduced. Ultimately the crystalline structure merges with the amorphous, which itself changes with increasing irradiation. After the irradiation has destroyed the crystallinity, further bombardment causes increasing constraint to even small-scale motions of molecular segments.

Acknowledgment.—We are grateful to Dr. A. Charlesby, formerly of the British Atomic Energy Research Establishment, Harwell, for the generous donation of some irradiated samples; and to Dr. W. L. Brown and Dr. V. L. Lanza of these laboratories for assistance with the electron irradiated samples.

INHIBITION BY HYDROGEN PEROXIDE OF THE SECOND EXPLOSION LIMIT OF THE HYDROGEN-OXYGEN REACTION[1]

BY W. FORST AND PAUL A. GIGUÈRE

Department of Chemistry, Laval University, Quebec, Que., Canada

Received October 26, 1957

The inhibiting action of hydrogen peroxide on the second limit of the hydrogen-oxygen reaction has been studied at 447° by the withdrawal technique as a function of the composition of the mixture. The pressure ratio p_1/p_2 of the inhibited limit to the normal second limit showed a quadratic dependence on the peroxide concentration. The simplest scheme that accounts for the results is obtained by adding the two reactions $H_2O_2 + H = H_2O + OH$ and $H_2O_2 + OH = H_2O + HO_2$ to the generally accepted mechanism for the second limit.

During a recent investigation of the homogeneous decomposition of hydrogen peroxide vapor carried out in this Laboratory[2] it was discovered incidentally that hydrogen peroxide acts as a strong inhibitor of the hydrogen–oxygen reaction at the second limit.[3] In view of the important rôle played by hydrogen peroxide in that reaction a detailed study of the novel effect seemed to be called for.

(1) This work was supported in part by the Office of Scientific Research of the U. S. Air Force under Contract No. AF 18(600)-492.

(2) P. A. Giguère and I. D. Liu, *Can. J. Chem.*, **35**, 283 (1957).

(3) P. A. Giguère and I. D. Liu, *J. Am. Chem. Soc.*, **79**, 5073 (1957).

Experimental

The apparatus was essentially the same as described previously[2] except for the addition of storage flasks for the various gases, and a flowmeter for controlling the rate of evacuation of the reaction vessel through insertion of capillaries of suitable size. The pressure was recorded by means of a transducer of the absolute type (Statham, Model PA 24 TCa-2-350), with a range of 0–100 mm., in combination with a Leeds and Northrup "Speedomax" recording potentiometer. The input voltage of the transducer (about 9 volts) was measured on a Leeds and Northrup Type K potentiometer. Calibration of the transducer against a mercury manometer showed its response to be linear within experimental error over the entire range at the working

temperature (80° to prevent condensation of peroxide and water vapor).

All the experiments were carried out at 447°. The temperature remained constant to within a few hundredths of a degree during a given run, and never changed by more than 0.5° from one run to the other. The reaction vessel was a 2-liter Pyrex flask cleaned with hot fuming sulfuric acid and conditioned by treatment with hydrogen peroxide vapor until reproducible rates were obtained for the homogeneous decomposition. The various gases were taken directly from commercial cylinders without purification, and were transferred to their storage vessels through a liquid-air trap. Argon was used as a diluent.

The explosion limits were determined by the withdrawal method. Hydrogen, argon and oxygen were first admitted into the reaction vessel, in that order, except in a few runs where the order had to be changed to oxygen–argon–hydrogen, due to the position of the limit. Then, a prepared mixture of hydrogen peroxide vapor with oxygen and/or argon was added quickly and the whole mixture immediately withdrawn. Total pressure prior to withdrawal was 65 mm. in all experiments.

The gaseous mixtures containing the inhibitor were prepared by evaporating some liquid hydrogen peroxide (99%) at 65° into a 5-liter Pyrex flask kept at 120°, and then adding oxygen and/or argon to bring the total pressure up to 100 mm. After allowing 5 minutes for mixing, the concentration of peroxide was determined by following its complete decomposition in the reaction vessel at 447°. A similar test at the end of a series of experiments on explosion limits made it possible to estimate by interpolation the concentration of peroxide at the beginning of each run, assuming the peroxide vapor in the storage vessel to decompose linearly with time. This was found to be true, within experimental error, the rate being of the order of 0.1% per minute at 120°.

Presumably due to some alteration in the surface activity of liquid hydrogen peroxide reservoir, it was difficult to prepare mixtures containing the desired concentration of inhibitor within close limits. In the final compilation of data only those runs were considered in which the initial peroxide concentration was between 85 and 90% of the nominal value.

Results

A first series of experiments served to establish the explosion limit of hydrogen–oxygen mixtures containing no inhibitor or diluent. The results are plotted in Fig. 1 in terms of partial pressures of each gas at the explosion boundary. The curves in Fig. 2 show the dependence of the explosion limit on composition for various amounts of inhibitor, and for a fixed concentration (in mole fraction) of either hydrogen or oxygen. The concentration of hydrogen peroxide at the explosion limit, a matter of considerable importance here, is subject to some uncertainty as the amount of hydrogen peroxide decomposed during withdrawal could not be estimated directly. It was found that if the "withdrawal time," that is the time elapsed between introduction of one-half of the inhibitor mixture and the explosion, was less than 25 sec., the limit was essentially independent of the rate of withdrawal, an indication that little peroxide had decomposed under these conditions. With slower pumping speeds the limit tended to increase appreciably. Therefore the "withdrawal time" was kept close to 20 sec. in all the runs reported here.

The rate of decomposition of hydrogen peroxide was measured in several preliminary tests, in the presence of inert gas and hydrogen at total pressures of about 65 mm. Neglecting the heterogeneous decomposition, which was unimportant at 447°,[2] a very liberal estimate based on these tests indicated that the decomposition suffered by

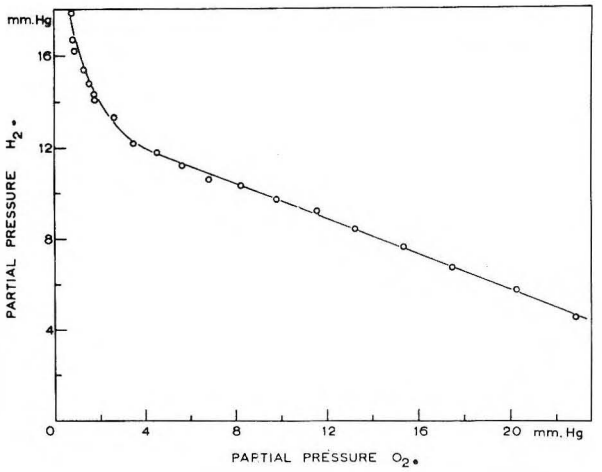

Fig. 1.—Second limit of hydrogen–oxygen mixtures at 447° in terms of the partial pressures of the two gases at the explosion boundary.

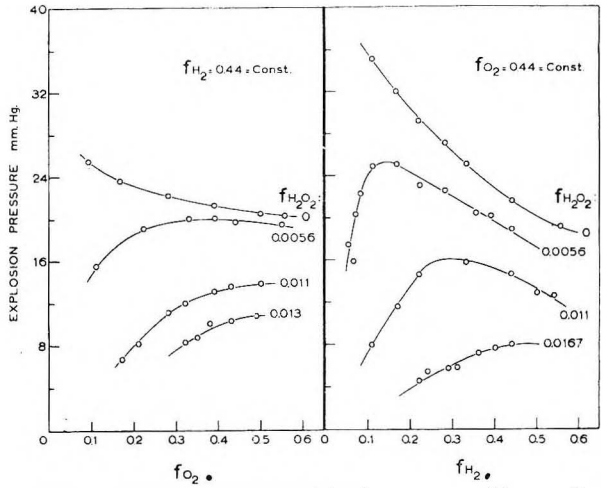

Fig. 2.—Inhibiting effect of hydrogen peroxide on the second explosion limit of hydrogen–oxygen mixtures of various compositions.

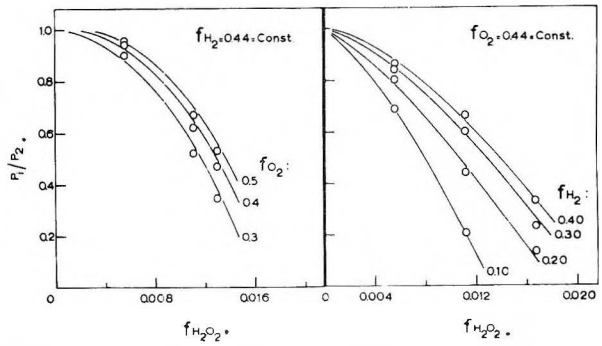

Fig. 3.—Dependence of the ratio $P_{\text{inhibited limit}}/P_{\text{second limit}}$ on the concentration of hydrogen peroxide.

the peroxide during the 20 sec. of withdrawal amounted to no more than about 5%, so that the uncertainty in the concentration of peroxide could not affect seriously the shape of the experimental curves nor the conclusions of this investigation.

Discussion

The plot in Fig. 1 is typical of a B_2O_3-type surface[4]

(4) A. Egerton and D. R. Warren, *Proc. Roy. Soc.* (*London*), **204A**, 465 (1951).

and can be represented by the equation

$$p_{H_2} + 0.33p_{O_2} = 11.24 + 5.09(p_{O_2})^{-1/2} \qquad (I)$$

The $(p_{O_2})^{-1/2}$ term, which is generally interpreted to represent the extent of second-order branching,[4,5] is responsible for the curvature of the plot. The linear portion, with an intercept of 13.5 on the p_{H_2} axis, corresponds to a region where second-order branching is unimportant; that is, where the term $5.09(p_{O_2})^{-1/2}$ does not exceed the value 13.5 − 11.24 = 2.26. This happens for $p_{O_2} > 5$. In the presence of an inert diluent, such as argon, a p_A term multiplied by a constant appears on the left-hand side of equation I; however, the right-hand side remains the same since the rate of branching is unaffected, and therefore the condition for negligible second-order branching is still given by $p_{O_2} > 5$. Inspection of Fig. 2 shows that this requirement is satisfied for all values of f_{H_2} (at $f_{O_2} = 0.44$), and for $f_{O_2} > 0.25$ (at $f_{H_2} = 0.44$). These data are replotted in Fig. 3 as p_i/p_2 (the ratio of the inhibited limit to the ordinary second limit) against $f_{H_2O_2}$. Thus, the dependence of the uninhibited limit on the mixture composition is eliminated. The curves show a quadratic or, more precisely, hyperbolic dependence of p_i/p_2 on $f_{H_2O_2}$, as found by selecting any five points on a curve and substituting their coördinates into the general equation of a conic.

According to the generally accepted mechanism,[6-11] the simplest reaction scheme to account for the essential features of the uninhibited second explosion limit, in the range of oxygen partial pressures of interest here, may be represented by the sequence

$$H + O_2 = OH + O \qquad (1)$$
$$O + H_2 = OH + H \qquad (2)$$
$$OH + H_2 = H_2O + H \qquad (3)$$
$$H + O_2 + M = HO_2 + M \qquad (4)$$

which leads to the condition for explosion

$$P_2 = 2k_1/k_4$$

Now, an explosion limit is met when the rate of chain breaking equals the rate of branching. Provided both processes are first order in chain carriers, the limit is independent of the rate of chain initiation, so that the OH radicals released into the gas phase by the decomposing peroxide[2] cannot affect the second limit. Therefore, the observed inhibition must be due to some other causes. Because of its low concentration, hydrogen peroxide cannot affect appreciably reaction 4 as a third body. Other reactions, notably with molecular hydrogen, may be ignored on the ground that they are not fast enough to be of importance here. The only remaining possibility seems to be one or more of the reactions of hydrogen peroxide with the chain particles

$$H_2O_2 + H = HO_2 + H_2 \qquad (9)$$
$$H_2O_2 + H = H_2O + OH \qquad (10)$$
$$H_2O_2 + 2H = 2H_2O \qquad (11)$$
$$H_2O_2 + OH = H_2O + HO_2 \qquad (12)$$
$$H_2O_2 + O = OH + HO_2 \qquad (13)$$
$$H_2O_2 + O = H_2O + O_2 \qquad (14)$$

From what is known of boric acid-type surfaces,[4,5,12] and of the decomposition of hydrogen peroxide itself,[2] the above reactions may be assumed essentially homogeneous. All of these reactions, first one by one, then two at a time in all possible combinations, were added to the mechanism for the uninhibited limit and the theoretical expressions for p_i/p_2 derived. It was found that only the sequence (1) − (4), (10) and (12) could account for the observed relationship between p_i/p_2 and $f_{H_2O_2}$.[13] This sequence is most significant in that it represents the simplest possible mechanism for the inhibiting action of hydrogen peroxide. Addition of three or more of reactions (9)–(14) to the (1)-(4) scheme might also explain the experimental results, but would lead to very complex expressions.

From the above sequence the inhibited limit is given by the equation

$$p_i = \frac{2k_1k_3f_{H_2}f_{O_2} - k_{10}k_{12}(f_{H_2O_2})^2}{k_3k_4f_{H_2}f_{O_2} - k_4k_{12}f_{H_2O_2}} \qquad [II]$$

Since the concentration of peroxide is presumably too small to affect the k_4 term, it follows from (II), after some reductions

$$\frac{p_i}{p_2} = \frac{1 - \frac{a}{f_{O_2}} \times \frac{b}{f_{H_2}}(f_{H_2O_2})^2}{1 + \frac{b}{f_{H_2}} \times f_{H_2O_2}} \qquad [III]$$

where $a = k_{10}/2k_1$ and $b = k_{12}/k_3$. Upon fitting the experimental results into (III) the value of "a" falls in the range from 50 to 80, and that of "b," from 4.8 to 5.7. However, these figures should be viewed with caution as they are quite sensitive to the mechanism assumed for the second explosion limit. For instance, addition of reactions 5, 6 and 7 to that mechanism, increases the value of "a" about fivefold, and that of "b," twenty-fold.

These findings receive some support from other sources. Thus Geib,[14] who studied briefly the reaction of hydrogen atoms with hydrogen peroxide, concluded that it takes place *via* step 10 rather than (9) or (11). His arguments were based on the relative abundance of the final products and on certain energy considerations. The latter may be worth restating here in terms of the latest thermochemical data. Using the fairly well established value $D(H - O_2) = 47$ kcal.,[15] it turns out that reaction 10 is more exothermic ($\Delta H = -68$ kcal.) than (9) by about 55 kcal. Also, the O-H bond

(5) G. Dixon-Lewis, J. W. Linnett and D. F. Heath, *Trans. Faraday Soc.*, **49**, 766 (1953).

(6) C. N. Hinshelwood and A. T. Williamson, "The Reaction between Hydrogen and Oxygen," Oxford University Press, 1934.

(7) G. von Elbe and B. Lewis, *J. Chem. Phys.*, **10**, 366 (1942).

(8) A. H. Willbourn and C. N. Hinshelwood, *Proc. Roy. Soc. (London)*, **185A**, 353, 369, 376 (1946).

(9) C. F. Cullis and C. N. Hinshelwood, *ibid.*, **186A**, 462, 469 (1946).

(10) C. N. Hinshelwood, *ibid.*, **188A**, 1 (1946).

(11) B. Lewis and G. von Elbe, "Combustion, Flames and Explosions," Academic Press, New York, N. Y., 1951.

(12) D. R. Warren, *Trans. Faraday Soc.*, **53**, 199 (1957).

(13) This is true also if the steps

$$HO_2 = {}^1/_2H_2O_2 + {}^1/_2O_2 \qquad (5)$$
$$HO_2 + H_2O_2 = H_2O + O_2 + OH \qquad (6)$$
$$H_2O_2 = 2OH \qquad (7)$$

are added to the scheme for the uninhibited limit.

(14) K. H. Geib, *Z. physik. Chem.*, **169A**, 161 (1934).

(15) S. N. Foner and R. L. Hudson, *J. Chem. Phys.*, **23**, 1364 (1955).

which must be broken in step 9, is twice as strong as the O–O bond involved in (10).[16] A recent reinvestigation of the reaction of atomic hydrogen with hydrogen peroxide has again been interpreted in favor of Geib's mechanism.[17] On the assumption that his measurements referred to reaction 10, Geib calculated the collision yield and, taking a steric factor of 0.1, he estimated the activation energy to be about 4.5 kcal. A rough calculation of E_{10} also may be attempted from the present results by obtaining first an estimate of k_1 at the temperature of our measurements.

Lewis and von Elbe[7] have given an expression for k_1 but there are reasons to believe that it is in error by a factor of 10^3 at 520°. According to Baldwin and Walsh[18] a more plausible value would be 10^{-14} cm.^{3} molecules^{-1} sec.$^{-1}$ at that temperature. Warren[19] has measured the temperature dependence of the second explosion limit, and obtained $E_{p_2} = (E_1 - E_4) = 20 \pm 1$ kcal. Now, Hoare and Walsh[20] have proposed for reaction 4 a negative activation energy of about -4 kcal., which makes $E_1 \simeq 16$ kcal. in good agreement with the endothermicity of that reaction, 17 kcal. at 700°K.[21] These data lead to $k_1 \simeq 3 \times 10^{-15}$ cm.^{3} molecules^{-1} sec.$^{-1}$ at 447°. Taking $a = 65$ one gets $k_{10} = 2ak_1 \simeq 4 \times 10^{-13}$ cm.^{3} molecules^{-1} sec.$^{-1}$ at the same temperature. Finally, using Geib's figures for the collision diameters of H and H_2O_2 the collision yield may be calculated, leading to $E_{10} \simeq 7$ kcal.[22] with a steric factor of 0.1. Considering the entirely different approach of the two methods, the agreement with Geib's estimate is gratifying. It is of course no proof for the value of the activation energy. The alternative interpretation of Geib's results proposed by Lewis and von Elbe[7] would thus appear doubtful.

As yet no quantitative measurements have been reported on the reactions of OH radicals. The mass spectrometric investigations of Foner and Hudson[15] point to a very high rate for reaction 12. From the value obtained here for constant "*b*," this reaction should be faster than 3 by a factor of at least five. It may also be noted that reaction 12 is twice as exothermic ($\Delta H = -32$ kcal.) as reaction 3.

An interesting question raised by the present findings concerns the possible influence of hydrogen peroxide on the second explosion limit under conditions of predominant second-order branching, *e.g.*, with a clean Pyrex surface, such as used here, but at higher temperatures. In Egerton and Warren's[4] derivation of equation I the coefficient of the $(p_{O_2})^{-1/2}$ term is proportional to the half-power of the rate of chain initiation. This has prompted Warren[19] to suggest that explosion sensitizers may expand the limits by affecting the rate of initiation. It is entirely conceivable that under appropriate conditions the increased chain-initiating effect of added hydrogen peroxide would far outweigh its chain-breaking effect through steps 10 and 12. Thus, at a high enough temperature, hydrogen peroxide might become an explosion sensitizer instead of an inhibitor. Such a conclusion seems all the more plausible as reactions 10 and 12 very likely have low activation energies, making their rates almost temperature independent, whereas the second-order branching term in equation I involves a large activation energy, of the order of 35 kcal.[4]

The authors are grateful to the National Research Council of Canada for financial assistance.

(16) T. L. Cottrell, "The Strengths of Chemical Bonds," Butterworths, London, 1954.

(17) J. S. Batzold, C. Luner and C. A. Winkler, *Can. J. Chem.*, **31**, 262 (1953).

(18) R. R. Baldwin and A. D. Walsh, *Disc. Faraday Soc.*, **17**, 97 (1954).

(19) D. R. Warren, *Proc. Roy. Soc.* (*London*), **211A**, 96 (1952).

(20) D. E. Hoare and A. D. Walsh, *Trans. Faraday Soc.*, **53**, 1102 (1957).

(21) F. D. Rossini, *et al.*, "Selected Values of Chemical Thermodynamic Properties," Vol. III, Circular 500, Washington, D. C., 1952.

(22) A value of 300 for "*a*" would make $E_{10} \simeq 5$ kcal. other things being equal.

THE CATALYSIS OF THE DECOMPOSITION OF CARO'S ACID[1]

BY DONALD L. BALL AND JOHN O. EDWARDS

Metcalf Chemical Laboratories of Brown University, Providence 12, R. I.

Received October 30, 1957

Evidence has been found for the catalysis of the decomposition of Caro's acid (peroxymonosulfuric acid) by specific substances in aqueous phosphate buffer. Cobalt(II) and molybdenum(VI) are especially effective, although some other metal ions also act as catalysts for the decomposition. The observed catalytic decompositions are first order in the concentration of Caro's acid with the exception of the cobalt-catalyzed decomposition which is second order in Caro's acid. The order in catalyst concentration could not be determined except in the case of molybdate wherein an order of one-half and an induction period were found.

Introduction

The decomposition of Caro's acid (*i.e.*, peroxymonosulfuric acid, H_2SO_5, to form oxygen and sulfuric acid) in aqueous buffer solutions is susceptible to catalysis by trace amounts of impurities.[1] Apparently these catalytic paths are eliminated by the addition of small amounts of ethylenediaminetetraacetic acid (EDTA). In the absence of EDTA, the observed rate of decomposition was dependent on the sample of phosphate used in preparing the buffer solutions; therefore the observed effect has been ascribed to the nature and amounts of the catalytic substances present as impurities in the phosphate. The fact[2] that dipicolinic acid stabilizes

(1) The Kinetics and Mechanism of the Decomposition of Caro's Acid. II; prior paper, *J. Am. Chem. Soc.*, **78**, 1125 (1956).

solutions of Caro's acid is further evidence for catalysis by trace impurities. Recently, Kuhn[3] has investigated the decomposition of Caro's acid by small amounts of nitric acid in strong sulfuric acid solutions.

Additional evidence for the catalysis of the Caro's acid decomposition was desirable. The present paper provides the results of a survey of the possible catalytic effect of various substances on the decomposition, also kinetic investigations have been made for the two most effective catalysts found. In view of the difficulties in interpretation, etc., only a summary of our work is presented here.[4]

Experimental

Most of the procedures used in this study have been discussed previously.[1] The catalytic survey was made in solutions buffered by phosphate (total phosphate = 0.75 *M*) in the *p*H range 6.6–6.8. The initial concentrations of Caro's acid were from 0.01 to 0.02 *M*. All experiments were conducted at 25.0°. The rate of decomposition before adding the test substance was apparently first order in Caro's acid.[1] With the sample of phosphate used in this survey, the original rate of decomposition (resulting from the spontaneous decomposition *plus* the catalytic rate due to catalysts originally present as impurities) was not rapid (k'_H = *ca.* 10^{-3} min.$^{-1}$).

In general, the test substance was dissolved in water before its introduction into the reaction solution. The element to be tested was added as its highest oxidation state, when available. The amount added was kept small enough that a stoichiometric reaction would not be mistaken for catalysis; usually the concentration of the test substance in the reaction solution was about 1×10^{-4} *M*. The effect of an added substance was assumed to be demonstrated by the difference between the rate of decomposition observed after the substance was added and the rate originally observed.

Results

Catalytic Survey.—Small amounts of cobalt(II), copper(II), nickel(II), ruthenium(II), iridium(III), vanadium(V), molybdenum(VI) and tungsten(VI) increased the rate of decomposition of Caro's acid. With the exception of the studies with cobalt(II), the catalytic decompositions appeared to be first order in Caro's acid; plots of the logarithm of the Caro's acid concentration *versus* time were linear.

The effects of cobalt and molybdenum appeared to be over ten times greater than that of any other catalyst observed. The other substances mentioned above appeared to have roughly the same small catalytic effect. No attempt to specify their relative effectiveness is justified; their concentrations were not equivalent in general and, in some instances, were not accurately known.

No observable catalytic effect was displayed by Ag(I), Tl(I), Cd(II), Pb(II), Hg(II), Pd(II), Zn(II), Sb(III), As(III), Bi(III), Ce(III), Fe(III), Pt(IV), Rh(IV) Th(IV), Zr(IV), I(V), Ta(V), Cr(VI) and Mn(VII). Some of the species declared catalytically inactive might have exerted an effect at a higher concentration. It is also possible that, in some cases, an impurity in the substance tested was responsible for the observed catalysis; a purer sample might not have shown any catalytic effect. In considering the results of the catalytic survey, these possibilities must be borne in mind.

(2) F. P. Greenspan and D. G. MacKeller, U. S. Patent 2,663,621 (Dec. 22, 1953).

(3) L. P. Kuhn, *J. Am. Chem. Soc.*, **79**, 3661 (1957).

(4) Further details especially for molybdate catalysis, may be found in the Ph.D. thesis of D. L. Ball, Brown University, 1956.

The Cobalt-catalyzed Decomposition.—Cobaltous ion at an apparent concentration of 10^{-8} *M* noticeably accelerates the decomposition of Caro's acid. Uniquely, the cobalt-catalyzed composition appears to be second order in the concentration of Caro's acid. Customarily observations were made over a period exceeding one "half-life"; plots of reciprocal Caro's acid concentration *versus* time gave straight lines when k_H' was small compared to the catalytic rate.

The observed rate law is of the form

$$-\frac{d[HSO_5^-]}{dt} = k_H'[HSO_5^-] + k_C'[Co(II)]^n[HSO_5^-]^2$$

where k_H' is the rate constant observed in the absence of cobalt(II), k_C' is the cobalt-catalyzed rate constant, and n is the order in the concentration of cobalt ion. In the *p*H range of these studies, Caro's acid exists primarily as the ion HSO_5^-.

The data obtained are summarized in Table I. Uncertainties in the nature of the cobalt catalyst in the system make a determination of n quite impossible at present. It is likely that the cobalt(II) is oxidized to cobalt(III) immediately upon its introduction. Sobol[5] reports a value of 3.2×10^{-45} for the activity solubility product constant of $Co(OH)_3$. A K_{sp} of this magnitude would require that essentially all the cobalt(III) in the system was in the form of precipitated cobaltic hydroxide. The possibility of precipitated cobaltous and/or cobaltic phosphates cannot be ignored; these salts are known to be very insoluble, although useful quantitative data are not available. The observed catalytic effect then could be heterogeneous in nature and the variation of rate with concentration is not inconsistent with this. Thus uncertainties regarding the appropriate solubility analysis make further consideration of the data unwarranted.

TABLE I

SUMMARY OF THE EXPERIMENTS ON THE COBALT-CATALYZED DECOMPOSITION OF CARO'S ACID

*p*H	[Co(II)] × 10^8, *M*	R_C[a]
6.09	5.3	1.3
6.11	23	2.5
6.62	1.4	*ca.* 0.28
6.61	2.8	*ca.* 0.45
6.65	430	6.0
6.65	770	7.1

[a] $R_C = k_C'[Co(II)]^n$. The units are (moles/l.)$^{-1}$ min.$^{-1}$.

The Molybdate-catalyzed Decomposition.—Small amounts ($\sim 10^{-5}$ *M*) of molybdenum have an effect on the rate of the decomposition of Caro's acid. The catalyst customarily was added as a solution of Na_2MoO_4; however comparable results were obtained using $(NH_4)_6Mo_7O_{24}$. The decomposition was first order in the concentration of Caro's acid; sample plots are given in Fig. 1. The observed first-order catalytic rate constant is defined as k_C.

An induction period was always observed after the addition of the catalyst. However, the length of this induction period (usually from five to ten

(5) S. I. Sobol, *Zhur. Obshchei Khim.*, 906 (1953); *C. A.*, **48**, 3109e (1954).

minutes) did not appear to have any correlation with other variables, such as *p*H, the concentration of Caro's acid, and the concentration of molybdate ion.

All runs were conducted in phosphate buffers at *p*H values ranging from 5.90 to 7.34. In this range, the decomposition appeared to be one-half order in the concentration of molybdenum(VI) as may be seen in Fig. 2. Molybdate ion is known to polymerize in the *p*H region of the kinetics experiments.[6] Therefore, the amount of molybdate added represents the total amount in all forms, both monomeric and associated.

The suggested rate law in the *p*H range investigated is

$$-\frac{d[HSO_5^-]}{dt} = k_H'[HSO_5^-] + k_c''[Mo(VI)]^{1/2}[HSO_5^-]$$

However, variations of k_c'' with *p*H were not entirely reproducible. The sample of phosphate used in the buffer had an apparent effect on the decomposition rate. Using phosphate(II) (1), the observed value for k_c'' was 0.66 ± 0.14 (moles/l.)$^{-1/2}$ min.$^{-1}$ (29 runs) in the *p*H range from 6.39 to 7.34. The value for k_c'' observed using phosphate(III) (1) was 0.33 ± 0.12 (19 runs) in the same *p*H range. At lower *p*H values (5 runs in the range 5.90 to 6.10) the observed value for k_c'' (phosphate(III)) was considerably lower (0.13 ± 0.01).

The data suggest that the monomer $HMoO_4^-$ participates in the catalytic mechanism, and that the dimer $Mo_2O_7^=$ is the principal form of molybdenum(VI) in the *p*H range studied. The decrease in the catalytic activity in the acidic extreme of the *p*H range studied could be explained by the formation of higher polymolybdates.

It should be noted that molybdate has no catalytic effect on the decomposition of Caro's acid in the presence of small amounts of EDTA. It appears that a third substance, or "co-catalyst," is necessary for the observed acceleration of the decomposition. Since a given buffer gave fairly reproducible data, whatever the source of molybdenum, it is believed that Mo(VI) is necessary for the catalytic decomposition; in other words, no impurity in the molybdate is solely responsible for the observed catalysis. Attempts to gain more reproducible data using conductivity water and recrystallized phosphate in the buffer solution were not successful. This observation compares with the failure of similar attempts to gain reproducible measurements of the rate of decomposition of Caro's acid in unmodified (no added EDTA) phosphate buffer solutions.

(6) H. J. Emeleus and J. S. Anderson, "Modern Aspects of Inorganic Chemistry," D. Van Nostrand Co., Inc., New York, N. Y., 2nd edition, 1952, pp. 213–216.

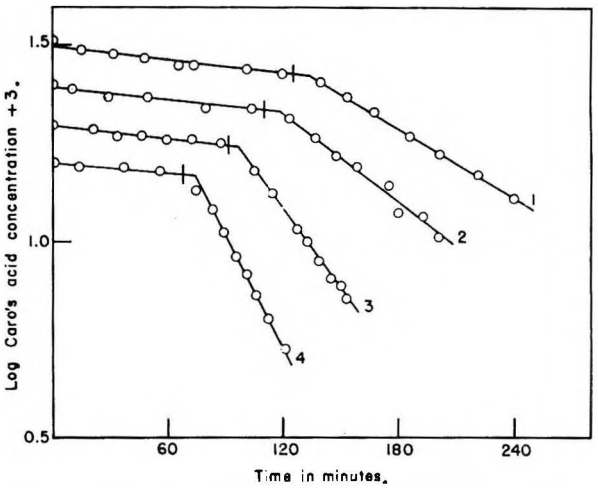

Fig. 1.—First-order plots of the molybdate-catalyzed decomposition at *p*H 6.42. The times of the addition of catalyst are indicated by the vertical bars. Runs with a total molybdate concentration of 4.8, 8.7, 41 and 68 × 10^{-5} *M* are given by curves 1, 2, 3 and 4, respectively.

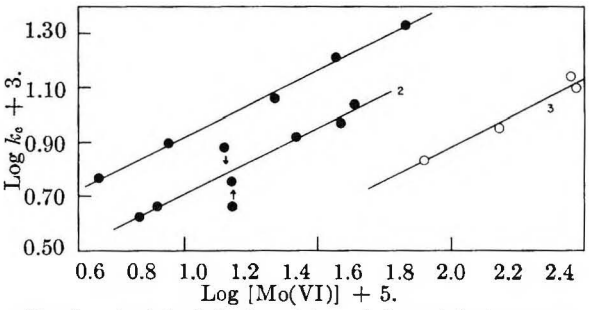

Fig. 2.—A plot of the logarithm of the catalytic rate constant, k_c (min.)$^{-1}$, *versus* the logarithm of the concentration of total molybdate. Runs buffered at average *p*H values of 6.42, 7.10 and 6.92 are given by curves 1, 2, and 3, respectively. The use of phosphates II and III is indicated by the symbols ● and ○, respectively.

Acknowledgment.—We are grateful to the Office of Ordnance Research of the U. S. Army for financial support, and D. L. B. is pleased to acknowledge the aid of a Union Carbide and Carbon Fellowship.

I. AN APPARATUS FOR USE WITH CONDENSED PHASES AT 10,000°[1] II. SOME THERMODYNAMIC AND RATE CONSIDERATIONS AT VERY HIGH TEMPERATURES[1]

BY H. TRACY HALL, BILLINGS BROWN, BRUCE NELSON AND LANE A. COMPTON

Brigham Young University, Provo, Utah

Received October 31, 1957

An apparatus is described wherein condensed phases may be heated to temperatures of 10,000° or higher for second to minute periods. Temperature is obtained by resistance heating of an electrically conducting element confined by a steel bomb. At the highest temperatures of operation, both the heating element and adjacent refractory material are molten. Some consideration is given to the various quantities that determine the equilibria between reactants and products under constant volume and also under constant pressure conditions. Kinetic problems at very high pressure and at very high temperature are discussed. Finally, there is some speculation as to the possibility of forcing external electrons into inner unfilled orbitals when condensed phases are maintained at constant volume and then subjected to extremely high temperatures.

I

An unexplored area for scientific research exists in the region above 5,000° wherein temperature could be maintained for second to minute periods in condensed phases. We have found it possible to obtain temperatures of at least 10,000° by resistance heating of an electrically conducting element confined within a bomb such as is shown in Fig. 1. During operation the thermal insulation immediately surrounding the central heating rod will grade-off radially from liquid to solid material with the radial temperature gradient that is established. The heating element will, of course, be liquid at the higher operating temperatures. The heat loss out the ends of the bomb along the axis will be such as to provide a thermal gradient from the central regions of the bomb toward the ends so that material will also grade from molten to solid here and in this wise eliminate the container problem. The material within the bomb is confined by tightening the nuts on the tension bolts. The pressure exerted upon the material within the bomb by this technique is small; indeed, it is insufficient to close up any voids initially present, so it is important to have good fitting components in order that the phases within the bomb might remain as condensed systems when the material becomes molten at the high temperature.

In the first bombs constructed the heating element was a carbon rod and the thermal insulation was a readily machinable, stony material known as pyrophyllite. Pyrophyllite is a naturally occurring, extremely fine-grained, hydrous aluminum silicate, which, when confined, melts to a glass-like substance at a temperature around 1,500°. A platinum–rhodium thermocouple element was imbedded in the carbon rod for the measurement of temperature. Power input (measured as watts) to the carbon heating element as a function of temperature indicated by the thermocouple was recorded. A plot of these two variables yields a straight line function, which was extrapolated to indicate higher temperatures. An additional point on this plot was obtained by finding the power input necessary to melt a small tungsten wire adjacent to the graphite rod. A sample of such a power input *versus* temperature plot is shown in Fig. 2.

(1) Supported by U. S. Army Office of Ordnance Research, Contract DA-04-495-ORD-792.

With a carbon rod heater and pyrophyllite insulator, it is possible to obtain extrapolated temperatures of the order of 6,000° for periods of 15 seconds. For periods of the order of minutes it is possible to obtain temperatures of the order of 4,000°. The maximum temperature obtainable with carbon heaters is limited by intrusion of molten pyrophyllite material across the carbon heating element. This intrusion, which seems to be a combination mechanical and chemical effect, results in interruption of the electric current and consequently limits the temperature obtainable. Substitution of thermal insulation materials for the pyrophyllite immediately surrounding the carbon rod was attempted in order to eliminate or minimize this current cut-off effect. Alumina, procelain, silica and glass were tried. Alumina and porcelain were no better than the pyrophyllite, silica was inferior, but Pyrex glass increased the temperature that could be obtained before cut-off occurred. A Pyrex glass sheath of approximately $^1/_{32}$-inch wall thickness immediately surrounding a $^1/_8$-inch diameter carbon rod allowed extrapolated temperatures of 15,000° to be obtained for 15-second periods. Some attempts were made to substitute compressed refractory powders for the pyrophyllite thermal insulation for use with various heating elements. This was without success. In the first place, it was difficult to obtain a dense compact mass free of minute voids. Of course, on heating such material, vaporization would take place into the voids and a condensed phase would not be maintained. Secondly, it soon became apparent that when operating at 10,000°, it matters little whether the refractory being used melts at 1,500 or 2,500°. In view of this, most of our experiments have been conducted with pyrophyllite as the refractory element. Of course, the principal advantage of pyrophyllite is that it can be readily machined to any shape.

Because there seemed to be some chemical reaction between carbon and the materials used as thermal insulation at the high temperatures being produced, we thought it advisable to experiment with some high melting metallic materials such as tungsten and molybdenum in place of carbon. Because of the much higher thermal conductivity of these materials over that of carbon, it was found that much larger wattages were required to obtain a

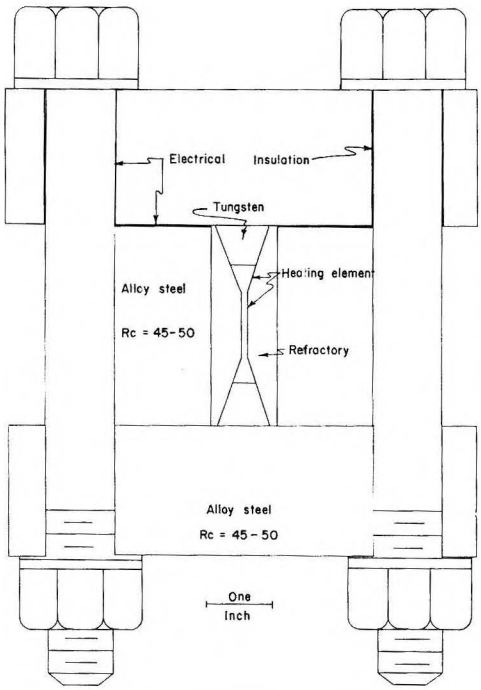

Fig. 1.—High temperature bomb.

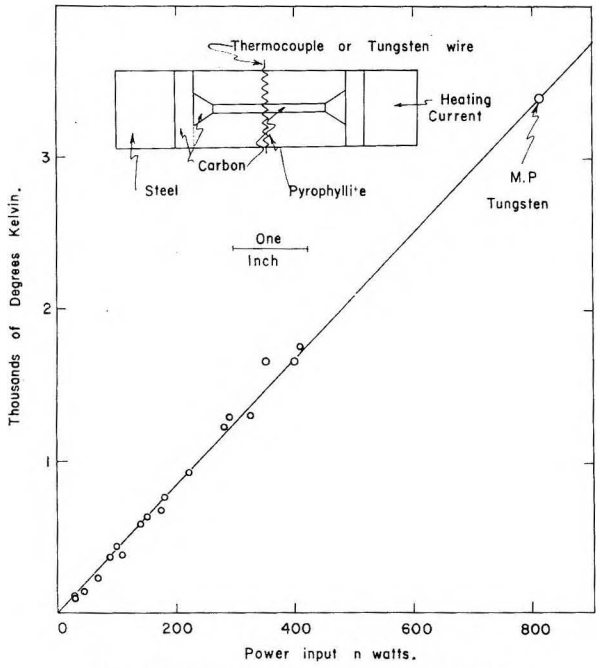

Fig. 2.—Typical temperature calibration.

given temperature with these substances. All other conditions of geometrical arrangement, etc., remained the same. (A new temperature calibration must be obtained for each change of materials or geometrical dimensions and arrangement.) With molybdenum and tungsten, the cut-off phenomenon was observed again. As before, the highest temperatures were obtained when the heating element was sheathed with Pyrex glass. With this arrangement, temperatures of 10,000° were maintained for 15 seconds before cut-off. There seemed to be no evidence of chemical reaction between the metal and the refractory. Cut-offs seemed to be caused by the molten metal withdrawing into a ball and by the molten refractory material flowing into the space from which the metal withdrew. The forming of this ball of metal might be due to two effects: (1) an actual electrical "pinch-off" effect due to the high current flowing through the metal; and (2) an attempt by the metal to reduce its surface area because of the large difference in surface energy between the metal and the refractory.

At this point, it seemed that this cut-off phenomenon might be eliminated if the heating element were composed of some material that when molten would possess cohesive forces more like that of the ceramic insulator and also if the electrical resistance of this element were a factor of 100 or so higher than that of tungsten. The higher resistance would require much lower currents to obtain the same wattage within the element and hence the electrical "pinch-off" effect would be reduced. The materials experimented with in this connection were, in general, semi-conductors such as silicon carbide, copper oxide and sulfide, elemental silicon, etc. Through these experiments a heating element was found in which it has not been possible to produce cut-off at power inputs available to us (20 kw.). This heating element is composed of an approximately 50-50-by-volume mixture of silicon carbide and graphite powders.

Extrapolations of power input–temperature curves such as that of Fig. 2 are hazardous above 10,000°. Consequently, equipment is being assembled to try to utilize thermal noise power in the measurement of temperatures that might be produced in bombs with C–SiC heating elements. If power inputs corresponding to 10,000° are maintained in C–SiC heaters for periods greater than one minute, considerable stirring of liquid material ensues, the C–SiC mixture is dispersed throughout a large volume of molten material with resultant enlargement of the cross section of the electrical conduction path. This leads to lower temperatures within the bomb. Initially, 3,000 watts corresponds to a conservative 10,000° when the conducting cross section is $^1/_8$-inch diameter. However, when the conducting cross section is $^1/_2$-inch diameter, 3,000 watts corresponds to only 3,000°. Application of very high pressures to the contents of the bomb would tend to stiffen the molten materials by squeezing out the molecular holes. The holes, of course, are necessary for liquid flow. High pressure would tend to maintain the original geometry of components within the bomb, thus allowing higher temperatures to be obtained and maintained for longer periods of time. To carry out high-temperature experiments within the bomb, it is necessary to surround the heating element with a sheath of the materials to be reacted. In some instances, it is possible to construct the heating element of the reacting materials. Limitations on the reactions will be imposed in many cases because of reaction with the heating element or the refractory liner. Regardless of these limitations, there are numerous experiments that can be performed with this high-temperature device.

II

A substance is completely characterized thermo-

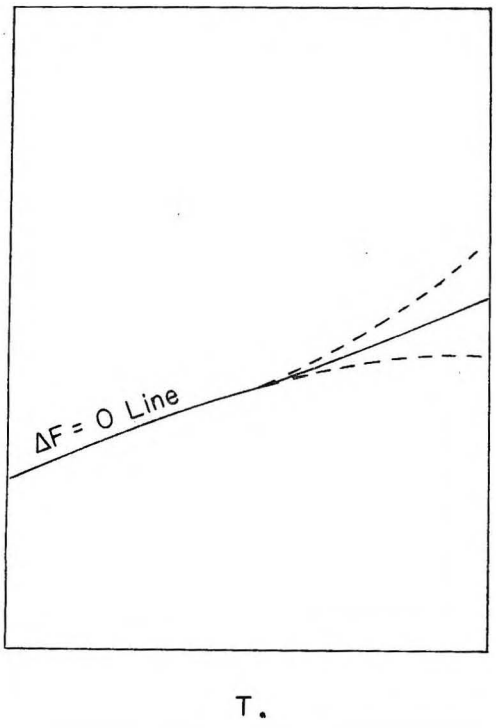

Fig. 3.—Plot showing $\Delta F = 0$ line on a P–T diagram.

dynamically if the volume is known as a function of the two intensive properties, pressure and temperature, and if the specific heat at constant pressure, say one atmosphere, is known as a function of temperature. If this information (in addition to ΔE and S at some pressure and temperature) were available for all possible substances, the thermodynamicist would have an easy time in predicting the course of chemical reactions. However, the amount of such information available even at moderate pressures and high temperatures is meager. The basic thermodynamic relationships for predicting the course of a chemical reaction are given below for the reaction A = B where A represents the reactants and B represents the products of the reaction. The difference in free energy be-

$$\begin{aligned} F_B &= P_B V_B + E_B - T_B S_B \quad (a) \\ F_A &= P_A V_A + E_A - T_A S_A \quad (b) \qquad (1) \\ \Delta F &= F_B - F_A \quad (c) \end{aligned}$$

tween the products and the reactants gives a measure of the extent to which the reaction will proceed in the direction A → B under the thermodynamic conditions involved. The points where the difference in free energy equals zero give convenient places of reference, since at such points the equilibrium constant is equal to one. For increasingly negative differences in free energy, the equilibrium is displaced toward the products and for positive differences in free energy, the equilibrium is displaced toward the reactants. The most common conditions under which a reaction takes place are those of constant pressure and constant temperature. The free energy equation 1c under these circumstances becomes equation 2 below.

$$\begin{aligned} \Delta F &= P(V_B - V_A) + (E_B - E_A) - T(S_B - S_A) \quad (a) \\ &= P\Delta V + \Delta E - T\Delta S \quad (b) \qquad (2) \\ &= P\Delta V + \Delta D \quad (c) \end{aligned}$$

Again, whether or not a chemical reaction will take place depends upon the sign of the change in free energy, ΔF. The balance between the various thermodynamic quantities which determine this sign may at times be quite delicate. The possibilities existing with respect to this balance are shown below.

Case I For ΔV positive, ΔD positive:
ΔF is positive everywhere

II For ΔV positive, ΔD negative:
ΔF is negative for $|\Delta D| > |P\Delta V|$

III For ΔF negative, ΔD positive:
ΔF is negative for $|P\Delta V| > |\Delta D$

IV For ΔV negative, ΔD negative:
ΔF is negative everywhere

From the standpoint of utilizing high pressure to bring about a chemical reaction in a condensed system that would not go otherwise, Case III is of primary interest. In such a situation, the positive thermal term ΔD would be larger than the negative mechanical term $P\Delta V$ at low pressures and would establish equilibrium in favor of the reactants. At sufficiently high pressure, however, the $P\Delta V$ term would become significant and favor the formation of the products. This is true in general (for reasonable volume decreases) because of the small effect of pressure on the thermal terms. The internal energy E changes with pressure as shown below. The first term in equation 3 gives the thermal expansion and the second term the compressibility.

$$\left(\frac{\partial E}{\partial P}\right)_T = -T\left(\frac{\partial V}{\partial T}\right)_P - P\left(\frac{\partial V}{\partial P}\right)_T \qquad (3)$$

Since these terms are of the same magnitude and of opposite sign, the change of internal energy with pressure is small.

The effect of pressure on entropy (see equation 4) is generally small.

$$\left(\frac{\partial S}{\partial P}\right)_T = -\left(\frac{\partial V}{\partial T}\right)_P \qquad (4)$$

The effect on potassium should be larger than for any other material. In this case a pressure of 12,000 atm. reduces the entropy by 30%. Pressures of millions of atm. are indicated to cause the entropy to approach zero. These pressure effects on E and S will generally be of the same magnitude for products and reactants and hence will have little effect on the outcome of the reaction providing ΔV is large.

When the change in free energy equals zero ($\Delta F = 0$), equation 2b transforms to equation 5

$$P = \frac{T\Delta S}{\Delta V} - \frac{\Delta E}{\Delta V} \qquad (5)$$

For Case III reactions above, a plot of pressure *versus* temperature would appear as shown in Fig. 3. The slope of the line equals the ratio of the change in entropy to the change in volume and the pressure axis intercept equals the ratio of the change in internal energy to the change in volume. The reaction A → B becomes thermodynamically more favorable in P–T regions above this line, whereas the reverse reaction, B → A, becomes increasingly favorable below the line. Actually, the changes in entropy, volume and internal energy are not constants, but depend on P and T so that the $\Delta F = 0$

line may deviate in either direction from the straight line, as shown by the dashed curves in the figure.

The reaction A = B may be useful or of interest only if the amount of B produced within a given time exceeds a certain minimum. By utilizing the absolute reaction rate theory as developed by Henry Eyring a minimum rate curve may be drawn on a pressure–temperature diagram. Three typical samples of the form taken by this curve for a positive $\Delta V^{\ddagger}$ are shown in Fig. 4. In a P–T region below a curve of Fig. 4, the elementary rate process proceeds faster than the pre-chosen value selected. Above the curve the rate is slower. For negative $\Delta V^{\ddagger}$ the curve on the P–T diagram will have a negative slope and the rate will proceed faster than the pre-chosen value in regions above the curve.[2]

In order to utilize the foregoing equilibrium considerations, it is necessary to have enough actual or estimated thermodynamic information to produce the $\Delta F = 0$ line on the P–T diagram. The rate information will be even more difficult to obtain. In some cases it is possible to obtain rate data on the reverse transformation, B → A. Then, making the assumption that the reaction proceeds in either direction along the same reaction path, it is possible to construct the *minimum rate line*. Figure 5 shows the $\Delta F = 0$ line and *minimum rate line* on the same diagram. In the region of overlap the products will be formed. Prediction of the course of a reaction at high pressure and high temperature is not only handicapped by lack of thermodynamic data for reactants and products, but is handicapped by not knowing what the products might be because the products of high pressure–high temperature experimentation might be substances heretofore unknown. An expression of this idea was recently given by Wentorf in regard to his synthesis of cubic boron nitride.[3] He reputedly said, "Attempting to make this material was like fishing for an unknown fish in an unknown lake." Of course, the making of cubic boron nitride was aided by analog-type reasoning, the analog being the diamond. However, the amount of analog-type reasoning that can be used in the synthesis of new materials is limited. The only course open seems to be one of "going out on a limb" with some unconventional ideas. One possibility is that at extremely high pressures, atoms will be forced into such close proximity that normal electronic configurations are grossly affected. Under such conditions the addition of high temperature and catalysts to the system to overcome activation barriers could lead to the formation of hitherto unknown compounds wherein the chemical bonding would be entirely new. Perhaps these compounds might have some properties that would be superior to those of materials in use today. In general these "new compounds" could be returned to ordinary conditions of pressure and temperature without disruption by reducing the temperature to normal before reducing the pressure. In some instances, rapid temperature quenching may be required.

(2) These considerations are given in detail by the author in the paper, "Chemistry at High Temperature and Pressure," "High-Temperature—a Tool for the Future," published and distributed by Stanford Research Institute, Menlo Park, California, 1956, pp. 161–166.

(3) R. H. Wentorf, Jr., *J. Chem. Phys.*, **26**, 956 (1957).

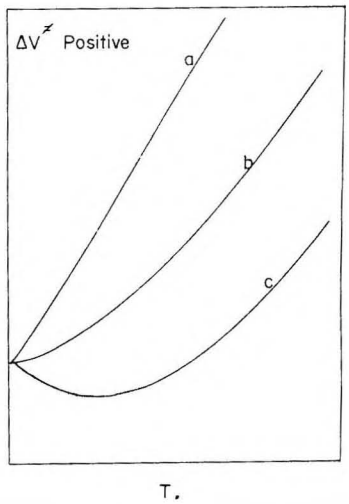

Fig. 4.—Minimum rate curves on P–T diagram for positive volume of activation.

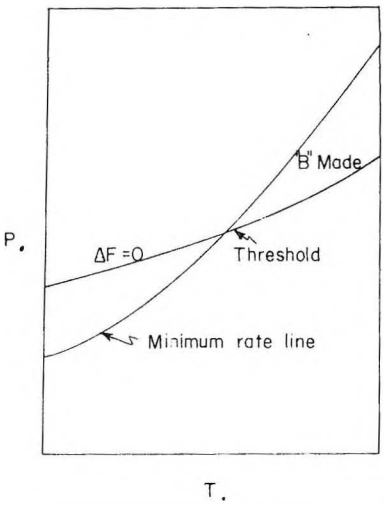

Fig. 5.—Minimum rate line and $\Delta F = 0$ line showing region of overlap where products are made.

The high-temperature bomb described above is loaded at a fixed volume and then high temperature is applied to the system. The bomb will, of course, try to maintain the volume existing at its initial loading. Because the materials of construction are compressible, however, there will be some increase in volume. Nevertheless, constant temperature, constant volume thermodynamics will be most applicable to this situation. Equation 1 shows that, at constant temperature and volume, equation 6 will apply.

$$\Delta F = V\Delta P + \Delta E - T\Delta S \qquad (6)$$

The balance established between the quantities ΔE, ΔP and ΔS will determine whether or not ΔF is negative. It will be important, therefore, to know the effect of temperature on the above quantities. The manner in which the pressure within the bomb changes with temperature is given by equation 7 below.

$$\left(\frac{\partial P}{\partial T}\right)_V = -\left(\frac{\partial V}{\partial T}\right)_P \Big/ \left(\frac{\partial V}{\partial P}\right)_T \qquad (7)$$

The data necessary to make an estimate of the magnitude of $(\partial P/\partial T)_V$ at the temperatures of in-

terest here are non-existent. However, something can be gained from examining data available at low temperature. Bridgman has measured P–V–T relationships for several liquids at temperatures from 0 to 95° and pressures to 12,000 atm.[4] A perusal of his data shows that the pressure generated by confining certain organic liquids to the volume they occupy at 0° and atmospheric pressure followed by heating to 95° will generate a pressure of about 1,200 atm. (This is an average for 30 organic liquids.) On a temperature *versus* pressure plot, curves for these liquids bend toward the temperature axis, indicating that the pressure generated by the temperature tends to fall off at higher temperatures. Mercury is in a different class than the organic liquids. If it is confined to the volume which it occupies at −30° and 1 atm. and then heated at constant volume to 200°, the pressure generated will be 7,000 atm. Curves for these materials cannot be extrapolated with any degree of reliability to temperatures greater than two or three hundred degrees.

Some measure of the pressures attained in the high-temperature bomb have been obtained by increasing the temperature until they explode. A bomb constructed similar to that shown in Fig. 1 except that the inside diameter is 1.5 inches will withstand an internal pressure in the neighborhood of 16,000 atm. Temperatures of 10,000° in the core of this bomb will cause it to burst. For the present, then, the approximate pressure developed within the bomb at 10,000° has been set at 16,000 atm. If, in the reaction A = B, the ratio of thermal expansion to compressibility is less for the products than for the reactants, high temperature will make the $V\Delta P$ component of ΔF more favorable with respect to product formation.

The internal energy of a substance is given by equation 8.

$$E = E_0 + \int_0^T C_v dT + \Sigma E_{\text{latent}} \qquad (8)$$

Other things being equal, the important quantity affecting the change of internal energy with temperature is C_v. If this quantity is smaller for the products than for the reactants (again, other things being equal) at the high temperature, ΔE will be negative and the reaction will be favored.

The entropy of a substance is affected by temperature, as shown below in equation 9.

$$\left(\frac{\partial S}{\partial T}\right)_V = \frac{C_v}{T} \qquad \text{(a)}$$

$$S = S_0 + \int_0^T \frac{C_v}{T} dT + \Sigma \frac{E_{\text{latent}}}{T} \qquad \text{(b)} \qquad (9)$$

Here, as in the case of internal energy, the quantity of importance as temperature is increased is the specific heat at constant volume. The relative change of the quantity TS with temperature will be larger than the change of internal energy E.

Thermodynamic data are not available to make quantitative use of the above relationships at very high temperatures. However, the influence of the various quantities in determining the sign of ΔF can be qualitatively weighed in some instances and the efficacy of the use of the high-temperature bomb in causing a reaction to proceed in the desired direction can be determined. Again, as in the constant P–T situation, the nature of the products that can be formed at high-temperature constant volume may not be known. *A priori*, it seems reasonable to state that "things resistant to heat must be born of heat." Perhaps solid materials could be produced that would remain solid at temperatures considerably above the melting points of the highest melting solids known today (on increasing the temperature of such a material at atmospheric pressure a melting point would not be reached, rather a transition temperature would be reached where the material would transform into its normal form).

At very high temperature and constant volume a process may take place that is reminiscent of that taking place at very high pressures, *i.e.*, electrons seeking empty orbitals closer to the nucleus. When a substance is heated at low pressure a temperature is eventually reached (approx. 7,000°) where ionization begins to take place. If the condensed material being heated is confined to constant volume, ionization of electrons, *i.e.*, electron escape, cannot take place in the usual sense. As an alternative to ionization, sufficiently high temperature could conceivably drive the electrons to occupy unfilled orbitals, thereby changing the ordinary chemistry of the atoms concerned. New chemical compounds might be formed under such conditions and could be "captured" for study at normal room temperature and pressure by rapid thermal quenching.

Up to the present time, the pressure inside the bomb prior to application of heat has been substantially one atm. There are certainly circumstances where it would be desirable to place an initial pressure on the contents of the bomb before increasing the temperature.

A limitation on the maximum pressure obtainable in conventional high-pressure apparatus is imposed by piston failure. Failure occurs because the piston must protrude a short distance from the cylindrical hole into which it is being driven. This leaves an unsupported portion of the piston wherein lies the region of greatest stress. Failure begins here. The maximum pressure obtainable with cemented tungsten carbide pistons is about 50,000 atm. It would be possible to make the piston of such length that at a pressure of 50,000 atm. the top of the piston would be driven flush with the top of the cylindrical hole, thereby eliminating any unsupported surface. The driving ram abutting the top of the piston and the top of the cylinder could now be driven with greater force against these components. The inside arrangement of the cylinder could be made similar to that of the high-temperature bomb. The temperature inside could then be raised to the neighborhood of 10,000° whereupon a pressure of 15,000 atm. or so would be generated from the inside. The total pressure inside would then be near 65,000 atm. The pistons, however, would not fail because there would be no unsupported surface.

Many reactions will proceed rapidly at very high temperature. The rate will depend especially on terms of the type $\exp(-\Delta F^{\ddagger}/RT)$ which means that rates may be appreciable at 10,000° even for

(4) Consult P. W. Bridgman, "The Physics of High Pressure," G. Bell and Sons, London, 1949.

$\Delta F^{\pm}$'s of 100 kcal. This fact ensures the usefulness of a high-temperature device such as that described herein even though the high temperatures can be maintained only for relatively short periods of time.

ACID DISSOCIATION CONSTANTS OF SOME POLYMETHINIUM SALTS[1]

By Seán P. McGlynn

Coates Chemical Laboratories, Louisiana State University, Baton Rouge 3, Louisiana

Received November 13, 1957

The pK_a values of bis-(dimethylamino)-methinium perchlorates of general formula 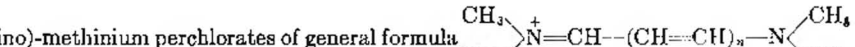 ClO_4^- are evaluated in terms of a resonance capability and an electrostatic energy. The results of the calculations are compared with such experimental data as are available, and the manner in which the resonance energy varies with chain length is discussed critically.

Introduction

The stability of polymethinium salts relative to their conjugate Lewis acids is known to decrease with increasing chain length. This effect was first observed qualitatively by LaMer and Burrows[2] for a series of cyanine dyes, and later verified quantitatively by Dauben and Feniak[3] for a series of linear symmetric polymethines. However, some controversy concerning the theoretical basis for the observed experimental behavior exists in the literature.

The group common to any polymethine series is vinylogous to the amidinium ion and is distinguished by two identical extreme resonance forms, a and b

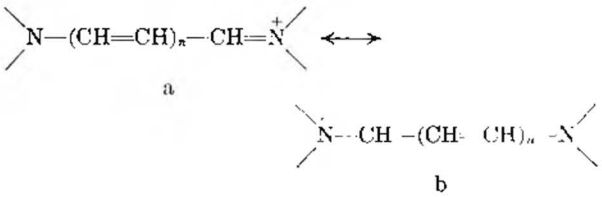

a b

where $n = 0, 1, 2, \ldots\ldots$ In the cyanine dyes each nitrogen atom is so linked that it forms part of a heterocyclic ring, whereas in the linear symmetric polymethines investigated by Dauben and Feniak, each nitrogen is directly attached to two methyl groups. Brooker[2,4] proposed that the decrease of basicity with chain length observed for these dyes was to be attributed to a corresponding decrease in the resonance energy, a $\longleftrightarrow$ b. He based his conclusions on structural considerations wherein proton addition yielding c

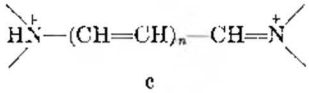

c

presumably led to destruction of the resonance possibility a $\longleftrightarrow$ b, and where ammonium ion type structures were assumed much more stable than those of carbonium type. However, this presumed decrease of resonance energy with increasing chain length has been questioned by some authors,[5] and disagrees with some of the calculations of others.[6] The ambiguities present are inherent, however, in the concept of resonance energy itself. The resonance energy defined by Brooker is a "spectroscopic" entity, while that of the Pullmans is referred as basis to either ethylene, or to the even-alternant with one less nitrogen atom. The conclusions of both sets of authors regarding the manner in which the different resonance energies should vary with chain length are undoubtedly correct; confusion enters only in the manner in which they should be related to pK_a values. This question has been discussed by Moffitt[7] for the amidinium ion, wherein it was shown that any such correlation should rather be concerned with the difference in ground state energies of the polymethinium salt and its conjugate acid.

The purpose of this note is then to present some calculations with a view to computational correlation of theory and such experimental pK_a values as are known, and finally to predict the pK_a values of such polymethinium salts as have not yet been either measured or isolated. It is hoped that some clarification of the confusing topic of resonance energy will result.

Theoretical

The difference in ground state energies of the salt and its conjugate acid can be approximately divided into two parts. These are described separately below.

A. Resonance Energy.—This is the energy difference of the species

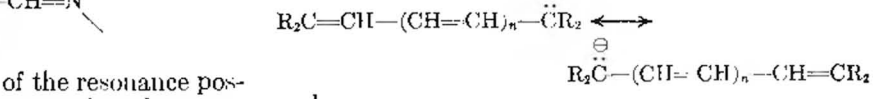

and

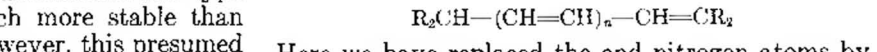

Here we have replaced the end nitrogen atoms by carbon, while at the same time keeping the all-carbon analog isoelectronic with its parent hetero-

(1) This research was done under an Esso Research Project, Contract Number 11-910.

(2) R. E. Burk and O. Grummitt, "Advances in Nuclear Chemistry and Theoretical Organic Chemistry," Interscience Publishers, Inc., New York, N. Y., 1945, p. 102.

(3) G. Feniak, Ph.D. Dissertation, University of Washington, Seattle 5, Wash., 1956.

(4) L. G. S. Brooker, *Rev. Mod. Phys.*, **14**, 275 (1942).

(5) A. Pullman and B. Pullman, *J. chim. phys.*, **46**, 212 (1949); B. Pullman, M. Mayot and G. Berthier, *J. Chem. Phys.*, **18**, 257 (1950).

(6) K. F. Herzfeld and A. L. Sklar, *Rev. Mod. Phys.*, **14**, 294 (1942).

(7) W. E. Moffitt, *Proc. Phys. Soc. (London)*, **63A**, 700 (1950).

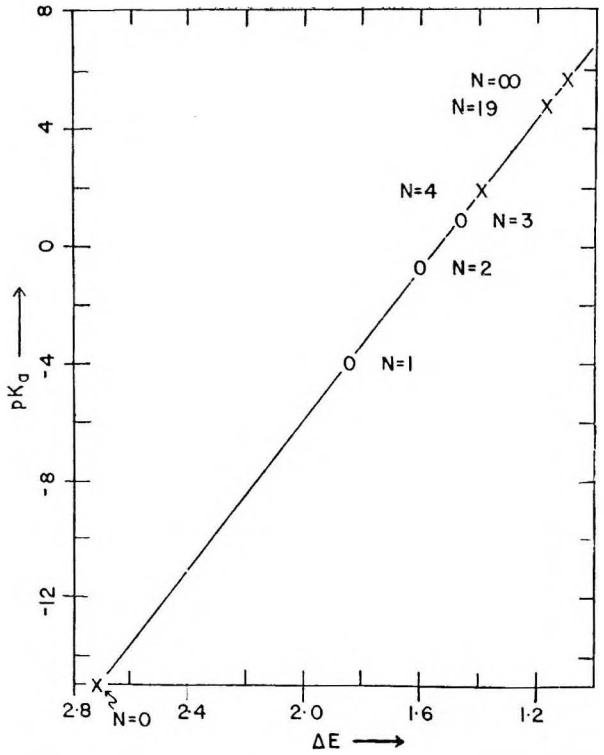

Fig. 1.—Experimental pK_a values are denoted by circles, those predicted are marked by crosses. The capital N of this figure corresponds to the small n of the text. This graph is for the case $D = 3$.

molecule. It is not expected[8] that replacement of nitrogen by carbon will lead to any gross error for molecules of this type, and it simplifies considerably the mathematics to be employed. It is apparent then that this energy difference is the same as the resonance energy of an odd alternant hydrocarbon with respect to the even alternant containing one carbon atom and two valence electrons less.

Simple Hückel theory is used,[9] and a solution of the determinant of order ν

$$\text{Det}(\nu) = \begin{vmatrix} \epsilon-\alpha & \beta & 0 & \cdots & \\ \beta & \epsilon-\alpha & \beta & \cdots & \\ 0 & \beta & \epsilon-\alpha & \cdots & \\ \cdots & \cdots & \cdots & \cdots & \\ 0 & 0 & 0 & \beta & \epsilon-\alpha \end{vmatrix} = 0$$

is required where ϵ is the MO energy, and β and α are the resonance and coulomb integrals, respectively, and where $\nu = 2n + 3$ for the odd alternant and $\nu = 2n + 2$ for the corresponding even alternant. This determinant may be written[10]

$$\text{Det}(\nu) = (-\beta)^{\nu} T_{\nu}\left(\frac{\alpha - \epsilon}{\beta}\right)$$

where $T_{\nu}[(\alpha - \epsilon)/\beta]$ is a Tchebycheff polynomial of the 2nd class, with a solution

$$\epsilon = \alpha + 2\beta \cos \frac{\pi l}{\nu + 1}, \; l = 1,2,3, \ldots, \nu$$

Considering now the species of interest: a π-electron system of $2n + 4$ electrons and $2n + 3$ carbon atoms is converted by protonation to a π-electron conjugation system of $2n + 2$ electrons and $2n + 2$ carbon atoms. The $(n + 1)$th MO (the π-MO for which $l = [\nu - 1]/2$) of the odd alternant is a "non-bonding MO" of energy α, and by summing over MO's the resonance energy is found to be

$$E_r = 2\alpha' + 4\beta \sum_{l=1}^{\frac{\nu-1}{2}} \left(\cos \frac{\pi l}{\nu + 1} - \cos \frac{\pi l}{\nu}\right)$$

where $2\alpha'$ represents the energy difference of two electrons in a σ C–H bond and two electrons in the $(n + 1)$th π-MO of the salt, and may be assumed to remain constant irrespective of the magnitude of n.

E_r may be shown[11] to be an increasing but fairly rapidly converging function of ν; the value of E_r at infinite chain length is given by

$$\begin{aligned} \lim_{\nu \to \infty} E_r &= 2\alpha' + 4\beta \int_0^{\pi/2} \frac{\nu + 1}{\pi} \cos\theta \, d\theta \\ &\quad - 4\beta \int_0^{\pi/2} \frac{\nu}{\pi} \cos\theta' d\theta' \\ &= 2\alpha' + 4\beta/\pi \end{aligned}$$

Accordingly, E_r is determined for all values of ν, but since our theory is based on a linear all-*trans* model for both salt and acid, it is of course restricted in this sense.

B. Electrostatic Energy.—This energy is occasioned by the rather large repulsion of the two positive charges which we presume to be located on the nitrogen atoms of the conjugate acid. The calculation of this quantity is dependent upon a knowledge of the internal dielectric constant, of its variation from place to place within the molecule, and of its change with n. Since any knowledge of such quantities is lacking, it seems best to assume D constant from molecule to molecule and even within a given molecule. This is not a very good assumption,[12] but it is of necessity adopted here.

Again the molecules are assumed to be linear all-*trans* species. All bond distances are set at 1.40 Å. length and all angles at 120°. The repulsive energies are evaluated as e^2/Dr, where D is to be determined by comparison with the pK_a values.

Theory and Experiment

The first interpretation of acid dissociation constants in terms of the resonance possibilities of both protonated and unprotonated forms seems to have been made by Albert and Goldacre.[13] Their conclusions have been verified to a large extent by a quantitative study by Longuet-Higgins[14] using the formula

$$(2.3RT)pK_a = \text{constant} - \Delta E$$

ΔE, for our purposes, is a difference in energy between

(8) S. P. McGlynn and W. T. Simpson, *J. Chem. Phys.*, in press.

(9) The use of Hückel theory for polyenes (*i.e.*, the conjugate acids) may be open to question. See W. T. Simpson, *J. Am. Chem. Soc.*, **77**, 6164 (1955); W. Drenth and E. H. Wiebenga, *Acta Cryst.*, **8**, 755 (1955).

(10) P. Tchebycheff, *Acta Math.*, **12**, 287 (1889); H. Bateman, "Higher Transcendental Functions," Vol. II, Ch. X, McGraw-Hill Book Co., Inc., New York, N. Y., 1953. For an inductive derivation of this formula see J. Lennard-Jones, *Proc. Roy. Soc.* (*London*), **A158**, 280 (1937).

(11) A. Zygmund, "Trigonometrical Series," M. Garasinski, Warsaw-Lwow, Poland, 1935.

(12) F. H. Westheimer and J. G. Kirkwood, *J. Chem. Phys.*, **6**, 506, 513 (1938); **1**, 437 (1939).

(13) A. Albert and R. J. Goldacre, *J. Chem. Soc.*, 454 (1943); 706 (1946); A. Albert, R. J. Goldacre and R. Phillips, *ibid.*, 2240 (1948).

(14) H. C. Longuet-Higgins, *J. Chem. Phys.*, **18**, 275 (1950).

acid and salt and may be written

$$\Delta E = E_r + E_{el} - 2\alpha'$$

where E_r and E_{el} are the resonance and electrostatic energies already defined, and where $2\alpha'$ is incorporated in the constant. The applicability of the above two equations has been discussed[14,15] at some length. Inherent in them is the assumption that the entropies of proton addition to the polymethines should remain constant with n. This is not too optimistic an assumption for the case of linear all-*trans* species, but anyway it cannot be avoided because no entropy data are available.

In Table I are listed the pK_a values of some simple polymethines; also included in the table are E_r, and ΔE and the predicted pK_a values for the illustrative case $D = 3$. Linearity of a plot of pK_a *versus* ΔE obtains within experimental error for any value of D within the range 1–4.5. The value $D = 3$ has been chosen as a mean value and has been used to plot Fig. 1; Fig. 1 has in turn been used to obtain the predicted values of pK_a quoted in Table I. The pK_a values predicted for any value of D in the range 1–4.5 do not differ significantly from those for $D = 3$.

TABLE I

Molecule[a]	Resonance energy, E_r	ΔE (ev.)[b]	pK_a (exp.)[c]	pK_a (theor.)
$n = 0$	$2\alpha' + 0.8284$	2.710	/	−15.0
$n = 1$	$2\alpha' + 0.9920$	1.856	−4.1	/
$n = 2$	$2\alpha' + 1.0676$	1.590	−0.7	/
$n = 3$	$2\alpha' + 1.1104$	1.461	1.0	/
$n = 4$	$2\alpha' + 1.1516$	1.397	/	1.75
:	:	:	:	:
:	:	:	:	:
$n = 19$	$2\alpha' + 1.2344$	1.171	/	4.65
:	:	:	:	:
:	:	:	:	:
$n = \infty$	$2\alpha' + 1.2732$	1.105	/	5.5

[a] Gives the value of n in the general formula $CH_3\diagdown\!\!\diagup N\!-\!(CH\!=\!CH)_n\!-\!CH\!=\!\overset{+}{N}\!\diagdown\!\!\diagup CH_3$ (with CH_3 on the left and CH_3 on the right). [b] With $\beta = 20.0$ kcal./mole and $D = 3$. [c] See reference 2 of text.

The observed trend of pK_a values consists then of the resultant of two parts. The resonance energy of the salt with respect to the conjugate acid increases as n increases, thus leading to a greater stabilization of the salt at larger n-values. Thus if the only operative part were the resonance energy one would expect pK_a to decrease with increasing n. This, however, is the reverse of that observed and is in part responsible for the many obscurities in the literature. The electrostatic repulsion energy in the conjugate acid decreases as n increases, thus leading to a greater stabilization of the salt at the smaller n-values. Both effects together lead to an increasing stabilization of the conjugate acid with increasing chain length, and produce the observed pK_a variation.

The following equilibria also have been measured,[16] and form a very illustrative example, since here there are no gross electrostatic effects operative

$$C_6H_5\overset{+}{N}H\!=\!C(CH_3)\!-\!(CH\!=\!CH)_n\!-\!NHC_6H_5 \longrightarrow C_6H_5N\!=\!C(CH_3)\!-\!(CH\!=\!CH)_n\!-\!NHC_6H_5 + H^+$$

where $n = 0$, 1 and 2. Here the polymethinium salt is now the conjugate acid, whereas formerly it was the base. If we refer to the acid dissociation constants of the polymethinium salts as pK_{a2}, we may call those above pK_{a1}. The resonance energy of the salt with respect to the conjugate base is still given by E_r, and thus increases as n. Accordingly the pK_{a1} values should also increase with chain length. However, the pK_{a1} values exhibit no well-defined trend, although their general tendency is to increase as expected. This development might suggest more experimentation, or perhaps further attests to the limitations of Hückel theory.

It is appropriate at this point to add a cautionary note. If one considers the various assumptions which have been made throughout (*i.e.*, entropy neglect, the use of Hückel theory for polyenes and the existence of a D) it becomes difficult to say with certainty that a resonance energy decrease with chain length is ruled out. This latter however is not the major concern of the present work. On the contrary interest is primarily directed to the fact that the experimental data can be reconciled to an increasing resonance energy if the compensating electrostatic part is made large enough.

The writer wishes to thank Professor W. T. Simpson for many informative discussions and criticisms. He is also grateful to Dr. R. V. Nauman for much help on the matter of dielectric constant behavior.

(15) L. P. Hammett, "Physical Organic Chemistry," McGraw-Hill Book Co., Inc., New York, N. Y., 1940.

(16) G. Schwarzenbach, *Z. Elektrochem.*, **47**, 40 (1941); G. Schwarzenbach and K. Lutz, *Helv. Chim. Acta*, **23**, 1179, 1147, 1163 (1940).

THERMODYNAMIC EVALUATION OF THE INERT PAIR EFFECT[1]

BY RUSSELL S. DRAGO

W. A. Noyes Laboratory of Chemistry, University of Illinois, Urbana, Illinois

Received December 16, 1957

A study of the thermodynamic data for chlorides of the elements of the boron and carbon families has indicated that the instability of thallium(III) chloride and of lead(IV) chloride can be attributed to the fact that in a given family the strength of the covalent bonds formed by these elements decreases as the atomic number of the element increases. It is further shown that Sidgwick's explanation of these stabilities, based on an inert pair of electrons, is not correct. A qualitative, quantum mechanical explanation for this phenomenon is proposed, and possible extensions of this concept are indicated.

Introduction

In contrast to the lighter elements, which usually use all their valence electrons in compound formation, the heavier elements of the boron and carbon families form more stable compounds when two of the valence electrons are not involved in bonding (*e.g.*, TlCl, $PbCl_2$ and $BiCl_3$). To explain this phenomenon, Sidgwick[2] postulated the existence of an "inert pair" of electrons in the heavy elements, thallium, lead and bismuth. Although this explanation is readily invoked to correlate behaviors of these elements,[3] an adequate theoretical explanation has not been advanced. An evaluation of the thermodynamic data pertaining to the stabilities of some of these compounds will be made, and a qualitative quantum mechanical explanation based upon the valence bond approach

(1) Presented at the Sept., 1956, Meeting of the Am. Chem. Soc., Atlantic City, N. J., Division of Chemical Education.

(2) N. V. Sidgwick, *Ann. Reports*, **20**, 120 (1933).

(3) E. S. Gould, "Inorganic Reactions and Structure," Henry Holt and Co., New York, N. Y., 1955, pp. 120, 246.

will be proposed to explain the stability relationships.

Discussion

The currently accepted explanation for the existence of an inert pair was originally proposed by Grimm and Sommerfeld.[4] The inertness in the heavy elements was attributed to stabilization resulting from a completion of the "s" shell of electrons, but more recently it is attributed to stabilization as a consequence of the "Lanthanide Contraction."[5]

If the reluctance of "s" electrons to participate in bond formation is truly a result of stabilization of these electrons, ionization potentials for these elements should indicate that a larger amount of energy is necessary to remove these electrons from the heavier atoms than from the lighter ones. However, from the values of ionization potentials given in Table I,[5] it can be seen that "s" electrons are stabilized to a larger extent for fourth row elements (Ga and Ge) than for sixth row elements (Tl and Pb). Since the inert pair effect is not encountered[2] in the compounds of gallium or germanium, the explanation advanced by Grimm and Sommerfeld that stabilization of "s" electrons occurs is not adequate.

TABLE I

IONIZATION POTENTIALS FOR REMOVAL OF THE "S" ELECTRONS

Element	Energy to remove "s" electrons (e.v.)	Element	Energy to remove "s" electrons (e.v.)	Element	Energy to remove "s" electrons (e.v.)
B	63.1	C	112.3	N	175.3
Al	47.3	Si	78.6	P	116.4
Ga	51.0	Ge	79.6	As	112.4
In	46.9	Sn	69.9	Sb	99.5
Tl	50.0	Pb	74.0	Bi	100.7

Causes for the occurrence of an inert pair can be ascertained by evaluating: (1) the instability of many of the solid compounds of the higher oxidation states of the heavier elements; and (2) the instability in solution of compounds in which the element is in the higher oxidation state.

Stabilities of the Solid Compounds.[6]—The decomposition reaction of the higher-valent halides can be summarized by the general equation

$$MX_n(\text{solid}) = MX_{n-2}(\text{solid}) + X_2(\text{gas}) \qquad (1)$$

where n is the maximum oxidation state of a particular element, and X is a halogen.

One of the first questions to be answered is whether the tendency of the heavy elements to decompose is due to thermodynamic instability or is due to a kinetic instability caused by the compounds of the heavier elements decomposing at an appreciable rate while the compounds of the lighter elements decompose infinitely slowly. As will be seen later, the thermodynamic data parallel the observed trends in stability, and the magnitude of the free energy of the decomposition reaction (equation 1) increases (*i.e.*, becomes more negative) as the atomic number increases in a family of elements. The instability is thus expected from the thermodynamic data and an explanation based on rate considerations is not necessary (see ΔH^0_{298} for equation 1 in Table III).

Any one or any combination of the following factors could result in an increase in the magnitude of the free energy value for equation 1 (*i.e.*, make it more negative) and could account for the decrease in stability of the higher oxidation states of the heavier elements: (1) an increase in the crystal stabilities of the compounds in which the heavier elements are in the lower oxidation state; (2) a decrease in the crystal stabilities of the compounds in which the heavier elements are in the higher oxidation state; (3) a decrease in the bond strength of the compounds of the heavier elements in the higher oxidation state (*i.e.*, MCl_n); (4) an increase in the bond strength of the compounds of the heavier elements in the lower oxidation state (*i.e.*, MCl_{n-2}).

Thermodynamic data are available (see Table II) to permit an evaluation of all four of these effects[7] and thus to ascertain the major cause of the observed stability relationships.

An explanation of the observed stabilities based on factors 1 and 2 would attribute the stability differences to crystal lattice effects. The standard heats of sublimation for the chloride compounds (Table II) indicate that these effects are of some importance in determining the standard free energies of equation 1; however, these effects are not large enough to account for the entire energy differences, and in many instances crystal lattice energies have almost no part in accounting for the observed stabilities. For example, the heats of formation (Table III) indicate that solid $GaCl_3$ is more stable than solid $TlCl_3$ with respect to decomposition into the monochloride by 68.5 kcal./mole (see ΔH^0 equation 1); however, the heats of sublimation indicate similar crystal lattice stabilities for these compounds. Also, it is very unlikely that the observed trends in stability for all the solid compounds of the elements of the boron, carbon or nitrogen families could be accounted for simply on the basis of crystal stabilities. The trends in bond energies (factors 3 and 4) may be of much greater general applicability in explaining many of the phenomena attributed to the inert pair.

The standard heats of reaction (2) can be used as a relative measure of the bond strengths of the chloride compounds of the elements in the highest oxidation state (factor 3)

(4) H. G. Grimm and A. Sommerfeld, *Z. Physik.*, **36**, 36 (1926).

(5) T. Moeller, "Inorganic Chemistry," John Wiley and Sons, Inc., New York, N. Y., 1952, p. 156.

(6) The evaluation will be limited to the chlorides of the elements of the boron and carbon families, for in other instances, sufficient thermodynamic data have not been reported.

(7) The sum of these terms is related to the standard free energy (ΔF^0) for equation 1 by the expression

$$\Delta F^0 = \Delta H^0 - T\Delta S^0$$

where T refers to the absolute temperature and S^0 refers to the standard entropy. In the comparison of the relative stabilities of the chloride compounds of any one family of elements, it will be assumed that the entropy effects can be neglected. The limited entropy data which are available are in accord with this assumption. Thus, an attempt will be made to correlate the trends in stabilities (*i.e.*, free energies) with the standard heats associated with the four factors listed above. Since, as it will be seen shortly (see Table III, eq. 1 such a correlation can be made, the assumption that the entropy can be neglected seems to be valid.

TABLE II

STANDARD HEATS OF FORMATION AND SUBLIMATION (KCAL./MOLE)

Compd. and state	ΔH^0_{298} formation	Ref.	ΔH^0_{298} sublimation ΔH^0_{298} evaporation	Ref.
BCl(g)	25.6	8	..	..
AlCl(g)	− 4.9	8	45	9
GaCl(g)	+ 9	8	..	..
InCl(g)	− 18	8	26.5	8
TlCl(g)	− 16	8	32.3	10
BCl_3(g)	− 94.5	8	..	..
$AlCl_3$(s)	−166.2	8	28	9, 12
$GaCl_3$(s)	−125.4	8	(19)	8
$InCl_3$(s)	−128.4	8	(39)	10
$TlCl_3$(s)[a]	− 83.9	8	(19)	13
$SnCl_2$(s)	− 83.6	8	(29)	10
$PbCl_2$(s)	− 85.9	8	44.3	10
CCl_4(g)	− 25.5	8	..	..
$SiCl_4$(g)	−145.7	8	..	..
$GeCl_4$(l)	−130	8	7.9(ΔHe^0)	8
$SnCl_4$(l)	−130.3	8	8.3(ΔHe^0)	8
$PbCl_4$(l)	− 78.85	14	9.0(ΔHe^0)	[b]
C			171.7	15
Si			88.04	15
Ge			78.44	15
Sn			72	15
Pb			46.34	15
PCl_3(g)	− 72.2	8	(8.8)	10
$AsCl_3$(g)	− 71.5	8	(11.1)	10
$SbCl_3$(g)	− 75.2	8	16.1	8
$BiCl_3$(g)	− 64.7	8	26.1	8
PCl_5(g)	− 95.3	8	(15)	11
$SbCl_5$(g)	− 93.9	8	14.1	10

[a] Klemm[13] indicates that the heats of sublimation of $TlCl_3$ and $GaCl_3$ are about the same order of magnitude. The ( ) indicate estimated values for the heats of sublimation at 25° from values at other temperatures. These values are probably correct to ±4 kcal. and since this evaluation is concerned with orders of magnitude larger than this, this accuracy will suffice. [b] Estimated by assuming Trouton's constant is 22 and employing the reported boiling point of 137°.[10]

TABLE III

STANDARD HEATS ($-\Delta H^0_{298}$) OF IMPORTANCE IN EVALUATING THE STABILITIES OF THE SOLID CHLORIDES

	$-\Delta H^0_{298}$ (kcal.)			
Element M	Eq. 1 $MCl_{n(s)} \rightarrow MCl_{(n-2)(s)} + Cl_2$	Eq. 2 $M(g) + n/2\ Cl_2(g) \rightarrow MCl_n(g)$	Eq. 6 $MCl_{(n-2)(g)} + Cl_2(g) \rightarrow MCl_n(g)$	Eq. 9 $M(g) + (n-2)/2Cl_2 \rightarrow MCl_{(n-2)}(g)$
B		191.7	120.1	71.6
Al	161.3	213.2	133.3	79.9
Ga	134.3	172.4	115.4	57.0
In	110.4	147.6	71.4	76.2
Tl	67.9	109.4	48.9	60.5
C		197.2		
Si		233.7		
Ge		200.3		
Sn	46.7	192.7	65.7	127
Pb	−5.0	115.2	27.3	87.9

(8) U. S. Bureau of Standards, "Selected Values of Chemical Thermodynamic Properties," Circular 500, 1949.

(9) F. Irmann, *Helv. Chim. Acta*, **33**, 1449 (1950).

(10) Kubaschewski and Evans, "Metallurgical Thermochemistry," 2nd ed., John Wiley and Sons, Inc., New York, N. Y., 1956.

(11) L. L. Quill, "Chemistry and Metallurgy of Miscellaneous Materials: Thermodynamics," McGraw-Hill Book Co., Inc., New York, N. Y., 1950.

(12) W. Fischer and O. Rahlfs, *Z. anorg. Chem.*, **205**, 1 (1932).

$$M(\text{gas}) + \frac{n}{2}\,Cl_2(\text{gas}) = MCl_n(\text{gas}) \qquad (2)$$

The standard heats calculated[16] for reaction 2 are listed in Table III along with values for other changes that are to be discussed shortly. With the exception of the compounds of the second row elements, the values indicate a decrease in the strengths of the bonds holding the atoms together as the atomic number of the central atom increases within a family. Since the electronegativities of the last three elements in any one family are approximately constant,[17] the ionic character is roughly constant, and the decrease in bond energy can be attributed to decrease in the strength of the covalent bonds holding the molecule together. Thus, an important factor causing the instability of thallium trichloride can be attributed to a decrease in the strength of the covalent bonds between the thallium and chlorine.

The difference in bond strength of the chlorides in the maximum oxidation state relative to the bond strength of the chlorides with an oxidation state of two less (*i.e.*, factors 3 and 4) can be obtained by considering the standard heat of the reaction (see Table III)

$$MCl_{n-2}(\text{gas}) + Cl_2(\text{gas}) = MCl_n(\text{gas}) \qquad (6)$$

Since the reverse of equation 6 represents the most common decomposition reaction of the higher-valent halides, and since lattice energies are not involved in this reaction, the values of ΔH^0 obtained are a true measure of the relative bond strengths in the two oxidation states of the metal. The values of ΔH^0 at 25° for this reaction can be calculated from the difference in the standard heats[18] pertaining to the reactions

$$M(\text{solid}) + \frac{n}{2}\,Cl_2(\text{gas}) = MCl_n(\text{gas}) \qquad (7)$$

$$M(\text{solid}) + \frac{n-2}{2}\,Cl_2(\text{gas}) = MCl_{n-2}(\text{gas}) \qquad (8)$$

Comparison of ΔH^0_{298} corresponding to equations 2 and 6 (see Table III) indicate that the instability of thallium(III) and lead(IV) chlorides is due to a decrease in covalent bond strength in these compounds; thus, of the four factors listed above, the

(13) W. Klemm, *Z. physik. Chem.*, **B12**, 17 (1931).

(14) F. Ya. Kulba, *J. Gen. Chem., U.S.S.R.*, **24**, 1677 (1954), Engl. Translation.

(15) W. M. Latimer, "Oxidation Potentials," 2nd ed., Prentice-Hall, Inc., New York, N. Y., 1952.

(16) The values for the standard heats, at 25°, of the gas phase reaction 2 can be calculated by the addition of the standard heats (at 25°) which refer to the general equations 3, 4 and 5.

$$M(s) + n/2\ Cl_2(g) \rightarrow MCl_n(s) \qquad (3)$$

$$MCl_n(s) \rightarrow MCl_n(g) \qquad (4)$$

$$M(g) \rightarrow M(s) \qquad (5)$$

The ΔH^0 values corresponding to equation 3 (the heats of formation of the solid chlorides) and equation 4 (the heats of sublimation of the solid chlorides) are contained in Table II. The ΔH^0 values for equation 5 can be obtained by multiplying the values for the heats of sublimation of the metals contained in Table II by −1. In those instances where the compounds concerned are liquids, the heats of evaporation are employed in step 4 of these calculations.

(17) H. O. Pritchard and H. A. Skinner, *Chem. Revs.*, **55**, 745 (1955).

(18) The ΔH^0_{298} values for equations 7 and 8 can be calculated from the data on the heats of formation and sublimation contained in Table II.

most important cause for the inert pair effect is factor 3.[19]

Since an important factor leading to instability of thallium(III) and lead(IV) chlorides has been identified, a reason for this instability can be proposed. Consideration of the hybrid bond types involved in the formation of these molecules and of the energy requirements of each type reveals the reason these molecules should be unstable with respect to decomposition into molecules that utilize two less valency electrons in bond formation. These considerations permit an extension of the information concerning the chlorides to other compounds of these elements.

Correlation between Bond Type and Stability.—The covalent contribution to the bonding for the elements of the boron family in the trivalent state can be described as due to "sp^2" hybrid bonds, while the bonding in the monovalent state probably involves only the "p" electron. The covalent bonding in the tetravalent compounds of the carbon family can be described as "sp^3," while the bonding in the dihalides involves only the "p^2" electrons. The standard heat corresponding to equation 2 can be considered as the resultant energy of the following steps

For the boron family elements

$$M(s^2p)(gas) \longrightarrow M(sp^2)(gas) \quad (10a)$$

$$M(sp^2)(gas) + \frac{3}{2}Cl_2 \longrightarrow MCl_3(sp^2)(gas) \quad (11a)$$

For the carbon family elements

$$M(s^2p^2)(gas) \longrightarrow M(sp^3)(gas) \quad (10b)$$

$$M(sp^3)(gas) + 2Cl_2(gas) \longrightarrow MCl_4(sp^3)(gas) \quad (11b)$$

From these reactions, it can be seen that ΔH^0 for equations 10a and 10b is the promotion energy involved in the hybridization of orbitals, and is an indication of the stabilization of the "s" electron relative to its promotion to the "p" orbital. ΔH^0 for equations 11a and 11b is the "bond forming ability" of the activated element. If ΔH^0 associated with reaction 10 is large, or if ΔH^0 associated with reaction 11 is small, compounds in the high oxidation state will become less stable and the elements will react by utilizing only the "p" electrons in bond formation. Because it is possible to calculate the promotion energy from reported spectral data on electronic transition in the atomic energy levels of the elements,[20,21] and because the bond forming ability can be determined by subtracting the promotion energy from the ΔH^0 values corresponding to equation 2, it is possible to decide which of these effects is of greater significance in causing the instability observed in the compounds of the heavier elements. The following values[22] were calculated for equations 10a and 11a

Element M[22]	ΔH^0_{298} kcal., eq. 10a $M(g)\ s^2p \rightarrow M(g)\ sp^2$	ΔH^0_{298} kcal., eq. 11a $M(g)\ sp^2 + \frac{3}{2}Cl_2 \rightarrow MCl_{3sp^2}(g)$
Al	83.67	−296.9
Ga	109.5	−281.9
In	100.8	−248.4
Tl	108	−217.4

The data indicate that the instability of thallium(III) and lead(IV) compounds can be attributed to a decrease in the covalent bond forming ability of thallium and lead (11a and b). For example: The difference in covalent bond forming ability (equation 11a) of the elements thallium and gallium is 64.5 kcal. while the ΔH^0_{298} for decomposition of solid gallium III chloride into the monochloride is 68.5 kcal. more negative than for the corresponding thallium compounds. In general, if the elements in the boron and carbon families can undergo chemical reactions and form strong enough covalent bonds (11a and b) to supply the energy for promotion (10a and b) and have enough energy in excess to make the magnitude of the free energy large, a stable compound utilizing all the valency electrons in bond formation will result. When weak covalent bonds are formed, as is the case for thallium(III) and lead(IV) chlorides, a lower energy state can be attained by the system by utilizing only the "p" electrons in compound formation. In this case, two less electrons will be involved in bond formation, and we observe the stability relationship attributed to the inert pair.

The decrease in covalent bond forming ability of these elements as the atomic number increases can be attributed to the following effects: (1) The radial part of the bond orbitals is changing in such a manner as to indicate a spread of the valence electrons over a larger area,[23] resulting in less overlap and weaker covalent bonding. (2) The number of inner shell electrons increases and the coulombic repulsion between these electrons and the inner electrons of the other bonded atoms increases.[24]

Although the thermodynamic data which would permit an evaluation for the compounds of the elements of the nitrogen family have not been obtained, it would be expected that similar effects will account for the observed stabilities of the compounds of these elements.

Stabilities in Solution.—The standard electrode potentials, E^0, for the boron and carbon family elements indicate decreased stability in solution of the high oxidation state of the heavy elements.

(19) The data pertaining to equation 9 indicate that the instability of gallium(I) chloride results in a large negative ΔH^0 value

$$M(g) + n - 2/2Cl_2(g) \longrightarrow MCl(m-2)(g) \quad (9)$$

for equation 6 and indicates the importance of factor 4 in explaining why the inert pair was reported not to occur in this compound. Similarly, on the basis of the heats of formation one would expect tin(IV) chloride to be nearly as stable as germanium(IV) chloride (see Table III, ΔH^0 for equation 2). The greater stability observed for germanium(IV) than for tin(IV) (equation 6) is probably due to the instability of germanium(II) relative to tin(II) chloride.

(20) C. E. Moore, "Atomic Energy Levels, Circular 467," National Bureau of Standards, Volumes I and II.

(21) Backer and Goudsmit, "Atomic Energy States," McGraw-Hill Book Co., Inc., New York, N. Y., 1932.

(22) The spectral data which are necessary for the calculation of the promotion energies for thallium and for the elements of the carbon family (other than carbon) have not been reported. The value of thallium was estimated from a derived relationship between the second ionization potential of gallium and indium and the promotion energies of these atoms. In the case of the elements of the carbon family it will be assumed that since the third ionization potentials are nearly the same, the promotion energies probably also are. These assumptions are very crude and more experimental work is required before a more reliable decision can be made.

(23) L. Pauling, THIS JOURNAL, **58**, 662 (1954).

(24) C. A. Coulson, "Valence," Oxford University Press, New York, N. Y., 1952, pp. 177–178.

For the carbon and nitrogen family elements, the E^0 parallels the stability of the oxides formed. The factors affecting the E^0's of the boron family elements can be evaluated by a process analogous to that employed by Latimer.[15] The over-all reaction can be divided into the following energy steps and ΔH^0_{298} for each step can be calculated from data contained in the literature.[15]

Eq. describing the energy step [25]		H^0_{298} (kcal.) Al	Ga	In	Tl
(12)	$M(s) \rightarrow M(g)$	75.0	66	58.2	44.5
(13)	$M(g) \rightarrow M^{+3}(g) + 3e^-$	1232.4	1322.5	1219.3	1303.6
(14)	$M^{+3}(g) \rightarrow M^{+3}(aq)$	−1432.8	−1438.9	−1309.5	−1301.3
(15)	$M(s) \rightarrow M^{+3}(aq) + 3e^-$	− 125.4	− 50.4	− 32.0	+ 45.8

Comparison of the above data pertaining to indium and thallium indicate that indium(III) is more stable because of the lower energy required to remove the three electrons, *i.e.*, step 13. The greater stability of gallium(III) as compared with thallium(III) can be attributed to the higher solvation energy of gallium(III) (step 14). Thus, both of these factors must be considered in order to explain the stability relationships of these ions in solution. Since the nature of the species represented by $M^{+3}(aq)$ is not known, it is not possible to give a quantum mechanical explanation for the stabilities in solution. It would also be of greater consequence to evaluate the stability of the trivalent ions relative to the monovalent ions but the necessary data are lacking for boron, aluminum and gallium.

Extensions of These Concepts.—The decrease in covalent bond forming ability with increase in atomic number is probably the principal cause for the instability of not only the chlorides, but also for most of the unstable compounds of lead and thallium. It is proposed that this factor is the main cause for the stability relationships attributed to the inert pair.

Since the bonding in the compounds thallium(III) methyl and thallium(III) fluoride is stronger than that in thallium(III) chloride, one would expect greater stability for these compounds. Coördination of thallium(III) chloride with strong Lewis bases might also enhance the stability of this compound by formation of stronger hybrid bond types.

Many of the stereochemical observations that have been attributed to the inert pair can be explained on the basis of the above proposal. If the covalent bond strength of the compound under consideration is large, there will probably be a large amount of "s" character in the bonds and the unshared electron pair will occupy a hybrid orbital having directional character. If the covalent bond strength is weak, then the lowest energy state will be obtained by keeping the electron pair in the nondirectional "s" orbit and a stereochemically inactive, inert pair will result. Thus, although the interatomic distances in the ion $SeBr_6^=$ are explained[26] by assuming inertness of the 4s electrons and use of $4p^34d^25s$ hybrid bonds, the molecule $Se(C_6H_5)_2Br_2$ has a structure in which the four bonds are directed toward four of the five apices of a trigonal bipyramid, one equatorial position being occupied by the stereochemically active pair of unshared electrons in a hybrid orbital.[26] The difference can now be explained by assuming the existance of stronger covalent bonds in $Se(C_6H_5)_2Br_2$.

Acknowledgment.—The author wishes to express his thanks to his fellow staff members and to Mr. Laurence Dempsey at the University of Illinois for their helpful suggestions regarding the preparation of this manuscript.

(25) Step 12 represents the heat of sublimation of the metal; step 13 is the sum of the energies of the first three ionization potentials; step 14 represents the heat of hydration of the gaseous ion, and, the sum of these three energies (step 15) represents the standard heat of the over-all reaction. It is indicated that steps 12 and 13 are endothermic while step 14 is exothermic. Since the values of ΔH^0_{298} parallel the values for the E^0's, the entropy charge can be considered to be nearly constant.

(26) L. Pauling, "Nature of the Chemical Bond," 2nd Ed. Cornell University Press, Ithaca, N. Y., 1948, p. 184.

NOTES

LIABILITY OF Cr(IV) TO SUBSTITUTION

BY ALLEN E. OGARD AND HENRY TAUBE

Contribution from the George Herbert Jones Laboratory, University of Chicago, Chicago 37, Ill.

Received August 26, 1957

We have studied the dissociation of $CrCl^{++}$ in acid solution as it is induced by 1 e^- oxidizing agents. The particular oxidizing agent used was Mn^{+++}, prepared *in situ* by oxidizing Mn^{++} with Ce(IV) or Co^{+++}. The dissociation is induced also by Ce(IV) or Co^{+++} alone, but the kinetic analysis of these systems is more difficult because the inducing agent is much more rapidly consumed than is the case when Mn^{+++} is used.

The rate of dissociation was followed spectrophotometrically and specific rates were calculated from the initial changes in optical density (OD). The curvature in a plot of $(CrCl^{++})$ *vs.* time (the curvature being attributable to slow consumption of Mn^{+3}) is slight enough so that the initial specific rates could be fixed reasonably well.

Experimental

Of the materials used, only the preparation of $CrCl^{++}_{aq}$ merits detailed description. Green $CrCl_3 \cdot 6H_2O$ is dissolved in 0.05 *M* $HClO_4$, and after remaining for *ca.* 12 hr. to permit $CrCl_2^+$ to dissociate, the solution is passed through a cation-exchange resin (Dowex 50-X4 was used). Ions such as $CrCl_2^+$ are eluted by washing with 0.15 *M* $HClO_4$, and $CrCl^{++}$ aq is brought through by washing with 1 *M* $HClO_4$.

This treatment leaves behind any Cr^{+++} which has been formed on the resin.

A typical experiment is reported in Table I. A plot of $\log(OD_t - OD_\infty)$ against time shows that at 90 min., which corresponds to the time at which reaction has proceeded half way to equilibrium, the specific rate is about 15% less than the initial value. Other sources of error, an important one of which is believed to be the difficulty of working with Mn^{+3} at concentrations far in excess of the equilibrium values (considering here the disproportionation to $Mn^{++} + MnO_2$), are more serious than that of fixing the initial specific rate from the data.

TABLE I

REPORT OF A TYPICAL EXPERIMENT

(Temp. 25 ± 1°; μ = 1.5; (H^+) = 1.0 OD_∞ = 0.080; the experiment is the first one in Table II)

Time, min.	$(OD_t - OD_\infty)$	Time, min.	$(OD_t - OD_\infty)$
2.3	0.120	69.5	0.070
5	.117	76	.067
10	.112	82	.064
16.5	.107	89	.061
21.3	.103	100	.057
30	.095	106	.055
39	.089	116	.052
42.5	.086	127	.047
49	.082	145	.043
58.3	.076	155	.041
		164	.039

TABLE II

DISSOCIATION OF $CrCl^{++}$ CATALYZED BY Mn^{+3}

t = 25 ± 1°, μ = 1.5, H^+ = 1.0 M except in expt. 10.

$(CrCl^{++})$ × 10²	(Cr^{+3}) × 10²	$(Mn^{+3})_0$ × 10²	(Co^{+3}) × 10⁴	(Cl^-) × 10²	$t_{1/2}$, min.	k_1, min.$^{-1}$
2.5	1.0	4.0	3.0	2.0	85	27.2
5.0	1.0	4.0	3.0	2.0	80	28.9
2.5	4.0	4.0	3.0	2.0	75	30.8
5.0	1.0	8.0	3.0	2.0	83	27.8
2 5	1.0	4.0	3.0	8.0	76	30.6
2.5	1.0	1.0	3.0	2.0	76	30.5
5.0	1.0	2.0	1.5	4.0	195	23.7
7.5	1.0	8.0	6.0	10.0	42	27.5
7.5	0.5	1.0	1.5	1.0	170	27.0
2.5	1.0	4.0	3.0	2.0	47	24.6[a]
2.5	1.0	4.0	3.0[b]	2.0	104	22.0
5.0	1.0	.25	1.0	2.0	150	15
5.0	1.0	.125	1.0	2.0	290	7.6

Av. (excluding last two) 27.3 ± 2 l. mole^{-1} min.$^{-1}$

[a] 0.5 M H^+ instead of 1.0 M H^+, $NaClO_4$ used to adjust ionic strength. [b] Ce(IV) used as the oxidizing agent in place of Co^{+3}.

A report of the experiments, except for preliminary ones, appears in Table II. The rate law used in calculating the specific rates was

$$\frac{-d(GCl^+)}{dt} = \frac{k(CrCl^+)(Mn^+)}{(H^+)}$$

The data are seen to conform to this rate law reasonably well over a considerable variation in initial $(CrCl^{++})$, (Cr^{++}), (Mn^{++}), (Mn^{+++}) (the last as determined by the Co^{+++} added.) The variation with (H^+) was least adequately tested, but the results suffice to show that in the acid range studied the term inverse in (H^+) is the dominant one in the rate law. The substantial agreement obtained when Ce(IV) is substituted for Co^{+++} (this agreement was even better in preliminary experiment in which a higher concentration of Mn^{++} was used) shows that the process is not a sole property of either oxidizing agent, and supports the view that those reagents serve, for the most part, merely to generate Mn^{+++}. The lower value observed with Ce(IV) can be attributed to this, that Ce(IV) is consumed more rapidly by Cr(III) than is Co^{+++}.

A mechanism which fits the data is

$$Mn^{+3} + CrCl^{++} \longrightarrow Cr(IV)\text{–}Cl^- + Mn^{+2} \text{ slow}$$
$$Cr(IV)\text{–}Cl^- = Cr(IV) + Cl^- \text{ (very rapid)}$$
$$Cr(IV) + Mn^{++} = Cr^{+++} + Mn^{+3} \text{ (rapid)}$$

To fit the observed kinetics and to be in accord with the estimates of the Cr^{+++}–Cr(IV) potential,[1] the ratio of $(Cr(IV))/(Mn^{+++})$ at the steady state must be very small. Thus the dissociation of the $Cr^{(IV)}$–Cl^- complex must take place very rapidly, at any rate more rapidly than the reaction of Cr(IV) with Mn^{++}, which itself must be rapid indeed. The high substitution lability of Cr(IV) is expected in view of its electronic structure, and is suggested also by the exchange of $Cr(H_2O)_6^{+++}$ with H_2O, as it is induced by Ce(IV).[2]

An alternative view is that Cl is transferred from $CrCl^{++}$ to Mn^{+++} during the reaction. If this is so, it represents a most unusual situation in which an electronegative group moves from reducing agent to oxidizing agent on electron transfer. While such a process is not impossible, there appears to be no particular reason why it should operate in this case; the substitution lability of Mn^{++} is certainly great, perhaps greater than for Cr(IV). This alternative mechanism is contra-indicated also by the fact that the activated complex for reaction contains also OH^-. Presumably this ion, rather than Cl^-, serves as bridging group in this reaction.

An experiment also was done using $(NH_3)_5CrCl^{++}$ in place of $CrCl^{++}$ (= $(H_2O)_5CrCl^{++}$). The induced dissociation with the ammino complex also proceeds, but at a slower rate, less by a factor of perhaps 25 in 1 M acid. The comparison lends some support to the view that when $(H_2O)_5CrCl^{++}$ is reactant, attack by Mn^{+++} is at an oxygen rather than at Cl.

It is interesting, and to us was disappointing to note that no kinetic evidence appeared in the work for the dissociation of $CrCl^{++}$ catalyzed by Cr(IV), as for example

$$Cr(IV) + CrCl^{++} \longrightarrow Cr^{+++} + Cr(IV) + Cl^-$$

Such a reaction is certainly possible, but its rate is apparently much less than that of Cr(IV) with Mn^{++}.

Acknowledgment.—This work was supported by the Atomic Energy Commission under contract AT (11-1)-378. Fellowship support for A. E. O. by the National Science Foundation, United States Rubber Co., and the du Pont Company is also gratefully acknowledged.

(1) F. H. Westheimer, *Chem. Revs.*, **45**, 419 (1948).
(2) R. A. Plane and H. Taube, THIS JOURNAL, **56**, 33 (1952).

THE SOLUBILITY OF *cis*- AND *trans*-DINITROTETRAMMINECOBALT(III) SULFATES IN MIXTURES OF WATER WITH ETHANOL AND WITH ACETONE

BY H. LAWRENCE CLEVER AND FRANK H. VERHOEK

McPherson Chemical Laboratory, The Ohio State University, Columbus 10, Ohio

Received September 9, 1957

This paper reports the results of a study of the change of solubility of the sulfates of *cis*- and *trans*-dinitrotetramminecobalt(III) ions as the dielectric constant of the solvent is changed by adding ethanol to water, and by adding acetone to water. The procedure and analytical method were as described by Mayper, Clever and Verhoek.[1] Measurements were made at 15 and 25°. The solubility data were corrected to zero ionic strength, using the Debye–Hückel limiting law, and the logarithms

(1) S. A. Mayper, H. L. Clever and F. H. Verhoek, THIS JOURNAL, **58**, 90 (1954).

TABLE I

ΔF^0, ΔH^0 AND ΔS^0 FOR THE SOLUTION OF *cis*- AND *trans*-DINITROTETRAMMINECOBALT(III) SULFATES IN MIXED SOLVENTS

Wt. %	Ethanol: Dielectric constant	Ethanol: ΔF^0_{298} (kcal.)	Ethanol: ΔH_0 (kcal.)	Ethanol: ΔS^0_{298} (e.u.)	Acetone: Dielectric constant	Acetone: ΔF^0_{298} (kcal.)	Acetone: ΔH_0 (kcal.)	Acetone: ΔS^0_{298} (e.u.)
				cis				
0	78.5	9.6	18.7	31	78.5	9.6	18.7	31
10	72.8	10.9	22.1	38	73.0	10.5	19.9	31
20	67.0	12.2	23.4	37	67.0	11.5	21.3	33
30	61.1	13.6	22.7	31	61.0	12.5	18.8	21
				trans				
0	78.5	10.2	16.4	21	78.5	10.2	16.4	21
10	72.8	11.6	19.1	25	73.0	11.4	17.9	22
20	67.0	12.9	22.3	32	67.0	12.5	21.7	31
30	61.1	14.4	22.4	27	61.1	13.8	23.4	32

of the corrected solubilities[2] are plotted against the reciprocal of the dielectric constant in Fig. 1, for 25°. Included on the plot is a point for the *trans* sulfate in 39.0% ethanol obtained by Hansen and Williams,[3] and the plot for dioxane–water.[1] Curves are obtained instead of the straight lines predicted by the Born equation.[4] This equation would interpret the differences in the three solvents in terms of a decreasing ionic radius in the order dioxane–water > acetone–water > ethanol–water, but the data would require a radius of the order of 1 Å. for the last two solvent pairs.

In Table I are given the values of ΔF^0 at 25° for the solution process, calculated from interpolated data for even 10% intervals at zero ionic strength, and of the less precise quantities ΔH^0 and ΔS^0, using the two temperatures. Comparison of these values with those for dioxane–water[1] shows that ΔS^0 tends to increase with decreasing dielectric constant, particularly in ethanol–water, with indications of a maximum, whereas in dioxane–water there is at first a decrease, followed by an increase at a lower dielectric constant. Again the entropy increase is, in the main, smaller for the salt of the *trans* than for that of the unsymmetrical *cis* ion. One might expect the opposite to be true, since the unsymmetrical ion would be expected to interact more strongly with the solvent. However, if the stronger interaction leads to a greater loosening of the *quasi*-crystalline structure of the solvent, the greater entropy increase would result for the *cis* salt. In the earlier paper[1] the discussion of this interaction was confused due to a misreading of the sign of the entropy change. Alternatively, the dissolved state may not be too dissimilar for the two ions, but the entropy of the solid may be less for the *cis* than for the *trans* salt. As in the dioxane–water system, ΔH^0 in ethanol–water and acetone–water is again positive; it increases with decreasing dielectric constant, perhaps with a maximum, and it has about the same value for both salts.

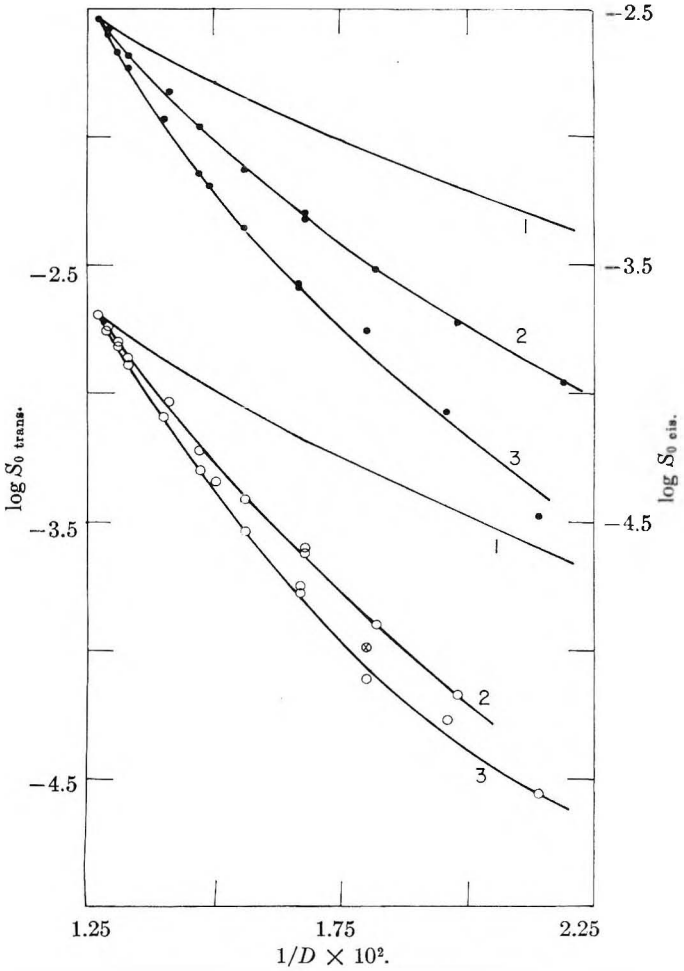

Fig. 1.—Solubilities of dinitrotetramminecobalt(III) sulfates in mixed solvents; upper 3 curves and scale at right, *cis;* lower 3 curves and scale at left, *trans*. Curves 1, dioxane–water (ref. 1); Curves 2, acetone–water; Curves 3, ethanol–water.

(2) The original data have been deposited as Document No. 5320 with the ADI Auxiliary Publications Project, Photoduplication Service, Library of Congress, Washington, D. C., U.S.A. A copy may be secured by citing the document number and by remitting $1.25 for photoprints, or $1.25 for 35 mm. microfilm, in advance by check or money order, payable to Chief, Photoduplication Service, Library of Congress.

(3) L. A. Hansen and J. W. Williams, *J. Am. Chem. Soc.*, **52**, 275 (1930).

(4) M. Born, *Z. Physik*, **1**, 45 (1920).

STABILITY OF NITRIC OXIDE OVER A LONG TIME INTERVAL

BY CHARLES S. HOWARD AND FARRINGTON DANIELS

Department of Chemistry, Worcester Polytechnic Institute, Worcester Mass., and the University of Wisconsin Chemistry Department, Madison 6, Wis.

Received September 9, 1957

Nitric oxide is thermodynamically unstable at room temperature and should decompose according to the reaction

$$2NO = N_2 + O_2$$

However, it is kinetically stable because the rate of decomposition is so very slow. Nitric oxide is colorless, but when an appreciable amount decomposes, the oxygen, produced by the decomposition, combines with the nitric oxide to give nitrogen dioxide which can be detected visually by its brown color. It is thus possible to study qualitatively the rate of this reaction with extremely simple equipment.

Nearly forty years ago, the authors sealed samples of nitric oxide in glass tubes with various substances which might act as catalysts for its decomposition.[1] There is still no trace of brown color in these tubes, and the results are negative, but they are recorded here because they constitute an unusually long experiment in chemical kinetics and because recent researches at high temperatures are now available which give some indication of the time which will be required for positive results.[2]

Long tubes of glass, 14 mm. and 20 mm. in diameter were cleaned with potassium dichromate and sulfuric acid and rinsed thoroughly. They were then constricted, giving tubes 2 to 5 inches long. Catalytic material was added and nitric oxide, purified by bubbling through concentrated sulfuric acid, was passed through. The tubes were sealed off at atmospheric pressure with a small flame. Previous sweeping of the tube with carbon dioxide was helpful in removing all the air. Without this precaution it was found by a sensitive chemical test for NO_2 that some air or nitrogen dioxide was still retained on the walls of the glass tubes. A blue color was obtained when a de-aerated solution of starch–iodide in a small sealed tube was broken in the larger tube containing the nitric oxide.

It was determined that in these tubes a concentration of about 2 mole % of nitrogen dioxide, corresponding to 2% decomposition of the nitric oxide, was necessary to give a detectable brown color by visual inspection. A tube containing 30 cc. of air and 5 mg. or more of anhydrous $Cu(NO_3)_2$ gave a detectable brown color when the $Cu(NO_3)_2$ was decomposed by heating. On cooling and standing the brown color disappeared as the $Cu(NO_3)_2$ was re-formed. This amount of copper nitrate gave about $^1/_{80}$ part by volume of NO_2 and any smaller amounts of $Cu(NO_3)_2$ did not give a detectable brown color. Three tubes were sealed off with different amounts of $Cu(NO_3)_2$ to be used as color standards upon heating, if needed.

Three tubes of pure nitric oxide were sealed up for blanks. One of these was heated to 300° for eight hours and then cooled to room temperature. No brown color developed and hence no decomposition occurred.

Two tubes of nitric oxide were purposely contaminated with a trace of air to give a light brown color. These tubes were to serve as checks against leakage and as tests for any possible autocatalytic effect. After these 40 years the nitric oxide tubes which contained a trace of NO_2 are still slightly brown, but qualitatively do not appear any browner nor less brown than when sealed up.

The remaining tubes were sealed up with small amounts of various oxides and other substances which might possibly exert a catalytic effect, as recorded in the following list. These materials, 1 to 2 grams, lie on the bottom of the tubes or adhere to the inside walls: aluminum powder[3]; beryllium oxide (4 tubes); bone black carbon; cerium oxide; chromium oxide; copper; fuller's earth; iodine; iron, iron oxide; lanthanum oxalate (2 tubes); lanthanum oxide; magnesium powder[3]; manganese dioxide; mercury; molybdenum oxide (2 tubes); naphthalene; neodymium oxide; nickel reduced with hydrogen from oxide (2 tubes); nickel, reduced with hydrogen from the oxide obtained by heating the nitrate; platinum black[3]; palladium; silver, precipitated powder; thorium and cerium oxides (ashes from Welsbach mantle); titanium oxide; tungsten oxide; tungsten wire[3]; uranium oxide from nitrate; partially nitrated cotton.

All of these tubes were heated to 300° for eight hours and then kept at room temperature. With two exceptions, all the tubes remained colorless for many weeks. One of the tubes containing beryllium oxide showed a brown color after a few weeks, and careful examination showed no visible sign of cracks. However, when this tube was allowed to stand for several hours in a starch-iodide solution, a blue color developed indicating that, after all, the tube did have a leak. One of the lanthanum oxalate tubes showed a brown color, but the other one did not. Leakage tests were negative and it is concluded that in this one tube, out of thirty-eight tubes, a trace of air got in accidentally during the filling.

Although there was no indication of a brown color in any of the other tubes, except in the two to which air had been purposely added, the senior thesis of 1918 states that "It is hoped that someone will be interested to look at these tubes at various intervals in the future, to see if any changes have taken place."

These tubes have been examined every few years and as of July 1957 there has been no change. The tubes indicated by footnote 3 became broken and the tests were lost. In May 1957 one of the tubes was opened by filing off one capillary end and exposing to the air. The pungent odor of nitrogen dioxide was detected immediately and the tube rapidly turned brown, showing that the nitric oxide was still present, that there were no minute cracks in the glass, that the glass is impermeable to both oxygen and nitric oxide and that 40 years is too short a time at room temperature for as much as 2% of the nitric oxide to decompose.

It is now possible to estimate the time required for the appearance of a brown color at 2% decomposition[2] by extrapolating to room temperature the rates of decomposition measured in the range of 600 to 1000° with tubes packed with pellets of oxides which act as catalysts. The decomposition rates would be considerably slower for the tubes sealed off as described in the present study because the surface of the solids is much less. The formula given by Fraser and Daniels for calcium oxide catalyst is

$$k = 43.6e^{-23,000/RT} \text{ mole}^{-1} \text{ sec.}^{-1}$$

for the zero order, surface-catalyzed reaction by calcium oxide gives an estimate of about 70 thousand years as the time required for 2% decomposition at 20°. Data on gallium oxide (not used in the 1918 experiments) give an extrapolated estimate of 13 hundred years. The value estimated for the homogeneous bimolecular gas phase decomposition by the formula

$$k = 1.9 \times 10^8 e^{-63,100/RT} \text{ atm.}^{-1} \text{ sec.}^{-1}$$

is of the order of 10^{29} years.

These formulas are, of course, unreliable for such a wide extrapolation from seconds to millions of years. In spite of the extraordinary long times predicted for positive results, these tubes will be

(1) More details of this work are available in the B. S. Thesis of C. S. Howard, Worcester Polytechnic Institute, Worcester, Mass., 1918.

(2) J. M. Fraser and F. Daniels, THIS JOURNAL, 61, 215 (1958).

(3) Broken and test lost.

left at the Chemistry Department of the University of Wisconsin and some will be offered to the Smithsonian Institution in Washington for future observations. Perhaps other investigators will be interested in repeating the experiments described here with new and improved catalysts which may bring the period required for detectable decomposition down to a reasonable time.

THE TRIPLE-POINT TEMPERATURE OF TELLURIUM

BY ROBERT E. MACHOL AND EDGAR F. WESTRUM, JR.

Contribution from the Department of Chemistry, University of Michigan, Ann Arbor, Michigan

Received September 25, 1957

The melting point of tellurium is given in standard references[1-3] as 450°. Critical examination of the highly discordant values in the literature, which are summarized in Table I, supports this value. However, recent publications by Weidel[4] and Lark-Horovitz,[5] who have worked with very pure material, give the melting point as 452 and 445°, respectively.

TABLE I
MELTING POINT OF TELLURIUM

Author	Year	M.p., °C.
Pictet	1879	525
Carnelley and Williams	1880	452, 455
Töpler	1894	420
Matthey	1901	450
Fay and Gillson	1902	446
Mönkemeyer	1905	428
Pellini and Vio	1906	450
Chickashige	1907	438
Pélabon	1909	452
Biltz and Mecklenberg	1909	455
Kobayashi	1910	437
Jaeger and Menke	1912	452.5
Damiens	1922	453
Umino	1926	446
Kraus and Glass	1929	451.1
Šimek and Strehlík	1930	452.0
Kracek	1941	449.8 ± 0.2
Weidel	1954	452
Epstein, *et al.*	1957	445
This research		449.5 ± 0.3

Experimental

The triple-point temperature of tellurium was determined directly by observing the halt in the heating and cooling curves of pure tellurium *in vacuo*. The tellurium was semiconductor grade, 99.999 + % pure, from American Smelting and Refining Company. It was placed in a vitreous silica tube with a re-entrant well for a thermocouple, connected to a vacuum of 10^{-6} mm., and boiled vigorously to eliminate possible volatile contaminants; sensitive tests[6] have shown that tellurium and silica do not react at these temperatures. The tube was then sealed and placed in a silver block in a furnace at 452°; melting occurred within the range 449.4 to 449.7° over a period of 30 minutes. The furnace was then cooled to 447° and the supercooled liquid shaken occasionally until freezing commenced, after an hour; the sample temperature then rose to 449.5° and remained constant for 20 minutes, after which it again fell to 447°.

The thermocouples (Pt. *vs.* Pt-Rh) were calibrated by freezing standard samples of zinc (419.50°) and aluminum (660.15°), obtained from the National Bureau of Standards, and copper–silver eutectic (779.2°), in graphite tubes under identical conditions to the above.

Discussion

Most of the discrepancies indicated in Table I can be explained. Many of the measurements were frankly inaccurate. Impurities may have played a part in some of the low values, but most of these were due to the phenomenon of supercooling.[5] Many of the measurements were incidental to thermal analysis designed to elucidate the phase diagram of binary systems containing tellurium, and the values given are often marked "start of crystallization," which is the phenomenon of interest in marking off a liquidus curve. Finally, in some instances where these criticisms are not applicable, and which deviate by one or two degrees from the results given here, the authors do not indicate how their temperature scales were derived, and it is well known that errors of several degrees can be made at these temperatures unless careful calibration procedures are observed. By these criteria, the only published reports worthy of consideration are those of Matthey,[7] Pellini and Vio,[8] Jaeger and Menke,[9] Kraus and Glass,[10] Simek and Strehlík,[11] Kracek[12] and this paper. The first two agree within the limitations of their accuracy. The errors in the measurements of Jaeger and Menke have been discussed by Damiens.[13] The deviation of Kraus and Glass remains unexplained. The measurements by Simek and Strehlík were exceedingly careful, and their relative temperatures must be considered accurate, so that, for example, their conclusion that hydrogen and carbon dioxide lower the melting point 0.15 and 0.20°, respectively, per atmosphere of pressure should be accepted; however, their calibration was obviously in error at the sulfur point and, as Kracek points out, if this is taken into account their result is in agreement. The work of Kracek appears to be the most accurate of all. Due to limitations in temperature measurement, the probable error of the present result is about 0.3°, slightly larger than that of Kracek.

Solid State Transition.—A solid state transition reported by Umino[14] was sought with the present apparatus by going through the temperature range from 300 to 450° in both directions at rates well below one degree per minute. No transition was found, though one a tenth as large as that reported would certainly have been evident. Simek and Strehlík have also remarked on the ab-

(1) "Selected Values of Chemical Thermodynamic Properties," National Bureau of Standards Circular No. 500, Washington, 1952.

(2) D. R. Stull and G. C. Sinke, "Thermodynamic Properties of the Elements," Washington, 1956.

(3) O. Kubaschewski, *Z. Metallkunde*, **41**, 445 (1950).

(4) J. Weidel, *Z. Naturforsch.*, **9a**, 697 (1954).

(5) A. S. Epstein, H. Fritzsche and K. Lark-Horovitz, *Phys. Rev.*, **107**, 412 (1957).

(6) R. E. Machol and E. F. Westrum, Jr., "The Vapor Pressure of Tellurium," to be published.

(7) E. Matthey, *Proc. Roy. Soc. (London)*, **68**, 161 (1901).

(8) G. Pellini and G. Vio, *Gazz. chim. ital.*, **36** [2], 469 (1906).

(9) F. M. Jaeger and J. B. Menke, *Z. anorg. Chem.*, **75**, 241 (1912).

(10) C. A. Kraus and S. W. Glass, THIS JOURNAL, **33**, 995 (1929).

(11) A. Šimek and B. Strehlík, *Coll. Czech. Chem. Comm.*, **2**, 304 (1930).

(12) F. C. Kracek, *J. Am. Chem. Soc.*, **63**, 1989 (1941).

(13) A. Damiens, *Ann. Chim.*, [9] **19**, 44 (1923).

(14) S. Umino, *Kinzoku-no-Kenkyu*, **3**, 498 (1926).

sence of this transition, as has Niwa[15] in a careful series of measurements of the vapor pressure of solid tellurium. Since only one experimenter has reported this transition, and that on the basis of weak evidence, it may be assumed that it does not exist.

(15) K. Niwa, *J. Fac. Sci. Hokkaido Imp. Univ.*, [III] **3**, 75 (1940).

THE VAPOR PRESSURE OF VANADIUM OXYTRIFLUORIDE[1]

BY LAVERNE E. TREVORROW

Chemical Engineering Division, Argonne National Laboratory, Lemont, Illinois

Received September 27, 1957

Very little information is available in the literature on the volatility of vanadium oxytrifluoride. Ruff and Lickfett[2] reported that the compound melted at 300° and boiled at 480°. Haendler[3,4] stated that vanadium(V) oxide reacted with fluorine at 475° to form volatile vanadium oxytrifluoride, VOF_3.

In the present work, a sample of the pure compound was prepared and identified by chemical analysis and by a vapor density determination. The vapor pressure of solid vanadium oxytrifluoride was measured at various temperatures from 72 to 123°.

Experimental

Materials.—Vanadium pentoxide of 99.5 to 99.7% purity was obtained from the Vanadium Corporation of America. High purity commercial fluorine was used. In previous work[5] this material was shown to be at least 99% fluorine by volume, and to contain less than 0.5% impurities.

Apparatus.—The preparation and vacuum manipulation of the vanadium oxytrifluoride were performed in a nickel and Monel system. Monel diaphragm and Teflon-seated bellows valves were used. The system used for the purification of the compound and the vapor pressure measurements was assembled from components which were joined by welds or by flare connectors with Teflon gaskets. This system was contained in a thermostated air box, and it was equipped with a Booth-Cromer pressure transmitter and self-balancing relay[6] which permitted pressure measurement with a mercury manometer.

Temperatures were measured to the nearest 0.1° with a copper-constantan thermocouple previously calibrated against a standard platinum resistance thermometer. The thermocouple was used with a Rubicon type B potentiometer for the vapor pressure measurements, and a Brown recording potentiometer was used to obtain thermal analysis curves. During the pressure measurement, the vanadium oxytrifluoride sample was contained immediately under the pressure transmitter in a $^3/_4$-inch nickel tube 6 inches in length. The thermocouple was inserted into a well in the bottom of the tube.

Procedure.—The vanadium oxytrifluoride was prepared by the reaction of vanadium pentoxide with fluorine at about 475°. The product was a pale yellow solid at room temperature. In order to rid the product of oxygen, fluorine and hydrogen fluoride, the whole sample was sublimed from one Fluorothene (poly-chlorotrifluoroethylene) tube and collected in another cooled in Dry Ice. The system was then evacuated. This procedure was repeated several times until the vapor pressure at a given temperature showed no further change after resublimation.

The vapor density of the sample used for the vapor pressure measurements was determined at 97.4°. A value of 124.6 g./G.M.V. was obtained. The formula weight is 123.95 g./mole. Chemical analysis of the sample indicated 40.6% vanadium and 43.0% fluorine. The theoretical values are 41.10% and 45.99%, respectively.

The vapor pressure measurements were made on a sample of 10–15 g. The equilibrium vapor pressures were approached experimentally from both higher and lower temperatures.

Results

The vanadium oxytrifluoride sample was examined briefly by the method of thermal analysis to determine whether melting or solid transitions occurred in the temperature range of 72 to 123°. The material showed no thermal halt when it was warmed through this temperature interval.

The results of the vapor pressure measurements are summarized in Table I.

Vanadium oxytrifluoride was found to be much more volatile than was indicated by the data of Ruff.[2] Interpolation of the results of the present work gives a vapor pressure of 760 mm. at 110°.

TABLE I

VAPOR PRESSURE OF VANADIUM OXYTRIFLUORIDE

Temp. (°C.)	Pressure, mm.	Temp. (°C.)	Pressure, mm.
72.1	122.7	109.3	749.7
72.1	124.1	109.3	752.0
72.1	124.7	111.3	791.6
80.8	175.3	111.4	795.1
84.0	200.4	111.4	795.7
84.1	201.9	116.7	1092
89.3	251.9	116.7	1093
89.5	251.6	122.8	1513
96.3	365.0	122.8	1519
96.3	365.2		

KINETICS OF YIELD DISTRIBUTION IN BIMOLECULAR SIMULTANEOUS–CONSECUTIVE REACTIONS

BY LOUIS GOLD

Massachusetts Institute of Technology, Cambridge, Massachusetts

Received August 12, 1957

The distribution of products to be expected in such synthetic systems where a reactant group R enters a bare benzene or monosubstituted nucleus M has been analyzed under the assumption that the sequence of simultaneous–consecutive reactions is essentially irreversible. Unlike the case of unimolecular or first-order reactions, the over-all rate of reaction of M cannot always be expressed as a sum of exponential terms as is usually supposed in biological tracer experiments.[1,2]

For M = benzene, a total of twenty reactions can occur to produce twelve distinct products which include one mono, three di, three tri, three tetra, one penta and one hexa substituted deriva-

(1) Work performed under the auspices of the U.S. Atomic Energy Commission.

(2) O. Ruff and H. Lickfett, *Ber.*, **44**, 2539 (1911).

(3) H. M. Haendler, "The Reaction of Fluorine with Titanium, Zirconium, and the Oxides of Titanium(IV), Zirconium(IV) and Vanadium(V)," NYO-6123, 1953.

(4) H. M. Haendler, S. F. Bartram, R. S. Becker, W. J. Bernard and S. W. Bukata, *J. Am. Chem. Soc.*, **76**, 2177 (1954).

(5) J. Fischer, J. Bingle and R. C. Vogel, *ibid.*, **78**, 902 (1956).

(6) S. Cromer, "The Electronic Pressure Transmitter and Self-Balancing Relay," SAM Laboratories, Columbia University, MDDC-803, 1947.

(1) See, for example, W. E. Siri, "Isotopic Tracers and Nuclear Radiations," McGraw-Hill Book Co., Inc., N. Y., 1949, Ch. 15, p. 388, *et seq.*

(2) Recent treatment in M. Berman and R. Schoenfeld, *J. Appl. Phys.*, **27**, 1361 (1956).

tive. The set of kinetic equations has the following appearance

$$-\frac{dM}{dt} = \lambda_1 MR$$
$$-\frac{dM_1}{dt} = RM_1(\lambda_2 + \lambda_3 + \lambda_4) - \lambda_1 MR \quad (1)$$
$$-\frac{dM_{21}}{dt} = RM_{21}(\lambda_5 + \lambda_7) - \lambda_2 M_1 R$$
$$\frac{dM_6}{dt} = \lambda_{20} RM_5$$

where M_1 is the concentration of mono product; M_2, is the concentration of one of the three possible di-products, etc. The pertinent rate constants are denoted by λ_i where $i = 1, 2, 3,..,20$. The over-all consumption of M is expressed by

$$\frac{dM}{dt} = -\sum_{i>j}\frac{dM_{ij}}{dt} = -\lambda_1 MR \quad (2)$$

and there are two conservation conditions

$$M_0 = M + \sum_{i>j} M_{ij} \quad (3a)$$

$$R_0 = R + \sum_{i>j} \omega_{ij} M_{ij} \quad (3b)$$

where M_0 and R_0 are the initial concentrations of M and R at $t = 0$. Characteristic weighting factors ω_{ij} take on such values as $i = 2$, $\omega_{ij} = 2$, $i = 3$, $\omega_{ij} = 3$, etc.

The distribution-like solution is arrived at inductively[3]; from the first two equations in (1)

$$\frac{dM_1}{dM} = \frac{\Lambda_1}{\lambda_1} \times \frac{M_1}{M} - 1, \; \Lambda \equiv \lambda_2 + \lambda_3 + \lambda_4 \quad (4)$$

which *via* the variable change $M_1 = \nu M$ has the solution

$$M_1 = \frac{M}{r_1 - 1}\left[1 - \left(\frac{M}{M_0}\right)^{r_1 - 1}\right], \; r_1 \equiv \frac{\Lambda_1}{\lambda_1} \quad (5)$$

Similarly

$$\frac{dM_{21}}{dM} = r_2\frac{M_{21}}{M} - r_3\frac{M_1}{M}, \; r_2 \equiv \frac{\lambda_5 + \lambda_6}{\lambda_1}, \; r_3 \equiv \frac{\lambda_2}{\lambda_1} \quad (6)$$

leads to

$$M_{21} = aM^{r_1} + bM \quad (7)$$

where

$$a = \frac{r_3}{(r_1 - 1)M_0^{(r_1 - 1)}} \times \frac{1}{r_1 - r_2} \quad (7a)$$
$$b = \frac{r_3}{(r_1 - 1)(r_2 - 1)}$$

Thus the general solution takes the form

$$M_{ij} = a_{ij} M^{r_1} + b_{ij} M \quad (8)$$

with a_{ij} and b_{ij} characteristic functions of λ_i. Stationary M_{ij} values correspond to $M = M^*$

$$M^* = \left(\frac{-b_{ij}}{r_1 a_{ij}}\right)^{\frac{1}{r_1 - 1}} \quad (9)$$

Furthermore since

$$R = R_0 - \sum_{i>j} \omega_{ij}(a_{ij} M^{r_1} + b_{ij} M) \quad (10)$$

the instantaneous value of M derives from

$$\int_M^{M_0} \frac{dM}{M\{R_0 - \sum_{i>j} \omega_{ij}(a_{ij} M^{r_1} + b_{ij} M)\}} = 1 - e^{-\lambda_1 t} \quad (11)$$

(3) This approach described earlier in L. Gold, *ibid.*, **24**, 88 (1953), for radioactive decay series.

This relation evidences the involved manner in which the various rate constants regulate the consumption of starting material. It clearly does not lead to a linear combination of exponential terms incorporating the λ_i; however, a decay-like behavior is manifest.

If $M \equiv M_1 = \phi x$ and $R \neq x$, a total of nineteen products originates *via* forty-two reactions, encompassing three mono, six di, six tri, three tetra and penta derivatives. Then in place of (1)

$$-\frac{dM_1}{dt} = (\lambda_1 + \lambda_2 + \lambda_3) RM_1$$
$$-\frac{dM_{21}}{dt} = (\lambda_4 + \lambda_5 + \lambda_6 + \lambda_7) RM_{21} - \lambda_1 M_1 R \quad (12)$$
$$\vdots$$
$$\frac{dM_6}{dt} = (\lambda_{40} M_{51} + \lambda_{41} M_{52} + \lambda_{42} M_{53})R$$

Analogous to (7) there obtains

$$M_{21} = \frac{M_1}{r_1 - 1}\left[r_2 - \left(\frac{M_1}{M_0}\right)^{r_1 - 1}\right] \quad (13)$$

with

$$r_1 \equiv (\lambda_4 + \lambda_5 + \lambda_6 + \lambda_7)/(\lambda_1 + \lambda_2 + \lambda_3)$$
$$r_2 \equiv \lambda_1/(\lambda_1 + \lambda_2 + \lambda_3) \quad (13a)$$

Hence the general solution parallels (8) with M_1 replacing M, so demonstrating the rather general applicability of the preceding formalism to related systems.

A SIMPLIFIED EXPRESSION FOR THE MOLAR POLARIZATION OF SOLUTES

BY KENNETH A. ALLEN

Oak Ridge National Laboratory, Oak Ridge, Tennessee[1]

Received October 10, 1957

It is well known that in obtaining extrapolated values for the molar polarization P_2 of solutes at infinite dilution, considerable uncertainty is often introduced in using plots of P_2 itself against concentration.[2] It has been shown theoretically[3] that at low concentrations the dielectric constant should be a linear function of the concentration, and equations based on this linearity, plus the linearity of the specific volume, have been proposed by Hedestrand[4] and by Halverstadt and Kumler,[5] which give unambiguous values of P_2 at zero concentration. The subject of this note is an alternative expression which, while equivalent to the foregoing in mathematical content, presents greater simplicity of form and ease of calculation.

The present derivation is based on the linearity of the function $(\epsilon_{12} - 1)/(\epsilon_{12} + 2)$ *vs.* concentration, plus the density linearity rather than that of the specific volume. It would seem from the Lorentz–Lorenz mixing law for molar refractivities that about as good a theoretical case could be made for this approach as for the above. The point is that

(1) Operated for the U.S.A.E.C. by Union Carbide Nuclear Company.

(2) C. P. Smyth, "Dielectric Behavior and Structure," McGraw-Hill Book Co., Inc., New York, N. Y., 1955, pp. 223–4.

(3) L. Onsager, *J. Am. Chem. Soc.*, **58**, 1486 (1936).

(4) G. Hedestrand, *Z. physik. Chem.*, **2B**, 428 (1929).

(5) I. F. Halverstadt and W. D. Kumler, *J. Am. Chem. Soc.*, **64**, 2988 (1942).

since all these derivations depend on the limiting values of the slopes at infinite dilution, it is quite immaterial which function of the dielectric constant or solute mass is used. This is illustrated in the table, where it is apparent that for values of $\epsilon_{12} - \epsilon_1$ up to 0.01, the slopes of the two dielectric functions are within 0.3% of each other, and that the same is true of the density and specific volume for density changes up to 0.002 g./ml. The more marked difference in slope between the density and specific volume is relatively unimportant, since such measurements are usually made with far more precision at low concentrations than is possible in the case of the dielectric constant measurements, although in dilute solutions of highly polar molecules the reverse may be true. Thus, since the values of $(\epsilon_{12} - 1)/(\epsilon_{12} + 2)$ usually have to be calculated at some stage anyway, and since the final expression for P_2 is simpler, the following approach has been used in this Laboratory.

We put

$$\frac{\epsilon_{12} - 1}{\epsilon_{12} + 2} = \frac{\epsilon_1 - 1}{\epsilon_1 + 2} + ax_2$$

where $x_2 = N_2/(N_1 + N_2)$, the mole fraction of solute. Similarly, for the density

$$d_{12} = d_1 + bx_2$$

By definition

$$P_{12} = x_1P_1 + x_2P_2 = \frac{\epsilon_{12} - 1}{\epsilon_{12} + 2}\frac{x_1M_1 + x_2M_2}{d_{12}}$$

hence

$$P_2 = P_1 + \frac{1}{x_2}\left\{\frac{\left(\frac{\epsilon_1 - 1}{\epsilon_1 + 2} + ax_2\right)(M_1 + x_2[M_2 - M_1])}{d_1 + bx_2} - P_1\right\}$$

which on rearrangement becomes

$$P_2 = P_1 + \frac{\frac{\epsilon_1 - 1}{\epsilon_1 + 2}(M_2 - M_1) + aM_1 + ax_2(M_2 - M_1)}{d_1 + bx_2} - \frac{\frac{bP_1}{d_1}}{1 + \frac{bx_2}{d_1}}$$

The last equation is in a form suitable for passing to the limit, and we obtain, at zero concentration

$$P_2 = \frac{P_1M_2}{M_1} + \frac{aM_1 - bP_1}{d_1}$$

That this expression is equivalent to that proposed by Halverstadt and Kumler, who used the linear forms $\epsilon_{12} = \epsilon_1 + \alpha x_2$ and $v_{12} = v_1 + \beta x_2$, is easily shown from the identities

$$\frac{\epsilon_1 + \alpha x_2 - 1}{\epsilon_1 + \alpha x_2 + 2} = \frac{\epsilon_1 - 1}{\epsilon_1 + 2} + ax_2$$

and

$$v_1 + \beta x_2 = \frac{1}{d_1 + bx_2}$$

on obtaining similarly the limiting expressions

$$\lim_{x_2 \to 0} a = \frac{3\alpha}{(\epsilon_1 + 2)^2}$$

and

$$\lim_{x_2 \to 0} b = -\frac{\beta}{v_1^2}$$

Thus, since Halverstadt and Kumler have amply demonstrated the applicability of their equation, it follows that the present expression is equally applicable, and we have in addition somewhat greater simplicity of form and ease of calculation.

TABLE I

LINEARITY COMPARISON; ϵ_{12} *vs.* $(\epsilon_{12} - 1)/(\epsilon_{12} + 2)$ AND d_{12} *vs.* v_{12}; SOLVENT VALUES BASED ON BENZENE AT 25°[6]

A.	$\epsilon_{12} - \epsilon_1$	$(\epsilon_{12} - 1)/(\epsilon_{12} + 2)$	$\frac{\Delta(\epsilon_{12} - 1)/(\epsilon_{12} + 2)}{\Delta(\epsilon_{12} - \epsilon_1)}$
	0.000	0.2980814	...
	.001	.2982456	0.1642[a]
	.002	.2984097	.1641
	.005	.2989016	.1639
	.01	.2997199	.1637
B.	$d_{12} - d_1$	v_{12}	$\Delta(v_1 - v_{12})/\Delta(d_{12} - d_1)$
	0.000	1.144951	...
	.001	1.143641	1.310
	.002	1.142335	1.306
	.005	1.138434	1.300
	.01	1.131990	1.289

[a] The numbers in this column also give the ratios a/α and $-\beta/b$ in Parts A and B, respectively.

(6) ϵ = 2.2740, C_6H_6, 25° from A. A. Maryott and E. R. Smith, Table of Dielectric Constants of Pure Liquids, Nat. Bur. Standards Circ. 514, August 10, 1951; d = 0.87340 g./ml., C_6H_6, 25° from "International Critical Tables," Volume III, McGraw-Hill Book Co., New York, N. Y., p. 29.

THE STRUCTURE OF LIQUID ANTIMONY PENTAFLUORIDE[1]

BY CHARLES J. HOFFMAN, BERT E. HOLDER AND WILLIAM L. JOLLY[2]

University of California, Radiation Laboratory, Livermore Site, Livermore, California

Received August 12, 1957

Antimony pentafluoride is an extremely viscous liquid at room temperature,[3] suggesting a high degree of polymerization. The fluorine nuclear magnetic resonance spectrum of the compound was examined in an attempt to determine the molecular structure.

Experimental

Samples of antimony pentafluoride were vacuum-distilled into 3 mm. i. d. Pyrex tubes and sealed off *in vacuo*. The material analyzed 99.2% pure antimony pentafluoride; the melting point, 8.5°, was comparable to values obtained recently for pure antimony pentafluoride.[4]

A Varian V-4300 high-resolution spectrometer was used at a fixed frequency of 40 mc. and a magnetic field of 9980 gauss. The system was capable of at least five cycles resolution without sample spinning. Resolution of the peaks in the spectra was limited by the separations and line widths of the signals themselves rather than by magnetic field inhomogeneity. Chemical shifts of the fluorine resonances were measured relative to trifluoroacetic acid by sample substitution after calibration of the linear magnetic field sweep by an appropriate side-banding of the trifluoroacetic acid sample.

The fluorine spectra for three temperatures (*ca.* −10°, room temperature, and *ca.* 80°) are given in Fig. 1. The lower temperature spectrum is the most interesting and

(1) The work described in this paper was sponsored by the U. S. Atomic Energy Commission.

(2) Department of Chemistry, University of California, Berkeley, California.

(3) A. A. Wolf and N. N. Greenwood, *J. Chem. Soc.*, 2200 (1950).

(4) C. J. Hoffman and W. L. Jolly, THIS JOURNAL, 61, 1574 (1957).

indicates the existence of three non-equivalent sets of fluorine atoms in antimony pentafluoride within this temperature range. Detailed data for the low temperature spectrum are given in Table I. The chemical shift, δ,[5] for the high temperature peak is 0.335.

TABLE I

LOW TEMPERATURE FLUORINE SPECTRUM OF SbF_5

Peak	No. of resolved lines	Nominal total half-width, gauss	δ	Spin–spin splitting, cycles	Relative area
A	..	0.065	0.085	....	1
B	7	.10	0.268	70± 10	2
C	3	.10	0.528	130± 15	2

Discussion

Any model which is proposed to explain the low temperature nuclear magnetic resonance spectrum of liquid antimony pentafluoride must be consistent with the existence of three non-equivalent sets of fluorine atoms in the over-all population ratio 1:2:2. In addition, the observed splittings must be satisfactorily explained. Various models can be used to explain the nuclear magnetic resonance data, but it is believed that the one chosen is not only consistent with the high viscosity of antimony pentafluoride but is also reasonable with respect to theories of chemical bonding.

The chosen model is pictured in Fig. 2. Liquid antimony pentafluoride is envisioned as a mixture of long chains of SbF_6^- groups, each group sharing two of its fluorine atoms with its two neighbors. The three groups of fluorine atoms are: type A (shared, or bridging fluorine atoms), type B (*trans* to type A fluorine atoms), and type C (*trans* to each other). It should be noted that the type A fluorine atoms are always *cis* to one another.

The distances of the fluorine atoms from the antimony atoms are presumed to increase in the order: type B, type C, type A. This order is the same as that of increasing ionic character for the individual Sb–F bonds. In Fig. 2, the fluorine atoms have been arranged approximately octahedrally about each antimony, but an attempt has been made to indicate a tendency for a tetrahedral arrangement of type B and type C fluorines.

The concept of shared or divalent fluoride ions is not without precedent. Brosset[6] has shown that the compound Tl_2AlF_5 contains infinite chains of hexafluoroaluminate octahedra in which the two opposite (*trans*) corners are shared. Bystrom and Wilhelmi[7] have shown that in $CsSb_2F_7$ the antimony atoms are surrounded by four fluorine atoms situated at the corners of an irregular tetrahedron. The two tetrahedra share one fluorine atom, so that $Sb_2F_7^-$ groups are formed. It recently has been suggested that the 2:1 addition compounds of boron fluoride with triethylamine and with pyridine existing in solution as well as in the pure phase have single fluorine bridge structures.[8]

I. Spectrum Interpretations in Terms of the Model.—Since the spin of the F^{19} nucleus is 1/2,

(5) $\delta = (H_i - H_{TFA})/H_{TFA} \times 10^4$, where H_i is the resonance field at 40 mc. for the peak in question and H_{TFA} is the corresponding field for trifluoroacetic acid.

(6) C. Brosset, *Z. anorg. Chem.*, **235**, 139 (1937).

(7) A. Bystrom and K. A. Wilhelmi, *Arkiv Kemi*, **3**, 373 (1951).

(8) H. C. Brown, P. F. Stehle and P. A. Tierney, *J. Am. Chem. Soc.*, **79**, 2020 (1957).

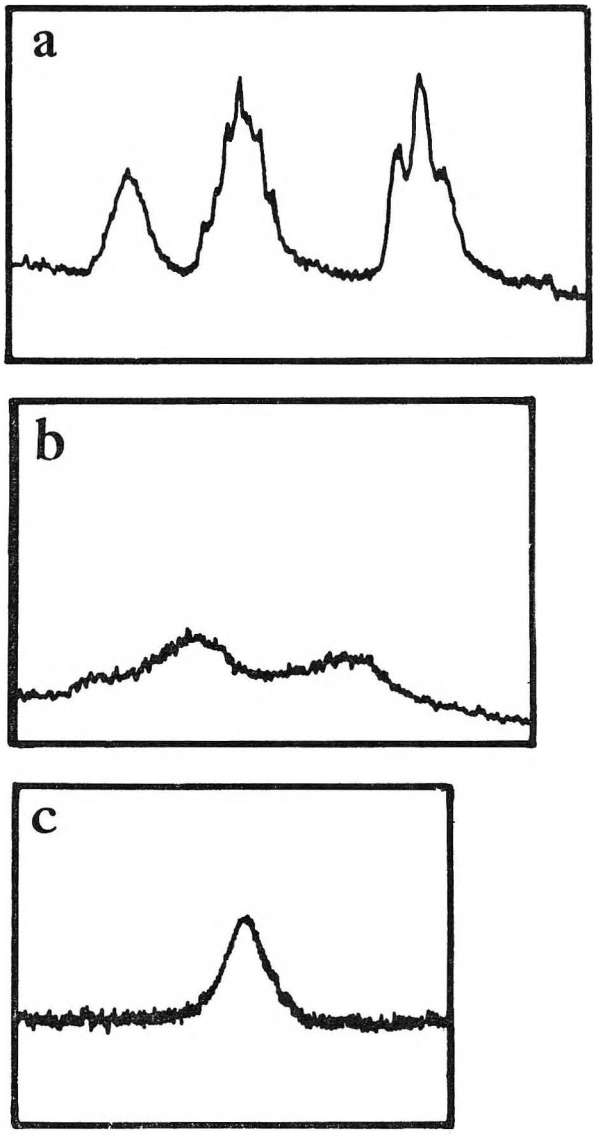

Fig. 1.—F^{19} spectrum of antimony pentafluoride at (a) ~−10°; (b) room temperature; and (c) ~80°.

the nuclear magnetic resonance line for a particular set of fluorine atoms will be split into $(n + 1)$ peaks by neighboring fluorine atoms of another type. It has been assumed that due to strong nuclear quadrupole relaxation, the Sb–F spin–spin coupling is ineffective in splitting the fluorine lines. The proposed model does not have electric field symmetry at the antimony nuclear site and can permit a strong relaxation interaction with the relatively large antimony quadrupole moment.

The spin–spin coupling constants estimated from the measured splittings are: $J_{AB} = 70 \pm 10$ cycles, $J_{AC} < 30 \pm 10$ cycles, and J_{BC} 130 ± 15 cycles. Peak A (Fig. 1) is split into a quintet with separations of 70 ± 10 cycles by the type B fluorines; these lines being further split by the type C fluorines overlap to make an unresolvable single broad peak. Peak B is split into a triplet with separations of 130 ± 15 cycles by the type C fluorines and each of these lines, in turn, is split into a triplet of separations of 70 ± 10 cycles by the type A fluorines. Since $J_{BC} \approx 2\,J_{AB}$, two pairs of

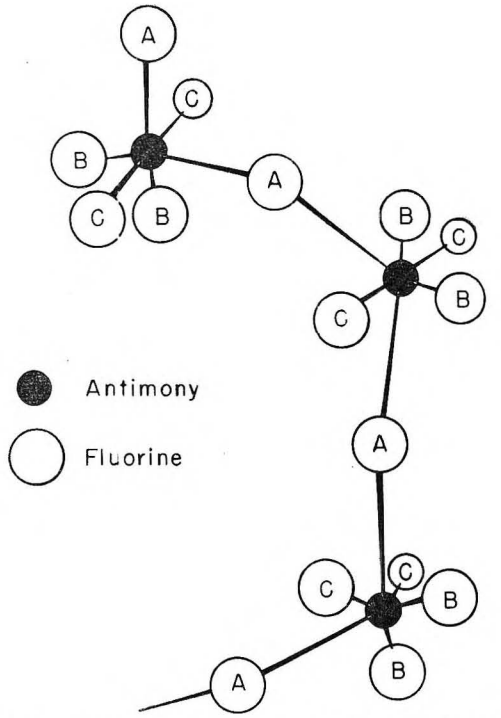

Fig. 2.—Schematic chain structure of SbF_5 polymer.

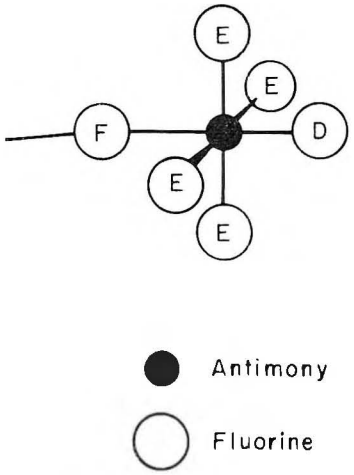

Fig. 3.—Active end of SbF_5 chain.

lines overlap and a septet of 1:2:3:4:3:2:1 intensity distribution results. Peak C is split into a triplet of 130-cycle separation by the type B fluorines. The splitting of this peak by the type A fluorines is unresolvable.

The loss of detail in the spectra obtained at room temperature and at *ca.* 80° indicates that the fluorine atoms exchange at these higher temperatures. At room temperature, the average lifetime for the exchange between fluorines of type A and B is calculated to be about 2×10^{-3} sec. and at 80°, the average lifetime for any type of fluorine is less than 10^{-4} sec.

II. The Model in Terms of Electrostatics and Polarization.—It is assumed that all the Sb–F bonds are principally ionic bonds, with little covalent character. The distance between neighboring Sb^{+5} ions is more than twice the Sb–F distance in the SbF_6^- ion not only as a result of coulombic repulsion of the Sb^{+5} ions, but also because of the decreased covalent character in the bonds between antimony ions and the "bridging" fluoride ions. A "bridging" fluoride cannot form two bonds each with as much covalent character as that of a singly bonded fluoride.

Figure 3 represents a terminal group of an SbF_5 chain. This may be considered as a basic group which is capable of reaction with an acidic group (*e.g.*, an SbF_5 monomer or the fluoride-deficient end of another SbF_5 chain). It is proposed that a type (D) fluoride ion is a less basic site than a type (E) fluoride ion as its electron cloud has been attracted toward the central Sb^{+5} ion more strongly than the others by virtue of a dipole induced in the Sb^{+5} ion. This induced dipole in the Sb^{+5} ion is the result of a virtual positive charge in the direction of fluoride ion (F) and is caused by (a) the neighboring Sb^{+5} ion in the chain (which is not shown in Fig. 3), and (b) the fact that fluoride ion (F) is farther from the terminal Sb^{+5} than the other five fluorides. Therefore the attachment of the acid group always occurs at one of the *cis* fluoride ions (E); never at the *trans* fluoride ion (D).

III. The Model in Terms of Atomic Orbitals.—Although the bonds in an SbF_5 chain are principally ionic, their fractional covalent character is of some importance. Antimony has available only four bonding orbitals[9] ($5s5p^3$), and yet it must form bonds with six fluorine atoms. The four bonds to the non-bridging fluoride atoms are more covalent in character than the other two, hence the most stable configuration will involve maximum utilization of the four available orbitals by these four bonds. Each of the three principal axes of antimony has available one and one-third orbitals for bonding ($s^{1/3}p$). If the bridging fluorides are *trans* to each other, the one and one-third orbitals in the direction of their axis are misspent on what are necessarily very ionic bonds. However, if the bridging fluorine atoms are *cis* to each other, it is then possible to utilize a full orbital in each of the bonds *trans* to the bridging fluorides, and a total of only two-thirds of an orbital is misspent on the very ionic bonds. In the *cis* configuration, the fluorine atoms *trans* to bridging fluorine atoms are the most strongly bound to the antimony and hence closer to the antimony. The bridging fluorine atoms are the most weakly bound and hence are farthest from the antimony.

Acknowledgment.—The authors wish to thank Prof. K. S. Pitzer for his helpful discussions of the bonding in antimony pentafluoride.

(9) The 5 d orbitals are theoretically available for sp^3d^2 hybridizations, but it is unlikely that they participate appreciably.

CALCIUM AMMONIUM PYROPHOSPHATES

BY EARL H. BROWN, WALTER E. BROWN, JAMES R. LEHR, JAMES P. SMITH AND ALVA W. FRAZIER

Division of Chemical Development, Tennessee Valley Authority, Wilson Dam, Ala.

Received October 12, 1957

One amorphous and two crystalline phosphates of interest as potential fertilizer materials were prepared by ammoniation of products of the hy-

drolytic degradation of vitreous calcium polymetaphosphate. Chromatograms of 5% acetic acid solutions of the crystals were identical with pyrophosphate chromatograms. Optical and X-ray properties are reported here.

When concentrated NH_4OH is added to the viscous, water-immiscible liquid product of the treatment of vitreous calcium polymetaphosphate with water,[1] a precipitate is formed. Initially amorphous, it crystallizes as spherulites when left in the mother liquor several days. Similar crystals are formed slowly when vitreous calcium polymetaphosphate is treated with concentrated NH_4OH. Average observed mole ratios $CaO:NH_3:P_2O_5:H_2O$ of 1.13:1.90:1:2.30 in the air-dried product suggest the formula $Ca(NH_4)_2P_2O_7 \cdot H_2O$.

The crystals are thin, colorless monoclinic blades, tabular on (100) or (001). The refractive indexes are $\alpha = 1.520$, $\beta = 1.537$, $\gamma = 1.540$. The crystals are biaxial (−) with $2V = 40°$ (obsd.) or 46° (calcd.), $\gamma = b$. Bx_a lies in the a-c plane and is inclined to the plate by 68°. Interplanar spacings and visually estimated intensities are shown in Table I.

TABLE I

X-RAY PATTERNS (Cu Kα RADIATION; CAMERA DIAM. 14.32 CM.; WEDGE-SHAPED SAMPLE)

$Ca(NH_4)_2P_2O_7 \cdot H_2O$				$Ca_3(NH_4)_2(P_2O_7)_2 \cdot 6H_2O$			
d, Å.	I	d, Å.	I	d, Å.	I	d, Å.	I
7.23	VS	2.52	M	7.27	VW	2.39	W
5.51	WM	2.44	VW	6.39	W	2.23	VW
4.86	S	2.39	VW	5.73	S	2.18	VW
4.23	WM	2.32	VW	5.56	M	2.13	VW
3.86	W	2.11	W	4.95	MS	2.09	W
3.56	VW	2.06	VW	4.20	WM	1.88	VW
3.39	MS	1.92	W	3.27	M	1.85	W
2.98	M	1.88	WM	3.19	M	1.80	W
2.90	M	1.72	VW	3.11	W	1.73	VW
2.85	VW	1.69	VW	3.07	S	1.64	VW
2.75	W	1.47	WM	2.84	W	1.56	VW
2.68	VW	1.45	WM	2.74	VW	1.50	VW
				2.70	VW	1.42	VW
				2.59	VW	1.41	VW

Exposure of $Ca_3H_2(P_2O_7)_2 \cdot 4H_2O$[1] to concentrated NH_4OH for several hours yields another product. Average $CaO:NH_3:P_2O_5:H_2O$ mole ratios of 1.51:0.99:1:3.52 in four preparations indicate the formula $Ca_3(NH_4)_2(P_2O_7)_2 \cdot 6H_2O$.

The crystals are monoclinic tablets or plates, tabular on (001). Principal forms are (201), $(\bar{2}0\bar{1})$, {012} and $(00\bar{1})$—modifying forms, {010} and {110}. The crystals are biaxial (−) with $2V = 60°$ (obsd.) or 61° (calcd.), OAP = 010. $N_z \wedge a$ is 27° in acute β. The refractive indexes are $\alpha = 1.520$, $\beta = 1.528$, $\gamma = 1.531$.

The powder pattern is shown in Table I. Lattice constants, as determined from b- and c-axis rotation and Weissenberg patterns, are $a = 7.67$, $b = 11.51$, $c = 11.00$ Å. and $\beta = 92.5°$. The systematic extinctions, $h0l$ with $h + l$ odd and $0k0$ with k odd, indicate the space group C_{2h}^5–$P2_1/n$. With a unit-cell content of $2[Ca_3(NH_4)_2(P_2O_7)_2 \cdot 6H_2O]$, the calculated density is 2.08 g./cc.—exactly the density calculated from refractive indexes. Reflections hkl with $h + l$ odd are weak or absent and are elongated parallel to c^*. When these are ignored, the above-mentioned unit cell becomes b-centered, and a smaller unit cell can be selected with the symmetry C_{2h}^2–$P2_1/m$ or C_2^2–$P2_1$ and the dimensions $a = 6.85$, $b = 11.51$, $c = 6.57$ Å. and $\beta = 110.2°$; cell content, $Ca_3(NH_4)_2(P_2O_7)_2 \cdot 6H_2O$.

The smaller translational distances of the subcell, along with the symmetry elements of C_{2h}^5 of the larger cell, generate the remaining symmetry elements of C_{2h}^2, which suggests that C_{2h}^2 is the more probable of the two possible subcell space groups. For this to be true, NH_4^+ and $P_2O_7^{4-}$ must be in special positions in the subcell. The Ca^{++} may be in either general or special positions, but in either event there would be a 1-in-4 deficiency of calcium to fulfill space-group requirements. This may account for the diffuse reflections.

All the crystals suitable for single-crystal X-ray study had overgrowths of the other calcium ammonium pyrophosphate. A comparison of the relative intensities of the diffuse reflections of two crystals with different amounts of overgrowth indicated only a remote possibility that the overgrowths could have caused the diffuse reflections. Prevalence of the overgrowths suggests that the two pyrophosphates may be structurally related or at least have similar unit-cell dimensions in two directions.

Both crystalline salts have been synthesized also from tetrasodium pyrophosphate, calcium chloride and ammonium salts.

(1) E. H. Brown, J. R. Lehr, J. P. Smith, W. E. Brown and A. W. Frazier, THIS JOURNAL, **61**, 1669 (1957).

VIBRATIONAL SPECTRA OF DIMETHYL ETHER IN THE LOWER FREQUENCY REGION

BY YO-ICHIRO MASHIKO AND KENNETH S. PITZER

Contribution from the Department of Chemistry, University of California Berkeley, California

Received October 17, 1957

There is some ambiguity in the assignments of the two torsional oscillations of methyl groups about the C–O axes of the dimethyl ether molecule.[1,2] It is the purpose of the present study to ascertain these frequencies by further measurements of the Raman and infrared spectra. Only Ananthakrishnan[3] observed the line at 160 cm.$^{-1}$ in the Raman effect and there is disagreement

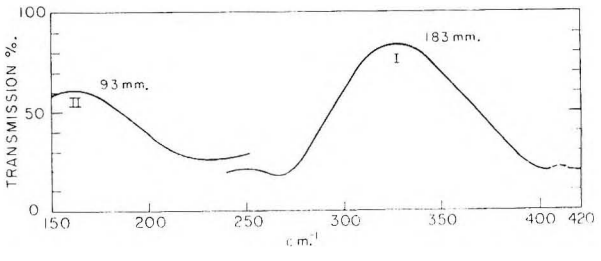

Fig. 1a.

(1) K. S. Pitzer, *J. Chem. Phys.*, **10**, 605 (1942).

(2) G. Herzberg, "Molecular Spectra and Molecular Structure. II. Infrared and Raman Spectra of Polyatomic Molecules," D. Van Nostrand Co., New York, N. Y., 1945, p. 353.

(3) R. Ananthakrishnan, *Proc. Ind. Acad. Sci.*, *A* **5**, 285 (1937).

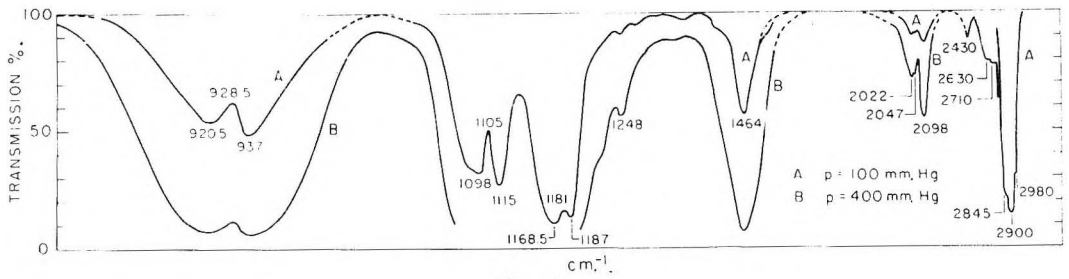

Fig. 1b.

among several authors in the observations near 300 cm.$^{-1}$.[3-6]

The Raman spectrum was taken in the liquid phase without a filter. The far infrared spectrum was studied through the region of 23 to 60 μ with a spectrometer described by Bohn, *et al.*[7] The usual rock salt region was studied with a Perkin–Elmer model 12C spectrometer. Both regions were measured in the gas phase under appropriate pressures.

Results obtained were as follows: Raman: 164(0b), (e); 251(0b), (e); 334(0), (e); 414(1vb), (e,K); 489(0b), (e); 530(0), (e,k); 918(7), (e,e,+, f,g,k,i); 1105(1b), (k); 1142(1vb), (k); 1377(0), (k); 1392(0), (k); 1451(4vb), (e,k); 2814(10), (q,p,l,k,i,e,f,g); 2685(7), (k,i,e,); 2886(1), (e,k); 2918(5), (q,p,k,i,e); 2951(4), (q,p,k,i,e); 2985(6), (q,p,k,i,e). Infrared (22–60 μ): 210–270 (m,b), ca. 410(m). Infrared (2.5–15 μ[8]): 921(m), 937(m), 1098(s), 1115(s), 1169(s), 1187(s), 1248(w) 1464 (m), 2022(w), 2047(w), 2098(m), 2430(w), 2630(w), 2710(w), 2845(s), 2900(s), 2980(s).

Here, frequencies are expressed in cm.$^{-1}$. (0), (7), etc., are the Raman intensities visually estimated on the plate; b or vb indicates that the line is broad or very broad; e, k, etc., denote the exciting mercury lines Hg-e, Hg-k, etc; w, m, and s denote weak, medium and strong infrared bands, respectively. The weakest Raman lines are on the border of detectability and cannot be taken as absolutely certain.

A plot of the infrared absorption spectrum is shown in Fig. 1.

In the lower frequency region there are five Raman lines and an infrared band in addition to 414 cm.$^{-1}$, which is clearly the C–O–C bending vibration. These are to be assigned as two modes of torsional vibration together with overtones and combinations. Assuming the point group of the molecule to be C_{2v}, one of these vibrations has a symmetry class A_2 (Raman active, infrared inactive) and the other B_2 (Raman and infrared active). One can quite definitely assign 265 cm.$^{-1}$ to B_2, since A_2 is infrared-inactive and 265 cm.$^{-1}$ is actually observed in the far infrared region. The peculiar infrared contour in the 200–270 cm.$^{-1}$ region is ascribed to a superposition of hot bands at lower frequencies on the 0–1 transition at 265 cm.$^{-1}$. From a consideration of the vibrational motions, B_2 should be higher in frequency than A_2[1,9] thus leaving 164 cm.$^{-1}$ to be assigned as the latter.

The B_2 torsional motion is expected to be very anharmonic, hence it is reasonable to take the 0–1 transition at 265 cm.$^{-1}$ and hot bands in the 200–230 cm.$^{-1}$ region. Similarly, 164 cm.$^{-1}$ should be regarded as a lowered value of the true fundamental frequency because of the contributions of the corresponding hot bands to the intensity of the Raman line. The true frequency was assumed to be 170 cm.$^{-1}$.

We propose as the torsional energy level pattern of dimethyl ether the following formula, which is limited in applicability to levels well below the top of the barriers to rotation.

$$\frac{E - E_0}{hc} = 170v_{A_2} + 265v_{B_2} - 3(v_{A_2} - 1)v_{A_2} - 21(v_{B_2} - 1)v_{B_2} - 35\,v_{A_2}v_{B_2}$$

where v_{A_2} and v_{B_2} are the quantum numbers of the two torsional vibrations. Thus, the remaining Raman bands at 334, 489 and 530 cm.$^{-1}$ have the v_{A_2} and v_{B_2} values (2,0), (0,2) and (2,1), respectively, in their upper states. The expected (1,1) band at 400 cm.$^{-1}$ would be buried under the strong 414 cm.$^{-1}$ band.

This pattern of levels is a refinement of the assignment of Hadni.[6] He has shown that this assignment of torsional vibrational levels yields thermodynamic properties in approximate agreement with those observed experimentally.[10-12]

We had hoped to discuss the vibrational assignment generally and to refine the thermodynamic calculations, but circumstances make it more feasible to continue this work separately.

Acknowledgment.—We wish to thank Dr. Roger Millikan and Dr. Edward Catalano for their aid in the far infrared measurements.

(4) S. C. Sirkar, *Ind. J. Phys.*, **7**, 257 (1932).
(5) N. G. Pai, *ibid.*, **9**, 121 (1934).
(6) A. Hadni, *Compt. rend.*, **239**, 349 (1954).
(7) C. R. Bohn, N. K. Freeman, W. D. Gwinn, J. L. Hollenberg and K. S. Pitzer, *J. Chem. Phys.*, **21**, 719 (1953).
(8) R. H. Pierson A. N. Fletcher and E. S. C. Gantz, *Anal. Chem.*, **28**, 1218 (1956), present an infrared spectrum identical to ours except for weak absorptions near 1600 and 1875 cm.$^{-1}$ which we did not find.
(9) K. S. Pitzer, *J. Chem. Phys.*, **12**, 310 (1944).
(10) G. B. Kistiakowsky and W. W. Rice, *ibid.*, **8**, 618 (1940).
(11) R. M. Kennedy, M. Sagenkahn and J. G. Aston, *J. Am. Chem. Soc.*, **63**, 2267 (1941).
(12) A. Eucken and E. U. Franck, *Z. Elektrochem.*, **52**, 195 (1948).

THE EFFECT OF AROMATIC NITRO COMPOUNDS ON MALONIC ACID

BY LOUIS WATTS CLARK

Department of Chemistry, Saint Joseph College, Emmitsburg, Maryland

Received October 21, 1957

Studies on the decarboxylation of malonic acid in non-aqueous, basic type solvents[1] have con-

(1) L. W. Clark, THIS JOURNAL, **62**, 79 (1958).

firmed the hypothesis of Fraenkel and co-workers[2] that malonic acid and the solvent form an intermediate transition complex, an electrophilic atom of the acid coördinating with a nucleophilic atom of the solvent. Analysis of the kinetic data for the reaction in 24 solvents indicated that, within the range of basicity where the malonic acid remains undissociated, the activation energy for the reaction decreases as the effective negative charge on the nucleophilic atom of the solvent increases.[1] A consideration of the structure of nitrobenzene and other aromatic nitro compounds suggested the possibility that such compounds possess sufficient nucleophilic character to coördinate with malonic acid and promote the decarboxylation reaction. Preliminary tests confirmed this suggestion. In order to obtain further information on the mechanism and energetics of the reaction kinetic studies were carried out in this Laboratory on the decomposition of malonic acid in four aromatic nitro compounds. The results of this investigation are reported herein.

Experimental

Reagents.—(1) The malonic acid was analytical reagent grade, 100.0% assay. (2) Solvents: (a) nitrobenzene, reagent grade, b.p. 210–212°; (b) *o*-nitrotoluene, reagent grade, m.p. −4 to −3°, sp. gr. 1.163; (c) *m*-nitrotoluene, highest purity grade, m.p. 15–16°; (d) 1,3-dimethyl-2-nitrobenzene, highest purity grade, m.p. 13–15°. Each sample of each liquid was distilled into the reaction flask immediately before the beginning of the decarboxylation experiment.

Apparatus and Technique.—The kinetic experiments were conducted in a constant-temperature oil-bath (±0.1°) by the technique previously described.[3] Temperatures were determined by means of a thermometer calibrated by the U. S. Bureau of Standards. In each experiment a 0.1857-g. sample of malonic acid (the amount required to produce 40.0 ml. of CO_2 at STP on complete reaction) was introduced in the usual manner into the reaction flask containing 50.0 ml. of solvent saturated with dry CO_2 gas.

Results and Discussion

The rate of reaction was measured in each solvent at three different temperatures over a 20° temperature range (Table I). When log $(a - x)$ was plotted against t (a being the final or maximum volume of CO_2 produced in an experiment and x the volume of CO_2 produced at the time t) straight lines resulted over the greater part of the reaction, indicating that the decomposition of malonic acid in aromatic nitro compounds is pseudo-first-order.

The parameters of the Eyring equation are listed in Table II. Data for aniline and *m*-toluidine are included for comparison.[1]

Nitrobenzene resembles aniline structurally in having a nitrogen atom joined to the benzene ring and to two other identical atoms. It differs from aniline in that oxygen is much more electronegative than hydrogen and that resonance occurs in the nitro group but not in the amino group. The essential condition for the formation of a transition complex between malonic acid and solvent is that the molecule of the solvent be sufficiently nucleophilic to coördinate with the malonic acid but not sufficiently nucleophilic to ionize the acid.[2]

(2) G. Fraenkel, R. L. Belford and P. E. Yankwich, *J. Am. Chem. Soc.*, **76**, 15 (1954).

(3) L. W. Clark, THIS JOURNAL, **60**, 1150 (1956).

TABLE I

APPARENT FIRST-ORDER RATE CONSTANTS FOR THE DECARBOXYLATION OF MALONIC ACID IN SEVERAL AROMATIC NITRO COMPOUNDS AT VARIOUS TEMPERATURES

Solvent	Temp. (°C.) (cor.)	Specific reaction velocity constant (sec.$^{-1}$)
Nitrobenzene	139.31	0.000268
	153.05	.000859
	161.78	.001711
o-Nitrotoluene	149.65	0.000671
	161.55	.001487
	167.37	.002168
m-Nitrotoluene	128.29	0.000910
	144.11	.003310
	149.94	.005210
2-Nitro-*m*-xylene	147.50	0.000398
	159.38	.001132
	167.67	.002260

TABLE II

KINETIC DATA FOR THE DECOMPOSITION OF MALONIC ACID IN SEVERAL AROMATIC NITRO COMPOUNDS AND AMINES

Solvent	$\Delta H‡$ (cal.)	$\Delta S‡$ (e.u.)	$k_{150°} \times 10^5$ (sec.$^{-1}$)
(1) 2-Nitro-*m*-xylene	30,000	− 3.12	16.2
(2) Nitrobenzene	28,100	− 7.15	28.3
(3) Aniline[1]	26,900	− 4.45	500.0
(4) *m*-Nitrotoluene	26,200	− 7.46	237.0
(5) *m*-Toluidine[1]	26,100	− 5.80	592.0
(6) *o*-Nitrotoluene	23,500	−17.92	33.6

The enthalpies of activation for the reaction in 2-nitro-*m*-xylene and in nitrobenzene (lines 1 and 2 of Table II) are higher than in aniline (line 3), suggesting that in these first two solvents the effective negative charge on the nucleophilic atom of the solvent is lower than in aniline.[1] In *m*-nitrotoluene and in *o*-nitrotoluene the enthalpies of activation are lower than in aniline, suggesting that in these solvents the effective negative charge on the nucleophilic atom of the solvent is higher than in aniline. A methyl group in the *meta*-position (line 4) increases the effective negative charge on the nucleophilic atom of the nitro group, by a positive inductive effect, sufficient to lower the enthalpy of activation below that of aniline, but has a relatively small steric effect as shown by the relative values of $\Delta S‡$ for nitrobenzene and *m*-nitrotoluene (lines 2 and 4). The large decrease in $\Delta H‡$ and the slight change in entropy results in a large increase in the rate of reaction on going from nitrobenzene to *m*-nitrotoluene. A methyl group in the *ortho*-position (line 6) decreases $\Delta H‡$ considerably due to the +I effect, and at the same time has a pronounced effect on $\Delta S‡$, a result which is consistent with the *ortho* effect.[4]

The effect of substitution of methyl groups in both *ortho* positions (line 1) appears to be anomalous, and suggests a possible difference in orientation of the solute molecules with respect to malonic acid between this liquid and the other nitro compounds studied.

(4) L. P. Hammett, "Physical Organic Chemistry," McGraw-Hill Book Co., Inc., New York, N. Y., 1940, p. 204.

Acknowledgments.—The support of this research by the National Science Foundation, Washington, D. C., is gratefully acknowledged. Distillations of the solvents were carried out by Miss Dolores Sicilia.

ON THE INTERPRETATION OF HYDRODYNAMIC DATA FOR DILUTE PROTEIN SOLUTIONS

BY HAROLD A. SCHERAGA AND LEO MANDELKERN

Department of Chemistry, Cornell University, Ithaca, New York, and Polymer Structure Section, National Bureau of Standards, Washington 25, D. C.

Received September 30, 1957

Several questions have recently been raised[1] about our method of interpretation of hydrodynamic data on dilute protein solutions,[2] and about a recent application of this method to measurements on bovine serum albumin.[3] We believe that the argument developed by Tanford,[1] in this connection, is misleading and thus necessitates further clarification.

As stated in his equation 1, Tanford chooses to express the effective hydrodynamic volume of a dissolved protein molecule in terms of its partial specific volume and a quantity δ_1, which he defines[4] as "the number of grams of solvent incorporated in the *hydrodynamic* particle per gram of dry protein." The arbitrariness of this assumption and its disregard of physical reality have already been discussed in great detail both by us[2] and by Sadron,[5] whose treatment is essentially equivalent to ours.

In addition to this arbitrary division of the effective *hydrodynamic* volume into two terms $(M/N)\bar{v}_2$ and $\delta_1(M/N)v_1^0$, Tanford's procedure is also very misleading since one is thereby tempted to attach reality to δ_1 as the mass of water actually bound to one gram of protein. Tanford, in fact, is inconsistent on this point since he makes this latter identity when he asserts[1] that the validity of his equation 1 is confirmed by Wang's considerations[6] of the self-diffusion of water in dilute aqueous protein solutions. It is incorrect to obtain δ_1 from self-diffusion since it is clearly stated by Wang and quite apparent in his theoretical development that the hydrodynamic behavior of the dissolved protein molecule does not enter into his calculation. Thus, it is not surprising that in Wang's treatment the appropriate and correct volume to be considered is that which describes the domain of the molecule, with δ_1, in this instance, being the specific solvation of the actual protein molecule. However, this latter conclusion is limited to problems involving the self-diffusion of water and has no application to the present matter concerned with the interpretation of the hydrodynamic data of protein solutions. A similar error is committed by Tanford and Buzzell,[4] who assume that the value of δ_1 obtained from intrinsic viscosity data and the aforementioned definition of the effective hydrodynamic volume is comparable with the value obtained from self-diffusion experiments. Hence, we re-affirm the statement[3] that "it is impossible to relate the effective hydrodynamic volume of a dissolved protein molecule to its partial specific volume."

Tanford agrees that two hydrodynamic properties have to be measured in order to deduce both the size and the shape of the effective hydrodynamic particle. However, he tries to imply a greater sensitivity in the interpretation of hydrodynamic data than actually exists by stating that our β (and presumably also our δ) function represents a poor choice of measurements. As emphasized previously,[2,3] whereas a single property (such as viscosity) varies considerably with axial ratio for *constant volume*, one doesn't know in advance what the volume is. Hence, one must use a function (*e.g.*, our β or δ function, or any other equivalent one) which depends on a pair of hydrodynamic measurements. A few calculations will show that any such function, which combines two hydrodynamic measurements, is very insensitive to changes in axial ratio.

(1) C. Tanford, THIS JOURNAL, **61**, 1023 (1957).

(2) H. A. Scheraga and L. Mandelkern, *J. Am. Chem. Soc.*, **75**, 179 (1953).

(3) G. I. Loeb and H. A. Scheraga, THIS JOURNAL, **60**, 1633 (1956).

(4) C. Tanford and J. G. Buzzell, THIS JOURNAL, **60**, 225 (1956).

(5) C. Sadron, *Prog. in Biophys.*, **3**, 237 (1953).

(6) J. H. Wang, *J. Am. Chem. Soc.*, **76**, 4755 (1954).

EXTRACTION OF INORGANIC SALTS BY 2-OCTANOL. III. ZINC AND CADMIUM CHLORIDES. AQUEOUS PHASE ACTIVITIES

BY T. E. MOORE, NORMAN G. RHODE AND ROBERT E. WILLIAMS

The Department of Chemistry, Oklahoma State University, Stillwater, Oklahoma

Received October 10, 1957

Preliminary experiments in these laboratories have shown that the extraction of both $Zn(ClO_4)_2$ and $Cd(ClO_4)_2$ from aqueous solutions (4 *m*) occurs readily. When solubilities of $ZnCl_2$ and $CdCl_2$ in 2-octanol are compared, however, a large difference is found, $ZnCl_2$ being over 1000 times as soluble at 25°. This suggested that effective separation might be achieved through the 2-octanol extraction of aqueous mixtures of the chlorides. This is in general agreement with earlier observations regarding the non-specificity of 2-octanol as an extraction solvent for metal perchlorates contrasted to the much more specific behavior of the corresponding chlorides.[2]

To test this theory, six series of solutions were extracted with the octanol at 25°. Figure 1 presents the variation of the distribution coefficients, k_d, of $ZnCl_2$ and $CdCl_2$ in the different series. The distribution coefficient is here defined as the ratio of the molal concentration in the non-aqueous phase to the molal concentration in the aqueous phase. The equilibrium mixtures of octanol and water are considered as solvents in each phase.

It is evident from the figure that separation factors, s, of the order of 50–60 ($s = k_d(ZnCl_2)/k_d(CdCl_2)$) are obtained with the $ZnCl_2$–$CdCl_2$ mixtures investigated. These values, however, are only about 50% of the values calculated from

(1) Supported under Contract AT(11-1)-71 No. 1 with the U. S. Atomic Energy Commission

(2) T. E. Moore, Roy J. Taran and Paul C. Yates, THIS JOURNAL, **59**, 90 (1955).

the ratio of the distribution coefficients in the binary solutions, the experimental results showing a definite mutual extraction-promoting effect of $ZnCl_2$ on the extraction of $CdCl_2$ and of $CdCl_2$ on the extraction of $ZnCl_2$. Whereas this mutual promoting effect (curves C and C′) may be regarded as normal, the existence of maxima and minima in the distribution coefficient curves (for the mixtures with $CaCl_2$, curves D and D′) has not been previously observed.

In order to understand better the interactions which are responsible for the concentration dependence of the distribution coefficients in these systems, the activity of $CdCl_2$ in 1 *m* $CdCl_2$ mixtures with $ZnCl_2$ and the activity of $ZnCl_2$ in 0.5 *m* $ZnCl_2$ mixtures with $CdCl_2$ were measured. Figure 2 shows ratios of the stoichiometric $CdCl_2$ activity coefficient in the mixtures to the activity coefficient of a 1 *m* $CdCl_2$ solution. In the same figure there are shown also the non-aqueous-phase acvitity coefficients calculated from the aqueous-phase activities and the distribution coefficients.[3] These are expressed relative to the octanol-phase activity coefficient of $CdCl_2$ calculated for zero molal $ZnCl_2$.

Unfortunately hydrolysis and the precipitation of a solid phase prevented measurements at concentrations above 1.5 *m* $ZnCl_2$; it is evident, however, that over the concentration range up to 1.5 *m* $ZnCl_2$ the observed increases in the $CdCl_2$ distribution coefficient can be largely attributed to the increases in the aqueous-phase activity coefficient of $CdCl_2$, arising probably from the effects of the ionic hydration of $ZnCl_2$.[4] From the constancy of the octanol-phase activity coefficients it is concluded that, as in the case of its aqueous solutions, $CdCl_2$ is only slightly dissociated in octanol.

The unusual shape of the distribution coefficient curve for $ZnCl_2$ in mixtures with $CaCl_2$ (Fig. 1) is better understood by reference to Fig. 3 where the aqueous-phase activity of $ZnCl_2$ is plotted as a function of the $CaCl_2$ concentration. Qualitatively, the initial rise in the activity curve can be interpreted as showing the effect of the common chloride ion and of ionic hydration. At higher concentrations of $CaCl_2$, however, ionic association reactions leading to the formation of ions such as $ZnCl^+$ and $ZnCl_4^{=}$[5] would cause the activity to reach a maximum and then fall to smaller values as the reactions become more complete. The literature value for the dissociation constant for the 1:1 chloro complex shows that it is but a weak complex (K = 0.65), and since the 1:1 complex is usually the most stable, higher complexes would be of importance only at high $CaCl_2/ZnCl_2$ ratios in concentrated solutions. The minimum at about 4 *m* $CaCl_2$ and the subsequent rise in the activity values then follow from the removal of additional solvent by $CaCl_2$ hydration at still higher concentrations of $CaCl_2$. The similarity of curve D of Fig. 1 and the curve for the aqueous-phase activity

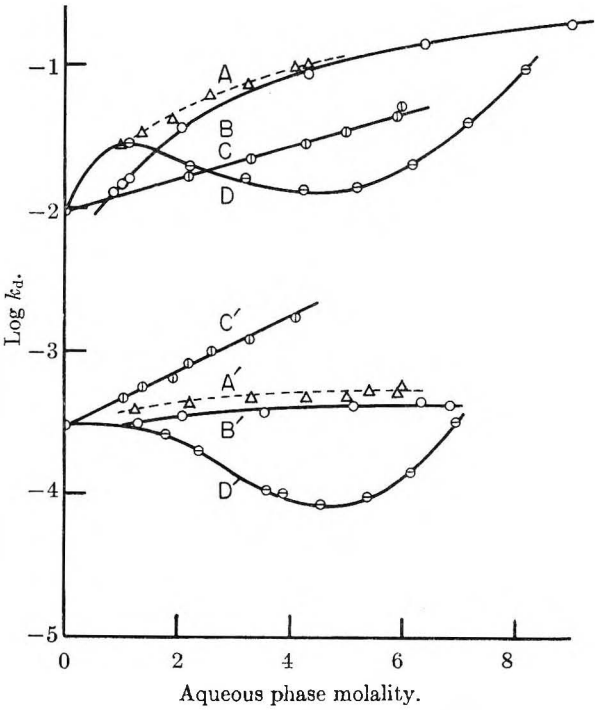

Fig. 1.—Distribution coefficients: A, $ZnCl_2$ + 1 *m* $CdCl_2$; B, $ZnCl_2$; C, 0.5 *m* $ZnCl_2$ + $CdCl_2$; D, 0.5 *m* $ZnCl_2$ + $CaCl_2$; A′, $CdCl_2$ + 0.5 *m* $ZnCl_2$; B′, $CdCl_2$; C′, 1 *m* $CdCl_2$ + $ZnCl_2$; D′, 1 *m* $CdCl_2$ + $CaCl_2$.

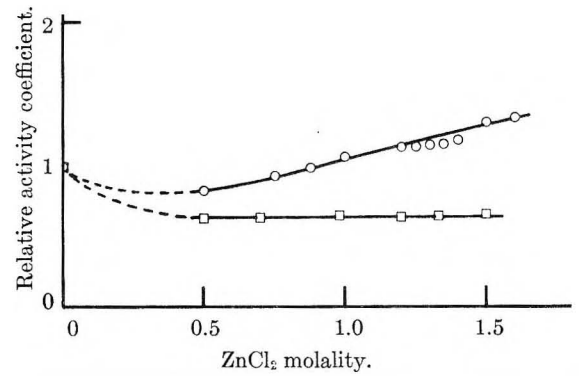

Fig. 2.—Activity coefficients of $CdCl_2$ in mixtures with $ZnCl_2$: ○, aqueous-phase coefficients relative to 1 *m* aqueous $CdCl_2$; □, calculated octanol-phase coefficients relative to that of an octanol solution of $CdCl_2$ in equilibrium with 1 *m* aqueous $CdCl_2$.

of $ZnCl_2$ (Fig. 3) is obvious and suggests a close correlation between the aqueous-phase activity and the distribution coefficient. It appears likely, therefore, that the anomalous behavior of the distribution coefficient in this system arises principally from aqueous-phase interactions of the kind described. A similar explanation should hold for the effect of $CaCl_2$ on the extraction of $CdCl_2$.

The results of these experiments further emphasize the difficulties in developing a really comprehensive theory for the extraction of metal halides in concentrated solutions. Diamond[6] has attempted this but has not quantitatively dealt with the effects of solvation in the aqueous-phase.

(3) T. E. Moore, R. W. Goodrich, E. A. Gootman, B. S. Slezak and P. C. Yates, *ibid.*, **60**, 564 (1956).

(4) R. H. Stokes and R. A. Robinson, *J. Am. Chem. Soc.*, **70**, 1870 (1948).

(5) R. A. Robinson and R. O. Farrelly, THIS JOURNAL, **51**, 704 (1947).

(6) R. M. Diamond, *ibid.*, **61** 69 (1957).

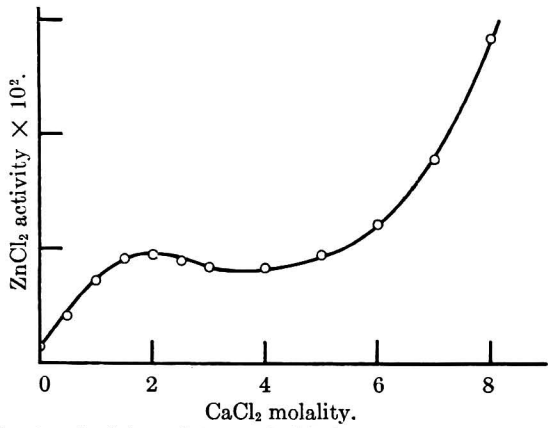

Fig. 3.—Activity of 0.5 *m* $ZnCl_2$ in mixtures with $CaCl_2$.

Experimental

Materials.—All chemicals were C.P. or reagent grades. The 2-octanol was the best grade furnished by the Matheson Coleman and Bell Co.

Extraction Procedures.—The equilibrations were made from approximately equal weights of the aqueous solutions and octanol sealed in glass-stoppered flasks and mechanically agitated overnight at 25.0 ± 0.1°. The phases were separated and analyzed.

Analytical Procedures.—The analytical procedures were for the most part standard. Octanol phases were back-extracted with water and zinc and cadmium determined polarographically either alone or together. Chloride was determined in the back-extracted samples volumetrically with $AgNO_3$.

The aqueous phases were similarly analyzed, calcium being found by difference.

Activity Measurements.—The activities of both $CdCl_2$ and $ZnCl_2$ were determined by electromotive force measurements. The cell was a conventional H-type cell with the metal amalgam electrode in one arm and the Ag–AgCl electrode in the other. The latter was prepared by the thermal reduction of Ag_2O according to the recommendations of Taniguchi and Janz.[7] Interagreement among the electrodes was of the order of 0.05 mv. The zinc amalgam electrode was an amalgam pool (*ca.* 2.5%). The e.m.f. values of the cell at equilibrium were very constant, varying by not more than 0.03 mv. over a period of several hours. The cadmium amalgam electrode (*ca.* 5.5%) also was a pool electrode and again the e.m.f. values at equilibrium were quite constant, the average deviation being only about 0.03 mv.

The electrolytic preparation of the amalgams followed the directions of Richards.[8]

In order to determine the standard potentials of the cells, the electromotive forces of standard solutions of $ZnCl_2$ and of $CdCl_2$ were measured. For $ZnCl_2$ the concentrations were 0.4320 and 1.031 *m*, and for $CdCl_2$ they were 0.0500 and 0.2325 *m*. Zinc chloride activity values were taken from those listed by Robinson and Stokes[9]; $CdCl_2$ activity values were those given by Harned and Fitzgerald.[10] The E^0 values at the two reference concentrations differed by 0.06 and 0.2 mv. for $ZnCl_2$ and $CdCl_2$, respectively. A potential of 0.2224 v. was used for the Ag-AgCl electrode.

All solutions were prepared by weight from stock solutions whose concentrations had been determined electrolytically. Anhydrous $CaCl_2$ was added to the ZnCl solutions to obtain the mixtures of $CaCl_2$ and $ZnCl_2$. Oxygen was removed from the solutions by a stream of oxygen-free nitrogen before the measurements were made.

(7) H. Taniguchi and G. J. Janz, "The Preparation and Reproducibility of the Thermal-Electrolytic Type Silver–Silver Chloride Electrodes," ARDC Contract No. AF 18(600)-333, Technical Note No. 3, 1955.

(8) T. W. Richards, "Electrochemical Investigation of Liquid Amalgams of Thalium, Tin, Zinc, Cadmium, Lead, Copper and Lithium," Carnegie Institution Publication, Washington, D. C., 1909.

(9) R. A. Robinson and R. H. Stokes, *Trans. Faraday Soc.*, **36**, 740 (1940).

(10) H. S. Harned and M. E. Fitzgerald, *J. Am. Chem. Soc.*, **58**, 2624 (1936).

THE SURFACE STRUCTURE OF SODIUM CHLORIDE

By L. G. Harrison[1] and J. A. Morrison

Division of Pure Chemistry, National Research Laboratories, Ottawa, Canada

Received September 25, 1957

Studies of isotopic exchange between gaseous chlorine and small particles of sodium chloride already have been reported.[2,3] Exchange of the surface layer of the solid obeyed first-order kinetics and proceeded rapidly at room temperature (velocity constant ~0.012 min.$^{-1}$). The energetics of the reaction suggested that the surface of the particles differed markedly from a normal crystal plane; however the possibility that their surface structure was strongly affected by adsorption of atmospheric gases during preparation and storage had to be considered. Accordingly, a similar investigation has been begun with films of sodium chloride prepared *in vacuo* and immediately exposed to carefully purified chlorine. Preliminary results indicate that exchange of the surface layer still occurs very readily, but that the first-order process is preceded by an extremely rapid exchange (within the first minute or so) amounting to about half the total reaction. This type of behavior had been observed in some of the earliest experiments on particles prepared and handled in dry nitrogen and dry air, and was attributed to impurities in the chlorine gas.[2] However, re-examination of these results in the light of the current experiments suggests an alternative explanation.

Experimental

Chlorine gas was circulated by convection in a closed system consisting of the jacket of a Geiger counter and a 15 mm. diameter Pyrex tube upon which the sodium chloride films were deposited. The counter was connected to a counting rate meter and graphic recorder. The sodium chloride (0.1 to 0.4 g.) containing radioactive ^{36}Cl was evaporated into the tube from a platinum crucible which was held on a quartz carriage and was heated by an induction furnace. The system, with the crucible *in situ*, was previously baked out at 400° and evacuated to ~10^{-8} mm.; the pressure was read with a Bayard–Alpert ionization gage. The evaporation took about an hour and the pressure never exceeded 10^{-6} mm. The crucible was then withdrawn by a magnetic device and the system sealed off (maximum pressure ~10^{-5} mm.). The chlorine gas, purified by two distillations (at 760 and ~1 mm.) and stored over a film of sodium chloride, was admitted through a break seal to give a pressure between 10 and 40 cm. The exchange reaction was followed for at least 24 hours, and the vessel was thereafter connected to an adsorption apparatus. The surface areas of the films, estimated by adsorption of nitrogen at 77°K., were ~10 m.^{2}/g.; the surface present in an experiment was 1–4 m.^{2}. The maximum amount of gas available to contaminate the film was estimated from the pressures during evaporation and sealing and the pumping speeds in the system.

Results and Discussion

Figure 1 is a typical record of the radioactivity of the gas phase, C (the background has been subtracted), showing an initial very rapid reaction up to C_1 and a subsequent process which obeys the first-order law

(1) National Research Laboratories Postdoctorate Research Fellow.

(2) L. G. Harrison, J. A. Morrison and G. S. Rose, Second International Congress of Surface Activity, London, April, 1957.

(3) L. G. Harrison, J. A. Morrison and G. S. Rose, This Journal, **61**, 1314 (1957).

$$C = C_1 + C_2\{1 - \exp(-kt)\}$$

Values of the rate constant k and of C_1 as a fraction of the over-all reaction $(C_1 + C_2)$ are given in Table I. In two of the three experiments, the values of k agree well with those for particles prepared in nitrogen (1.2×10^{-2} min.$^{-1}$), sintered after preparation ($1.3 - 2.3 \times 10^{-2}$ min.$^{-1}$), and precipitated from solution (0.9×10^{-2} min.$^{-1}$). The results thus lend further support to the conclusion[2] that the first-order reaction involves the solid surface in thermal equilibrium and not an impurity or metastable surface structure specific to the method of preparation.

TABLE I

Run	$C_1/(C_1 + C_2)$	$10^2 k$, min.$^{-1}$
1	0.49	1.7
2	.51	0.3
3	.48	1.0

The very rapid initial process was previously observed only in some early experiments with relatively impure chlorine, and was ascribed to impurities.[2] In the present experiments, the maximum amount of impurity present was very much less and corresponded to a different fraction of the total surface (in the range 10–40%) in each experiment. The reappearance and reproducibility of the very rapid reaction under these conditions suggest that it is not to be accounted for in terms of impurities.

Re-examination of the earlier results has shown that both the method of preparation and the age of the particles may be significant; Table II is a summary of the data from this point of view, and shows the following features of the reaction: (i) It has appeared in every experiment with particles prepared by volatilization in nitrogen or under vacuum and used within four months; $C_1/(C_1 + C_2)$ is reasonably reproducible. (ii) It has not been observed with particles over six months old or material precipitated from solution. (iii) It has not appeared with sintered particles, except for one specimen, from a freshly prepared lot (D), which was given a very mild sintering treatment.

TABLE II

Sodium chloride particles Age, weeks	Lot	No. of expts.	$C_1/(C_1 + C_2)$ Range	Mean
0	Evap. films	3	0.48–0.51	0.49
2	A	1	.....	.43
0–4	B	3	0.44–0.54	.49
10–16	C	4	0.30–0.46	.40
55	A	1	.....	0
49–68	B	5	0	0
30	D	1	.....	0
9	From soln.	1	.....	0
2	D sintered[a]	1	.....	0.30
21	C sintered[a]	1	.....	0
52–63	B sintered[a]	3	0	0

A,B,C,D—4 lots of particles prepared by volatilization in nitrogen

[a]Lot	Sintering procedure	Final area/initial area
D	Heated *in vacuo*	0.6
C	Contact with moist air	.2
B	Heated in chlorine	< .3

From this analysis of the results, the phenomenon may be attributed tentatively to the existence, on particles prepared by volatilization at high temperatures, of metastable surface structure, which reverts to equilibrium very slowly at room temperature and more rapidly on sintering. This structure appears to cover at least half the total surface; the over-all exchange $(C_1 + C_2)$ has been found to correspond roughly to the B.E.T. surface area. The remainder of the surface is at equilibrium and exchanges by the first-order process. The reproducibility of $C_1/(C_1 + C_2)$ is a remarkable feature for which we have at present no explanation, and an attempt to find a continuous change in this ratio with the progress of aging or sintering is obviously required.

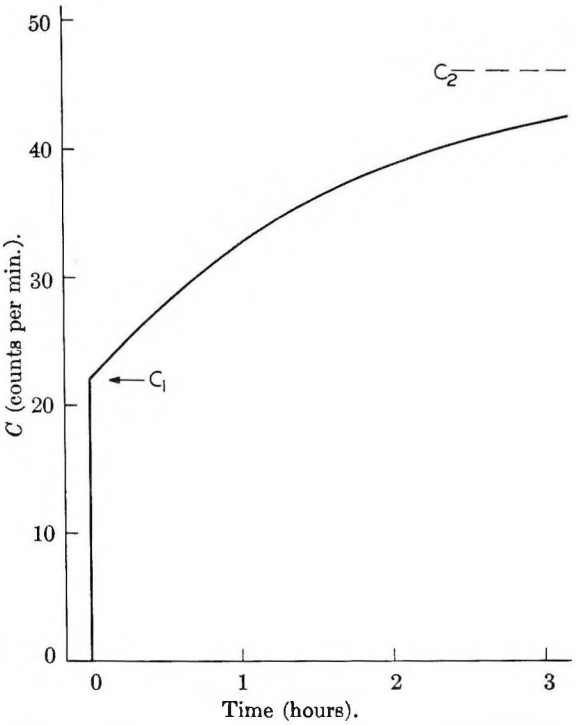

Fig. 1.—Results of run 3, showing the two successive reactions, plotted from a continuous record of the radioactivity of the gas phase.

A priori, it seems quite likely that similar phenomena may occur on many other solid surfaces, and particularly on evaporated films. From the point of view of studying such surfaces, perhaps the most interesting feature of the present results is the great length of time during which the surface structure seems to be changing.

The authors wish to thank Dr. R. Rudham for helpful suggestions on the experimental technique, Mr. G. Ensell for the construction of special glassware, and Mr. J. E. Desnoyers for assistance with the adsorption measurements.

PYROLYSIS OF DECABORANE

BY BERNARD SIEGEL AND JULIUS L. MACK

Research and Development Department, U. S. Naval Powder Factory, Indian Head, Md.

Received January 6, 1958

Very little has been reported about this reaction. In a paper on the chemical and physical properties

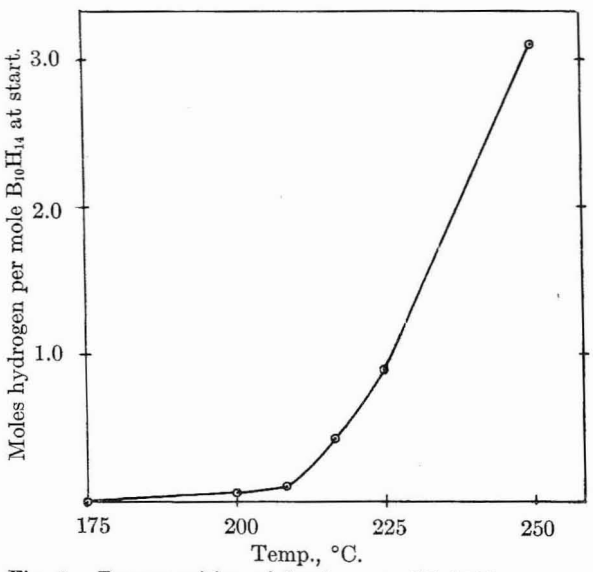

Fig. 1.—Decomposition of decaborane, 175–250°: comparison of hydrogen evolutions after one hour.

of decaborane,[1] Stock reported that the latter was not appreciably decomposed after long heating at 200° but that it did decompose extensively, to hydrogen and non-volatile solids of approximate composition $BH_{0.6}$, after long heating at 250°. We were therefore surprised to find, during experiments on the preparation of non-volatile boron hydride solids, that decaborane is far less thermally stable than was implied by Stock's observations. This led to the present study, in which decaborane samples were decomposed in evacuated glass bulbs over a wide temperature range, taking quantitative data on the disappearance of decaborane and the formation of products.

Experimental

Purification of Decaborane.—Since small amounts of impurities might possibly affect the rates of decaborane pyrolysis, the latter (obtained from the American Potash Corporation) was very carefully purified. It was recrystallized from methylene chloride, followed by two successive vacuum sublimations. The purified decaborane melted sharply at 99.5°. Mass spectrometric analysis indicated the absence of even traces of volatile impurities. Infrared analysis failed to detect impurities. An ultimate method of elemental analysis[2] gave a value of 11.53% hydrogen compared to a theoretical value of 11.54%.

Pyrolyses.—The decaborane samples, in Pyrex bulbs fitted with break seals, were sealed onto a high vacuum apparatus and thoroughly evacuated. They were subsequently sealed and placed in a thermostated oven kept within ±0.2°. Zero time for the pyrolysis was after a short period to allow the oven to reach the reaction temperature after inserting the reactor, usually about ten minutes. Upon removal from the oven the reactions were quenched by immersal of the reactors in cold water.

Analyses.—The hydrogen evolved was determined by resealing the bulb to a high vacuum apparatus, freezing the bulb with liquid nitrogen, and transferring the hydrogen, with a Toepler pump, to a calibrated volume whose pressure could be measured. After removal of the evolved hydrogen, the liquid nitrogen-bath was removed and the condensable contents of the bulb were transferred to another bulb for mass spectrometric analysis. In some runs, the entire reaction contents were examined mass spectrometrically without prior removal of the hydrogen.

After removal of the hydrogen and condensable material, the bulb was taken off the high vacuum apparatus and smashed. Its contents were analyzed for unreacted decaborane by extraction with ethyl acetate, and then ultraviolet spectrophotometric analysis of the ethyl acetate solution, using the wave length, 2650 Å. Since it was difficult to separate the non-volatile boron hydride solids from bits of glass, the compositions of these solids were calculated from the decaborane and hydrogen data.

(1) A. Stock and E. Pohland, *Ber.*, **62**, 90 (1929).

(2) E. L. Simons, E. W. Balis and H. A. Liebhafsky, *Anal. Chem.*, **25**, 635 (1953).

Results

The results are summarized in Table I. They show that decaborane is far more susceptible to thermal decomposition than is implied by the few semi-quantitative observations made previously.[1] Most of the present pyrolyses were carried out under conditions chosen so that the entire sample was in the gas phase within minutes after exposure to the reaction temperature. These resulted in the formation of amorphous polymers evenly coated on the walls of the reactors. In one case conditions were chosen for a liquid phase reaction in which an appreciable hydrogen atmosphere would form (5.9 atm. after 15 hours). This reaction was faster than the corresponding gas phase reaction and resulted in a glassy polymer, formed in a lump where the decaborane was introduced.

TABLE I

Time, hr.	Temp., °C.	Moles H_2 evolved per mole decaborane at start	Decomposition, %	Empirical formula of polymer
1[a]	175	0	0	No polymer formed
1[a]	200	0.0625	3.13[b]	.....
1[a]	208	.106	5.30[b]	.....
1[a]	217	.432	21.6[b]	.....
1[a]	225	.901	45.4	$(BH_{1.00})_x$
1[a]	250	3.10	100	$(BH_{.78})_x$
8[a]	200	0.687	30.7	$(BH_{.95})_x$
19[a]	200	1.65	66.1	$(BH_{.90})_x$
15[c]	200	1.826	89.6	$(BH_{.99})_x$

[a] 1.000 gram of $B_{10}H_{14}$ in 1 liter bulbs; gas phase reactions. [b] Based on $B_{10}H_{14} \rightarrow 10/x(BH)_x + 2H_2$. [c] 0.125 gram $B_{10}H_{14}$ in 12.5-cc. bulb; a liquid phase reaction.

In every pyrolysis, hydrogen and non-volatile boron hydrides were the principal products. However trace quantities of pentaborane-9 were also products, even in the pyrolysis at 225°. The latter was the only other product found by mass spectrometric analysis.

Acknowledgment.—The authors wish to acknowledge the helpful advice of Dr. Sol Skolnik. Dr. George Wilmot performed the infrared analyses. The mass spectrometric analyses were performed by Mrs. Mary Joslyn of the National Bureau of Standards under the direction of Dr. Fred Mohler.

EQUILIBRIUM DISTRIBUTION OF MASS IN CENTRIFUGAL FIELDS

BY MARSHALL FIXMAN

Department of Chemistry, Harvard University, Cambridge, Massachusetts

Received September 27, 1957

The equations governing the distribution of mass[1] may be given a particularly simple and

(1) R. J. Goldberg, THIS JOURNAL, **57**, 194 (1953).

rigorous form by a suitable selection of variables. We hope also to illuminate the significance of the buoyant force on a macromolecule in solution. The equilibrium distribution of n components in an external field of acceleration $\mathbf{g}$ is determined by $\nabla\mu_i = \mathbf{g}$, $i = 1, 2, \ldots, n$, where μ_i is the chemical potential (in units of energy/mass). Let the concentrations (in mass/volume), of the n components be ρ_i. Then

$$\nabla\rho_i = \sum_{k=1}^{n} (\partial\rho_i)/\partial\mu_k)_\mu \mathbf{g} \qquad (1)$$

where we suppress a subscript indicating constant temperature. In the derivative all μ except μ_k are held constant. We introduce the partial specific volumes $\bar{v}_i$ by means of the equation

$$\sum_{k=1}^{n} \bar{v}_k(\partial\rho_i/\partial\mu_k)_\mu = \kappa\rho_i \qquad (2)$$

where κ is the compressibility. Equation 2 is derived readily from the Gibbs-Duhem equation and $\bar{v}_i = \kappa(\partial P/\partial\rho_i)\rho$, where P is the pressure. We multiply eq. 2 by an arbitrary constant Q and subtract the result from eq. 1

$$\nabla \ln \rho_i = \mathbf{g}\left[\sum_{k=1}^{n} (1 - Q\bar{v}_k)(\partial \ln \rho_i/\partial\mu_k)_\mu + Q\kappa\right] \qquad (3)$$

We will select a convenient value of Q later. Now we use an expression from Kirkwood and Buff[2]

$$RT(\partial \ln \rho_i/\partial\mu_k)_\mu = M_k\delta_{ik} + N\rho_k G_{ik} \qquad (4)$$

where M_k is the molecular weight of component k, R is the gas constant, N is Avogadro's number, δ is the Kronecker δ, and G_{ik} is a cluster integral

$$G_{ik} = \int [g_{ik}(R) - 1]\, d\mathbf{R}$$

where g_{ik} is a radial distribution function. Equation 4 is valid for non-electrolytes, or for electrolytes if applied to individual ion species. If i and k refer to macromolecules, G_{ik} reduces to an osmotic second virial coefficient G_{ik}^0 in the limit of low macromolecule concentration. Thus $\pi = RT\cdot[\Sigma(\rho_i/M_i) - \Sigma\Sigma(\rho_i\rho_k/2M_iM_k)G_{ik}^0 + \ldots]$, where the sums go over macromolecular components i, k, ...

In terms of the G_{ik}, eq. 3 becomes

$$RT\nabla \ln \rho_i = \mathbf{g}\left[(1 - Q\bar{v}_i)M_i + N\sum_{k=1}^{n} (1 - Q\bar{v}_k)\rho_k G_{ik} + RTQ\kappa\right] \qquad (5)$$

In the subsequent discussion we take i to be a macromolecule. In the particular case where there is only one solvent component, say n, all macromolecule–solvent interactions may be made to vanish identically from eq. 5 by taking $Q = 1/\bar{v}_n$. If several solvent components are present, macromolecule–solvent interactions cannot be rigorously eliminated from eq. 5. If, however, the solvent molecules are much smaller than the macromolecules, and do not interact with macromolecules strongly or specifically, we may assume that G_{ik} is independent of which solvent component k is chosen. (Under these circumstances, G_{ik} will equal the "volume" of macromolecule i). Then macromolecule–solvent interactions may be removed explicitly from eq. 5 by setting $\Sigma(1 - Q\bar{v}_k)\rho_k = 0$, where the sum goes over solvent components. Thus

$$Q = \rho_s/\varphi_s \qquad (6)$$

where ρ_s is the total density of solvent components, and φ_s is the total volume fraction of solvent components. The equation $Q = 1/\bar{v}_n$ for the single solvent case forms an example of eq. 6.

(2) J. G. Kirkwood and F. Buff, *J. Chem. Phys.*, **19**, 774 (1951).

THE SOLUBILITY OF XENON IN SOME HYDROCARBONS[1]

BY H. LAWRENCE CLEVER[2]

Contribution from the Department of Chemistry, Duke University, Durham, N. C.

Received October 1, 1957

The solubility of xenon has been determined at a total pressure of one atmosphere and temperatures of about 16, 25, 34.5 and 43° in benzene, cyclohexane, *n*-hexane, isoöctane and *n*-dodecane.

Experimental

The solubility apparatus, procedure and solvents were those used and described before.[3] The pure xenon was furnished by the Linde Air Products Co., Tonawanda, N. Y.

Results and Discussion

The solubilities of xenon in the hydrocarbons corrected to one atmosphere of xenon by Henry's law are given in Table I expressed as the Ostwald coefficient and mole fraction. Included are least square constants for the equation

$$\log \text{solubility} = \frac{a}{T} + b$$

in both solubility units. The slope intercept equations reproduce the experimental solubilities with an average deviation of 2.8% in benzene, 2.2% in cyclohexane, 1.1% in *n*-hexane, 1.0% in isoöctane and 0.7% in *n*-dodecane. Much of the departure from linearity is in the low temperature determination where temperature control was difficult.

Entropy of Solution.—Entropies for the transfer of one mole of xenon from the gas phase to the hypothetical unit mole fraction (Fig. 1a, curve 1) are slightly more negative than values found before for the other rare gases in the same solvents.[3] However, they are not as negative as the entropy calculated from either compressing and condensing the xenon (Fig. 1a, curve 2) or the corresponding entropy of condensation of the solvent (Fig. 1a, curve 3).

Solubility and Solvent Surface Tension.—The Uhlig plot[4] of the logarithm of the Ostwald coefficient against the solvent surface tension (Fig. 1b) shows more scattering of the points than the same plot for the other rare gases in the same solvents.[3]

Hildebrand Equation.—Xenon, critical temperature 16.7°, is a gas with physically real constants from which to evaluate solubility param-

(1) Presented before the Division of Physical and Inorganic Chemistry, 127th National Meeting of the American Chemical Society, Cincinnati, Ohio, April, 1955.

(2) Department of Chemistry, Emory University, Emory University, Georgia.

(3) H. L. Clever, R. Battino, J. H. Saylor and P. M. Gross, THIS JOURNAL, **61**, 1078 (1957).

(4) H. H. Uhlig, *ibid.*, **41**, 1215 (1937).

TABLE I

THE SOLUBILITY OF XENON IN SEVERAL HYDROCARBONS UNDER ONE ATMOSPHERE PRESSURE

Solvent	Temp., °C.	Solubility Ostwald	Solubility Mole fraction	$\log \text{sol.} = \frac{a}{T} + b$ (1) Ostwald (2) Mole fraction a	b
Benzene	16.0	3.59	0.0132		
	25.0	3.08	.0111	(1) 297.4	−0.4878
	34.45	2.98	.0106	(2) 372.6	−3.1825
	43.1	2.90	.0101		
Cyclo-	16.0	5.26	.0233		
hexane	26.0	4.42	.0192	(1) 385.1	−0.6226
	34.45	4.25	.0181	(2) 463.8	−3.2483
	43.1	4.00	.0168		
n-Hexane	16.0	5.60	.0298		
	25.3	4.84	.0254	(1) 491.6	−0.9552
	34.4	4.45	.0229	(2) 558.7	−3.4610
	43.1	3.95	.0201		
Isoöctane	16.0	4.68	.0313		
	25.5	4.08	.0264	(1) 475.0	−0.9720
	34.4	3.70	.0241	(2) 537.0	−3.3674
	43.0	3.36	.0214		
n-Dodecane	16.0	3.78	.0348		
	25.0	3.35	.0304	(1) 414.0	−0.8561
	34.4	3.08	.0274	(2) 496.3	−3.1753
	43.0	2.84	.0247		

eter δ_2, molar volume V_2, and ideal solubility X_2^i, for use in the Hildebrand and Gjaldbaek equation.[5]

$$-\log X_2 = -\log X_2^i + \log \frac{V_2}{V_1} + 0.434 \left(1 - \frac{V_2}{V_1}\right) + \frac{V_2}{4.575T}(\delta_1 - \delta_2)^2$$

Values with physical significance for V_2 include (1) the volume at the xenon b.p., 43, (2) van der Waals b, 108.4, and (3) the critical volume, 113.7 cm.^{3}/mole.

Values for the solubility parameter, δ_2, include (1) 8.0, the value at the normal b.p., (2) 5.4, calculated from the normal b.p. value to 25° by[6]

$$\frac{d \ln \delta}{dT} = -1.25\alpha$$

where α, the coefficient of thermal expansion is assumed temperature independent and equal to the corresponding state value of 0.68 T_c[7] and (3) 7.0, the maximum in a plot of mole fraction solubility against solvent solubility parameter (Fig. 2) which would correspond to the gas solubility parameter if the volume of mixing terms cancelled or were negligible. Included in Fig. 2 are the solubilities in methylcyclohexane and perfluoromethylcyclohexane given before.[8]

The Hildebrand and Gjaldbaek equation was solved for the ideal solubility using the experimental solubility in seven solvents and all possible combinations of δ_2 and V_2. The combination giving the most constant "ideal solubility" value was

(5) J. Chr. Gjaldbaek and J. H. Hildebrand, *J. Am. Chem. Soc.*, **71**, 3147 (1949).

(6) J. H. Hildebrand and R. L. Scott, "Solubility of Nonelectrolytes," 3rd ed., Reinhold Publ. Corp., New York, N. Y., 1950.

(7) E. A. Guggenheim, *J. Chem. Phys.*, **13**, 253 (1945).

(8) H. L. Clever, J. H. Saylor and P. M. Gross, THIS JOURNAL, **62**, 89 (1958).

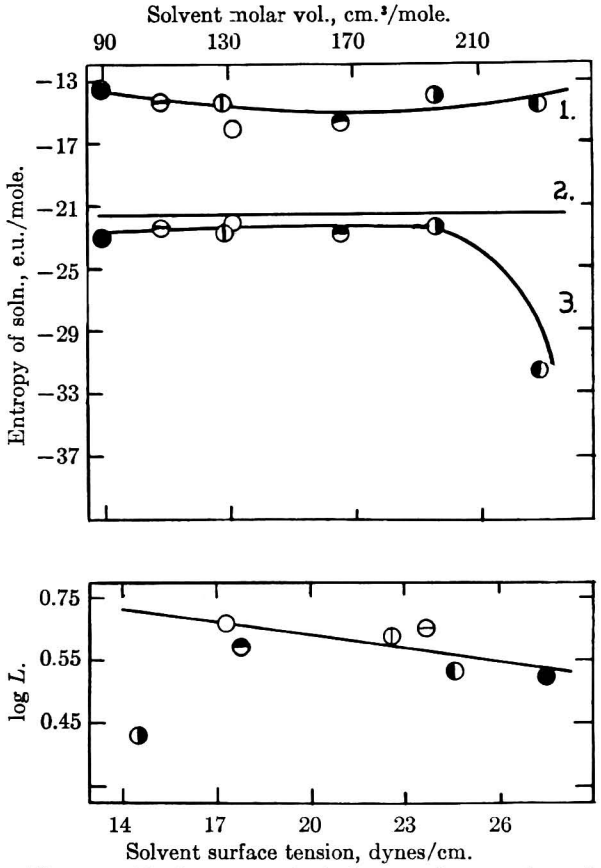

Fig. 1a.—(Top) entropy of solution *vs.* solvent molar volume. 1b.—(Bottom) logarithm of Ostwald coefficient *vs.* solvent surface tension: •, benzene; ⊖, cyclohexane; ⊕, methylcyclohexane; ○, *n*-hexane; ◓, isoöctane; ◑, perfluoromethylcyclohexane; ◐, *n*-dodecane.

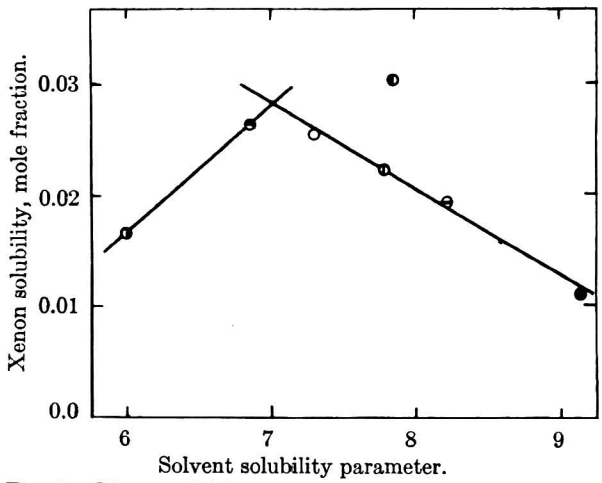

Fig. 2.—Xenon solubility *vs.* solvent solubility parameter, same symbols for solvents as Fig. 1.

$\delta_2 = 7.0$ and $V_2 = 108.4$ which reproduced the hydrocarbon solubilities to within 5% but was 54% in error for the fluorocarbon solubility. The calculated ideal solubility was 0.0257 ± 0.0008 which is 50% higher than the value calculated from xenon vapor pressure.

Acknowledgment.—The author is indebted to Professors P. M. Gross and J. H. Saylor for helpful discussions.

THE SURFACE CHEMISTRY OF BONE MINERAL. X. THE LACK OF INTERACTION BETWEEN SODIUM AND CARBONATE IONS[1]

BY W. R. STOLL AND W. F. NEUMAN

From the Division of Pharmacology, Department of Radiation Biology, School of Medicine and Dentistry, University of Rochester, Rochester, New York

Received October 14, 1957

Sodium ions have been shown to compete with calcium ions for the crystalline surface of hydroxy apatite on a mole for mole basis.[2] Under physiological conditions, the magnitude of this passive sodium exchange by hydrated hydroxy apatite is adequate to account for the sodium content of bone *in vivo*. A similar crystal surface competition has been shown recently to exist between carbonate and phosphate ions.[3] In this case, although the primary ion in solution is bicarbonate, infrared studies have demonstrated that the ion in the crystal surface is the carbonate ion.[4]

The few studies in the literature of sodium and carbonate mobilization from bone have revealed that these two ions are closely associated, a decrease of one being associated with a decrease in the other.[5-7] This association might be explained either on a physiological or a physicochemical basis: (a) to deplete bone carbonate, the animal must be made acidotic and, physiologically, most acidotic states are accompanied by a sodium loss or (b) some specific interaction between sodium and carbonate ions occurs at the mineral crystal surfaces. Experiments were performed *in vitro* to test the physicochemical explanation. No specific physicochemical interaction was observed.

Experimental Procedures

Two series of equilibrating solutions were used. The first series contained varying amounts of sodium and potassium as chlorides; the second contained mixtures of sodium and potassium as bicarbonates. Each solution was 0.005 *M* with respect to diethylbarbituric acid which served as a buffer. The ionic strength of each solution was approximately 0.16 *M*.

Two grams of a sodium-free, synthetic hydroxy apatite[2,3,8] was equilibrated with one liter of the test solution. The temperature was maintained at 37° by means of a water-bath, the *p*H was maintained at 7.4 ± 0.1, and the time of equilibration was from 2–6 hours, a time proven adequate for the establishment of equilibrium by earlier experiments (the techniques of equilibration, of sampling the solutions, and the separation of the solid phase are described elsewhere).[2,3] After separation from the solution, the wet solid was divided into four parts and centrifuged at a force of 8000 × gravity for 1 hour to remove the last traces of the bulk solution leaving the crystals with their hydration shells intact for subsequent analysis.[3,9] Following centrifugation, the solid phase was dried and dissolved in a fixed quantity of dilute nitric acid. The liberated carbon dioxide was determined gravimetrically.[3] Aliquots of the acid solutions were then taken for sodium and potassium analyses by flame photometry.[2] A second aliquot was taken for chloride analyses by displacement of iodate from silver iodate by chloride. The released iodate in the supernatant was then reduced by potassium iodide and the free iodine was titrated with sodium thiosulfate. This method, an adaption of the method of Sendroy[10] was not affected by variations in the amount of dissolved apatite, but it was quite sensitive to variations in the concentration of acid.

Samples of the equilibrating solutions were analyzed for calcium by titration with ethylenediaminetetraacetic acid[2] and for phosphorus by the method of Fiske and SubbaRow.[11] The concentration of phosphate in the hydration shell of the crystals and on the crystalline surface itself was estimated by isotope dilution techniques using carrier-free $P^{32}O_4$ as described previously.[12]

Each set of equilibrations was repeated. The two sets of data were then averaged as duplicate analyses.

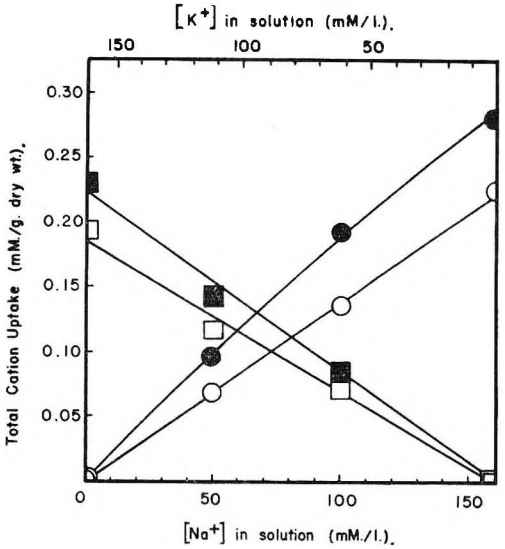

Fig. 1.—Uptake of sodium and potassium by hydrated hydroxy apatite in the presence of chlorides and bicarbonates: ○, sodium uptake from chloride solutions; ●, sodium uptake from bicarbonate solutions; □, potassium uptake from chloride solutions; ■, potassium uptake from bicarbonate solutions.

Results and Discussion

The uptake of potassium and sodium by the hydrated hydroxy apatite is shown in Fig. 1 as a function of the sodium ion concentration in the equilibrating solution. The potassium concentration can be obtained by the relation: $[K^+] = 160 - [Na^+]$ in millimoles per liter. Where chloride was the anion present, the uptake of the sodium by the hydrated solid was greater than the uptake of potassium in equivalent concentrations, in excellent quantitative agreement with an earlier study.[2] When bicarbonate was the anion present, the uptake of both sodium and potassium ions was increased slightly.

(1) This paper is based on work performed under contract with the United States Atomic Energy Commission at the University of Rochester Atomic Energy Project, Rochester, New York.

(2) W. R. Stoll and W. F. Neuman, *J. Am. Chem. Soc.*, **78**, 1585 (1956).

(3) W. F. Neuman, T. Y. Toribara and B. J. Mulryan, *ibid.*, **78**, 4263 (1956).

(4) (a) A. S. Posner and G. Dukaerts, *Experientia*, **10**, 424 (1954); (b) A. L. Underwood, T. Y. Toribara and W. F. Neuman, *ibid.*, **77**, 317 (1955).

(5) W. H. Bergstrom, *J. Biol. Chem.*, **206**, 711 (1954).

(6) W. H. Bergstrom, *J. Clin. Invest.*, **34**, 997 (1955).

(7) G. Nichols, Jr., and N. Nichols, *Metabolism, Clin. and Exp.*, **5**, 438 (1956).

(8) W. F. Neuman, Univ. of Rochester Atomic Energy Report. UR-238 (1953).

(9) W. F. Neuman, T. Y. Toribara and B. J. Mulryan, *J. Am. Chem. Soc.*, **75**, 4239 (1953).

(10) P. B. Hawk, B. L. Oser and W. H. Sumerson, "Practical Physiological Chemistry," 12th Edition, Blakiston Co., Philadelphia, Penna., 1949, p. 895.

(11) C. H. Fiske and Y. SubbaRow, *J. Biol. Chem.*, **66**, 375 (1925).

(12) J. H. Weikel, W. F. Neuman and I. Feldman, *J. Am. Chem. Soc.*, **76**, 5202 (1954).

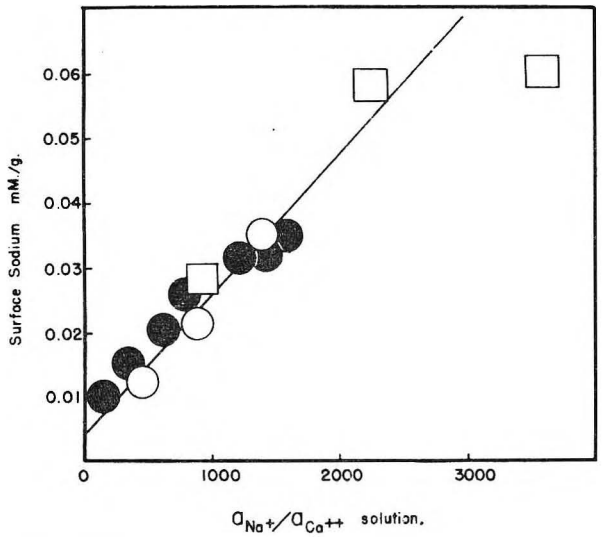

Fig. 2.—Competition of sodium and calcium for the surface of hydroxy apatite, plotted according to mass law: O, chloride solutions; □, bicarbonate solutions; ●, chloride solutions from previous data.[2]

Previously, the conclusion was drawn[2] that potassium ions do not displace calcium from the crystalline surface to any significant extent; rather, the potassium found by analysis of the apatite was assumed to be the result of a simple equilibrium between the bulk solution and the hydration shell of the solid phase. With the reasonable assumption that the content of sodium of the hydration shell is the same as the potassium content at equivalent concentrations in solutions, the difference between the total uptake of these two cations approximates the concentration of sodium actually in the crystalline surface as a result of an exchange displacement of calcium ion.[2] Since sodium displaces calcium from the surface on an equal molar basis, the net sodium uptake ($Na_{solid} - K_{solid}$) should be proportional to the activity ratios of sodium to calcium in the solution.[2] This function is given in Fig. 2 and, for comparison, previous data[2] are also included. The same line describes the sodium–calcium relationship equally well, regardless of the anion species present in the solution.

Despite the consistency of the exchange-interpretation of the earlier study,[2] it is possible to account for the preference of the solid phase for sodium ion on the basis solely of activity coefficients. For example, the apparent activity coefficient, γ_{K^+}, in the hydration shell has been calculated to be 0.55,[2] suggesting the *effective* ionic strength of the hydration shell to be about 1.5. At this ionic strength, the activity coefficient of sodium ($\gamma_{Na^+ \text{ hydration shell}}$) can be expected to be even smaller than $\gamma_{K^+ \text{ hydration shell}}$, by about 20%.[13] Thus sodium would *concentrate* at the crystal: solution interface and the resultant electrostatic inbalance would release other cations, principally calcium. In any case, whether sodium uptake by the solid represents true exchange or whether the ordinate in Fig. 2 represents the quantity, $(\gamma_{Na \text{ hydration shell}} - \gamma_{K^+ \text{ hydration shell}}) \times [Na]_{soln.}$, the presence of carbonate has no specific influence.

A comparison of the effect of the anion present (chloride *vs.* bicarbonate) on the composition of the solid phase and of the solution is given in Table I. It is true that the concentrations of sodium and of calcium ion influence the composition of the hydration shell and of the solution.[12, 14] However, these changes are insignificant in comparison with the changes induced by replacing chloride with bicarbonate as the anion present. In Table I, therefore, the averages of all the bicarbonate and all the chloride mixtures are given irrespective of the cation, potassium or sodium.

TABLE I

EFFECT OF ANION (Cl^- *vs.* HCO_3^-) ON SOLID AND SOLUTION COMPOSITION[a]

Compn. of solid	Anion in soln. Chloride 160 in mole/l.	Bicarbonate 152 in mole/l.	Net change
H_2O	53 ± 0.6	53 ± 0.8	
Cl	0.155 ± .005	.....	
CO_2	.....	0.31 ± .03	
$P_{hydration\ shell}$	.2 ± .01	.1 ± .01	−0.1 ± 0.02
$P_{surface}$	.4 ± .1	.1 ± .1	− .3 ± .2
Compn. of soln.			
Ca	.24 ± .006	.11 ± .01	− .13 ± .02
P	.12 ± .004	.41 ± .016	+ .29 ± .02

[a] Results are av. ± av. deviation of four analyses, expressed as mmoles/g. in solid or mmoles/l. in solution. For a comparison of net changes, solid *vs.* solution, the mmoles/g. must be multiplied by two since 2 g. of solid was equilibrated with one liter of solution.

There were no detectable changes in the size of the hydration shell. Phosphate ions appeared to be displaced by carbonate ions both from the hydration shell and from the crystal surface. The average error of the total amount of phosphate displaced, 0.4 ± 0.2 mmole per gram, was too large to permit any conclusion regarding the molar ratio of the carbonate–phosphate displacement. The displaced phosphate appeared in the solution and repressed the amount of calcium dissolved from the solid. On a molar basis, the *extra* phosphate which appeared in solution, $(P_{bicarbonate} - P_{chloride}) = 0.29 \pm 0.02$ corresponded almost exactly to the *extra* carbonate taken up by the 2 g. of solid, $(CO_{3solid} - Cl_{solid}) \times 2 = 0.31 \pm 0.06$. This suggests an equimolar displacement but it is by no means conclusive.

From these data, it appears that there is no physicochemical basis for a direct interaction between sodium and carbonate ions at the surface of hydroxy apatite crystals. Carbonate ions do increase the amount of monovalent ions bound by the solid in a non-specific way, possibly by increasing the charge asymmetry at the crystal:solution interface.[15] The close association between sodium and carbonate concentrations in bone seen *in vivo* must,

(13) H. S. Harned and B. B. Owen, "The Physical Chemistry of Electrolytic Solutions," Reinhold Publ. Corp., New York, N. Y., 1950, p. 562.

(14) G. J. Levinskas and W. F. Neuman, THIS JOURNAL, **59**, 164 (1955).

(15) W. F. Neuman and M. W. Neuman, Chapter IV, "Chemical Dynamics of Bone Mineral," Univ. of Chicago Press, 1958.

therefore, be the result of physiological mechanisms mentioned earlier.

Summary

Both sodium and carbonate ions have previously been shown to be incorporated in the surface of hydroxy apatite crystals by ion exchange processes. Because, in bone *in vivo*, these two ions appear to be related, an attempt was made to test whether any specific interaction between sodium and carbonate ions occurs at the hydroxy apatite surface *in vitro*. Carbonate ions did increase incorporation by apatite of both sodium and potassium ions but the effects were small and non-specific. The association between sodium and carbonate ions in bone is, therefore, probably the result of physiological mechanisms.

ISOTOPIC EXCHANGE REACTIONS. II. THE RAPID HALOGEN EXCHANGE BETWEEN $SiCl_4$ AND $(CH_3)_4NCl$, AND A CONVENIENT METHOD FOR THE PREPARATION OF Cl^{36} LABELED CHLOROSILANES

BY ROLFE H. HERBER

Department of Chemistry and Chemical Engineering, University of Illinois, Urbana, Ill.

Received November 1, 1957

In a detailed study[1] of the halogen exchange kinetics in the system $SiCl_3{}^nCl^{36}$–HCl^n (in which n denotes the natural isotopic composition) it was pointed out that isotopically labeled silicon tetrachloride could be prepared by a homogeneous gas phase exchange with HCl^{36}. The reaction half-times for reactant concentrations of 10^{-2} mole per liter were found to be on the order of 10^4 seconds at 90°. Since, under these conditions the total quantity of $SiCl_4$ which can be labeled in a given run is small, we have looked for a more suitable exchange path.

Schomaker and Stevenson[2] have suggested that the difference between the sum of the covalent bond radii (2.16 Å.) and the observed interatomic distance in $SiCl_4$ (2.02 Å.) is due to partial ionic bond character contributions of the type $SiCl_3{}^+Cl^-$. As Lewis and Wilkins[3] have shown in the case of NOCl, such ionization should lead to rapid exchange with appropriate ionized solutes and hence we have explored the exchange between $(CH_3)_4NCl$ and $SiCl_4$ since the former is known to ionize readily in a number of non-aqueous solvents.[4]

In a typical exchange run, Cl^{36}-labeled $(CH_3)_4NCl$ was prepared by dissolving the reagent grade salt in a minimal volume of water, adding one drop of HCl^{36} stock solution[5] and evaporating off the water and HCl under high vacuum conditions. The resulting solid was subjected to high vacuum pumping for one hour at 100°. Into a cold finger containing 4.6 mmoles of this labeled salt were then distilled 1.62 mmoles of $SiCl_4$, using liquid N_2 as a refrigerant. Since HCl^{36}, formed by the hydrolysis of $SiCl_4$ by any traces of moisture still remaining in the tetramethylammonium chloride, would simulate exchange (especially in exchange runs between labeled $SiCl_4$ and unlabeled salt, see below) the cold finger was momentarily warmed to 0°, then cooled with acetone–Dry Ice slush, and subjected to high vacuum pumping to remove any HCl present. The cold finger was warmed to 0° and aliquots of $SiCl_4$ removed at known time intervals, radioassayed and returned to the reaction cold finger. The counting technique for the assay of volatile labeled materials has been described in detail.[6] The activity observed in the silicon tetrachloride as a function of time is shown in Fig. 1. In a second experiment, $SiCl_4$ and labeled $(CH_3)_4NCl$ maintained for 3 hours at 50°, resulted in an activity of 220 c.p.m./cm. $SiCl_4$. We have also noted the reverse exchange in which labeled silicon tetrachloride with an initial specific activity of 200 c.p.m./cm. was contacted with unlabeled $(CH_3)_4NCl^n$ at room temperature. The observed c.p.m./cm. were 182 for 5 minutes, 129 after 10 minutes, 77.3 after 20 minutes and 70.7 after 30 minutes. Calculation of the fraction of total exchange, based on the observed "infinite time" activity, appears to indicate that the exchange may proceed *via* a heterogeneous mechanism. A further experiment in which $(CH_3)_3SiCl^n$ was substituted for the tetrachloro species indicates that this material, too, exchanges halogens at room temperature with $(CH_3)_4NCl^{36}$.

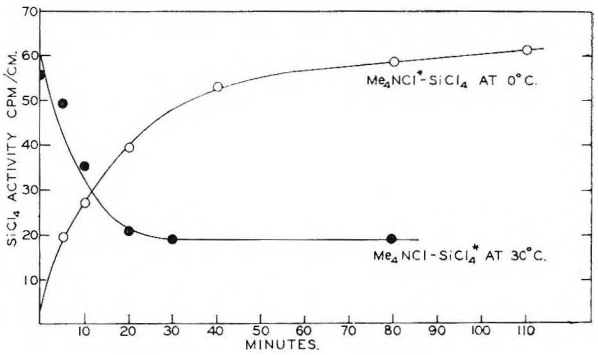

Fig. 1.—Activity of silicon tetrachloride.

The use of high specific activity tetramethylammonium chloride thus provides a convenient starting point for the preparation of chlorine labeled $SiCl_4$ and $(CH_3)_3SiCl$ and the exchange is noted to be reasonably rapid at room temperature. Due to the condensed nature of this system, relatively large quantities of labeled product can be prepared in a single exchange run.

This research has been supported in part by the U. S. Atomic Energy Commission. The assistance of Mr. W. Cordes in this work is gratefully acknowledged.

(1) R. H. Herber, *J. Chem. Phys.*, **27**, 653 (1957).

(2) V. Schomaker and D. P. Stevenson, *J. Am. Chem. Soc.*, **63**, 37 (1941).

(3) J. Lewis and R. G. Wilkins, *J. Chem. Soc.*, 56 (1955).

(4) A. B. Burg and D. E. McKenzie, *J. Am. Chem. Soc.*, **74**, 3143 (1952); V. Gutmann, *Z. anorg. allgem. Chem.*, **266**, 331 (1951).

(5) Item Cl-36-P, Oak Ridge National Laboratory, Isotopes Division.

(6) R. H. Herber Paper #24, 132nd Meeting Am. Chem. Soc., New York City, 1957; R. H. Herber, *Rev. Sci. Inst.*, in press.

DETERMINATION OF THE RATE CONSTANT RATIOS IN THREE-STEP COMPETITIVE CONSECUTIVE SECOND-ORDER REACTIONS

By W. J. Svirbely

Contribution from the Chemistry Department, University of Maryland, College Park, Maryland

Received December 4, 1957

Recently,[1] McMillan described a procedure in which the ratio of the rate equations for a two-step competitive consecutive second-order reaction was solved so as to yield the rate constant ratio as an implicit function of any two simultaneous concentrations of components other than that of the reactant common to the two steps. In this paper, we have applied the same analysis to a three step competitive consecutive second-order reaction. The pertinent reactions are illustrated by

$$A + B \xrightarrow{k_1} C + E$$
$$A + C \xrightarrow{k_2} D + E$$
$$A + D \xrightarrow{k_3} F + E$$

As in the previous case,[1] we shall only be interested in obtaining our results from a knowledge of the concentrations of components other than A.

The rate equations for B, C and D are

$$\frac{dB}{dt} = -k_1AB \quad (1)$$

$$\frac{dC}{dt} = k_1A(B - KC) \quad (2)$$

$$\frac{dD}{dt} = k_2A(C - JD) \quad (3)$$

respectively, where $K = k_2/k_1$ and $J = k_3/k_2$. In terms of the dimensionless parameters

$$\beta = \frac{B}{B_0}, \gamma = \frac{C}{B_0} \text{ and } \eta = \frac{D}{B_0} \quad (4)$$

The ratios of equation 2 to 1 and of equation 3 to 1 become

$$\frac{d\gamma}{d\beta} = \frac{(K\gamma - \beta)}{\beta} \quad (5)$$

$$\frac{d\eta}{d\beta} = \frac{K(J\eta - \gamma)}{\beta} \quad (6)$$

The solution of equation 5 is given by

$$\gamma = \frac{\beta}{K - 1}(1 - \beta^{K-1}) \quad (7)$$

where the constant of integration was determined by the initial condition that when $\beta = 1$, $\gamma = 0$. Substitution of equation 7 into 6 yields an equation which on integration gives

$$\eta = \left[-\frac{K}{(K-1)}\frac{\beta}{(1-JK)} + \frac{\beta^K}{(K-1)(1-J)} + \frac{\beta^{JK}}{(1-JK)(1-J)} \right] \quad (8)$$

where the constant of integration was determined by the initial condition that when $\beta = 1$, $\eta = 0$.

As in the case of the two step reaction, for any measured pair (β,γ) of experimental concentrations, one may find the value of K which satisfies equation 7. If η is measured simultaneously, or for any other measured pair (β,η) of experimental concentrations, and from a knowledge of K one may find the value of J which satisfies equation 8. The KJ product would yield the k_3/k_1 ratio.

(1) W. G. McMillan, *J. Am. Chem. Soc.*, **79**, 4838 (1957).

ETHERATES OF LITHIUM BOROHYDRIDE. III. THE SYSTEM LITHIUM BOROHYDRIDE–DIISOPROPYL ETHER

By John J. Burns, S.J., and George W. Schaeffer

The Department of Chemistry, St. Louis University, St. Louis, Missouri

Received November 19, 1957

Pressure–composition isotherms at 0, 10, 15 and 20° for the system lithium borohydride–diisopropyl ether have been determined. The data, listed in Table I, are clear evidence for the existence of a single solid etherate in the temperature range examined. The abrupt pressure change at lithium borohydride mole fraction (n_2) of 0.50 denotes a phase transformation between lithium borohydride mono-(diisopropyl etherate) and lithium borohydride and the absence of discontinuities

$$LiBH_4{\cdot}O[CH(CH_3)_2]_2(s) = LiBH_4(s) + [(CH_3)_2CH]_2O(g) \quad (1)$$

at $n_2 = 0.33$ and 0.67 shows that neither a bis-(diisopropyl etherate) nor an hemi-(diisopropyl etherate) of lithium borohydride exists in the temperature range, 0 to 20°, examined. In this regard the lithium borohydride–diisopropyl ether system is in distinct contrast to the lithium borohydride-dimethyl ether system in which both a stable bis-(etherate) and hemi-(etherate) are formed.[1] The present system resembles the lithium borohydride–diethyl ether system in not forming a stable bis-(etherate), but is distinguished from this latter system in that no hemi-(etherate) is found.[2]

The heat of dissociation of lithium borohydride mono-(diisopropyl etherate) into lithium borohydride and the ether, equation 1, was determined from the dissociation pressures at various temperatures. The data are well represented by the simple linear relation

$$\log p_{mm} = 11.274 - 2772.0/T$$

as can be seen by the comparison of Table II. Values for the various thermodynamic quantities associated with the dissociation process at 25° described by equation 1 are $\Delta H_d = 12.68$ kcal./mole; $\Delta F_d = 1.24$ kcal./mole and $\Delta S_d = 38.4$ e.u. These values may be combined with data for lithium borohydride[3] and diisopropyl ether[4]

(1) G. W. Schaeffer, T. L. Kolski and D. L. Ekstedt, *J. Am. Chem. Soc.*, **79**, 5912 (1957).

(2) T. L. Kolski, H. B. Moore, L. E. Roth, K. J. Martin and G. W. Schaeffer, *ibid.*, **80**, 549 (1958).

(3) $\Delta H_f^0 = -46.36$ kcal./mole; $\Delta F_f^0 = -30.74$ kcal./mole; and $S^0 = 18.13$ e.u. Taken from "Thermodynamic Properties of Boron Compounds at 25°," National Bureau of Standards, Washington 25, D. C., April, 1954.

(4) For diisopropyl ether the following values were employed: $\Delta H_f^0 = -69.8$ kcal./mole (calculated by a modified Franklin method, *cf.* G. W. Wheland, "Resonance in Organic Chemistry," John Wiley and Sons, Inc., New York, N. Y., 1955, pp. 94-96); $S^0 = 70.4$ e.u. (G. S. Park and H. M. Huffman, "The Free Energies of Some Organic

TABLE I

DATA FOR PRESSURE–COMPOSITION ISOTHERMS AT VARIOUS TEMPERATURES FOR THE SYSTEM LITHIUM BOROHYDRIDE–DIISOPROPYL ETHER

0.0°		10.0°		15.0°		20.0°	
Comp., n_2	Press., mm.	Comp., n_2	Press., mm.	Comp., n_2	Press., mm.	Comp., n_2	Press. mm.
0.128	44.8	0.128	75.2	0.143	95.4	0.129	120.5
.143	44.6	.297	75.2	.164	95.4	.144	119.9
.163	44.4	.337	75.0	.298	95.5	.194	119.4
.232	44.3	.490	73.6	.339	95.4	.235	119.5
.295	44.3	.512	36.8	.471	94.5	.299	119.4
.366	44.2	.515	29.6	.493	92.4	.373	119.4
.464	43.9	.634	30.2	.503	80.0	.475	119.0
.485	43.4	.672	30.3	.513	46.1	.497	113.9
.496	43.0	.732	31.0	.641	44.5	.504	87.0
.502	41.0	.915	30.8	.675	44.5	506	68 0
507	33.5			.739	45.4	.517	66.3
.510	24.2			.923	44.5	.522	65.1
.512	16.5					.645	65.1
.630	13.2					.681	65.0
.666	13.2					.743	66.0
.906	13.6					.935	65.2

to allow calculation of the standard heat of formation, standard free energy of formation and absolute entropy at 25° for lithium borohydride mono-(diisopropyl etherate). The values so obtained are: $\Delta H_f^0 = -128.9$ kcal./mole, $\Delta F_f^0 = -55.5$ kcal./mole and $S^0 = 75.6$ e.u.

TABLE II

DISSOCIATION PRESSURES OF $LiBH_4 \cdot O[CH(CH_3)_2]_2$

t, °C.	0	10	15	20
p_{mm} (obsd.)	13.2	30 2	44.5	65.1
p_{mm} (calcd.)	13.2	30.1	44.6	65.0

Experimental

The apparatus and techniques are described in the monograph of Sanderson[5] and in a previous paper.[1]

(a) **Materials.**—Lithium borohydride was purified in the manner previously described. Diisopropyl ether was refluxed over lithium aluminohydride for ten hours, fractionated (67.0–67.4° at 752 mm.) and introduced into the high vacuum system. The ether was further dried over $LiAlH_4$ (20 hours) and $LiBH_4$ (16 hours) and it was then fractionated through traps held at −78, −112 and −186°. The −112° fraction exhibited a vapor pressure of 155 mm. at 25°.

(b) **Determination of the Isotherms.**—For the measurement of diisopropyl ether quantities, the pressure of the sample was kept at less than one-half its saturation pressure at room temperature to minimize deviations from ideal gas behavior. Temperature control was maintained within 0.1 degree by a small constant-temperature water-bath around the sample tube above 0.0° and by a water-crushed ice-bath at 0.0°.

Compounds," Chemical Catalog Company, New York, N. Y., 1932, p. 169); $\Delta F_f^0 = -23.5$ kcal./mole (calculated from above values); $\Delta H_{(vaporization)} = 7.61$ kcal./mole (estimated from vapor pressures of D. R. Stull, *Ind. Eng. Chem.*, **39**, 525 (1947)).

(5) R. T. Sanderson, "Vacuum Manipulation of Volatile Compounds," John Wiley and Sons, Inc., New York, N. Y., 1948.

POSSIBLE BORON HYDRIDE IONS

BY WILLIAM N. LIPSCOMB

School of Chemistry, University of Minnesota, Minneapolis 14, Minnesota

Received November 11, 1957

The present form of the topological theory of boron hydrides by Dickerson and Lipscomb[1] is here extended to include ions. For a boron hydride B_pH_{p+q}, containing s H bridges, x extra B–H groups, t three-center BBB bonds and y two-center BB bonds, the equations of balance may be written in a simplified form as follows. The hydrogen atom balance is simply $s + x = q$. Since each boron supplies four orbitals but only three electrons the total number of three-center bonds in the molecule is the same as the number of boron atoms, $s + t = p$. Finally if we consider BH as the bonding unit, each of which then supplies one electron pair, these p pairs are used up as three-center BBB bonds, two-center BB bonds, and in supplying half of each pair to each extra hydrogen, *i.e.*, $p = t + y\ q/2$. It is quite easy to extend these equations to include a description of ions of the type $B_pH^c_{p+q+c}$, where c is the charge including its sign. The resulting generalization may be formulated as

$$s + x = q + c$$
$$s + t = p + c$$
$$t + y = p - \frac{c}{2} - \frac{q + c}{2} = p - c - \frac{q}{2}$$

An examination of ions based on icosahedral, octahedral and tetrahedral polyhedra and fragments has been made for $c = -2, -1, +1$ and $+2$. These ions supplement our earlier predictions[1] for $c = 0$, and are described by listing the numbers s, t, y and x just preceding the appropriate molecular formula.

1. Ions Similar in Geometrical Structure to Known Hydrides.—The 4450 $B_{10}H_{14}^{-2}$ ion of C_{2v} symmetry is the only ion of this type, and is probably the most interesting of all of the ions. Except for a probable contraction of the two 2.0 Å B· · ·B contacts toward a more normal value, the geometry of this ion is probably very similar to that of the well known 4620 $B_{10}H_{14}$ structure.

2. Ions Similar in Electronic Structures to Known Hydrides.—The prediction[2] of the B_5H_9-like ions $B_4H_7^-$ and $B_6H_{11}^+$ was based upon analogies of these compounds to C_5H_6, $C_5H_5^-$ and $C_7H_7^+$. Equivalent orbital transformations reduce these to 3030 $B_4H_7^-$ and 5210 $B_6H_{11}^+$ in the present description.

3. Ions Derived from Known Hydrides by Removal of H^+ from a BHB Bridge Bond.—These structures satisfy our rules if the electron pair is used to form a B–B bond. It is obvious how a list of these ions can be made from the known and hypothetical neutral hydrides, and hence such a list will not be given here. However the 2013 $B_3H_8^-$ ion[3] is probably either a member of this class or of Class 4.

4. Ions Derived from Known Hydrides by Removal of H^+ from a B–H Terminal Bond.—Terminal hydrogens tend to be less negative[4] than bridge hydrogens, and might ionize off more readily, although the resulting ion usually does not have as satisfactory a valence structure as the ion produced

(1) R. E. Dickerson and W. N. Lipscomb, *J. Chem. Phys.*, **27**, 212 (1957).

(2) W. N. Lipscomb, *J. Chem. Phys.*, **28**, 170 (1958).

(3) W. V. Hough, L. J. Edwards and A. D. McElroy, *J. Am. Chem. Soc.*, **78**, 689 (1956).

(4) W. C. Hamilton, *Proc. Roy. Soc. (London)*, **A235**, 395 (1956).

in Class 3. The various terminal hydrogen atoms in the known hydrides are attached to borons of different formal charge,[5] and those attached to the more positive boron atoms will presumably ionize off more readily. The borons of type[5] II or I in $B_{10}H_{14}$ are more positively charged than the others, and hence possible ionization of one or more of the attached hydrogens may be suggested. There is some evidence that $B_{10}H_{14}$ has an ionizable hydrogen,[6] and the series of salts $NaB_{10}H_{13}$, $Na_2B_{10}H_{12}$, etc., may be suggested. When this suggestion is combined with the Class I type, $Na_2B_{10}H_{14}$, we expect another series beginning with $Na_3B_{10}H_{13}$, etc.

5. Ions Derived from Addition of H^+ to a Single B–B Bond on the Edge.—The $B_6H_{11}^+$ ion derived by addition of a proton to the strained single B–B bond in the known[7] 4220 B_6H_{10} structure is expected to be stable. Although no other of the known hydrides based upon icosahedral fragments have this structural feature, several of the possible hydrides and ions do, and might become stabilized by the addition of one or two protons.

6. Other Ions Based upon Icosahedral Fragments.—Ions like the 3122 $B_5H_{10}^-$ ion and the 3100 $B_3H_6^+$ ion may also exist, as may the 2113 $B_4H_9^-$ and 2440 $B_8H_{10}^{-2}$ both of which have one or more single B–B bonds along the edge (*cf.* Class 5). Probably the most promising[8] ion of this type is $B_{12}H_{12}^{-2}$, which is an 0.10.3.0 resonance hybrid in our localized-bond description.

7. Ions Based upon Tetrahedra, Octahedra or Their Fragments.—Our bonding scheme applies to any geometrical framework in which one can say that only close contacts represent valence interactions, and hence include 0230 $B_4H_4^{-2}$, (0400 B_4H_4), 2040 $B_4H_6^{-2}$, 3030 $B_4H_7^-$ also listed in Class 2, (4020 B_4H_8), 5010 $B_4H_9^+$ and 6000 $B_4H_{10}^{+2}$ all based on a tetrahedral boron arrangement; 2240 $B_6H_8^{-2}$, 3230 $B_6H_9^-$, 0430 $B_6H_6^{-2}$ (see ref. 5), 1420 $B_6H_7^-$, (2410 B_6H_8) and 3400 $B_6H_9^+$ all based on an octahedral boron arrangement; and a similar series based on the B_5H_9 arrangement. Within each of these groups these ions are interrelated by the process describing Class 5 as the charge increases, or Class 3 as the charge decreases. Ions involving features not present in the known hydrides have been omitted.

While the above classifications and lists probably do not exhaust all possibilities, it may be hoped that the omissions do not overlook any obviously promising stable ions. For example, we have not considered ions based on linked polyhedra or linked fragments of polyhedra. We have not tried to list completely the results of applying the processes of Classes 3, 4 and 5 to all ions listed above. Finally, these principles are applicable to types of polyhedra other than those discussed here.

The available experimental evidence for ionic boron hydride fragments suggests that much careful experimental work is desirable. Stock[9] mentions $Na_2B_2H_6$ and $Na_2B_4H_{10}$, from which the original hydrides B_2H_6 and B_4H_{10} are at least partly recoverable. He also describes[10] $Na_2B_5H_9$ and $Na_2B_4H_8$ as a decomposition product of $Na_2B_4H_{10}$. Recent work[3,11] has shown that the diborane reaction gives $NaBH_4$ and NaB_3H_8. The remarkable $B_2H_7^-$ ion[12] prepared by reaction of BH_4^- with B_2H_6 may possibly be formed only when BH_4^- can react with the double hydrogen bridge which occurs in B_2H_6 but not in the higher hydrides. However, similar studies have not yet appeared for the higher hydrides.

In summary, the more stable ions are probably $B_{12}H_{12}^{-2}$, $B_{10}H_{14}^{-2}$, $B_{10}H_{13}^-$, $B_6H_{11}^+$, $B_3H_8^-$, $B_4H_7^-$, $B_6H_6^{-2}$, $B_5H_{10}^-$, $B_3H_6^+$. The fact that both positive and negative ions might exist leads to the suggestion of purely ionic hydrides possibly prepared by reactions of salts of these ions with one another.

(5) W. H. Eberhardt, B. L. Crawford, Jr., and W. N. Lipscomb, *J. Chem. Phys.*, **22**, 989 (1954).

(6) G. A. Guter and G. W. Schaeffer, *J. Am. Chem. Soc.*, **78**, 3546 (1956).

(7) F. L. Hirshfeld, K. Eriks, R. E. Dickerson, E. L Lippert, Jr., and W. N. Lipscomb, *J. Chem. Phys.*, **28**, 56 (1958).

(8) H. C. Longuet-Higgins and M. de V. Roberts, *Proc. Roy. Soc. (London)*, **A230**, 110 (1955).

(9) A. Stock, "Hydrides of Boron and Silicon," Cornell University Press, Ithaca, N. Y., 1933.

(10) A. Stock, W. Sutterlin and F. Kurzen, *Z. anorg. Chem.*, **225**, 225, 243 (1935); **228**, 178 (1936).

(11) J. S. Kasper, L. V. McCarty and A. E. Newkirk, *J. Am. Chem. Soc.*, **71**, 2583 (1949).

(12) H. C. Brown, P. F. Stehle and P. A. Tierney, *ibid.*, **79**, 2020 (1957).

MEASUREMENT OF THE ABSORPTION SPECTRA OF NEPTUNIUM IONS IN HEAVY WATER SOLUTION FROM 0.35 TO 1.85 μ

BY W. C. WAGGENER

Contribution from the Chemistry Division, Oak Ridge National Laboratory, Oak Ridge, Tennessee

Received November 27, 1957

Numerous inorganic ions undoubtedly have characteristic aqueous absorption bands which occur above 1.2 μ where the strong absorption of ordinary water precludes their measurement. The spectral region between 1.2 and 1.8 μ is easily accessible to measurement by changing to heavy water aqueous media since D_2O is much more transparent than H_2O to radiation in the near infrared.[1]

The following preliminary study of the spectra of neptunium ions in heavy water solution suggests a fruitful extension for spectroscopy of aqueous solutions in general into the range from 1.2 to at least 1.8 μ. By following the progressive catalytic reduction of a solution of $NpO_2(ClO_4)_2$ in 1 *M* $DClO_4$–D_2O over the range from 0.35 to 1.85 μ ten new absorption maxima have been characterized (see Table I). Five of these maxima, including the strong peak for Np(VI) ion at 1.223 μ, were first measured in light water solutions.

Experimental

The neptunium solution used was prepared by evaporating a 30 mg. sample[2] of Np^{237} to dryness twice with $HClO_4$. An excess of $HClO_4$, then added, was converted to $DClO_4$ by repeated dilution and evaporation with D_2O (99.8%). Finally, constant boiling acid was evaporated to requisite weight for dilution to unit molarity in $DClO_4$.

(1) W. C. Waggener, *Anal. Chem.*, in press.

(2) Courtesy of P. M. Lantz and G. W. Parker, Chemistry Division, Oak Ridge National Laboratory.

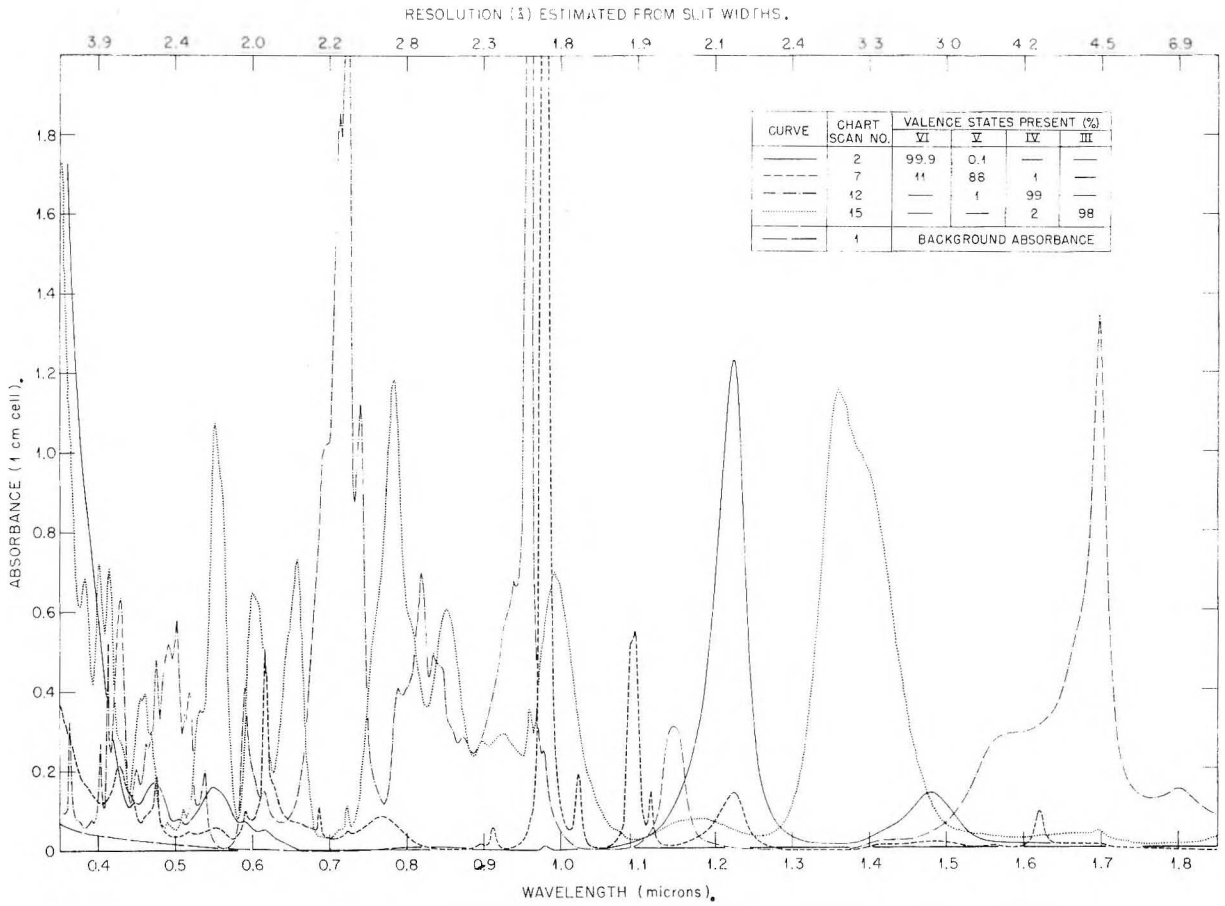

Fig. 1.—Absorption spectra of 0.0276 *M* neptunium perchlorate in 1 *M* $DClO_4$–D_2O from 0.35 to 1.85 μ.

The concentration of Np^{237} in the deuterated sample was 0.0276 *M* by radiometric assay. One molar $DClO_4$ for the reference cell was prepared from $HClO_4$ in the manner described for the neptunium sample.

The sample was held in a conventional 1 cm. fused quartz cell which was fitted with a long neck and a Teflon stopper. Reduction of the sample was done outside the spectrophotometer by inserting a fine platinized Pt capillary helix through which a slow stream of $D_2(g)$ was passed.

The Cary Model 14M Spectrophotometer was used with cell compartments thermostated at 25°. Undispersed radiation was passed through the cells, and slit operation was automatic, providing a constant power signal from the reference beam to the PbS detector.

Background absorbance was determined from 0.35 to 1.85 μ with 1 *M* $DClO_4$ in both cells. The oxidized sample was then scanned and reduced alternately until the neptunium was 98% converted into the III state.

Results and Discussion

The spectral curves in Fig. 1 represent the maximum concentration recorded, respectively, for Np(VI), (V), (IV) and (III) ions in the deuterated medium during reduction.

The valence composition given in Fig. 1 for each curve was determined from the data with the aid of published results for neptunium ions in 1 *M* $HClO_4$.[3]

Beer's law behavior and a negligible effect of change of solvent were assumed. The molar absorptivities computed for 19 bands between 0.428 and 1.023 μ are in reasonable agreement with the data of Sjoblom and Hindman if their entire curve for Np(V) is dropped 4 absorptivity units: $\epsilon_{obs}/\epsilon_{SH} = 0.95 \pm 0.05$. No evidence has been found for this background absorption, either in $HClO_4$ or $DClO_4$; it is also not shown by the spectrum of Np(V) in HCl as measured by Hindman and co-workers.[4]

TABLE I

ESTIMATED MOLAR ABSORPTIVITIES AND VALENCE ASSIGNMENTS OF NEW NEPTUNIUM MAXIMA BELOW 1.85 μ

λ (μ)	Valence	ϵ	λ (μ)	Valence	ϵ
1.800	4	5	1.223	6	45
1.697	4	49	1.180	3	3
1.620	5	4	1.145	4	11
1.480	6	5	1.117	5	6
1.360	3	43	1.096	5	23

None of the absorption maxima were tested for constancy of ϵ. However, the intensities of the sharpest bands, *e.g.*, 0.9600 and 0.9800 μ of Np(IV) and (V), respectively, did not appear to be sensitive to appreciable changes in slit width.

Acknowledgment.—The author acknowledges the assistance of his wife, Rose Marie, in preparing the graph.

(3) R. Sjoblom and J. C. Hindman, *J. Am. Chem. Soc.*, **73**, 1744 (1951).

(4) J. C. Hindman, L. B. Magnusson and T. J. LaChapelle, "National Nuclear Energy Series," IV, 14B No. 15.2, McGraw-Hill Book Co., Inc., New York, N. Y., 1949.

THE THERMAL STABILITY OF COPPER PHTHALOCYANINE[1]

BY EMIL A. LAWTON[2]

Contribution from Battelle Memorial Institute, Columbus, Ohio

Received November 21, 1957

In the course of investigating the thermal properties of copper phthalocyanine and related materials, a sample of copper phthalocyanine was quickly heated to 900° in a sealed evacuated Vycor ampule with no visible change in its properties. A second sample maintained at 800° for one hour was also apparently unchanged and its infrared spectrum was identical to unheated material from the same preparation. Although it has been long known that copper phthalocyanine can be sublimed at atmospheric pressure at 580°,[3] this unusually high thermal stability is much greater than might be expected for such a complex organic molecule.[4] These results suggested that dicopper heptabenzobis-(tetraazaporphin) (I) might also be sublimable. Using a modification of the method of Ebert and Gottlieb[5] for nickel phthalocyanine, a mixture of copper phthalocyanine I and higher polymers was prepared by treating excess phthalic anhydride with pyromellitic anhydride in the presence of urea and $CuCl_2 \cdot 2H_2O$. I and higher polymers are characterized by absorption bands at 7.5-7.6, 9.1-9.2 and 13.5-13.6μ.

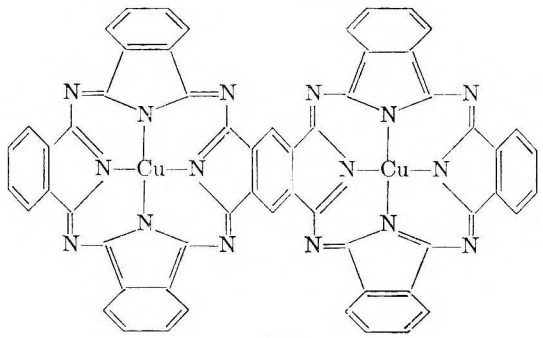

I

(1) This research was supported by the United States Air Force under Contract No. AF 33(616)-3477, monitored by the Aeronautical Research Laboratory, Wright Air Development Center.

(2) Rocketdyne, Canoga Park, California.

(3) C. E. Dent and R. P. Linstead *J. Chem. Soc.*, 1027 (1934).

(4) Vanadyl porphyrin is also very stable, subliming *in vacuo* at 880°, W. H. Bonner, Jr., U. S. 2,740,794 (April 3, 1956).

(5) A. A. Ebert, Jr., and H. B. Gottlieb, *J. Am. Chem. Soc.*, **74**, 2806 (1952).

The copper phthalocyanine was removed easily from the mixture by sublimation in high vacuum below 530°. Further increasing the temperature slowly to 696° gave no additional sublimate but led to total decomposition of the sample. The residue represented 81 weight % of the original sample and contained free copper, carbon and an amorphous nitrogen-containing material. Condensable gaseous decomposition products were collected at −196°. The condensate contained HCN (90%) and NH_3 (10%) by mass spectographic analysis.

The stability of copper phthalocyanine for one hour at 800° in a closed system contrasts with the total decomposition of similar polymeric materials at 700° under continuous pumping. This difference in behavior seemed to indicate an unusual reversible dissociation as a first step in the pyrolysis of this type of compound. An attempt was made to determine whether a reversible decomposition of copper phthalocyanine could be observed by measuring its sublimation pressure in a static system.

Pure sublimed copper phthalocyanine (230 mg.) was sealed off at a pressure of less than 10^{-5} mm. of mercury in a quartz Bourdon gage having a precision of better than ±2 mm. up to a total pressure of three atmospheres.

The gage registered no pressure until the sample was heated above 500°. The pressure rose slowly at temperatures above 550°, but an equilibrium pressure never was attained. For example, after two days it had risen to 945 mm. and was still increasing. The sample evolved gaseous products corresponding to a maximum of about 9% decomposition during a five-day period. Five days at temperatures between 550 to 575° resulted in the formation of 3.6 cc. of gas. The per cent. decomposition was calculated from the measured volume of the gaseous decomposition products. By analogy with the measured decomposition of I, it was assumed that the evolved gas was HCN and it represented one-fifth of the total decomposition products.

It must be concluded that the stability displayed by copper phthalocyanine at 800° and higher is due to a very slow rate, *i.e.*, high activation energy, of decomposition and is not a measure of the intrinsic thermal stability of this compound.

Acknowledgments are due Mr. Jerry W. Moody for the initial measurements and Mrs. Donna D. McRitchie for preparing the compounds employed in this investigation.